An Anticipatory-Lifecycle Approach Towards Increasing the Environmental Gains from Photovoltaic Systems Through Improved Manufacturing and Recycling

by

Dwarakanath Triplican Ravikumar

A Dissertation Presented in Partial Fulfillment
of the Requirements for the Degree
Doctor of Philosophy

Approved November 2016 by the
Graduate Supervisory Committee:

Thomas Seager, Co-Chair
Matthew P. Fraser, Co-Chair
Mikhail Chester
Parikhit Sinha
Meng Tao

ARIZONA STATE UNIVERSITY

December 2016

ABSTRACT

Photovoltaics (PV) is an environmentally promising technology to meet climate goals and transition away from greenhouse-gas (GHG) intensive sources of electricity. The dominant approach to improve the environmental gains from PV is increasing the module efficiency and, thereby, the renewable electricity generated during use. While increasing the use-phase environmental benefits, this approach doesn't address environmentally intensive PV manufacturing and recycling processes.

Lifecycle assessment (LCA), the preferred framework to identify and address environmental hotspots in PV manufacturing and recycling, doesn't account for time-sensitive climate impact of PV manufacturing GHG emissions and underestimates the climate benefit of manufacturing improvements. Furthermore, LCA is inherently retrospective by relying on inventory data collected from commercial-scale processes that have matured over time and this approach cannot evaluate environmentally promising pilot-scale alternatives based on lab-scale data. Also, prospective-LCAs that rely on hotspot analysis to guide future environmental improvements, (1) don't account for stake-holder inputs to guide environmental choices in a specific decision context, and (2) may fail in a comparative context where the mutual differences in the environmental impacts of the alternatives and not the environmental hotspots of a particular alternative determine the environmentally preferable alternative

This thesis addresses the aforementioned problematic aspects by (1)using the time-sensitive radiative-forcing metric to identify PV manufacturing improvements with the highest climate benefit, (2)identifying the environmental hotspots in the incumbent CdTe-PV recycling process, and (3)applying the anticipatory-LCA framework to identify the most

environmentally favorable alternative to address the recycling hotspot and significant stakeholder inputs that can impact the choice of the preferred recycling alternative.

The results show that using low-carbon electricity is the most significant PV manufacturing improvement and is equivalent to increasing the mono-Si and multi-Si module efficiency from a baseline of 17% to 21.7% and 16% to 18.7%, respectively. The elimination of the ethylene-vinyl acetate encapsulant through mechanical and chemical processes is the most significant environmental hotspot for CdTe PV recycling. Thermal delamination is the most promising environmental alternative to address this hotspot. The most significant stake-holder input to influence the choice of the environmentally preferable recycling alternative is the weight assigned to the different environmental impact categories.

DEDICATION

To Thara, Miyuki and my family without whose love, support, and sacrifice this effort would not have been possible.

ACKNOWLEDGMENTS

The guidance and advise from my committee members has contributed immensely towards the research presented in this dissertation and my intellectual and professional growth over the last four years. I am grateful to Dr. Thomas Seager who has spent a significant amount of his time emphasizing the importance of systems thinking while analyzing large-scale environmental challenges, the significance of thermodynamics as a tool to understand the lifecycle impacts of renewable energy technologies, and improving my scientific presentation skills. I thank Dr. Matthew Fraser for the guidance on the environmental chemistry aspects of this research, laboratory facilities for the photovoltaic delamination experiments and the support for photovoltaic (PV) environmental research as a part of the Quantum Energy and Sustainable Solar Technologies (QESST) engineering research center at Arzona State University. Dr. Parikhit Sinha has been very generous with his time while providing an industry perspective on PV recycling research and was instrumental in me getting introduced to the recycling team and gaining access to the recycling plant at First Solar. This ensured that the findings in this dissertation can guide the PV industry towards environmentally improved pathways or recycling. I thank Dr. Mikhail Chester for the difficult, but immensely valuable, questions on Lifecycle Assessment (LCA) of emerging technologies which has significantly influenced the methodological basis of this dissertation. I thank Dr. Meng Tao for helping me gain a deeper understanding of PV device fundamentals and how this can inform recycling processes. I am lucky to have been part of many informative discussions with Ben Wender and Valentina Prado on how LCA can guide environmental improvements in emerging technologies. These discussions have influenced my approach towards prospectively assessing the environmental impacts of novel PV recycling technologies.

I am thankful for the organizational support received from First Solar's recycling team over a two-year period and the findings in this dissertation would not have been possible without their data on recycling operations and the constructive feedback received from their leadership team.

This dissertation is primarily supported by the National Science Foundation (NSF) and the Department of Energy (DOE) under NSF CA No.EEC-1041895 and 1140190. Any opinions, findings and conclusions or recommendations expressed in this material are those of the author and do not necessarily reflect those of NSF or DOE.

TABLE OF CONTENTS

Page

APPENDIX Page

LIST OF TABLES

Table Page

LIST OF FIGURES

Figure Page

Figure Page

CHAPTER 1

INTRODUCTION

Global cumulative PV installations have increased from 1.4 GW in 2000 to 177 GW in 2014 [1][2] to meet climate goals and transition away from fossil fuels for electricity generation [3][4]. The environmental benefit of a PV system accrues during the use phase, when PV electricity displaces carbon-intense electricity, and is predicated upon environmental investments in the manufacturing and recycling phases. To date, the dominant approach to increase the environmental benefits of PV systems is to improve the module efficiency as this increases the renewable electricity generated over the lifespan of a PV system [5]. While achieving significant environmental and economic improvements, this approach fails to address the environmental burdens in the manufacturing and recycling processes. For example, manufacturing processes like silicon purification and wafer sawing continue to be energetically burdensome and have significant material losses[6][7]. Further, end-of-life modules are projected to reach 78 million tonnes by 2050 [8].The gradual shift in and PV manufacturing activities to GHG-intensive regions like China [9] and possible resource constraints [10][11] [12][13] further underscore the need to identify novel, environmentally improved pathways for PV manufacturing and recycling.

The typical approach to realize such environmental improvements is identifying existing hotspots, addressing them through alternate, less environmentally burdensome processes and analyzing the corresponding environmental trade-offs through a lifecycle assessment (LCA). LCA is a retrospective framework as it depends on material and energy inventory datasets that are available only after a process has technologically matured and commercialized over time [14]. Such inventory data is lacking for the emerging lab scale

processes (e.g. novel PV recycling methods) and investigators, during the research and development stage, focus primarily on the feasibility of the process and not on reporting energy and material requirements. The lack of technological maturity in the early stage of research of development, unavailability of inventory data and the retrospective mode of analysis limits the application of a traditional LCA approach in evaluating the environmental performance of emerging PV recycling and manufacturing methods.

Anticipatory LCA [15], a recent methodological innovation, addresses these problematic aspects by stochastically comparing the environmental impacts of the incumbent and the novel methods, identifying the environmental hotspots through a sensitivity analysis and prioritizing the future research to address the hotspots and maximize the environmental benefits of commercializing novel alternatives. The material and energy inventory data required for the environmental impact assessment for the novel recycling methods are determined from laboratory experiments and secondary literature sources. This thesis applies the aLCA framework and presents the environmental rationale for extending beyond the dominant approach of improving the use-phase PV module efficiency to increase the lifecycle environmental gains from a PV system through improved manufacturing and recycling practices. Environmental hotspots in the existing PV manufacturing and recycling phases are identified and the aLCA framework is applied to quantify the environmental benefit of addressing the PV recycling hotspots through seven alternate recycling processes.

Environmental benefits of improved PV manufacturing

Improving the environmental performance of PV manufacturing processes requires an understanding of trends that drove past improvements and using this to prospectively

analyze the potential for further improvements. For example, reduction in the silicon wafer thickness which drove past manufacturing improvements, may not be a viable strategy in the future as breakage and cracking rates in wafer manufacturing operations increase below a threshold thickness [16]. To establish historical environmental gains from manufacturing improvements, this thesis presents an experience curve depicting manufacturing energy improvements over the past two decades for the four main PV technologies –amorphous silicon, CdTe, multi and mono crystalline silicon. This manufacturing experience curve will be based on a data harmonization of previously published PV manufacturing environmental lifecycle studies. Significant reductions in manufacturing energy for the four PV technologies in the experience curve are identified and the corresponding manufacturing process improvements that resulted in these reductions are investigated.

Manufacturing improvements, identified in the experience curve, reduce electricity requirements and the corresponding emissions which depend on the GHG intensity of electricity at the PV manufacturing site. Further, the GHGs avoided in the manufacturing phase temporally precede emissions avoided in the use phase when PV electricity displaces GHG intensive electricity. Previous research has demonstrated that the global warming impacts of GHG emissions are dependent on the timing of the emission and is directly proportional to the residence time in the atmosphere [17]. Therefore, a mass of GHG emission avoided in the manufacturing phase has a greater environmental benefit than that in the use phase. This thesis uses the time sensitive radiative forcing metric [18] [19]to account for geographical and temporal sensitivities of the environmental impacts of GHGs emitted and avoided over the PV lifecycle and determine if future PV manufacturing improvements offer significant environmental gains. To demonstrate the significance of the climate benefits through manufacturing improvements the equivalent increase in module

efficiency required to achieve the same climate benefit is calculated. An increase in module efficiency increases the renewable electricity generation at the deployment site and therefore increases the climate benefit by avoiding electricity generated from fossil fuels.

Environmentally improved pathways for CdTe PV recycling

With rapid global deployments, the volume of end of life PV systems will increase after a typical lifetime of 25 years. An environmentally efficient strategy to manage this PV waste requires an assessment of the environmental performance and hotspots in existing processes that recycle the entire PV system (module, balance of system and electrical systems). To date, there is no comprehensive study that evaluates the environmental impact of transporting and recycling an entire PV system and identifies recycling process hotspots. This thesis addresses this knowledge gap through an energetic analysis of CdTe PV recycling operations at First Solar, which is the world's largest recycler. The outcomes of this section includes quantifying the energetic impacts of PV recycling, calculating benefits of recovering secondary materials and identifying process hotspots that can be addressed in the future.

Furthermore, the aLCA framework is applied to identify environmentally favorable pathways for addressing recycling hotspots by replacing the incumbent process with novel alternatives. The novel methods are selected based on a detailed literature review of PV recycling studies and the inventory requirements are determined from laboratory experiments and from published studies. The environmental performance of the incumbent and novel methods is compared using the aLCA framework. Furthermore, to prioritize future research effort, the parameters that significantly improve the environmental performance of the novel recycling methods at a commercial scale are identified through a global sensitivity analysis.

To manage PV waste from deployments across disperse geographies, PV recyclers can either transport end of life modules to centralized plants operating the incumbent method or recycle modules at the deployment site through decentralized mobile plants operating the novel methods. The environmental trade-off between the increased transportation burden to centralized recycling sites and the environmental gains from mature processes and economies of scale at centralized plants are calculated to determine the optimal strategy for locating recycling infrastructure. The optimal strategy for locating the recycling plant is determined by applying aLCA framework to two scenarios (1) centralized recycling in Kuala Lumpur, Malaysia and decentralized recycling in Biejing, China, and (2) centralized recycling in Perrysburg, Ohio and decentralized recycling at the Topaz Solar plant, California. China and California are selected for decentralized recycling as PV deployments in these geographies are increasing rapidly and corresponding end- of-life waste is expected to increase in the next 25 years. Kuala Lumpur and Perryburg are chosen as sited for centralized plants as First Solar, the world's largest PV recycler, is currently operating commercial scale CdTe PV recycling plants at these locations to manage PV waste from multiple locations.

Chapter-wise Summary

Table 1 Chapter 2 summary

Chapter 2: Intertemporal Cumulative Radiative Forcing Effects of Photovoltaic Deployments	
Research questions	Do current PV LCAs underestimate the climate impacts of PV manufacturing emissions that occur earlier than the emissions avoided gradually over the use-phase of the PV module? How can the time-sensitive climate impact of PV manufacturing emissions be quantified? What are the existing hotspots in the crystalline silicon PV manufacturing process that drive this climate impact?
Approach	Analyze the climate-trade-off between the emissions emitted and avoided during the manufacturing and use-phase, respectively, using the time-sensitive cumulative radiative forcing (CRF) metric. Using a sensitivity analysis determine the operational parameters in the PV manufacturing process that can minimize this climate impact.
Deliverable	Journal article in Environmental Science and Technology (ES&T)
Intellectual Merit	This study demonstrates that existing PV environmental studies underestimate manufacturing improvements by failing to account for the time sensitive radiative forcing impacts of manufacturing emissions. The CRF payback-time is greater than the GHG payback-time. The most significant climate hotspots in the PV manufacturing is the GHG intensity of mono and poly Si manufacturing processes.

Key figure

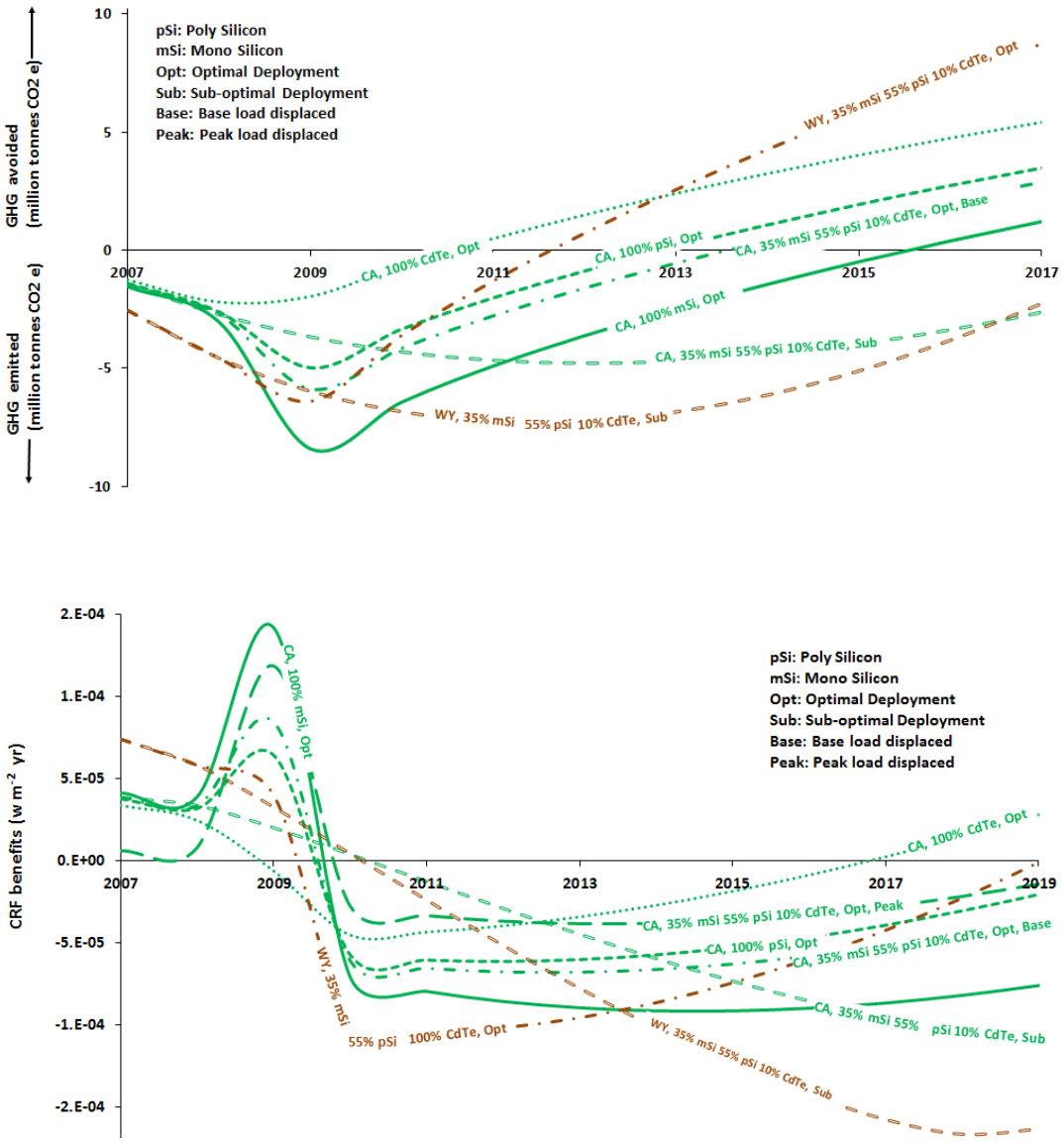

Figure 1 PV GHG and CRF payback times.
GHG (upper plot) and CRF (lower plot) payback times for PV systems manufactured in China and deployed in California and Wyoming. If the curve is below the X axis then GHG/CRF cost exceeds GHG/CRF benefit. If the curve is above the X axis GHG/CRF benefit exceeds the GHG/CRF cost. GHG/CRF payback occurs when the curve crosses the X axis. The CRF payback time in the (lower plot) exceeds the GHG payback time (upper plot) for all the scenarios.

Table 2 Chapter 3 summary

Chapter 3: A Compelling Climate Rationale for Carbon Efficiency in Photovoltaics Manufacture	
Research questions	What are the manufacturing experience curves for the four main PV technologies –amorphous silicon, CdTe, multi and mono crystalline silicon? Are there any distinct trends in the four curves and can they inform future PV manufacturing? Is there a climate rational for extending beyond the dominant approach of improving module efficiency and improving the lifecycle environmental performance of a PV module through manufacturing improvements?
Approach	Review previous PV manufacturing studies and harmonize manufacturing energy trends for 1 m^2 of a PV module. Identify and explain key transitions in the manufacturing energy trends and identify scenarios for future manufacturing improvements. Compare the climate benefit of manufacturing and module efficiency improvements using the CRF metric.
Deliverable	Conference proceeding in IEEE Photovoltaic Specialists Conference (PVSC). Journal article in Applied Energy.
Intellectual Merit	This study demonstrates that crystalline mono-silicon panels show a higher (74%) reduction in manufacturing energy from 1998 to 2008 than thin film technologies. This resulted from silicon PV industry reducing the silicon feedstock requirements for module manufacturing. The climate benefit of increased carbon-efficiency in mono-silicon manufacturing

	operations is equivalent to increasing the module efficiency from 17 to 21.7%.

Key figure

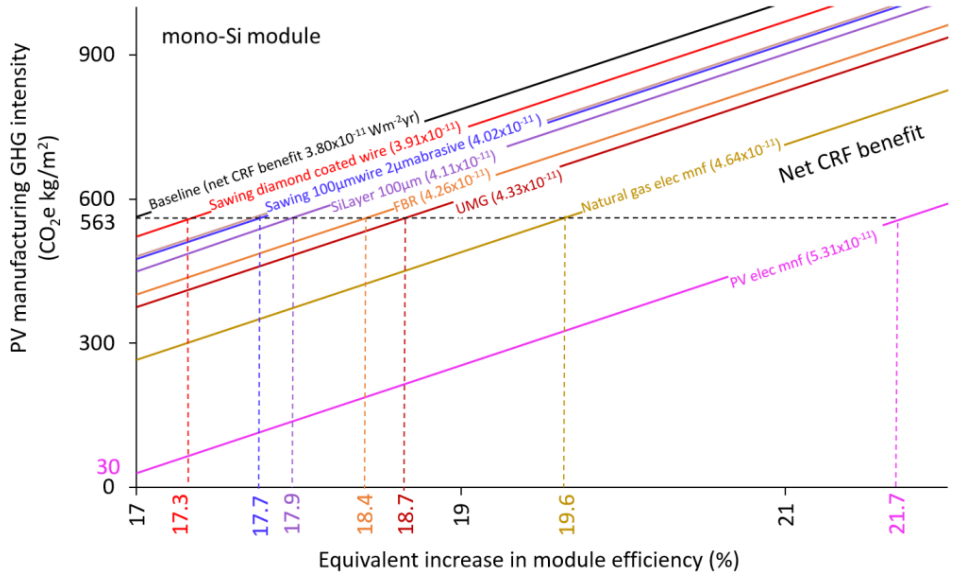

Figure 2 Equivalence between manufacturing and module efficiency imporvements. The equivalence in the CRF benefits between addressing hotspots in PV manufacturing and an increase in module efficiency for mono-Si modules manufactured in China and deployed in California. The manufacturing improvement that addresses the hotspot is accounted for by lowering the manufacturing GHG intensity (y-axis). The equivalent increase in module efficiency is determined by projecting the difference between the CRF benefit equivalence lines of the baseline and the improved manufacturing scenario to the x-axis.

Table 3 Chapter 4 summary

Chapter 4: An Anticipatory Approach to Quantify Energetics of Recycling CdTe Photovoltaic Systems	
Research questions	What is the net energetic impact of recycling a CdTe PV system and what are the hotspots in the recycling process? What is the energetic trade-off between centralizing and decentralizing the three steps of PV recycling – system disassembly, unrefined semiconductor material (USM) separation, USM refining?
Approach	Calculate the net energy benefit of recycling as the difference between the energetic gains of recovering secondary materials and the energetic cost of the recycling process. Identify hotspots in the recycling process that significantly impact the net energy benefit of CdTe PV recycling. Determine the threshold distance at which transportation energy impacts to centralized locations exceed the energetic benefits of economies of scale at a centralized recycling plant.
Deliverable	Journal article in Progress in Photovoltaics : Research and Applications
Intellectual Merit	Recovery of bulk secondary materials (e.g. steel, aluminum, glass) reduces the lifecycle energy footprint by approximately 24% of the energy required to manufacture the CdTe PV system. Eliminating EVA in the semiconductor recovery step is an energetic hotspot. Centralized recycling is favorable for USM refining and decentralized

	recycling is favorable for system disassembly and unrefined semiconductor material (USM) separation.

Key Figure

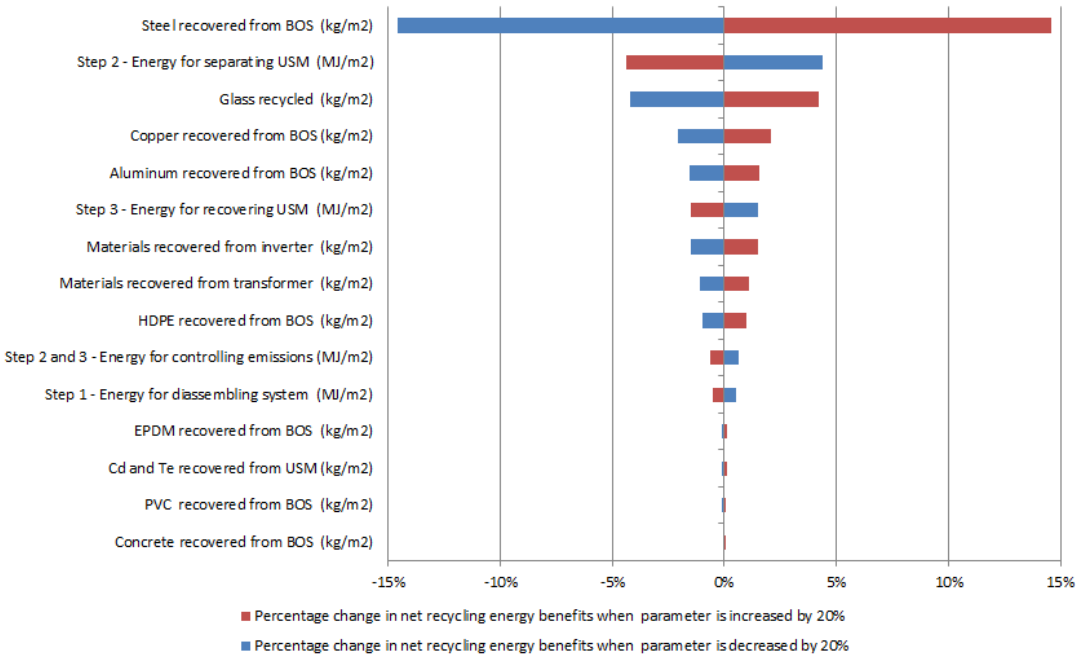

Figure 3 Sensitivty analysis of CdTe PV recycling energetics.
Sensitivity of recycling energy benefits to parameters under the control of a recycler. The parameter is incremented and decremented by 20% and the horizontal bars depict the corresponding percentage change in recycling energy benefit from the base value (0% line).

Table 4 Chapter 5 summary

Chapter 5: Anticipatory Lifecycle Assessment of CdTe Photovoltaic Recycling	
Research questions	What are the novel CdTe PV recycling methods proposed in literature? Which among these novel CdTe PV recycling methods is the most environmentally preferred to address the hotspot of EVA elimination in the incumbent recycling process (identified in chapter 3)? Will recycling the CdTe PV module through a novel method in decentralized plants be environmentally preferable to recycling in a centralized plant? What are the research priorities to further reduce the environmental impact when commercializing the most favorable novel method?
Approach	The environmental impact of the incumbent and six emerging PV recycling processes are stochastically aggregated and compared using the aLCA and stochastic multi-attribute analysis (SMAA) framework. The environmental impacts of operating the most environmentally promising novel method in a decentralized plant at the deployment site is compared with the impacts of transporting and recycling the module in a centralized plant. Using a global sensitivity analysis, the most significant parameters that influence the environmental performance of the novel method is determined.
Deliverable	Journal article in Energy and Environmental Science
Intellectual Merit	Thermally delaminating the EVA and recovering the cadmium and tellurium through leaching and precipitation is the most favored novel

	recycling process and environmentally outperforms the incumbent recycling process. Also, this novel method, operating in decentral plants, environmentally outperforms the centralized recycling when the dominant mode of transportation to centralized plants is road. When the dominant mode of transport is shipping, centralized recycling is environmentally preferable. The environmental performance of the novel method is most sensitive to weights assigned by the stakeholders to the environmental impact categories. If the weights are not included in the global sensitivity analysis, the environmental impact of the novel recycling method can be improved by decreasing the electricity consumption or using less GHG-intense sources of electricity.

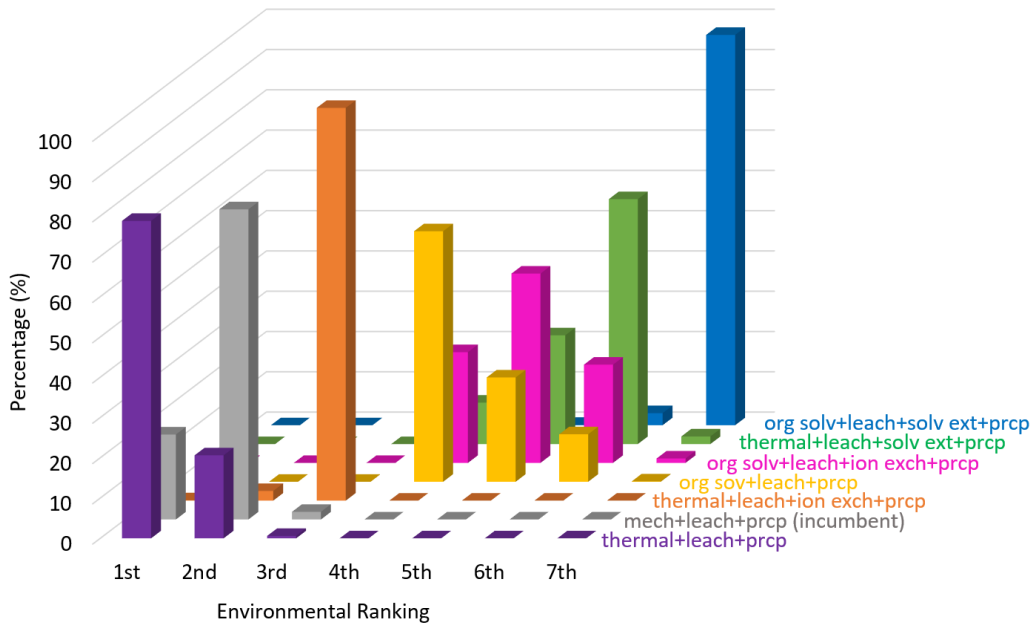

Figure 4 Environmental rankings of CdTe PV recycling alternatives. Percentage number of times the incumbent and six novel CdTe PV recycling methods obtain a particular environmental rank (based on an aggregated environmental score) in 1000 stochastic runs of the aLCA and SMAA framework. Rank one is environmentally the most favored. The aggregated environmental score for the novel method, which eliminates the EVA thermally and subsequently recovers cadmium and tellurium through leaching and precipitation (thermal+leach+prcp), is ranked one 78% of times and is, therefore, environmentally the most favored.

References

[1] European Photovoltaic Industry Association, "Global market outlook for photovoltaics until 2016," p. 12, 2012.

[2] International Energy Agency, "2014 Snapshot of global PV markets," p. 6, 2014.

[3] European Comission, "Renewable energy directive," 2009. [Online]. Available: https://ec.europa.eu/energy/en/topics/renewable-energy/renewable-energy-directive.

[4] Environmental Protection Agency, "Clean Power Plan," 2015. [Online]. Available: http://www2.epa.gov/cleanpowerplan/clean-power-plan-existing-power-plants.

[5] Office of Energy Efficiency and Renewable Energy, "Photovoltaics Research and Development," 2015. [Online]. Available: http://energy.gov/eere/sunshot/photovoltaics-research-and-development.

[6] E. Alsema and M. de Wild-Scholten, "Reduction of Environmental Impacts in Crystalline Silicon Photovoltaic Technology: An Analysis of Driving Forces and Opportunities," *MRS Proc.*, vol. 1041, Feb. 2011.

[7] A. Goodrich, P. Hacke, Q. Wang, B. Sopori, R. Margolis, T. L. James, and M. Woodhouse, "A wafer-based monocrystalline silicon photovoltaics road map: Utilizing known technology improvement opportunities for further reductions in manufacturing costs," *Sol. Energy Mater. Sol. Cells*, vol. 114, pp. 110–135, Jul. 2013.

[8] International Renewable Energy Agency, "End of Life Management: Solar Photovoltaic Panels," 2016.

[9] Fraunhofer Institute for Solar Energy Systems ISE, "Photovoltaics Report," no. August, p. 4, 2015.

[10] K. Burrows and V. Fthenakis, "Glass needs for a growing photovoltaics industry," *Sol. Energy Mater. Sol. Cells*, vol. 132, pp. 455–459, 2015.

[11] C. Candelise, M. Winskel, and R. Gross, "Implications for CdTe and CIGS technologies production costs of indium and tellurium scarcity," *Prog. Photovoltaics Res. Appl.*, vol. 20, no. 6, pp. 816–831, 2012.

[12] D. Ravikumar and D. Malghan, "Material constraints for indigenous production of CdTe PV: Evidence from a Monte Carlo experiment using India's National Solar Mission Benchmarks," *Renew. Sustain. Energy Rev.*, vol. 25, pp. 393–403, Sep. 2013.

[13] M. Redlinger, R. Eggert, and M. Woodhouse, "Evaluating the availability of gallium, indium, and tellurium from recycled photovoltaic modules," *Sol. Energy Mater. Sol. Cells*, vol. 138, pp. 58–71, 2015.

[14] B. a. Wender, R. W. Foley, T. a. Hottle, J. Sadowski, V. Prado-Lopez, D. a. Eisenberg, L. Laurin, and T. P. Seager, "Anticipatory life-cycle assessment for responsible research and innovation," *J. Responsible Innov.*, vol. 1, no. 2, pp. 200–207, 2014.

[15] B. a Wender, R. W. Foley, V. Prado-Lopez, D. Ravikumar, D. a Eisenberg, T. a Hottle, J. Sadowski, W. P. Flanagan, A. Fisher, L. Laurin, M. E. Bates, I. Linkov, T. P. Seager, M. P. Fraser, and D. H. Guston, "Illustrating anticipatory life cycle assessment for emerging photovoltaic technologies.," *Environ. Sci. Technol.*, vol. 48, no. 18, pp. 10531–8, Sep. 2014.

[16] S. Pingel, Y. Zemen, O. Frank, T. Geipel, and J. Berghold, "Mechanical stability of solar cells within solar panels," in *Proc. of 24th EUPVSEC*, 2009, pp. 3459–3464.

[17] A. Kendall, "Time-adjusted global warming potentials for LCA and carbon footprints," *Int. J. Life Cycle Assess.*, vol. 17, no. 8, pp. 1042–1049, May 2012.

[18] R. Pachauri and A. Reisinger, "IPCC Fourth Assessment Report: Climate Change 2007 (section 2.2)," 2012. [Online]. Available: http://www.ipcc.ch/publications_and_data/ar4/wg1/en/faq-2-1.html.

[19] T. F. Stocker, Q. Dahe, and G. K. Plattner, "IPCC Fifth Assessment Report - Climate Change 2013: The Physical Science Basis (Chapter 8 Supplementary Information Section 8.SM.11.3.1)," 2013.

CHAPTER 2

INTERTEMPORAL CUMULATIVE RADIATIVE FORCING EFFECTS OF PHOTOVOLTAIC DEPLOYMENTS

This chapter has been published in *Environmental Science & Technology* and appears as published. The citation for the article is: Ravikumar, D., Seager, T. P., Chester, M. V., & Fraser, M. P. (2014). Intertemporal cumulative radiative forcing effects of photovoltaic deployments. *Environmental Science & Technology*, 48(17),10010-10018.

Introduction

Global photovoltaic (PV) electricity generating capacity has increased from 0.3 GW in 2000 to 32.2 GW in 2012 and is projected to grow further [1, 2, 3], increasing to about 11% of total electricity generated worldwide by 2050 [4]. In the United States (US), the Department of Energy's (DoE) Sun Shot initiative seeks to deploy 632 GW by 2050, representing over 200 times the 2010 US capacity of 2.5GW [3, 5]. The primary motive for increasing PV is to reduce dependence on fossil fuels for electricity generation and prevent the global warming impacts of the associated greenhouse gas (GHG) emissions [4, 6]. However, production of new PV is itself energy intensive, and consequently creates GHG emissions during raw material extraction and purification, panel manufacturing and module installation that are gradually offset by the GHG avoided when PV electricity displaces grid electricity generated from fossil fuels. Consequently, rapid expansion of PV capacity can temporarily *increase* global warming impacts [7].

Life Cycle Assessment (LCA) is the preferred analytic framework for evaluating the systemic environmental consequences of competing energy technologies [8]. LCA quantifies

the environmental impacts of the material and energy flows at each stage of the product supply chain, to ensure that mitigation efforts do not simply shift impacts from one life cycle stage to another [9]. PV LCAs typically rely on 'grams/kWh' to compare the CO_2 footprint of PV electricity with other traditional electricity sources[10, 11, 12, 13]. This metric is determined by aggregating the PV lifecycle net CO_2 emissions over the total electricity generated during the use phase of the PV modules, without regard to the timing of these emissions [14]. By ignoring the CO_2 footprint of the electricity displaced at the deployment location, existing PV studies [11, 13, 15, 16] do not measure temporal trade-off of CO_2 over the PV lifecycle and cannot measure the corresponding short-term global warming impacts.

With regard to energy analysis, the primary temporal assessment metric for PV systems is Energy Payback Time (EPBT), expressed as a ratio between the total energy invested in manufacture and the annual energy produced during use [17] [18]. However, EPBT does not quantify the inter-temporal GHG tradeoffs or differences between the GHG intensity of energy supplies at panel manufacturing and deployment locations. These shortcomings limit the utility of EPBT to assess the global warming impacts of PV deployments.

Time sensitive warming impacts of GHG emissions

The Cumulative Radiative Forcing (CRF) metric provides a time sensitive quantitative measure of the atmospheric warming induced by GHG emissions. The CRF impact is determined by (i) radiative forcing (in Wm^{-2}) which is a measure of the change in the balance of incoming solar and outgoing infrared radiation in the atmosphere due to the emission of a specific GHG [19] and (ii) time period (in years) over which the annual radiative forcing impacts are cumulatively summed. For a fixed time period, earlier emissions have

relatively longer atmospheric residence time and therefore, cause higher CRF impacts than emissions occurring later in time. The quantitative framework to measure the time sensitive CRF impacts of GHG emissions is explained in the methods section.

Recent LCA studies highlight the necessity of understanding time-sensitive impact assessment methods in LCA of energy and infrastructure investments and the difference in the magnitude of CO_2 and CRF benefits and the time frames over which benefits accrue. The CRF metric has been used to quantify the difference in climate impacts for different diffusion rates and timing of carbon capture and storage (CCS) deployments and efficiency improvements for coal-fired power plants [20]. LCAs of bio-fuels and transportation systems have used CRF to develop correction factors that account for the timing of the GHG emission during the product lifecycle [21, 22, 23] and calculate the difference between the CO_2e and CRF payback times [24]. Another analysis shows that the CRF benefits of PV system deployments outweigh the CRF impacts of reduced albedo due to large scale deployments of dark surfaced PV systems [25].

This paper presents the results of a novel CRF-based model specifically for PV systems and calculates GHG and CRF-based payback times. The model also incorporates the prevailing geographical heterogeneities in the global PV supply chain to assess the impact of PV module manufacturing in coal-intensive geographies and deployment in comparatively less carbon-intensive electricity grids, under different conditions of solar insolation. We present an optimization framework that minimizes the CRF impacts of deploying PV modules to meet California Solar Initiative (CSI) policy targets and conduct a scenario analysis to demonstrate variations in GHG emissions and CRF with geographic locations, deployment strategies and technology mixes. Through a sensitivity analysis, we identify the

most important technology and supply chain parameters that, when improved, can significantly decrease CRF impacts of future PV deployments.

Methods

Factors impacting magnitude of GHG emitted and avoided over PV lifecycle

The parameters that influence the global warming impacts of new PV installations are depicted in Figure 5.

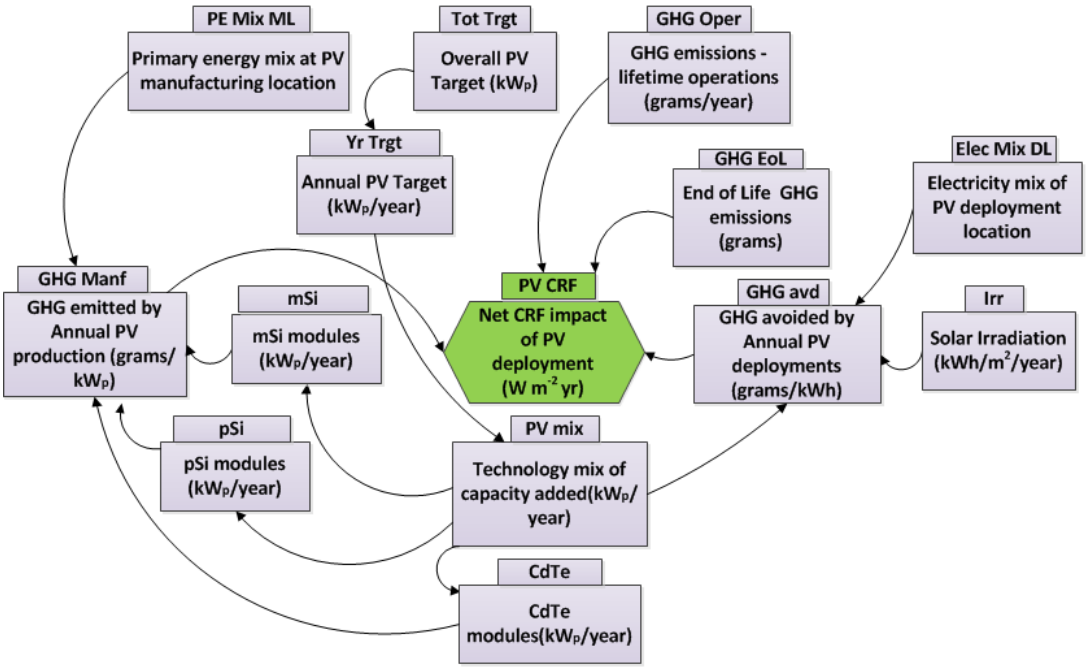

Figure 5 Factors impacting net GHG emissions over PV lifecycle

PV supply chain and technology parameters that impact the magnitude of GHGs emitted and avoided over the PV lifecycle

The annual PV target (Yr Trgt) is modeled as being fulfilled by a technology mix (PV mix) of monocrystalline silicon (mSi), polycrystalline silicon (pSi) and thin film CdTe (CdTe) modules as these technologies constitute around 95% of the world PV market [26]. The GHGs emitted over the manufacturing phase of the PV lifecycle (GHG Manf) is dependent on the primary energy mix at the manufacturing location (PE Mix ML) and the

manufacturing energy requirements of the PV technology. The manufacturing GHG footprint includes raw material extraction and purification, cell and module manufacturing (including frames) and the balance of systems (inverters, mounting, cables and connectors The GHGs emitted during manufacture of mSi (MCI china mono si) and CdTe (MCI Malaysia CdTe) modules are the highest and lowest, respectively (Table S6 in Appendix B). Crystalline silicon PV modules are primarily manufactured in China where coal contributes to around 70% of the primary energy mix [27]. By contrast, CdTe cells are produced predominantly by First Solar, Inc., which locates 70% of its manufacturing capacity in Malaysia [28]. This results in a lower GHG footprint for CdTe due to both the less intensive processes associated with materials purification and a less GHG-intensive primary energy mix at the manufacturing location.

The environmental benefit of PV deployments is determined by the GHG emissions avoided annually (GHG avd) as PV electricity offsets grid electricity generated from fossil fuels. GHG avd is dependent on the electricity grid mix (Elec Mix DL), solar irradiation at the deployment location (Irr) and the rated PV capacity deployed in that year (PV Mix). The GHGs emitted while maintaining, decommissioning and recycling PV modules (GHG Oper, GHG EoL) are assumed to be 10% of the overall GHG emitted to manufacture PV modules [29]. The magnitude and timing of GHG Manf ,GHG avd, GHG Oper and GHG EoL determine the net CRF impact (PV CRF) over the policy time frame.

CRF calculations for GHGs

CRF (in W m^{-2} yr) for a GHG pulse over a time period of TH years is given by

$$CRF = \int_0^{TH} \left(a_{ghg} \times c(t)\right) dt \qquad (1)$$

where c(t) is the fraction of the initial GHG emission (in kg) that remains in the atmosphere after 't' years have elapsed. The radiative efficiency (aghg) of the GHG, in W m^{-2} kg^{-1}, is the radiative forcing per unit mass of the GHG in the atmosphere [30] [31]. Radiative efficiency values are tabulated in Section 1 in Appendix B. The calculated CRF for methane is incremented by 40% to account for the indirect impacts of methane emissions on ozone and stratospheric water vapor concentrations [32].

The lifetime of atmospheric CO_2 described by c(t) is defined by the Bern carbon cycle model [33] and is given by

$$c(t) = 0.217 + (0.259 * e^{-t/172.9}) + (0.338 * e^{-t/18.51}) + (0.186 * e^{-t/1.186}) \qquad (2)$$

For GHGs apart from CO_2, c(t) is given by [34]

$$c(t) = e^{(-t/\tau)}dt \qquad (3)$$

where τ is the time required (years) for the GHG emission to decay to 1/e times the initial emission (perturbation time).

GHGs considered for CRF calculations

Typical GHG emissions for PV manufacturing processes and electricity production are reported as an aggregate CO_2e value calculated over a hundred year time frame (GWP_{100}). This masks the CRF impacts of GHGs which are potent over shorter time frames (e.g. CH_4). To disaggregate CO_2e emissions, the SimaPro software package was used to develop a GHG inventory for mSi and pSi manufacturing in China, CdTe manufacturing in Malaysia and grid emissions in California and Wyoming (Section 7, 8 in Appendix B).

For PV manufacturing CRF calculations, this study considers CO_2, CH_4, SF_6 and HFC-152a for mSi and pSi modules and CO_2 and CH_4 for CdTe modules. These gases contribute 97.74%, 98% and 99% of the total 10 year CRF impact for mSi, pSi and CdTe

manufacturing, respectively (Tables S14, S15, and S16 in Appendix B). For CRF calculations of grid emissions avoided at Wyoming and California, we consider only CO_2 and CH_4 as they contribute 99% of the total 10 year CRF impact (Tables S17, S18 in Appendix B). The CRF calculations also include the negative forcing impacts of SO_2 and NO_x emissions as they have significant short-term cooling impacts when there is a change in the fuel mix used to generate electricity [35, 36]. CRF values are determined by calculating the product of net SO_2 and NO_x emitted each year by the radiative efficiencies of SO_2 and NO_x, respectively. The CRF in a particular year is equal to the annual instantaneous RF in that year as the atmospheric residence times of SO_2 and NOx are less than two weeks [37, 38].

The net SO_2 and NO_x emission in any year is the difference between the PV SO_2 and NO_x emitted and avoided at the manufacturing and deployment location, respectively (Figure S4 and S5 in Appendix B). The radiative efficiencies of SO_2 and NO_x is determined by calculating the ratio of the annual global average radiative forcing attributed to SO_2 and NO_x and the annual global emissions [39] (Table S10 in Appendix B).

Timing of GHGs emitted and avoided over PV lifecycle

The decision to increase PV deployments earlier during the policy time frame (front loading) to displace more fossil fuel electricity versus the decision to postpone deployments to a later date (back loading) must weigh potential technology improvements in the PV system which may produce greater electricity with lower manufacturing impacts. Technology improvements over time are modeled by a decrease in PV manufacturing GHG emissions (grams/kWp) due to increasing manufacturing and module efficiencies (Section 3 in Appendix B).

Consider the following strategies for deploying 1 GW of PV capacity:

- **Front loading strategy (FLS):** 1 GW in year 1
- **Back loading strategy (BLS):** 1 GW in year 3

The GHG trade-off, which influences the CRF impacts, for FLS and BLS are shown in Figure 6 and Figure 7, respectively.

Timing of GHG emissions for FLS

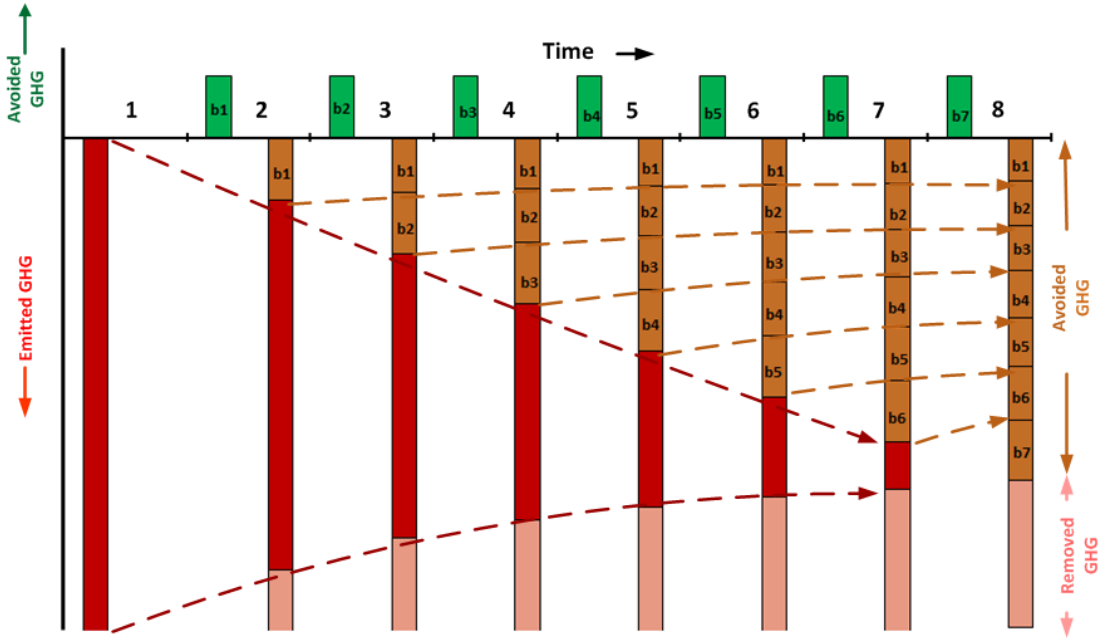

Figure 6 GHG flows for front loading of PV systems.
GHG flows for FLS. The positive Y axis represents GHG benefits and the negative Y axis the GHG costs of deploying PV systems. The PV system is deployed in year 1 and the corresponding PV manufacturing GHG emission is represented by the solid red bar. The pink bar represents the portion of the emitted GHG which is removed from the atmosphere annually (determined by equation (2) and(3)). The solid green bars from year 2 onwards (e.g., b1, b2, b3) represent the GHG emissions avoided as PV electricity displaces grid electricity and this is cumulatively deducted from the red bar (represented by the solid brown bars). The dashed brown line represents the removal of the avoided GHG had it been emitted. The dashed red arrows represent the gradual removal of PV manufacturing GHG emissions from the atmosphere.

The magnitude of the PV manufacturing emissions is a product of the PV capacity deployed and the GHG intensity of the manufactured PV modules.

$$mGHG_t = \sum_{\substack{i=monoSi,\\ PolySi,\\ CdTe}} W_{t\_i} \times MCI_{t\_i} \quad (4)$$

Where:

- mGHGt = PV manufacturing GHG emissions in year 't' (grams),
- i = PV technology deployed. Three types of PV technology are considered: mSi, pSi, CdTe,
- W t_i = capacity of a particular PV technology 'i' deployed in the year 't' (kWp),
- MCI t_i = GHG intensity of the manufactured PV modules in the year't' for technology 'i' (grams/kWp).

The GHGs avoided every year (solid green bars) is mathematically defined as

$$aGHG_t = \sum_{\substack{i=monoSi,\\ PolySi,\\ CdTe}} \left(\sum_{k=1}^{t} W_{k\_i} \right) \times pr \times irr \times (1-op) \times (1-tl) \times DGI_t \times apd \quad (5)$$

Where:

- aGHGt is the GHG emission avoided in year 't' (grams),
- W k_i is the cumulative rated PV capacity addition till the year t (kWp),
- pr is the performance ratio, the ratio between the AC power generated to the rated DC power,
- irr is the annual average solar irradiation at the deployment location (kWh/m^2/year),
- op is the ratio of energy spent on the operations and maintenance of the PV module to the total energy generated by the PV module,
- tl is the transmissions losses during electricity distribution (%),

- DGI t_i is the GHG intensity of the grid (grams/kWh), at the deployment location in the year 't',
- apd is the annual performance degradation (in %) for the PV module.

In the FLS strategy (Figure 2), the GHG benefits of a PV module accrue slowly over time; only in the 8th year is there a net GHG benefit.

Timing of GHG emissions for BLS

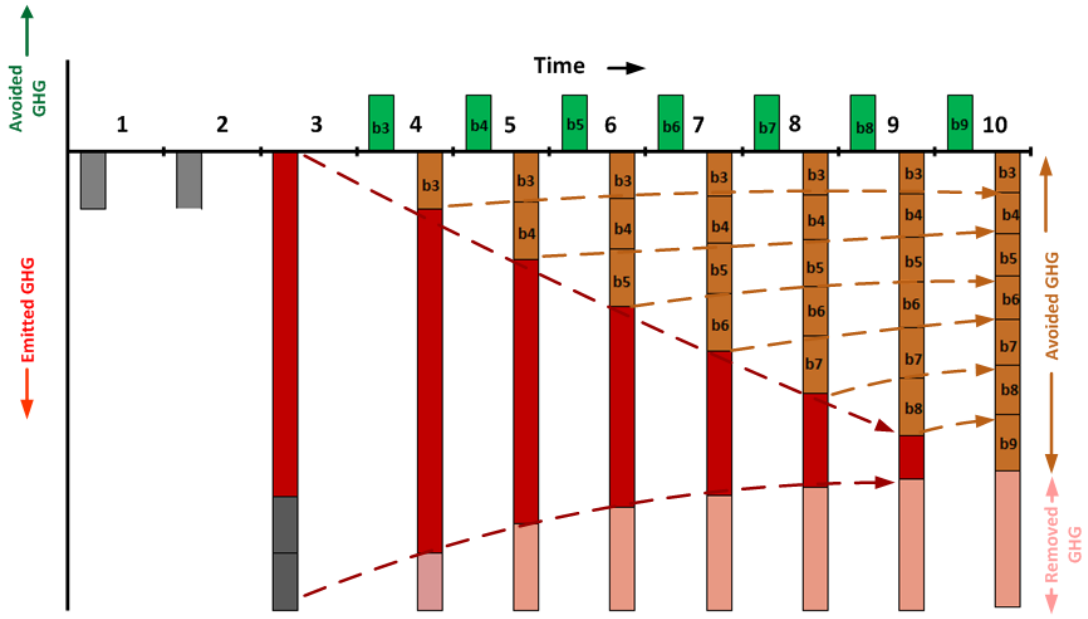

Figure 7 GHG flows for back loading of PV systems.
GHG flows for BLS. The PV capacity is deployed in year 3 and the grey bars in year 1 and 2 represent the GHG emissions due to continued reliance on grid electricity. The other depictions are similar to Figure 6.

One benefit of BLS is that PV modules deployed in the future will have higher efficiencies and lower manufacturing energy requirements than present day PV modules and this increases environmental benefits. However, the environmental cost of BLS is that users continue to rely on fossil fuels in the interim. In Figure 3, year 1 and 2 GHG emissions are

due to the continued reliance on fossil fuels for electricity. These emissions are equal to those that are displaced by the PV electricity from year 3 on (equation(5)). GHG emissions due to back loading can be mathematically defined as

$$bGHG_t = \sum_{\substack{i=monoSi,\\ PolySi,\\ CdTe}} \left(C - \sum_{k=1}^{t} W_{k\_i} \right) \times pr \times irr \times (1-op) \times (1-tl) \times DGI_t \times apd \qquad (6)$$

where, C is the total policy target (in kWp). The remaining terms in equation (6) are the same as in equation (5)

Optimization framework for PV deployment

The model presented herein arrives at the optimal PV deployment strategy (FLS or BLS) for minimal CRF impacts over the ten year time frame defined in the CSI [40] incorporating the PV supply chain and technology factors depicted in Figure 1.
The optimal deployment strategy is obtained by maximizing the objective function Z which quantifies the difference between PV CRF benefits and costs.

$$Z = \sum_{t=1}^{n} CRF_{av(t)} - CRF_{mnf(t)} - CRF_{bl(t)} \quad (7)$$

CRFav(t) is the CRF benefit due to the avoided GHGs (equation (5)) and is mathematically defined as

$$CRF_{av(t)} = \sum_{\substack{CO_2,CH_4,\\ SO_2,NO_x}} \sum_{t=1}^{n} (aGHG_t \times k_t) \qquad (8)$$

kt is the time sensitive CRF impact per unit mass of CO_2, CH_4, N_2O, and SF_6 emitted. kt is calculated for a ten year horizon (2007 to 2017) and is dependent on the year in which the GHG is emitted. The values are tabulated in tables S2, S3, S4, S5 in the Appendix B.

CRFmnf(t) is the CRF cost due to manufacturing GHGs emissions (equation (4)) and is mathematically defined as

$$CRF_{mnf}(t) = \sum_{\substack{CO_2,CH_4,\\ SF_6,HFC152a\\ SO_2,NO_x}} \sum_{t=1}^{n} \left(mGHG_t \times k_t \right) \qquad (9)$$

CRFbl(t) is the CRF cost due to back loading (equation (6)) and is mathematically defined as

$$CRF_{bl}(t) = \sum_{\substack{CO_2,CH_4,\\ SO_2,NO_X}} \sum_{t=1}^{n} \left(bGHG_t \times k_t \right) \qquad (10)$$

The decision variable is the annual PV deployment (Wt), which determines aGHG, bGHG, mGHG (equations(4), (5), and(6)) and therefore determines CRFav(t), CRFmnf(t) and CRFbl(t). By either deploying Wt during the initial years (FLS) or delaying it for the final years (BLS), Z can be optimized for maximum CRF benefits. The only constraint on Wt is that it should be less than the total PV target

$$\sum_{1}^{n} W_t \leq C \qquad (11)$$

The CSI goal is to add 1940 MW of PV capacity between 2007 and 2016 [40]. Based on the data published by the California Energy Commission, 81 MW and 169 MW were deployed in 2007 and 2008 and therefore these values are modeled as fixed [41]. The deployment of the remaining 1690 MW ('C') will be optimized between 2009 and 2016 with no annual constraints being imposed other than equation(11). The optimal strategy is a

choice between deploying all the capacity in 2009 (FLS) or in 2016 (BLS). FLS is optimal if CRF gains are maximized by displacing fossil fuel electricity with PV electricity (maximizing $CRF_{av(t)}$ in Equation (7)). This results in all the capacity being deployed in 2009. BLS is optimal if CRF gains are maximized when the PV manufacturing emissions resulting from PV technology improvements over time and the GHG footprint of the displaced grid electricity are minimal ($CRF_{mnf(t)}$ and $CRF_{bl(t)}$ in Equation (7)). This results in all the capacity being deployed in 2016. Any intermediate deployment strategy, apart from these two feasible policy extremes, is environmentally suboptimal as it staggers deployments across intermediate years which decrease maximum possible FLS or BLS CRF gains. The data assumptions for the optimization framework are explained in Section 2 in Appendix B.

Scenario and Sensitivity Analysis

We calculate the variations in GHG and CRF impacts for eleven scenarios with different PV technology mixes, type of loads displaced and deployment strategies in California and Wyoming. The different PV technology mixes consist of 100% for a particular technology as well as a 35% mSi, 55% pSi and 10% CdTe mix, based on a worldwide market share of 30 to 40% for mSi, 50 to 60% for pSi and 6 to 10% for CdTe from 2004 to 2010 [26]. We consider two scenarios in California where PV displaces base and peak loads each having different grid GHG intensities and we also include two scenarios for FLS and sub-optimal deployment strategies. For FLS in CA and WY, 81MW and 169 MW are deployed in 2007 and 2008 and the remaining capacity of 1689 MW is deployed in 2009. For sub-optimal deployment, 81MW and 169 MW are deployed in 2007 and 2008 and the remaining capacity of 1689 MW is equally deployed between 2009 and 2016. California and Wyoming were chosen to demonstrate the difference in GHG and CRF benefits for

different grid GHG intensities and solar insolation at the deployment location (DGI and Irr values in Table S6 in Appendix B).

We perform a sensitivity analysis (Figure 10) to quantify the change in the CRF value calculated when PV supply chain and technology parameters (depicted in Figure 5) are varied. The CRF is calculated for a base scenario in which capacities of 81, 169 and 1690 MW were deployed in California in 2007, 2008 and 2009, respectively, with a technology mix of 35% mSi, 55% pSi and 10% CdTe. Calculations assume Si technologies are manufactured in China, CdTe technologies are manufactured in Malaysia, and the CRF is measured over a 10 year period. After calculating the base scenario CRF, 12 runs were conducted by increasing and decreasing each parameter by 10% of its base condition value while keeping the other 11 parameters constant. CRF values for each of the 12 runs were recorded and plotted as a percentage change from the base condition CRF. A similar approach is used to quantify the variations in CRF impacts when the radiative efficiencies of GHGs are varied within the uncertainty range identified by IPCC (Section 9 in Appendix B).

Results and Discussion

Optimal PV deployment strategy and Scenario Analysis for GHG and CRF impacts

FLS is optimal for California and Wyoming for any technology mix that is chosen when the CRF impacts are considered from 2007 to 2017 (Section 4 in Appendix B). Figure 8 and Figure 9 depict scenarios that bracket the trends for GHG flows and the CRF impacts which are applicable to all the scenarios (Section 5 in Appendix B).

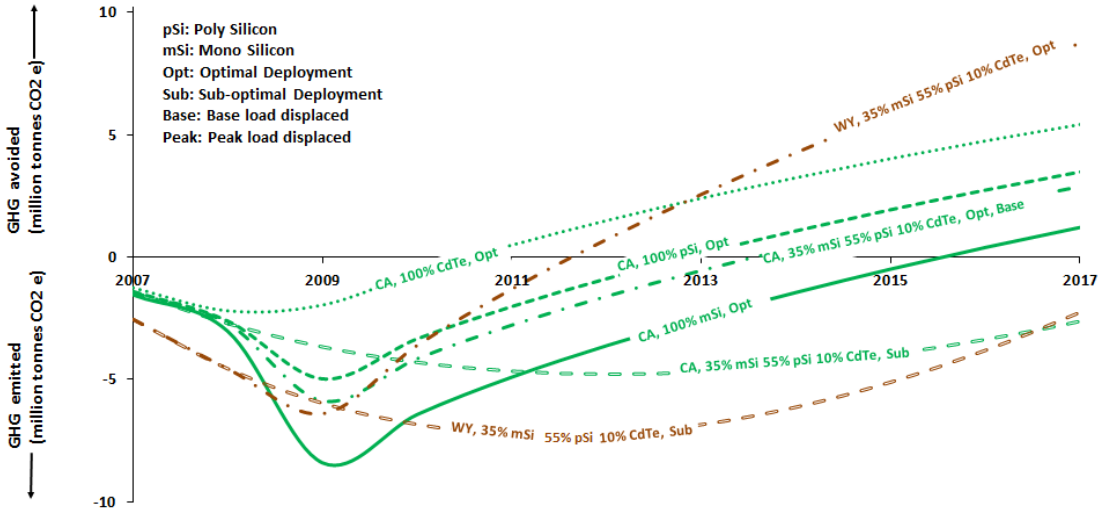

Figure 8 GHG payback time of PV systems.
Aggregated GHG benefits of PV deployments in California and Wyoming plotted from 2007 to 2017. Emissions due to PV manufacturing and the continued reliance on fossil fuels (for sub-optimal deployment) are the GHG costs of PV deployments. GHGs avoided when PV electricity offsets grid electricity represents the GHG benefit. If the curve is below the X axis then GHG costs exceed GHG benefits. If the curve is above the X axis GHG benefits exceed the GHG costs. GHG payback occurs when the curve crosses the X axis. At the chosen Y axis scale, curves for CA,35% mSi, 55% pSi, 10% CdTe, Opt – Base and Peak overlap as the difference in the grid GHG intensities is 8% [42].

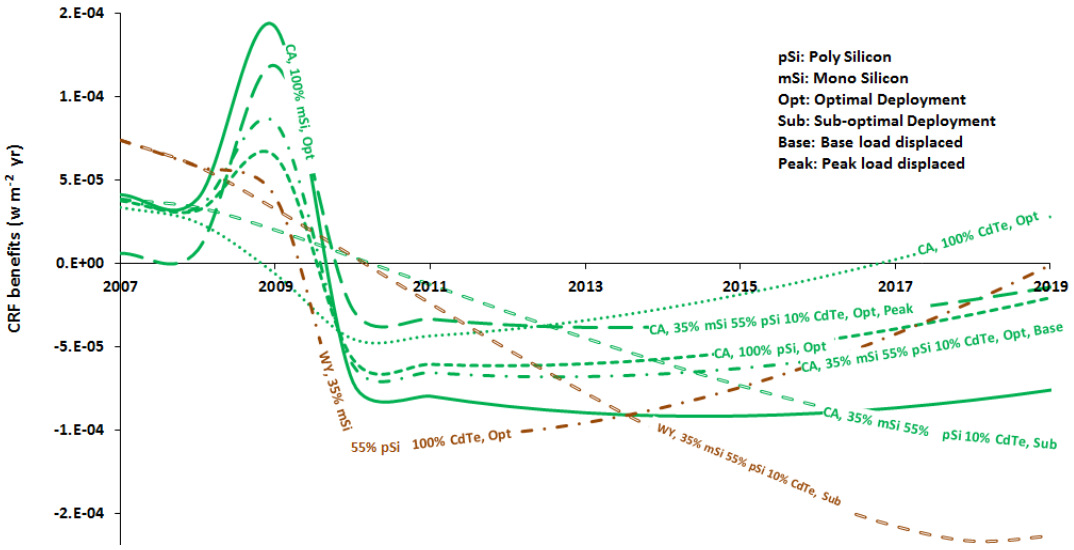

Figure 9 CRFpayback time of PV systems.
CRF benefits of PV deployments in California and Wyoming plotted from 2007 to 2017. CRF impacts of manufacturing emissions and emissions due to the continued reliance on fossil fuels (for sub-optimal deployment) represent PV CRF costs. The CRF impacts avoided when PV electricity offsets grid electricity represent the CRF benefits. If the curve is below the X axis then CRF costs exceed CRF benefits of deploying the PV module and if the curve is above the X axis then CRF benefits exceed CRF costs. CRF payback occurs when the curve goes from below to above the X axis.

The CRF benefit is positive from 2007 to 2010 due to the cooling impacts of short-lived SO_2 and NO_x emissions during PV manufacturing. As the short term negative forcing impact decrease and the positive forcing impacts of longer lived manufacturing GHG emissions (CO_2, CH_4, SF_6, HFC-152a) dominate, the calculated net CRF benefit becomes negative. The net CRF benefit is positive only when the CRF benefits of the GHGs displaced at the deployment location exceed the CRF costs incurred during PV manufacturing.

In all cases, CRF payback times are greater than GHG payback times. GHG payback occurs when the mass of GHG avoided is equal to the GHG emitted and is insensitive to

the timing and atmospheric residence time of emissions. CRF payback is sensitive to the magnitude and timing of emission and the residence time of GHG in the atmosphere. Early manufacturing emissions have a higher CRF impact than emissions avoided after deployment and this increases the payback time required to offset the CRF impacts of manufacturing GHG emissions

The GHG displaced and CRF impacts are dependent on the optimal rate of PV capacity deployment. For the sub-optimal strategy (e.g., WY, 35% mSi 55% pSi 100% CdTe, Sub), the grid continues to rely on electricity that is generated from fossil fuels and the CRF impacts of the resulting GHG emissions are greater than benefits of reduced GHG emissions resulting from manufacturing process improvements overtime. The optimal FLS (e.g., WY, 35% mSi 55% pSi 100% CdTe, Opt) yields greater CRF benefits as it displaces fossil fuel based grid electricity emissions early during the policy time frame. Thus, in California and Wyoming, aggressive upfront PV deployments at the current state of technology will yield greater benefits than a strategy of delayed deployments.

The difference between the CRF benefits when PV displaces either base and peak electrical loads is depicted by the CA, 35% mSi 55% pSi 100% CdTe, Opt base and peak scenarios. The CRF benefits are higher for the peak scenario as the grid GHG intensities for California's peak load is greater than base load by 8% [42].

GHG and CRF benefits depend on the GHG intensity of the grid electricity being offset at the deployment location. PV electricity will displace more emissions for locations with higher grid GHG intensities and this will decrease the GHG and CRF payback time. Thus, Wyoming's GHG and CRF payback times are less than that calculated for California's (WY and CA scenarios in Figure 8 and Figure 9). An earlier GHG and CRF payback implies

that the GHG and CRF benefits for all the Wyoming strategies are higher than the corresponding strategies in California for a 10 year time frame.

The choice of PV technology influences the GHG and CRF impacts. For example, among the three technology mixes in California – (i) CA, 100% mSi, Opt, (ii) CA, 100% pSi, Opt, and (iii) CA, 100% CdTe, Opt - the 100% CdTe mix has the highest GHG and CRF benefits and the earliest GHG and CRF break even time because CdTe has the lowest manufacturing GHG emissions among the three technologies (MCI malayisa cdte, MCI china poly Si, MCI china mono Si in Table S6 in Appendix B). Thus, with the current state of technology, a deployment mix relying more on CdTe and pSi will have lower environmental impacts than mSi.

Sensitivity Analysis

Figure 10 depicts the sensitivity analysis results and identifies parameters that significantly influence CRF impacts of PV deployments from 2007 to 2017. CRF impacts are most and least sensitive to the parameters at the top and bottom of the graph, respectively.

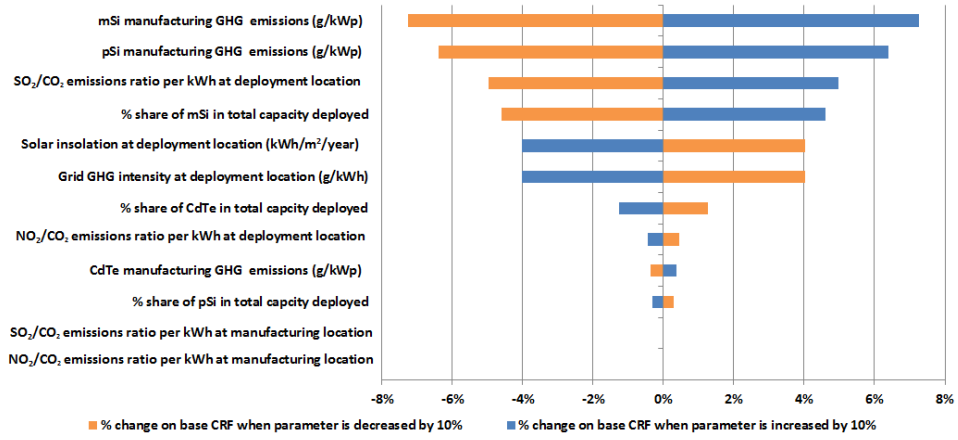

Figure 10 Sensitivity analysis of PV CRF impacts
Sensitivity analysis results identifying parameters that significantly influence CRF impacts of PV deployments. Variations in the most significant parameters result in the greatest percentage change in CRF from the base condition. The base scenario's CRF value is represented by the vertical line passing through zero.

CRF impacts are most sensitive to the GHG emitted while manufacturing mSi and pSi modules. This is due to the 90% share of pSi and mSi technology in the PV market and most of the world's Si PV modules being manufactured in China [2] with GHG intense electricity. Less energy intensive PV manufacturing processes and increased energy and material efficiencies in manufacturing Si modules will substantially reduce CRF impacts. The energy required to manufacture a unit area of mSi module has decreased by only 6% from 2006 to 2011 [43,44]. A decrease in the energy requirements of upstream metallurgical refining processes that contribute around 63% and 79% of the total energy footprint for pSi and mSi modules [44], respectively, will reduce CRF impacts and manufacturing costs. Recent studies identify reducing kerf loss through improved wafering techniques, decreasing cell thickness, lowering energy required for ingot growth and recycling kerf as potential pathways to reduce the environmental impacts and economic costs of manufacturing crystalline Si PV modules [45, 46]. Also, significant CRF gains can be achieved by reducing the GHG intensity of energy supply in China through the use of renewable energy sources at manufacturing locations[16].

PV system deployments will temporarily increase CRF impacts if the electricity displaced at the deployment location has a significant SO_2 footprint. However, as the time frame of analysis increases, the long term warming impacts of long-lived GHGs become more significant than temporary cooling impacts of displaced SO_2 emissions[35]. Further, the significance of this parameter will decrease as environmental regulations continue to reduce power plant SO_2 emissions to mitigate aerosol formation[47].

A PV deployment mix with a higher share of pSi and CdTe will offer greater CRF benefits as the GHG intensity of manufacturing mSi is 80% and 475% greater than pSi and

CdTe, respectively (MCIchina mono Si , MCIchina poly Si , MCImalayisa CdTe in Table S6 in Appendix B).

Grid GHG intensity and solar insolation at the deployment location have significant influence on CRF impacts. PV deployments will have the maximum CRF benefits when PV panels are deployed in locations with a higher grid GHG footprint and solar insolation which increases the displacement of grid electricity. All scenarios (for different technology mixes, deployment and manufacturing locations) show greater CRF benefits over 10 or 25 year time frames for early deployments when compared to delayed deployments.

Model limitations and uncertainties

Using a SimaPro model to disaggregate the GHG inventory introduces uncertainties in the actual emissions and corresponding CRF calculations. With the availability of a disaggregated PV lifecycle GHG inventory, CRF impacts can be determined as explained in Section 7 of the Appendix B. The model does not incorporate regional climate impacts of SO_2 and NO_x emitted and avoided over the PV lifecycle. We assume constant radiative efficiency values for emissions over ten years and do not include the impact of changing background atmospheric concentrations[31]. We analyzed the change in the CRF value calculated (Figures S6, S7 in Appendix B) when the radiative efficiencies of GHGs is varied within the uncertainty range defined by IPCC. This uncertainty is significant for certain GHGs (e.g. + 116/- 124% for NO_x in Table S19 in Appendix B). The CRF impact in 2017, calculated using IPCC's upper (and lower) radiative efficiency estimate, is greater (and lesser) than the CRF calculated using the base radiative efficiency estimate by 22% (Figure S6 in Appendix B). Also, the CRF payback time decreases and increases by one year and one and a half years for IPCC's upper and lower radiative efficiency estimates, respectively. The net

CRF impacts of PV deployments are most sensitive to uncertainty in radiative efficiency estimates of SO_2 over 10 years and CO_2 over 25 years (Figure S7 and S8 in Appendix B). Over longer time frames, the uncertainties in the radiative efficiency estimates of long lived CO_2 emissions dominate the CRF impacts.

Acknowledgements

This study is primarily supported by the National Science Foundation (NSF) and the Department of Energy (DOE) under NSF CA No.EEC-1041895 and 1140190. Any opinions, findings and conclusions or recommendations expressed in this material are those of the author and do not necessarily reflect those of NSF or DOE. The authors are thankful for the feedback received from colleagues at the Quantum Energy and Sustainable Solar Technologies (QESST) center, Dr. Susan Spierre Clark, members of the Sustainable Energy & Environmental Decision Science (SEEDS) studio at ASU and the anonymous reviewers.

References

1.Masson, G.; Latour, M.; Biancardi, D., Global market outlook for photovoltaics until 2016. *European Photovoltaic Industry Association* **2012**.

2.Green Tech Media,GTM Research: Yingli Gains Crown as Top Producer in a 36 GW Global PV Market. http://www.greentechmedia.com/articles/read/Yingli-Gains-Crown-As-Top-Producer-in-a-36-GW-Global-PV-Market.

3.US Department of Energy, Sunshot Vision Study. **2012**.

4.IEA,*Technology Roadmap: Solar photovoltaic energy*; 2010.

5.US Department of Energy,*2010 Solar Technologies Market Report*; 2011.

6.Drury, E.; Denholm, P.; Margolis, R. M., The solar photovoltaics wedge: pathways for growth and potential carbon mitigation in the US. *Environmental Research Letters* **2009,** *4* (3), 034010.

7.Ravikumar, D.; Chester, M.; Seager, T. P.; Fraser, M. P. In *Photovoltaic Capacity Additions: The Optimal Rate of Deployment with Sensitivity to Time-Based GHG Emissions*, International Symposium on Sustainable Systems and Technologies, 2013.

8.Fthenakis, V.; Kim, H. C., Photovoltaics: Life-cycle analyses. *Solar Energy* **2011,** *85* (8), 1609-1628.

9.ISO, 14040 Environmental management-life cycle assessment-principles and framework. *London: British Standards Institution* **2006**.

10.Hsu, D. D.; O'Donoughue, P.; Fthenakis, V.; Heath, G. A.; Kim, H. C.; Sawyer, P.; Choi, J. K.; Turney, D. E., Life cycle greenhouse gas emissions of crystalline silicon photovoltaic electricity generation. *Journal of Industrial Ecology* **2012,** *16* (s1), S122-S135.

11.Kim, H. C.; Fthenakis, V.; Choi, J. K.; Turney, D. E., Life Cycle Greenhouse Gas Emissions of Thin-film Photovoltaic Electricity Generation. *Journal of Industrial Ecology* **2012,** *16* (s1), S110-S121.

12.Peng, J.; Lu, L.; Yang, H., Review on life cycle assessment of energy payback and greenhouse gas emission of solar photovoltaic systems. *Renewable and Sustainable Energy Reviews* **2013,** *19*, 255-274.

13.Kato, K.; Hibino, T.; Komoto, K.; Ihara, S.; Yamamoto, S.; Fujihara, H., A life-cycle analysis on thin-film CdS/CdTe PV modules. *Solar Energy Materials and Solar Cells* **2001,** *67* (1), 279-287.

14.Alsema, E., Energy pay-back time and CO2 emissions of PV systems. *Progress in photovoltaics: research and applications* **2000,** *8* (1), 17-25.
15.Held, M.; Ilg, R., Update of environmental indicators and energy payback time of CdTe PV systems in Europe. *Progress in photovoltaics: research and applications* **2011,** *19* (5), 614-626.

16.Fthenakis, V. M.; Kim, H. C.; Alsema, E., Emissions from photovoltaic life cycles. *Environmental science & technology* **2008,** *42* (6), 2168-2174.

17.Gutowski, T. G.; Gershwin, S. B.; Bounassisi, T. In *Energy payback for energy systems ensembles during growth*, Sustainable Systems and Technology (ISSST), 2010 IEEE International Symposium on, IEEE: 2010; pp 1-5.

18.Fthenakis, V.; Alsema, E., Photovoltaics energy payback times, greenhouse gas emissions and external costs: 2004–early 2005 status. *Progress in photovoltaics: research and applications* **2006,** *14* (3), 275-280.

19.Pachauri, R.; Reisinger, A. IPCC fourth assessment report (Section 2.2). http://www.ipcc.ch/publications_and_data/ar4/wg1/en/faq-2-1.html.

20.Sathre, R.; Masanet, E., Long-term energy and climate implications of carbon capture and storage deployment strategies in the US coal-fired electricity fleet. *Environmental science & technology* **2012,** *46* (17), 9768-9776.

21.Kendall, A.; Price, L., Incorporating time-corrected life cycle greenhouse gas emissions in vehicle regulations. *Environmental science & technology* **2012,** *46* (5), 2557-2563.

22.Kendall, A.; Chang, B.; Sharpe, B., Accounting for time-dependent effects in biofuel life cycle greenhouse gas emissions calculations. *Environmental science & technology* **2009,** *43* (18), 7142-7147.

23.Kendall, A., Time-adjusted global warming potentials for LCA and carbon footprints. *The International Journal of Life Cycle Assessment* **2012,** *17* (8), 1042-1049.

24.Chang, B.; Kendall, A., Life cycle greenhouse gas assessment of infrastructure construction for California's high-speed rail system. *Transportation Research Part D: Transport and Environment* **2011,** *16* (6), 429-434.

25.Nemet, G. F., Net radiative forcing from widespread deployment of photovoltaics. *Environmental science & technology* **2009,** *43* (6), 2173-2178.

26.FRAUNHOFER *Photovoltaics Report - Fraunhofer institute for solar energy systems*; 2012.

27.Administration, U. E. I. China Energy Analysis. http://www.eia.gov/countries/cab.cfm?fips=CH.

28.Personal Communication with First Solar. 2013.

29.FirstSolar *Life Cycle Carbon Impacts of Utility Scale Photovoltaic Projects*; 2011.

30.Joos, F.; Roth, R.; Fuglestvedt, J.; Peters, G.; Enting, I.; Bloh, W. v.; Brovkin, V.; Burke, E.; Eby, M.; Edwards, N., Carbon dioxide and climate impulse response functions for the computation of greenhouse gas metrics: a multi-model analysis. *Atmospheric Chemistry and Physics Discussions* **2012,** *12* (8), 19799-19869.

31.Stocker, T. F., Dahe, Q., & Plattner, G. K *IPCC Fifth Assessment Report - Climate Change 2013: The Physical Science Basis (Chapter 8 Supplementary Information Section 8.SM.11.3.1)*; 2013.

32.Stocker, T. F., Dahe, Q., & Plattner, G. K, IPCC Fifth Assessment Report - Climate Change 2013: The Physical Science Basis (Chapter 8 Supplementary Information Section 8.SM.11.3.2). **2013**.

33.Pachauri, R.; Reisinger, A. IPCC fourth assessment report (Table 2.14 notes). http://www.ipcc.ch/publications_and_data/ar4/wg1/en/ch2s2-10-2.html.

34.Stocker, T. F., Dahe, Q., & Plattner, G. K, IPCC Fifth Assessment Report - Climate Change 2013: The Physical Science Basis (Chapter 8 Supplementary Information Section 8.SM.11.1). **2013**.

35.Hayhoe, K.; Kheshgi, H. S.; Jain, A. K.; Wuebbles, D. J., Substitution of natural gas for coal: climatic effects of utility sector emissions. *Climatic Change* **2002,** *54* (1-2), 107-139.

36.Shindell, D.; Faluvegi, G., The net climate impact of coal-fired power plant emissions. *Atmospheric Chemistry and Physics* **2010,** *10* (7), 3247-3260.

37.Hobbs, P. V., *Introduction to atmospheric chemistry (Section 8.3)*. Cambridge University Press: 2000.

38.Ehhalt, D.; Prather, M.; Dentener, F.; Derwent, R.; Dlugokencky, E. J.; Holland, E.; Isaksen, I.; Katima, J.; Kirchhoff, V.; Matson, P. *Atmospheric chemistry and greenhouse gases (Section 4.2.3.3)*; Pacific Northwest National Laboratory (PNNL), Richland, WA (US): 2001.

39.Shine, K. P.; Fuglestvedt, J. S.; Hailemariam, K.; Stuber, N., Alternatives to the global warming potential for comparing climate impacts of emissions of greenhouse gases (page297). *Climatic Change* **2005,** *68* (3), 281-302.

40.California Public Utilities Commission,California Solar Initiative. http://www.cpuc.ca.gov/puc/energy/solar/aboutsolar.htm.

41.California Energy Commission,California Solar Photovoltaic Statistics & Data. http://energyalmanac.ca.gov/renewables/solar/pv.html.

42.US Environmental Protection Agency,State Level Emissions data. http://cfpub.epa.gov/egridweb/view_st.cfm.

43.Fthenakis, V.; Kim, H.; Held, M.; Raugei, M.; Krones, J. In *Update of PV energy payback times and life-cycle greenhouse gas emissions*, 24th European Photovoltaic Solar Energy Conference and Exhibition, 2009; pp 21-25.

44.Wild-Scholten, M. J. M. d., Energy payback time and carbon footprint of commercial photovoltaic systems. *Solar Energy Materials and Solar Cells* **2013,** *119*, 296-305.

45.Alsema, E.; WildScholten, M. In *Reduction of environmental impacts in crystalline silicon photovoltaic technology: an analysis of driving forces and opportunities*, Materials Research Society Fall 2007 Symposium, Boston, Cambridge Univ Press: 2007; p 10.

46.Goodrich, A.; Hacke, P.; Wang, Q.; Sopori, B.; Margolis, R.; James, T. L.; Woodhouse, M., A wafer-based monocrystalline silicon photovoltaics road map: Utilizing known technology improvement opportunities for further reductions in manufacturing costs. *Solar Energy Materials and Solar Cells* **2013,** *114*, 110-135.

47.United States Environmental Protection Agency,National Trends in Sulfur Dioxide Levels. http://www.epa.gov/airtrends/sulfur.html.

CHAPTER 3

A COMPELLING CLIMATE RATIONALE FOR CARBON EFFICIENCY IN PHOTOVOLTAICS MANUFACTURE

Introduction

Global photovoltaic (PV) installations are projected to exceed 1 terawatt as policy-makers strive to reduce global warming impacts of electricity production. For example, the SunShot Initiative launched by the United States Department of Energy proposes more than 630 GW of installed PV capacity by 2050 [1] and China is targeting 150 GW of installed capacity by 2020 [2]. The climate benefits of PV are determined by the displacement of non-renewable electricity sources during the use phase of the PV life-cycle, compared to the GHG emissions required to manufacture PV modules. Thus, improvements in the life-cycle GHG emissions of PV can take two forms (1) increasing module efficiencies to generate more electricity during use, and, (2) reducing GHG emissions associated with PV manufacturing processes.

To date, the dominant PV research and development (R&D) strategy is to improve life-cycle environmental and economic performance by increasing PV module efficiency [3][4]. In response to R&D, use phase efficiencies for commercial and emerging PV technologies have increased significantly over the last 3 decades [5], albeit at irregular rates [6]. Nonetheless, the upstream silicon feedstock purification processes necessary to produce high-efficiency modules continue to be energetically expensive, accounting for 40% of the energy consumed in manufacturing crystalline silicon modules [7]. Furthermore, as PV manufacturing increasingly migrates to locations sourced by GHG-intensive electric mixes, the GHG emissions of global PV manufacture may also increase. For example, China's

contribution in the worldwide module production market has increased from 5% in 2005 to 69% in 2014 [8]. Therefore, current PV R&D efforts focusing on module efficiency improvements may forgo opportunities to enhance the climate and environmental performance of PV systems through manufacturing improvements, as well as derive concomitant benefits like reduced toxicity, better human health and safety [9] and decreased reliance on materials with limited availability [10][11][12].

Reducing the climate impact of upstream processes associated with PV technologies requires understanding the technology specific trends that drove historical improvements and using this to prospectively analyze the potential for further incremental improvements as intrinsic material and manufacturing limits are approached. For example, reduction in the silicon wafer thickness which drove past manufacturing improvements, may not be a viable strategy in the future as breakage and cracking rates in wafer manufacturing operations increase below a threshold thickness [13]. Additionally, it is necessary to compare the potential of hypothetical improvements in current PV manufacturing processes to those that may be available by increases to module efficiency that could achieve the same climate benefit. Because manufacturing occurs prior to use, such a comparison must account for temporal dimensions of radiative imbalances in the atmosphere [14][15][16][17][18]. Thus, for an equal mass of GHG emitted and offset, the climate impact of manufacturing emissions is greater than the global warming burdens avoided by the GHGs offset later in the use phase.

Existing PV environmental studies quantify PV manufacturing improvements using the GHG and energy payback time metrics [7][19][20][21] and do not account for this time-sensitive climate impact of GHG emissions [16]. In this way, current practices may underestimate the global warming impacts of manufacturing emissions and cannot inform

the PV R&D policy on the actual magnitude of the climate gains to be achieved by reducing the manufacturing energy and GHG footprint. Although there have been recent reviews and harmonization studies on the GHG intensity of PV electricity[16][17] and research on optimally locating manufacturing and deployment sites for reducing the GHG and energy impacts during rapid growth phases of global PV installations [24][25], these stopped short of analyzing the potential for future gains in time-sensitive climate benefits of improving PV manufacturing. One study presented manufacturing trends over a shorter time frame of 5 years [26], but does not quantify the climate benefit of GHG and energy reduction in PV manufacturing processes using a time sensitive metric.

To address the above knowledge gaps and identify strategies to increase the climate benefit of future PV installations, this research presents an environmental experience curve that plots manufacturing energy trends over the past three decades for the dominant PV technologies (Figure 11). Through analysis of the historical factors that resulted in significant manufacturing improvements, this research quantifies the climate benefit of PV manufacturing improvements using the time sensitive cumulative radiative forcing (CRF) metric [27]. The CRF metric is a time integrated measure of the radiative forcing (in Wm^{-2}) due to an imbalance in the incoming and outgoing infrared radiation in the atmosphere induced by a GHG emission and depends on the mass and timing of the GHG emission [28]. By calculating the net CRF benefit over the PV lifecycle as the difference between the CRF impacts of PV manufacturing emissions and the CRF benefit through the GHGs subsequently offset by PV electricity generation, this research determines the time-sensitive climate benefit of GHG emission reductions through PV manufacturing improvements. Further, this approach demonstrates that the use of conventional GHG metrics underestimate the climate benefits of PV manufacturing improvements (Figure 12). To

accelerate the development of less climate-intensive PV manufacturing pathways for the future, this work identifies CRF hotspots in existing PV manufacturing processes (Figure 14). Finally, the short and long-term climate benefits of addressing manufacturing hotspots are compared to equivalent increases in module efficiency (Figure 13 and Figure 15).

Methods

Data collection, harmonization and generation of PV manufacturing experience curve

To analyze temporal trends in the manufacturing energy embodied in a PV module, data from published PV studies must be harmonized for the primary energy required to produce one peak watt of a PV module (MJ/W_p) [7], [19]–[21], [26], [29]–[101]. Four commercially dominant PV technologies – mono-crystalline silicon (mono-si), multi-crystalline silicon (multi-si), cadmium telluride (CdTe) and amorphous silicon – account for around 99% of the world PV market. A broad review results in 214 data points, covering energy requirements for raw material extraction, purification, fabrication of PV cells, and PV module assembly. However, data from studies with ambiguous system boundary definitions or assumptions for the material and energy used in PV production must be eliminated. For example, [73] does not mention if frames are included in the energy required to manufacture the module and, therefore, this data point is excluded from our analysis. To avoid duplications, data points which were repeated across multiple studies are considered only once as a part of the final analysis. For example, [101] cited values for CdTe originally reported in [54] and only the original value is included to avoid duplication.

After this initial data screening, the system boundaries and assumptions for the remaining data points are examined to facilitate consistent comparisons across data from

across different studies. For crystalline silicon modules, the following processes are included as a part of the system boundary: quartz processing and purification of metallurgical grade silicon, production of solar-grade silicon from metallurgical grade silicon, cell and module manufacturing, and capital equipment. For amorphous silicon and CdTe the system boundary includes cell production, module manufacturing, and capital equipment. If the reported energy values did not include energy requirements for all the steps in the system boundary, we assume values based on contemporary studies published on the same PV technology. For example,[50] published in 1991, does not include the energy requirements for up-stream silicon purification and, therefore, we include the value reported from [69] which was published two years earlier. The data harmonization exercise resulted in the inclusion and rejection of 51 and 163 data points, respectively.

Based on the 51 data points collected and harmonized between 1988 and 2013, we generate a manufacturing experience curve by plotting the primary energy requirements for manufacturing 1 peak watt of the module for each PV technology as a function of time (Figure 11). The complete list of the literature surveyed, PV manufacturing energy data points, justification for the inclusion or rejection of data points, ambiguous boundary conditions and duplications is listed in section S1 of Appendix C.

Cumulative Radiative Forcing (CRF) of PV installations

The CRF impact of one kg of a GHG emission for a time period t is given by

$$CRF_{ghg} = \int_0^t [RE_{ghg} \times f(t)_{ghg}]\, dt \qquad 12$$

In equation 12 RE, the radiative efficiency of the GHG ($Wm^{-2}kg^{-1}$), is the radiative forcing induced per unit mass of the gas in the atmosphere and f(t) represents the fraction of

the initial GHG emission remaining in the atmosphere after a time t. f(t) for CO_2 (equation 13) and CH_4 (equation 14) is given by [27]

$$f(t)_{CO_2} = 0.217+0.259e^{-t/172.9}+0.338e^{-t/18.51}+0.186e^{-t/1.186} \quad 13$$

$$f(t)_{CH_4} = e^{-t/12}d(t) \quad 14$$

RE_{CO2} and RE_{CH4} have the values of $1.75x10^{-15}$ and $1.30x10^{-13}$ $Wm^{-2}kg^{-1}$, respectively [16]. The CRF impact of CH_4 is increased by 40% to include the indirect impacts of CH_4 emissions on stratospheric water vapor and ozone concentrations [102]. The CRF analysis in this paper considers only carbon dioxide and methane as a previous study shows that these two GHGs are responsible for 97% of the CRF impacts over the PV lifecycle [16].

The net global warming benefit (CRF_{benf_t}) in year t of the PV use-phase is given by the difference between the global warming impact avoided (CRF_{avd_t}) when PV electricity displaces fossil-fuel derived electricity, and the global warming impact of PV manufacturing GHG emissions (CRF_{mnf}).

$$CRF_{benf\_t} = CRF_{avd\_t} - CRF_{mnf} \quad 15$$

The avoided global warming impact, CRF_{avd_t} is given by

$$CRF_{avd\_t} = \sum_{x=1}^{t} avd_{ghg\_x} \times \int_{0}^{x} [RE_{ghg} \times f(t)_{ghg}]\, dt] \quad 16$$

where, avd_{ghg_t} is the mass of GHG emissions avoided in year t per m^2 of the PV module and is given by

$$avd_{ghg} = deply\_gGHG\_kWh \times kWp\_m^2 \times irrd \times perf\_rat \times (1-perf\_deg)^t \quad 17$$

where, deply_gGHG_kWh is the GHG intensity of the grid electricity displaced by the PV system at the deployment location (g/kWh), kWp_m^2 is the peak wattage per m^2 of the PV module (kW), irrd is the annual solar irradiation (kWh m^{-2} yr^{-1}) at the deployment location,

perf_rat (performance ratio) is the ratio of the AC to DC power generated by the PV system and perf_deg is the annual performance degradation of the PV module (%).

The global warming impact of PV manufacturing GHG emissions, CRF_{mnf}, is given by

$$CRF_{mnf} = mnf_{ghg} \times \int_0^t [RE_{ghg} \times f(t)_{ghg}]dt \quad 18$$

where mnf_{ghg} ,the PV manufacturing emission, is given by

$$mnf_{ghg} = (fdstk\_kWh + non\_fdstk\_kWh) \times mnf\_gGHG\_kWh \quad 19$$

where fdstk_kWh is the electricity required per m^2 of the module for feedstock purification processes (kWh/ m^2), non_fdstk_kWh is the electricity required for non-feedstock processes per m^2 of the module (kWh/ m^2), and mnf_gGHG_kWh is the GHG intensity of the electricity at the PV manufacturing location (g/kWh).

The electricity required for feedstock purification, fdstk_kWh, is given by

$$fdstk\_kWh = kWh\_Si \times Si\_Wp \times Wp\_m^2 \quad 20$$

where kWh_Si is the electricity required to produce one gram of solar grade silicon (kWh/g) and Si_Wp is the number of grams of silicon required to manufacture 1 peak watt of the PV module (g/Wp).

As 69% of the world's mono and multi-crystalline PV modules are manufactured in China [8], we assume the Chinese grid mix for CO_2 and CH_4 intensity of the electricity used at the PV manufacturing location.

The list of abbreviations, the assumptions for the module efficiency and the module manufacturing energy requirements for mono-Si and multi-Si and the parameters used to

calculate the avoided CRF, PV manufacturing CRF and the CRF pay back time (PBT, equations 12 to 21) are tabulated in section S2 in the Appendix C.

The CRF PBT is calculated as the year in which CRF burdens of PV manufacturing is equal to the CRF benefits of avoided GHG emissions from PV deployments and is given by

$$CRF_{avd\_t} = CRF_{mnf} \quad 21$$

The CRF PBT is a short-term temporal metric as it quantifies the minimum time for the PV system to realize CRF benefits and the long-term CRF benefits are expected to accrue beyond the CRF PBT period over the 25-year lifetime of the PV system (equation 15). This study reports short-term CRF PBT in addition to long-term impacts, as rapid cumulative PV capacity additions can have short-term negative GHG and CRF burdens [16][17].

Difference between the GHG and CRF metric

To demonstrate the difference between the climate impacts as measured by the GHG and CRF metric, we plot the net GHG and CRF benefit equivalence lines for a baseline scenario representing the current state of commercial PV technology and improved PV manufacturing scenarios (Figure 12). The equivalence lines represent combinations of the GHG-intensity of PV manufacturing and the module efficiency that result in the same net GHG and CRF benefit, respectively. The net GHG benefit is the difference between the total GHG avoided over 25-year lifespan of the PV installation (avd_{ghg} in equation 17) and the GHG emission from PV manufacturing (mnf_{ghg} in equation 19). The net CRF benefit is determined from equation 15. Manufacturing improvements are simulated by decreasing the

GHG intensity of PV manufacturing from the current value to a lower value representing less-GHG intensive PV manufacturing practice.

A difference in the climate benefits as measured by the GHG and the time-sensitive CRF metric is demonstrated by a difference in the (1) sensitivity of the CRF and GHG equivalence lines to the GHG intensity of PV manufacturing and (2) magnitude of benefits between the two GHG and CRF benefit equivalence lines corresponding to the baseline and improved manufacturing scenario.

Short-term equivalence between module efficiency increase and manufacturing improvements

To demonstrate the comparability of short-term climate benefits between a reduction in energy and material intensity of PV manufacturing processes and an increase in the module efficiency improvements, we generate an equivalence plot between the two strategies using the CRF payback time (CRF PBT) metric (Figure 13). The plot contains a series of CRF PBT lines which represent combinations of module efficiency and manufacturing material and energy intensity values that result in a particular CRF PBT (calculated using equations 15 to 21). Moving vertically downwards on the plot, from a higher to lower CRF PBT line, represents a decrease in CRF PBT through a reduction in manufacturing material and energy intensity. Moving horizontally towards the right, between the same pair of CRF PBT lines, represents an equivalent decrease in CRF PBT through an increase in module efficiency. This downward or rightward movement between the same pair of lines represents an equivalence in reducing CRF PBT by decreasing the manufacturing energy and material intensity or increasing the module efficiency, respectively.

The CRF benefits of PV are dependent on the GHG intensity of the electricity avoided at the deployment location (deply_gCO_2_kWh in equation 17 and CRF_{avd} in equation 15). For example, PV that displaces hydropower will result in lesser comparative climate benefits than PV that displaces coal combustion. To account for this geographical sensitivity, we will generate the CRF PBT equivalence plot based on grid emissions in Wyoming and California which are assumed to represent upper and lower extremes for grid GHG intensity, respectively (deply_gCO_2_kWh_CA and deply_gCO_2_kWh_WY in Table 1 in Appendix C). The difference in the grid GHG intensity is a result of Wyoming's reliance on coal when compared to California's reliance on renewable sources and natural gas for electricity generation.

Climate hotspots in PV manufacturing

To maximize the long-term CRF benefits of future PV deployments, we identify the PV manufacturing hotspots by modeling the energy and flows for manufacturing 1 m^2 of a multi-silicon module. The parameters in the hotspot analysis include energy for purifying metallurgical grade silicon from quartz, energy and feedstock requirements for solar grade polysilicon production, manufacturing cells, wafers and panel and the GHG intensity of electricity at the manufacturing location. Multi-silicon technology is selected as it is the most widely installed PV technology with a 56% PV market share [8]. To investigate sensitivity, each parameter is increased and decreased by 10% from the baseline value (section S4 in Appendix C) while keeping other parameters fixed. The net change in the CRF benefit is calculated from equation 15. The most significant hotspots result in the highest variation in the CRF benefit resulting from the sensitivity investigation.

Climate benefits of addressing PV manufacturing hotspots

Based on the hotspots identified, this paper explores five scenarios that simulate improvements in PV manufacturing parameters that are assumed to be within the operational control of the PV manufacturer and quantify the corresponding CRF benefits. The scenarios simulate both: 1) incremental energy and material efficiency improvements in incumbent PV manufacturing processes, and 2) replacement of incumbent processes with novel methods that are expected to gradually gain a market share in the future.

Reducing the energy intensity of the Siemens' process ("Siemen's energy reduction"): The Siemen's chemical vapor deposition process produces between 80 to 90% of the world's solar grade silicon [103][104]. Design improvements that can potentially reduce the manufacturing energy requirements of the Siemen's process include : reducing the radiative losses in the reactor by using thermal shields, capture and recycling of waste heat, increasing the reactor capacity, and optimizing deposition conditions and growth rate [104][105][106][107][108]. In this scenario, the energy requirements for the Siemen's process is reduced by 48 kWh/kg (from baseline conditions) by increasing the number of reactor rods, improving the properties of the reactor wall and introducing thermal shields [106].

Alternatives to the Siemen's process ("FBR" and "UMG"): Two scenarios simulate the gradual market adoption of alternate solar-grade silicon production processes through either: (1) the fluidized bed reactor route which has a 6% share of the polysilicon market [103] and is currently the main, commercially significant, alternative to the Siemen's process [104], or (2) the upgraded metallurgical grade (UMG) route which is an emerging process that requires less energy but has no appreciable market share.

The energy estimates for FBR energy requirements range between 30 to75 kWh per kg of polysilicon [104][109][110] and a middle value of 50 kWh/kg is assumed for this scenario (FBR). The energy requirements for UMG range between 18 to 55 kWh per kg of purified polysilicon [104][111][112] and this scenario (UMG) assumes a middle value of 35 kWh/kg.

Reducing kerf losses ("sawing 100μmwire 2μmabrasive" and "sawing diamond coated wire"): Around 50% of the purified and energetically intensive polysilicon is wasted as kerf loss during the wafer sawing process in the PV manufacturing industry [113]. The kerf loss in the incumbent multi-wire slurry sawing (MWSS) process is linearly related to the steel wire thickness and the diameter of the abrasive silicon carbide particles in the slurry [114]. Currently, the standard values for steel wire and abrasive particle diameters for MWSS in the industry are 120-140 μm and 9.3 μm diameter, respectively [113][114]. Strategies to reduce kerf loss include: reducing the abrasive particle and steel wire diameter, replacing MWSS with diamond coated wire sawing, recycling the solar grade silicon kerf from the slurry and novel kerfless sawing processes [115][116][117][118][113]. This paper models improvements in future wafer sawing process through two scenarios:

(1) " sawing 100μmwire 2μmabrasive" where the kerf loss in MWSS is decreased by reducing the steel wire diameter and silicon carbide particle size to 100 μm and 2 μm, respectively, and this decreases kerf loss by 50% [119], and

(2)"sawing diamond coated wire" where diamond coated wire sawing replaces MWSS which reduces kerf loss by 25% [120]. Diamond coated wire sawing has been considered to replace MWSS as it is expected to be increasingly adopted in the PV manufacturing industry, is compatible with the incumbent upstream Siemen's process, does not decrease the cell

efficiency or wafer quality for downstream processes relative to the MWSS process and doesn't require slurry based sawing [121][118][122]. For these reasons, this approach avoids silicon losses in the slurry and the calculation for the reduced silicon feedstock requirement in these two scenarios is explained in section S8 of Appendix C.

Reducing silicon wafer thickness ("SiLayer 100μm"): A reduction in the silicon wafer thickness will reduce energy and material contributions from upstream silicon purification processes that represent around 40% of the silicon PV module's energetic footprint [7]. At present, the silicon wafer is 180 μm thick and this incremental scenario assumes that the thickness can be reduced to 100 μm without a significant loss in efficiency or wafer breakage[123].

Sourcing manufacturing energy from low-carbon sources ("PV elect mnf", "Natural gas elec mnf"): Apart from decreasing the material and energy intensity of processes, the environmental performance of PV manufacturing can be improved by utilizing electricity from less GHG intensive sources. With domestic PV deployments increasing rapidly in China [2] and natural gas expected to meet 10% of China's total energy needs in 2020 [124], this scenario assumes that the electricity requirements for PV manufacturing in China will be sourced from PV installations and combined cycle natural gas systems. The CRF benefits will be calculated based on a GHG intensity of 51 and 450 gCO_2/kWh for electricity sourced from PV installations and combined cycle natural gas systems (section S3 in Appendix C).

Long-term equivalence between module efficiency increase and manufacturing improvements

Addressing the PV manufacturing hotspots results in GHG improvements that could also be achieved by increasing the PV module efficiency, as both the approaches increase the CRF benefits over the PV systems life-span. We demonstrate this equivalence (Figure 15) by calculating the increase in the CRF benefit (using equation 15) for the strategies that address the PV manufacturing hotspots when compared to the baseline scenario. The manufacturing parameters are then fixed at the baseline value (Table 2 in Appendix C) and the increase in baseline value of module efficiency required to achieve the same increase in CRF benefit over the 25-year lifetime of a PV module is determined.

Results and Discussion

PV manufacturing environmental experience curve

The results of the data harmonization of the PV manufacturing energy values reported in the literature from 1987 to 2013 is depicted in Figure 11.

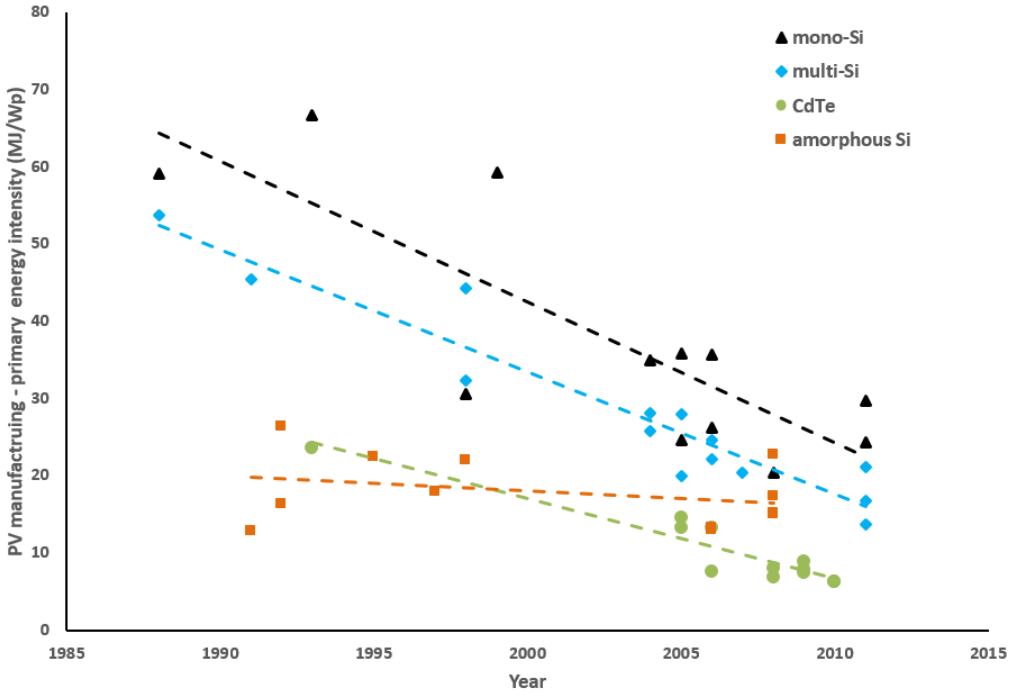

Figure 11 PV manufacturing energy trends
PV manufacturing energy trends for mono-silicon, multi-silicon, CdTe and amorphous silicon. The lines depict a linear fit for the data points.

Data indicates that mono-Si, multi-Si and CdTe have shown a reduction of approximately 40, 32 and 18 MJ/Wp (Figure 11) between 1988 and 2012, 1988 and 2012, and 1993 and 2010, respectively. These historical energetic improvements in manufacturing crystalline PV technologies were driven by the shift in feedstock from electronic grade silicon to solar grade and the reduction in the mass of silicon feedstock per m^2 of the module. The shift in the feedstock to solar grade silicon was driven by a worldwide shortage in the supply of electronic grade silicon [83][104]. The energy intensity of manufacturing solar grade silicon (100-150 kWh/kg [83]), produced via the modified Siemen's process, is lower by 50-100 kWh/kg than electronic grade silicon (200-250 kWh/kg [83][69][50]) due to the lower purity requirement of solar grade silicon. A reduction in wafer thickness in crystalline PV modules from 350 μm in 1999 to 270-300 μm in 2005 resulted in a 25% reduction in embodied energy [26]. For the period from 2004 to 2008, Fthenakis et al have

reported a 40% reduction in manufacturing energy requirements for mono-Si cells from a reduction in cell thickness [101]. For the CdTe PV industry manufacturing energy improvements can be attributed to incremental process improvements, improved production yields and a reduction in CdTe layer thickness [125].

Underestimation of the climate benefit of PV manufacturing improvements as measured by GHG metrics

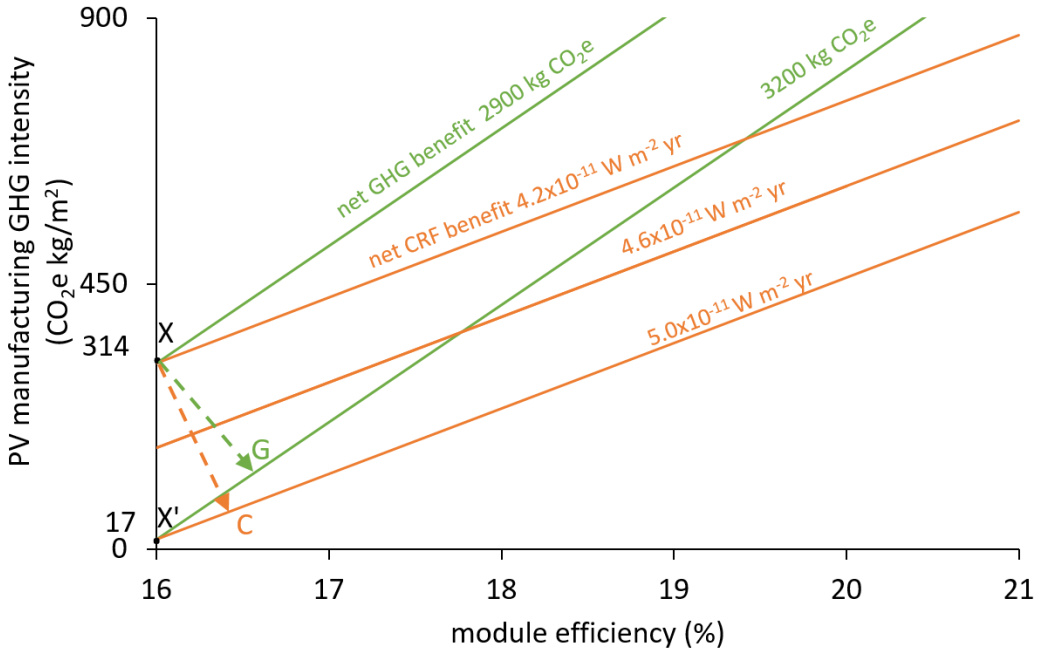

Figure 12 Difference between GHG and CRF impacts
Difference in the climate benefit of improved PV manufacturing as measured by the net GHG and net CRF benefits for multi-Si modules manufactured in China and deployed in California. The green and orange lines represent combinations of PV manufacturing GHG intensity and module efficiency that result in the same net GHG and net CRF benefit over the 25-year lifespan of a module, respectively. A reduction in the GHG intensity of PV manufacturing from 314 to 17 kg CO_2e/m^2 increases the net GHG benefit by only 10% (2900 to 3200 kg CO_2e) when compared to 20% increase in the net CRF benefit ($4.2x10^{-11}$ to $5.0x10^{-11}$ $Wm^{-2}yr$), as CRF is more sensitive to timing of the PV manufacturing GHG emissions.

To demonstrate the difference between the climate impacts as measured by the GHG and CRF metric, we use the current state of technology for commercial multi-silicon

PV modules with a baseline efficiency of 16% and a manufacturing GHG intensity of 314 kg CO_2e/m^2 (point X in Figure 12). This corresponds to a net GHG and CRF benefit of 2900 kg CO_2e and $4.2x10^{-11}$ $Wm^{-2}yr$, respectively, over the 25-year lifespan of the PV module. The upper GHG (green) and CRF (orange) equivalence lines represent combinations of module efficiency and PV manufacturing GHG intensity resulting in the same net GHG and CRF benefit, respectively, as the baseline scenario. Each of the lower green and orange line represents a 10% increase in the net GHG and CRF benefit (versus the upper line), respectively, due to lowered GHG intensity of PV manufacturing. For example, reducing the GHG intensity of PV manufacturing to 17 kg CO_2e/m^2 (X->X' by using low GHG electricity for PV manufacturing) increases the net GHG and CRF benefit to 3200 kg CO_2e and $5.0x10^{-11}$ $Wm^{-2}yr$, respectively. The optimal pathway of achieving the same increase in GHG benefit is to move from X->G along the shortest distance between the two GHG equivalence lines. However, the optimal pathway when accounting for the climate forcing benefit of reducing the GHG intensity of PV manufacturing is X->C.

The difference in the trajectories of X->C and X->G calls attention to the fact that the CRF metric is more sensitive to the GHG intensity of PV manufacturing than the net GHG benefit metric. Improved PV manufacturing (X->X') increases the net GHG benefit by only 10% (2900 to 3200 kg CO_2e) when compared to a 20% increase ($4.2x10^{-11}$ to $5.0x10^{-11}$ $Wm^{-2}yr$) in the net CRF benefit. Similar results are observed for multi-Si and mono- Si modules manufactured in China and deployed in California and Wyoming (section S9 in Appendix C). Manufacturing emissions avoided earlier in the PV lifecycle, by lowering the GHG intensity of PV manufacturing, have an immediate climate benefit (as measured by the CRF metric) than emissions avoided later in the use phase which are dependent on the module efficiency. Therefore, conventional time-insensitive GHG based metrics

underestimate the climate benefit of PV manufacturing improvements. Policies based on GHG gas targets[126] might emphasize investments on module efficiency at the expense of manufacturing improvements. By comparison, policies based on a CRF metric will correspond better with eventual climate impacts [16].

Due to the significant difference in magnitude of impacts measured by the time-insensitive GHG metric and the CRF metric (Figure 12), this paper uses the CRF metric to quantify the short-term and long-term benefits of PV manufacturing improvements in subsequent results.

Short-term climate benefit of improved PV manufacturing

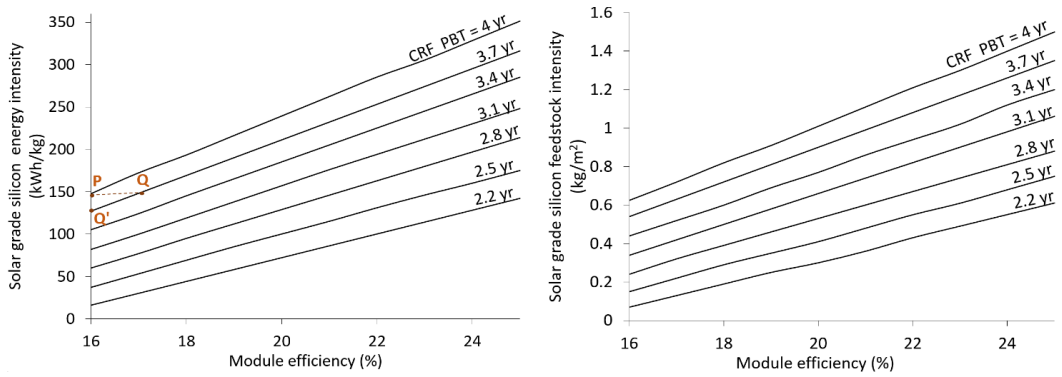

Figure 13 Short-term climate benefit of PV manufacturing imporvements
CRF payback time (PBT) equivalence between module efficiency improvements and reduction in feedstock energy intensity (left plot) and feedstock material intensity (right plot) for multi-Si modules. Moving vertically downwards or moving horizontally towards the right decreases the CRF PBT by reducing feedstock energy intensity (or feedstock material intensity in the right plot) or increasing the module efficiency, respectively.

Figure 13 depicts the equivalence between increasing the module efficiency and decreasing the energy and material intensity of PV manufacturing in reducing the CRF PBT for multi-Si PV modules manufactured in China and deployed in California. The slanted lines represent combinations of solar grade silicon energy intensity (kWh/kg) and module efficiencies that result in a particular CRF payback time (PBT). For example, points Q' (130 kWh/kg, 16%) and Q (150kWh/kg, 17%) represent combinations of feedstock energy intensity and module efficiency for a CRF PBT of 3.7 years. A reduction in feedstock energy intensity and an equivalent increase in module efficiency is represented by moving down vertically and moving right horizontally, respectively, between two CRF PBT lines. As an example, reducing the feedstock energy by 20kWh/kg (P to Q') is equivalent to increasing the module efficiency from 16 to 17%(P to Q) as both these approaches reduce the CRF PBT from 4 to 3.7 years. Similar CRF PBT equivalence plots for multi-silicon PV deployments in Wyoming and mono-Si modules manufactured in China and deployed in

California and Wyoming are shown in section S5 in Appendix C. The results show that, for mono-Si and multi-Si modules, decreasing the feedstock energy intensity by 15-17 kWh/kg or feedstock material intensity by 0.065-0.120 kg/m^2 is equivalent to increasing the module efficiency by 1% when considering the resulting decrease in CRF PBT (Table 3 and Table 4, section S5 in Appendix C).

Climate hotspots in current PV manufacturing processes

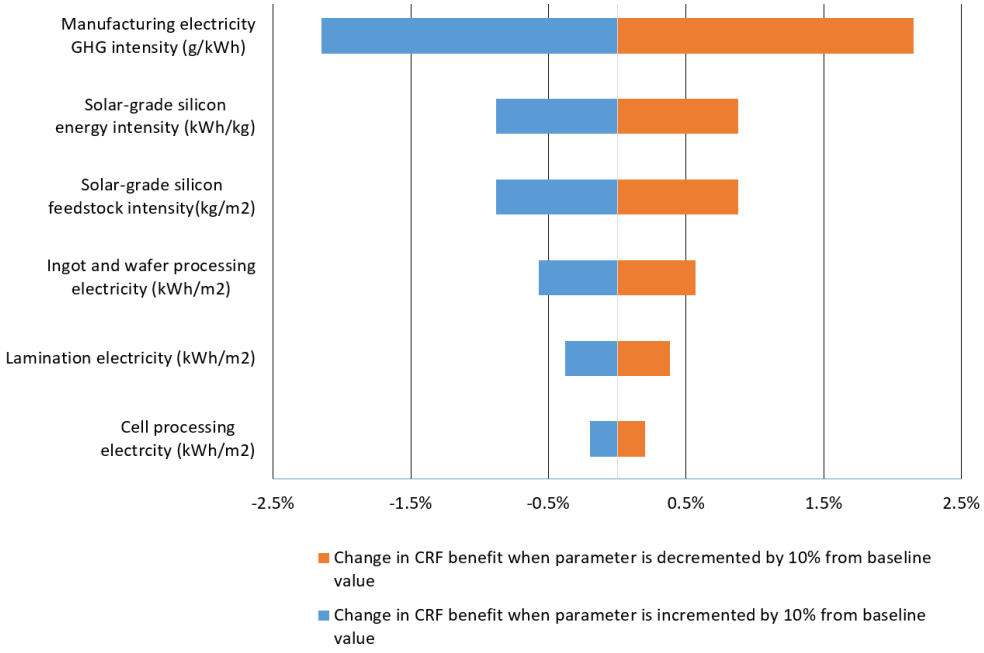

Figure 14 CRF hotspots multi-silicon PV modules
CRF hotspots multi-silicon PV modules manufactured in China and deployed in California. The width of the bars indicate the percentage change in the CRF benefit of the baseline scenario when a parameter in the manufacturing process is incremented and decremented by 10%. The widest bars correspond to the PV manufacturing process parameters with the highest CRF impacts.

The results in Figure 14 demonstrate the percentage change in the baseline CRF benefits (equation 15) when a particular PV manufacturing parameter is increased or decreased by 10% while keeping the other parameters constant at the baseline value (section S4 in Appendix C). The CRF benefit in the baseline scenario is represented by the vertical

0% line. Figure 14 suggests that sourcing electricity from less GHG intensive sources has the most potential to reduce the CRF footprint of a multi-Silicon PV module. The corresponding CRF benefit is evaluated in the "Natural gas elec mnf" and "PV elec mnf" scenario in Figure 15. Furthermore, for material and energy parameters that are within the control of a manufacturer, reducing the polysilicon feedstock per m^2 of the module and energy required to purify this polysilicon are two other significant CRF hotspots in the current crystalline PV manufacturing processes. Similar results are observed for multi-Si and mono- Si modules manufactured in China and deployed in California and Wyoming (section S10 in Appendix C).

Equivalence between manufacturing and module efficiency improvements

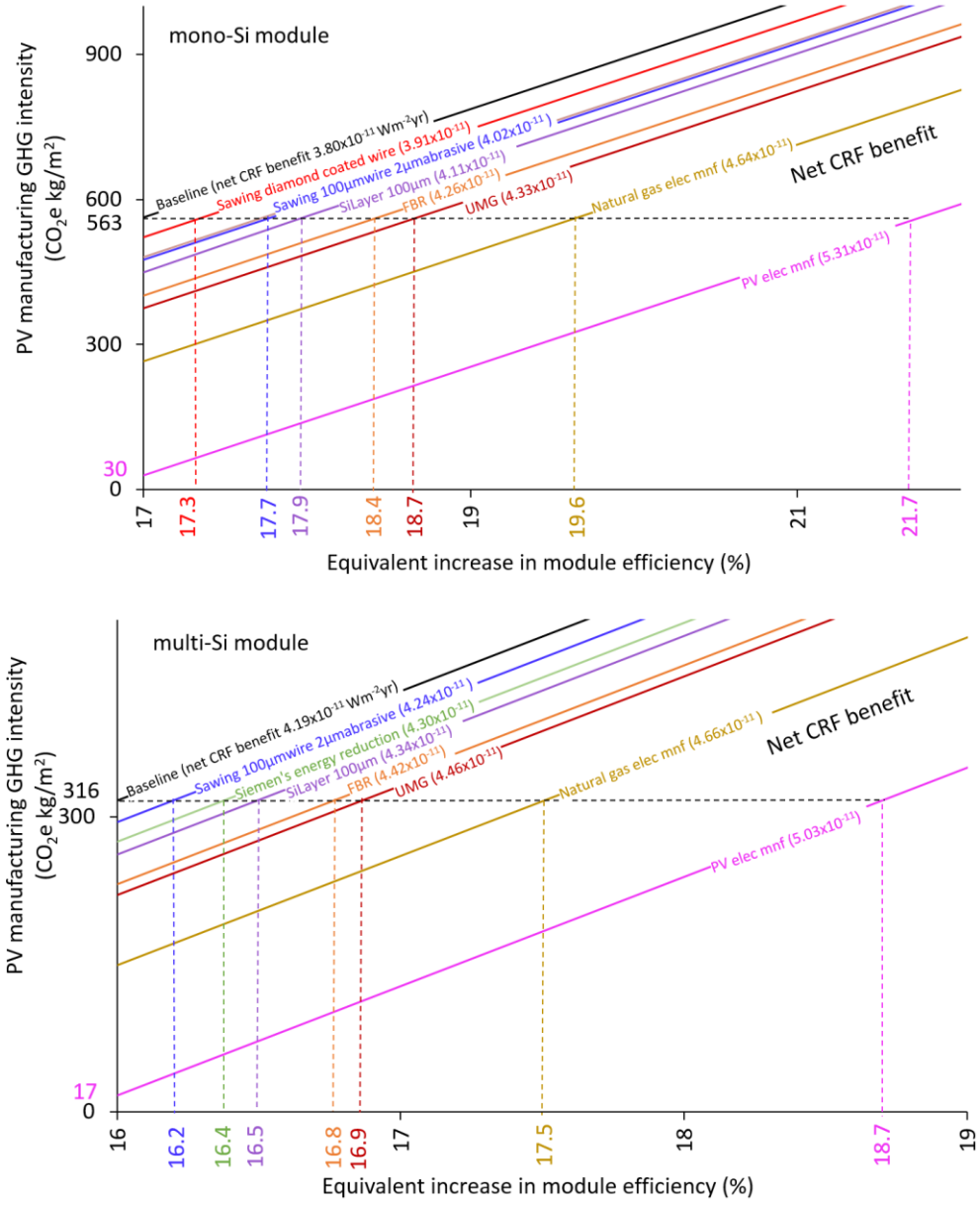

Figure 15 The equivalence between manufacturing and module efficiency imporvements

The equivalence in the CRF benefits between addressing hotspots in PV manufacturing (Figure 14) and an increase in module efficiency for mono-Si (upper plot) and multi-Si (lower plot) modules manufactured in China and deployed in California. The manufacturing improvement that addresses the hotspot is accounted for by lowering the manufacturing GHG intensity (y-axis). The equivalent increase in module efficiency is determined by projecting the difference between the CRF

benefit equivalence lines of the baseline and the improved manufacturing scenario to the x-axis.

In Figure 15, the CRF benefit equivalence line of each scenario represents a combination of PV manufacturing GHG intensity and module efficiency resulting in the same net CRF benefit over the 25-year life span of a PV module. The PV manufacturing improvement in a particular scenario is quantified by starting the net CRF benefit equivalence line from a point that is lower than the baseline scenario on the y-axis. For example, the manufacturing improvement between the baseline and the "PV elec mnf" scenario for mono-Si modules (upper plot) is a reduction in the PV manufacturing GHG intensity from 563 to 30 CO_2e kg/m^2 and the corresponding CRF benefit increases from $3.80x10^{-11}$ to $5.31x10^{-11}$ $Wm^{-2}yr$ (black and pink lines).

As the GHG intensity of electricity used in the PV manufacturing process is the most significant CRF hotspot (Figure 14), using electricity from less GHG-intensive sources like PV at the manufacturing location (PV elec mnf) offers the greatest CRF benefit. While reducing manufacturing emissions receives relatively little PV R&D focus compared to increasing use-phase efficiency, the analysis shows it is equivalent to increasing the mono-Si and multi-Si module efficiency from the baseline value of 17% to 21.7% and 16% to 18.6%, respectively. Alternate solar grade silicon refining processes like UMG and FBR also offer a significant CRF benefit equivalent to increasing the baseline efficiency to a value between 18.4 and 18.7% for mono-Si modules and 16.7 and 16.85% for multi-Si modules.

The incremental strategies of improving existing manufacturing processes by reducing the silicon layer thickness to 100μm, decreasing the energy footprint of the Siemen's process, reducing the wire thickness and abrasive particle diameters in the MWSS process and using the diamond coated wire sawing process yield lower CRF benefits that provide an equivalent module efficiency gain between 17.3% to 17.9% for mono-Si modules

and, 16.2% and 16.5% for multi-Si modules. The equivalent increase in module efficiency from short and long-term CRF benefits of PV manufacturing improvements (as calculated in Figure 13 and Figure 15) is significant as commercial multi-silicon PV modules have shown an average year on year efficiency increase of only 0.25% from 2004 to 2016 (section S7 in Appendix C). It is important to note that the equivalent improvement in module efficiency is independent for each scenario and implementing multiple manufacturing process improvements would yield an additive CRF benefit and a corresponding module efficiency gain. Further, the Siemen's energy reduction, UMG and the FBR scenarios are mutually exclusive as they represent alternate solar-grade silicon refining processes.

For modules manufactured in China and deployed in Wyoming, the CRF benefit of using PV electricity for manufacturing (PV elec mnf) is equivalent to increasing the module efficiency from 17 to 20% for mono-Si and 16 to 17.7% for multi-Si modules, respectively (section S6 in Appendix C). Wyoming has a higher GHG intensity of grid electricity than California and, therefore, the net CRF benefit (CRF_{bnf} in equation 15) is more sensitive to the CRF impact of GHGs avoided per unit of PV electricity generated (CRF_{avd}) than CRF impacts of lowered PV manufacturing emissions (CRF_{mnf} in equation 15). Thus, the equivalent increase in module efficiency is lower in Wyoming than California. The results demonstrate that shifting to low-carbon electricity sources for PV manufacturing in GHG intensive geographies like China results in the greatest increase in the climate benefit of PV systems.

Recent reports show that commercial PV electricity in China will reach grid parity in the next five years [127][128][129] and, therefore, this transition to low-carbon electricity at manufacturing sites is economically favorable and may not impact module prices. Natural gas electricity, with a cost comparable to coal electricity in China [127], is a potential

intermediate source that can enable a transition to a less carbon intensive electricity sources (like PV) in the future for PV manufacturing. The climate benefit from this transition is also significant as this is equivalent to increasing the efficiency of multi-Si and mono-Si modules from 16 to 17.5% and 17 to 19.6%, respectively. Further, sourcing electricity from these low-carbon sources will not impact PV manufacturing costs significantly as energy contributes to less than 2% of the wafer, cell and module costs in China [130].

While the adoption of UMG and FBR for silicon purification also result in significant CRF benefits, a large scale transition to these processes in the near future will be limited by the advantages of the incumbent Siemen's process including market dominance, the economic gains realized from scale and the cumulative technical experience of manufacturers over the last 60 years [103][131]. To increase the economic and environmental attractiveness of FBR refining methods, PV manufacturing research should address loss of silicon yields in trichlorosilane (TCS) based FBR reactors due to reverse reactions [132] and the formation of fine particles and consequent contamination of silicon in silane based FBR reactors [133]. Market adoption of UMG silicon can be accelerated through focused research on reducing light induced degradation due to boron-oxygen clusters [134], improving defect gettering in UMG silicon feedstock [135], increasing efficiencies through novel cell fabrication processes [136], and reducing carbon, boron and phosphorus impurity levels [137][138] to avoid cell performance issues in downstream PV processing activities. In addition to the novel silicon refining processes, pursuing incremental manufacturing improvements, as highlighted by the last four scenarios in Figure 15, will offer significant climate benefits. Further research is required to enable a transition to thinner wafers by analyzing the physical limits and potential issues that downstream PV manufacturing processes will face with incremental improvements like reducing the

thickness of the silicon absorber layer. Past studies have indicated that at values below 100 μm, current manufacturing processes will require changes to avoid an increase in breakage in the robotic handling and transfer steps, manage increased flexibility, lower temperature soldering, kerf-free wafer processes, advanced light trapping methods and improved surface passivation methods to reduce surface recombination [139][140][13][141].

Conclusion

The current practice of using GHG metrics underestimates the climate benefit of addressing PV manufacturing hotspots (Figure 12) that can be realized through PV R&D focusing on upstream PV manufacturing processes. The PV manufacturing experience curve generated by harmonizing PV manufacturing data from the last three decades (Figure 11) shows that reducing the thickness of the silicon wafer and replacing electronic grade silicon with less energetically intensive solar grade silicon historically drove PV manufacturing energy improvements. Further improvements are suggested by a hotspot analysis for the current crystalline silicon module manufacturing processes (Figure 14), which identifies the GHG intensity of the electricity used for manufacturing processes and the material and energy intensity of solar-grade silicon feedstock as the most significant opportunities to improve the climate benefit from PV manufacturing and deployment. Based on the short-term CRF payback time analysis (Figure 13), reducing solar-grade silicon's energy intensity by 15-17 kWh/kg or the solar-grade silicon material intensity by 0.065-0.120 kg/m^2 is equivalent to a 1% increase in the baseline efficiency for mono-Si or multi-Si modules. Furthermore, by using low-carbon electricity sources like PV for manufacturing, the climate benefit realized over the 25-year lifetime of a PV module is equivalent to increasing the efficiency of multi-Si and mono-Si modules from 16% to 18.7% and 17% to 21.7%,

respectively (Figure 15). These potential efficiency gains that can be realized by pursuing PV manufacturing improvements are significant as the commercial crystalline silicon module efficiencies have increased annually by only 0.25% over the last 12 years. Thus, prospective CRF benefits of possible manufacturing improvements demonstrate the climate case for complementing the dominant PV R&D strategy of increasing the module efficiency with manufacturing improvements to increase the climate benefit of a terawatt scale of PV installations.

Acknowledgements

This study is primarily supported by the National Science Foundation (NSF) and the Department of Energy (DOE) under NSF CA No.EEC-1041895 and 1140190. Any opinions, findings and conclusions or recommendations expressed in this material are those of the author and do not necessarily reflect those of NSF or DOE.

References

[1] US DOE, "SunShot Vision Study," 2012. [Online]. Available: http://energy.gov/sites/prod/files/2014/01/f7/47927_executive_summary.pdf. [Accessed: 01-Jan-2016].

[2] PV Magazine, "China aims for 150 GW of solar PV by 2020," 2015. [Online]. Available: http://www.pv-magazine.com/news/details/beitrag/china-aims-for-150-gw-of-solar-pv-by-2020_100021548/#ixzz418vtDQAo. [Accessed: 01-Jan-2016].

[3] European Commission, "Solar Photovoltaics: An overview of European research and policy," p. 14, 2014.

[4] Office of Energy Efficiency and Renewable Energy, "Photovoltaics," 2015. [Online]. Available: http://energy.gov/eere/renewables/solar.

[5] NREL, "Best Research-Cell Efficiencies," 2016. [Online]. Available: http://www.nrel.gov/ncpv/images/efficiency_chart.jpg. [Accessed: 01-Jan-2016].

[6] B. a Wender, R. W. Foley, V. Prado-Lopez, D. Ravikumar, D. a Eisenberg, T. a Hottle, J. Sadowski, W. P. Flanagan, A. Fisher, L. Laurin, M. E. Bates, I. Linkov, T. P. Seager, M. P. Fraser, and D. H. Guston, "Illustrating anticipatory life cycle assessment

for emerging photovoltaic technologies.," *Environ. Sci. Technol.*, vol. 48, no. 18, pp. 10531–8, Sep. 2014.

[7] M. J. De Wild-Scholten, "Energy payback time and carbon footprint of commercial photovoltaic systems," *Sol. Energy Mater. Sol. Cells*, vol. 119, pp. 296–305, 2013.

[8] Fraunhofer Institute For Solar Energy Systems, "Photovoltaics Report," 2015. [Online]. Available: https://www.ise.fraunhofer.de/de/downloads/pdf-files/aktuelles/photovoltaics-report-in-englischer-sprache.pdf. [Accessed: 01-Jan-2016].

[9] V. M. Fthenakis and P. D. Moskowitz, "Photovoltaics: Environmental, Health and Safety Issues and Perspectives," *Prog. Photovoltaics Res. Appl.*, vol. 8, no. 1, pp. 27–38, 2000.

[10] V. Fthenakis, "Sustainability metrics for extending thin-film photovoltaics to terawatt levels," *MRS Bull.*, vol. 37, no. 04, pp. 425–430, 2012.

[11] C. S. Tao, J. Jiang, and M. Tao, "Natural resource limitations to terawatt-scale solar cells," *Sol. Energy Mater. Sol. Cells*, vol. 95, no. 12, pp. 3176–3180, 2011.

[12] D. Ravikumar and D. Malghan, "Material constraints for indigenous production of CdTe PV: Evidence from a Monte Carlo experiment using India's National Solar Mission Benchmarks," *Renew. Sustain. Energy Rev.*, vol. 25, pp. 393–403, Sep. 2013.

[13] S. Pingel, Y. Zemen, O. Frank, T. Geipel, and J. Berghold, "Mechanical stability of solar cells within solar panels," in *Proc. of 24th EUPVSEC*, 2009, pp. 3459–3464.

[14] A. Kendall, "Time-adjusted global warming potentials for LCA and carbon footprints," *Int. J. Life Cycle Assess.*, vol. 17, no. 8, pp. 1042–1049, May 2012.

[15] A. Kendall and L. Price, "Incorporating time-corrected life cycle greenhouse gas emissions in vehicle regulations.," *Environ. Sci. Technol.*, vol. 46, no. 5, pp. 2557–63, Mar. 2012.

[16] D. Ravikumar, T. P. Seager, M. V Chester, and M. P. Fraser, "Intertemporal Cumulative Radiative Forcing Effects of Photovoltaic Deployments," *Environ. Sci. Technol.*, vol. 48, no. 17, pp. 10010–10018, 2014.

[17] D. Ravikumar, "Photovoltaic Capacity Additions: The optimal rate of deployment with sensitivity to time-based GHG emissions," Masters Thesis, Arizona State University, 2013.

[18] D. Ravikumar, M. Chester, T. P. Seager, and M. P. Fraser, "Photovoltaic Capacity Additions: The optimal rate of deployment with sensitivity to time-based GHG emissions," in *International Symposium of Sustainable Systems and Technologies (ISSST)*, 2013.

[19] V. M. Fthenakis, R. Betita, M. Shields, R. Vinje, J. Blunden, M. Shields, R. Betita, and R. Vinje, "Life cycle analysis of high-performance monocrystalline silicon photovoltaic systems: Energy payback times and net energy production value," *27th Eur. Photovolt. Sol. Energy Conf. Exhib.*, pp. 4667–4672, 2012.

[20] V. M. Fthenakis and H. C. Kim, "Photovoltaics: Life-cycle analyses," *Sol. Energy*, vol. 85, no. 8, pp. 1609–1628, Aug. 2011.

[21] E. A. Alsema, "Energy pay-back time and CO2 emissions of PV systems," *Prog. Photovoltaics Res. Appl.*, vol. 8, no. 1, pp. 17–25, Jan. 2000.

[22] H. C. Kim, V. Fthenakis, J. K. Choi, and D. E. Turney, "Life Cycle Greenhouse Gas Emissions of Thin-film Photovoltaic Electricity Generation: Systematic Review and Harmonization," *J. Ind. Ecol.*, vol. 16, no. S1, pp. S110–S121, 2012.

[23] D. D. Hsu, P. O'Donoughue, V. Fthenakis, G. A. Heath, H. C. Kim, P. Sawyer, J. K. Choi, and D. E. Turney, "Life Cycle Greenhouse Gas Emissions of Crystalline Silicon Photovoltaic Electricity Generation: Systematic Review and Harmonization," *J. Ind. Ecol.*, vol. 16, no. S1, pp. S122–S135, 2012.

[24] K. Kawajiri, T. G. Gutowski, and S. B. Gershwin, "Net CO_2 emissions from global photovoltaic development," *RSC Adv.*, vol. 4, no. 102, pp. 58652–58659, 2014.

[25] K. Kawajiri and Y. Genchi, "The right place for the right job in the photovoltaic life cycle.," *Environ. Sci. Technol.*, vol. 46, no. 13, pp. 7415–21, Jul. 2012.

[26] E. A. Alsema, "The real environmental impacts of crystalline silicon PV modules: an analysis based on up-to-date manufacturers data," *20th Eur. Photovolt. Sol. Energy Conf.*, vol. 6, p. 10, 2005.

[27] G. K. Stocker, T.F., Dahe, Q., & Plattner, "IPCC Fifth Assessment Report - Climate Change 2013: The Physical Science Basis (Chapter 8 Supplementary Information Section 8.SM.11.1)," 2013.

[28] P. Forster, V. Ramaswamy, P. Artaxo, T. Berntsen, R. Betts, D. W. Fahey, J. Haywood, J. Lean, D. C. Lowe, G. Myhre, J. Nganga, R. Prinn, G. Raga, M. Schulz, and R. Van Dorland, "Changes in Atmospheric Constituents and in Radiative Forcing.," *Clim. Chang. 2007 Phys. Sci. Basis. Contrib. Work. Gr. I to Fourth Assess. Rep. Intergov. Panel Clim. Chang.*, 2007.

[29] D. Ravikumar, P. Sinha, T. Seager, and M. P. Fraser, "An anticipatory approach to quantify energetics of recycling CdTe photovoltaic systems," *Prog. Photovoltaics Res. Appl.*, 2015.

[30] F. Filippidou, P. N. Botsaris, K. Angelakoglou, and G. Gaidajis, "A comparative analysis of a cdte and a poly-Si photovoltaic module installed in North Eastern Greece," *Appl. Sol. Energy*, vol. 46, no. 3, pp. 182–191, 2010.

[31] M. Ito, K. Kato, K. Komoto, T. Kichimi, and K. Kurokawa, "A comparative study on cost and life-cycle analysis for 100 MW very large-scale PV (VLS-PV) systems in deserts using m-Si, a-Si, CdTe, and CIS modules," *Prog. Photovoltaics Res. Appl.*, vol. 16, no. 1, pp. 17–30, 2008.

[32] M. Ito, M. Kudo, M. Nagura, and K. Kurokawa, "A comparative study on life cycle analysis of 20 different PV modules installed at the Hokuto mega-solar plant," *Prog. Photovoltaics Res. Appl.*, vol. 19, no. 7, pp. 878–886, 2011.

[33] F. Kreith, P. Norton, and D. Brown, "A comparison of CO2 emissions from fossil and solar power plants in the United States," *Energy*, vol. 15, no. 12, pp. 1181–1198, 1990.

[34] G. Bizzarri and G. L. Morini, "A Life Cycle Analysis of roof integrated photovoltaic systems," *Int. J. Environ. Technol. Manag.*, vol. 7, no. 1/2, pp. 134–146, 2007.

[35] K. Kato, T. Hibino, and K. Komoto, "A life-cycle analysis on thin-film CdS/CdTe PV modules," *Sol. Energy Mater. …*, vol. 67, pp. 279–287, 2001.

[36] D. H. W. Li, S. K. H. Chow, and E. W. M. Lee, "An analysis of a medium size grid-connected building integrated photovoltaic (BIPV) system using measured data," *Energy Build.*, vol. 60, pp. 383–387, 2013.

[37] M. Ito, K. Kato, K. Komoto, T. Kichimi, H. Sugihara, and K. Kurokawa, "An analysis of variation of very large-scale PV(VLS-PV) systems in the world deserts," *Photovolt. Energy Conversion, 2003. Proc. 3rd World Conf.*, vol. 3, pp. 2809–2814, 2003.

[38] K. M. Hynes, a. E. Baumann, and R. Hill, "An assessment of the environmental impacts of thin film cadmium telluride modules based on life cycle analysis," *Proc. 1994 IEEE 1st World Conf. Photovolt. Energy Convers. - WCPEC (A Jt. Conf. PVSC, PVSEC PSEC)*, vol. 1, pp. 958–961, 1994.

[39] K. Knapp and T. Jester, "An Empirical Perspective on the Energy Payback Time for Photovoltaic Modules," *Proc. Sol. Conf.*, pp. 641–648, 2000.

[40] G. a Keoleian and G. M. Lewis, "Application of life-cycle energy analysis to photovoltaic module design," *Prog. Photovoltaics*, vol. 5, no. February, pp. 287–300, 1997.

[41] D. Gürzenich and H. J. Wagner, "Cumulative energy demand and cumulative emissions of photovoltaics production in Europe," *Energy*, vol. 29, no. 12–15 SPEC. ISS., pp. 2297–2303, 2004.

[42] P. Zhai and E. D. Williams, "Dynamic hybrid life cycle assessment of energy and carbon of multicrystalline silicon photovoltaic systems.," *Environ. Sci. Technol.*, vol. 44, no. 20, pp. 7950–7955, 2010.

[43] J. L. Bernal-Agustín and R. Dufo-López, "Economical and environmental analysis of grid connected photovoltaic systems in Spain," *Renew. Energy*, vol. 31, no. 8, pp. 1107–1128, 2006.

[44] I. Nawaz and G. N. Tiwari, "Embodied energy analysis of photovoltaic (PV) system based on macro- and micro-level," *Energy Policy*, vol. 34, no. 17, pp. 3144–3152, 2006.

[45] R. Prakash and N. K. Bansal, "Energy analysis of solar photovoltaic module production in India," *Energy Sources*, vol. 17, no. 6, pp. 605–613, 1995.

[46] K. E. Knapp, T. L. Jester, and G. B. Mihaiik, "Energy balances for photovoltaic modules: status and prospects," *Photovolt. Spec. Conf. 2000*, pp. 1450–1455, 2000.

[47] A. Tiwari, P. Barnwal, G. S. Sandhu, and M. S. Sodha, "Energy metrics analysis of hybrid - photovoltaic (PV) modules," *Appl. Energy*, vol. 86, no. 12, pp. 2615–2625, 2009.

[48] K. Kato, A. Murata, and K. Sakuta, "Energy pay□ back time and life□ cycle CO2 emission of residential PV power system with silicon PV module," *Prog. Photovoltaics …*, vol. 115, no. December 1997, pp. 105–115, 1998.

[49] O. Perpiñan, E. Lorenzo, M. A. Castro, and R. Eyras, "Energy payback time of grid connected PV systems: comparison between tracking and fixed systems," *Prog. Photovoltaics Res. Appl.*, vol. 17, no. 2, pp. 137–147, 2009.

[50] W. Palz and H. Zibetta, "Energy Pay-Back Time of Photovoltaic Modules," *Int. J. Sol. Energy*, vol. 10, no. 3–4, pp. 211–216, 1991.

[51] M. de Wild-Scholten, "Energy payback times of PV modules and systems," *Work. Photovoltaik-Modultechnik*, 2009.

[52] E. A. Alsema, "Energy Requirements and CO2 Mitigation Potential of PV Systems," *Present. BNL/NREL Work. "PV Environ. 1998,"* 1998.

[53] E. Alsema, "Energy requirements of thin-film solar cell modules—a review," *Renew. Sustain. Energy Rev.*, 1998.

[54] V. Fthenakis and H. C. Kim, "Energy Use and Greenhouse Gas Emissions in the Life Cycle of CdTe Photovoltaics," *MRS Proc.*, vol. 895, pp. 83–88, 2005.

[55] E. A. Alsema and E. Nieuwlaar, "Energy viability of photovoltaic systems," *Energy Policy*, vol. 28, no. 14, pp. 999–1010, Nov. 2000.

[56] Y. Tripanagnostopoulos, M. Souliotis, R. Battisti, and a. Corrado, "Energy, cost and LCA results of PV and hybrid PV/T solar systems," *Prog. Photovoltaics Res. Appl.*, vol. 13, no. 3, pp. 235–250, 2005.

[57] E. . Alsema, "Environmental Aspects of Solar Cell Modules Summary Report," *Netherlands Agency Energy Environ.*, 1996.

[58] E. Alsema and Mar, "Environmental impacts of crystalline silicon photovoltaic module production," *MRS Proc.*, vol. 895, pp. 0895–G03, 2005.

[59] E. A. Alsema and M. J. De Wild-scholten, "Environmental impacts of crystalline silicon photovoltaic module production," *13th CIRP Int. Conf. Life Cycle Eng.*, 2006.

[60] E. A. Alsema, M. J. de Wild-Scholten, and V. M. Fthenakis, "Environmental impacts of PV electricity generation-a critical comparison of energy supply options," *21st Eur. Photovolt. Sol. Energy Conf.*, vol. 3201, 2006.

[61] G. Phylipsen and E. Alsema, "Environmental life-cycle assessment of multicrystalline silicon solar cell modules (NOVEM Report 95057)," *Netherlands Agency Energy Environ. Hague*, 1995.

[62] L. Lu and H. X. Yang, "Environmental payback time analysis of a roof-mounted building-integrated photovoltaic (BIPV) system in Hong Kong," *Appl. Energy*, vol. 87, no. 12, pp. 3625–3631, 2010.

[63] F. Cucchiella and I. D'Adamo, "Estimation of the energetic and environmental impacts of a roof-mounted building-integrated photovoltaic systems," *Renew. Sustain. Energy Rev.*, vol. 16, no. 7, pp. 5245–5259, 2012.

[64] P. N. Botsaris and F. Filippidou, "Estimation of the Energy Payback Time (EPR) for a PV Module Installed in North Eastern Greece," *Appl. Sol. Energy*, vol. 45, no. 3, pp. 166–175, 2009.

[65] R. Battisti and A. Corrado, "Evaluation of technical improvements of photovoltaic systems through life cycle assessment methodology," *Energy*, vol. 30, no. 7, pp. 952–967, Jun. 2005.

[66] S. A. Pacca, "Global Warming Effect Applied to Electricity Generation Technologies," 2003.

[67] V. M. Fthenakis and H. C. Kim, "Greenhouse-gas emissions from solar electric- and nuclear power: A life-cycle study," *Energy Policy*, vol. 35, no. 4, pp. 2549–2557, 2007.

[68] H. Schaefer and G. Hagedorn, "Hidden energy and correlated environmental characteristics of P.V. power generation," *Renew. Energy*, vol. 2, no. 2, pp. 159–166, 1992.

[69] G. Hagedorn, "Hidden energy in solar cells and photovoltaic power stations," *9th Eur. Photovolt. Sol. Energy Conf.*, pp. 542–545, 1989.

[70] K. E. Knapp and T. L. Jester, "Initial empirical results for the energy payback time of

photovoltaic modules.," *Proc. 16th Eur. PVSEC*, pp. 2053–2056, 2000.

[71] B. Azzopardi and J. Mutale, "Life cycle analysis for future photovoltaic systems using hybrid solar cells," *Renew. Sustain. Energy Rev.*, vol. 14, no. 3, pp. 1130–1134, Apr. 2010.

[72] A. Müller, K. Wambach, and E. Alsema, "Life Cycle Analysis of Solar Module Recycling Process," *Mater. Res. Soc. Symp. Proc.*, vol. 895, 2005.

[73] R. Laleman, J. Albrecht, and J. Dewulf, "Life cycle analysis to estimate the environmental impact of residential photovoltaic systems in regions with a low solar irradiation," *Renew. Sustain. Energy Rev.*, vol. 15, no. 1, pp. 267–271, 2011.

[74] M. Held and R. Ilg, "Life Cycle Assessment (LCA) of CdTe thin film modules and Material Flow Analysis of cadmium within EU27," *23rd Eur. Photovolt. Sol. Energy Conf. (EU PVSEC)*, vol. 10, pp. 2551–2557, 2010.

[75] M. Raugei, S. Bargigli, and S. Ulgiati, "Life cycle assessment and energy pay-back time of advanced photovoltaic modules: CdTe and CIS compared to poly-Si," *Energy*, vol. 32, no. 8, pp. 1310–1318, Aug. 2007.

[76] N. Jungbluth, C. Bauer, R. Dones, and R. Frischknecht, "Life cycle assessment for emerging technologies: Case studies for photovoltaic and wind power," *Int. J. Life Cycle Assess.*, vol. 10, no. 1, pp. 24–34, 2005.

[77] S. A. F. Sherwani, J. A. Usmani, Varun, "Life cycle assessment of 50 kWp grid connected solar photovoltaic (SPV) system in India," *Intern. J. Energy Environ.*, vol. 2, no. 1, pp. 49–56, 2011.

[78] T. Muneer, S. Younes, N. Lambert, and J. Kubie, "Life cycle assessment of a medium-sized photovoltaic facility at a high latitude location," *Proc. Inst. Mech. Eng. Part A J. Power Energy*, vol. 220, no. 6, pp. 517–524, 2006.

[79] H. Kim, K. Cha, V. M. Fthenakis, P. Sinha, and T. Hur, "Life cycle assessment of cadmium telluride photovoltaic (CdTe PV) systems," *Sol. Energy*, vol. 103, pp. 78–88, 2014.

[80] N. Jungbluth, "Life cycle assessment of crystalline photovoltaics in the Swiss ecoinvent database," *Prog. Photovoltaics Res. Appl.*, vol. 13, no. 5, pp. 429–446, Aug. 2005.

[81] A. Stoppato, "Life cycle assessment of photovoltaic electricity generation," *Energy*, vol. 33, no. 2, pp. 224–232, 2008.

[82] R. Dones and R. Frischknecht, "Life Cycle assessment of photovoltaic systems: results of Swiss studies on energy chains," *Prog. Photovoltaics Res. Appl.*, vol. 6, no. 2, pp. 117–125, 1998.

[83] N. Jungbluth, M. Tuchschmid, and M. de Wild-Scholten, "Life Cycle Assessment of Photovoltaics: Update of ecoinvent data v2. 0," *ESU-services Ltd.*, 2008.

[84] S. Pacca, D. Sivaraman, and G. a Keoleian, "Life Cycle Assessment of the 33 kW Photovoltaic System on the Dana Building at the University of Michigan : Thin Film Laminates, Multi-crystalline Modules, and Balance of System Components (Report No. CSS05-09)," *Univ. Michigan*, 2006.

[85] R. García-Valverde, C. Miguel, R. Martínez-Béjar, and A. Urbina, "Life cycle assessment study of a 4.2kWp stand-alone photovoltaic system," *Sol. Energy*, vol. 83, no. 9, pp. 1434–1445, 2009.

[86] R. Kannan, K. C. Leong, R. Osman, H. K. Ho, and C. P. Tso, "Life cycle assessment study of solar PV systems: An example of a 2.7kWp distributed solar PV system in Singapore," *Sol. Energy*, vol. 80, no. 5, pp. 555–563, 2006.

[87] R. Dones, C. Bauer, R. Bolliger, B. Burger, M. Faist Emmenegger, R. Frischknecht, T. Heck, N. Jungbluth, A. Röder, and M. Tuchschmid, "Life Cycle Inventories of Energy Systems: Results for Current Systems in Switzerland and other UCTE Countries," *Ecoinvent Rep. No 5*, 2007.

[88] M. Pehnt, A. Bubenzer, and A. Räuber, "Life Life Cycle Assessment of Photovoltaic Systems –Trying To Fight Deep-Seated Prejudices," in *Photovoltaics guidebook for decision-makers : technological status and potential role in energy economy*, Springer, 2003, pp. 179–213.

[89] M. Ito, K. Komoto, and K. Kurokawa, "Life-cycle analyses of very-large scale PV systems using six types of PV modules," *Curr. Appl. Phys.*, vol. 10, no. 2 SUPPL., pp. S271–S273, 2010.

[90] A. Sumper, M. Robledo-García, R. Villafáfila-Robles, J. Bergas-Jané, and J. Andrés-Peiró, "Life-cycle assessment of a photovoltaic system in Catalonia (Spain)," *Renew. Sustain. Energy Rev.*, vol. 15, no. 8, pp. 3888–3896, 2011.

[91] P. J. Meier, "Life-Cycle Assessment of Electricity Generation Systems and Applications for Climate Change Policy Analysis," *PhD Thesis*, 2002.

[92] A. Meijer, M. a. J. Huijbregts, J. J. Schermer, and L. Reijnders, "Life-cycle assessment of photovoltaic modules: Comparison of mc-Si, InGaP and InGaP/mc-Si solar modules," *Prog. Photovoltaics Res. Appl.*, vol. 11, no. 4, pp. 275–287, Jun. 2003.

[93] P. J. Meier and G. L. Kulcinski, "Life-Cycle Energy Costs and Greenhouse Gas Emissions for Building-Integrated Photovoltaics," *Energy Cent. Wisconsin*, 2002.

[94] J. K. Kaldellis, D. Zafirakis, and E. Kondili, "Optimum autonomous stand-alone

photovoltaic system design on the basis of energy pay-back analysis," *Energy*, vol. 34, no. 9, pp. 1187–1198, 2009.

[95] S. Pacca, D. Sivaraman, and G. a. Keoleian, "Parameters affecting the life cycle performance of PV technologies and systems," *Energy Policy*, vol. 35, no. 6, pp. 3316–3326, 2007.

[96] Alsema and M. J. E. De Wild-Scholten, "Reduction of the environmental impacts in crystalline silicon module manufacturing," *22nd Eur. Photovolt. Sol. Energy Conf.*, pp. 829–836, 2007.

[97] P. Frankl, A. Masini, M. Gamberale, and D. Toccaceli, "Simplified life-cycle analysis of PV systems in buildings: Present situation and future trends," *Prog. Photovoltaics*, vol. 6, no. 2, pp. 137–146, 1998.

[98] T. Williams, J. Guice, and J. Coyle, "Strengthening the Environmental Case for Photovoltaics: A Life-Cycle Analysis," *2006 IEEE 4th World Conf. Photovolt. Energy Conf.*, pp. 2509–2512, 2006.

[99] R. Wilson and A. Young, "The embodied energy payback period of photovoltaic installations applied to buildings in the U.K.," *Build. Environ.*, vol. 31, no. 4, pp. 299–305, 1996.

[100] M. Held and R. Ilg, "Update of environmental indicators and energy payback time of CdTe PV systems in Europe," *Prog. Photovoltaics Res. Appl.*, vol. 19, no. January, pp. 614–626, 2011.

[101] V. M. Fthenakis, H. C. Kim, M. Held, M. Raugei, and J. Krones, "Update of PV energy payback times and life-cycle greenhouse emissions," *24th Eur. Photovolt. Sol. Energy Conf.*, no. September, p. 4412, 2009.

[102] T. F. Stocker, Q. Dahe, and G. K. Plattner, "IPCC Fifth Assessment Report - Climate Change 2013: The Physical Science Basis (Chapter 8, Supplementary Information Section 8.SM.11.3.2)," 2013.

[103] R. Fu, T. L. James, and M. Woodhouse, "Economic measurements of polysilicon for the photovoltaic industry: Market competition and manufacturing competitiveness," *IEEE J. Photovoltaics*, vol. 5, no. 2, pp. 515–524, 2015.

[104] G. Bye and B. Ceccaroli, "Solar grade silicon: Technology status and industrial trends," *Sol. Energy Mater. Sol. Cells*, vol. 130, pp. 634–646, 2014.

[105] G. Del Coso, C. Del Canizo, and A. Luque, "Disclosing the polysilicon deposition proess," in *Proc. 25th European Photovoltaic Solar Energy Conf. and Exhibition, 5th World Conf. on PV Energy Conversion*, 2010, pp. 1216–1219.

[106] G. Del Coso, C. Del Canizo, and A. Luque, "Radiative energy loss in a polysilicon

CVD reactor," *Sol. Energy Mater. Sol. Cells*, vol. 95, no. 4, pp. 1042–1049, 2011.

[107] A. Ramos, J. Valdehita, J. C. Zamorano, and C. del Cañizo, "Thermal Shields for Heat Loss Reduction in Siemens-Type CVD Reactors," *ECS J. Solid State Sci. Technol.*, vol. 5, no. 3, pp. P172–P178, 2016.

[108] J. R. Hamilton and A. C. Rami, "Best in Class Polysilicon Technology," in *ECS Transactions*, 2010, vol. 27, no. 1, pp. 1007–1013.

[109] N. Jungbluth, M. Stucki, F. Karin, R. Frischknecht, and S. Büsser, "Life Cycle Inventories of Photovoltaics," 2012.

[110] M. Tao, *Terawatt Solar Photovoltaics: Roadblocks and Challenges*. 2014.

[111] J. Odden and G. Halvorsen, "Comparison of the energy consumption in different production processes for solar grade silicon," *Silicon Chem. …*, pp. 1–16, 2008.

[112] M. J. de Wild-Scholten, R. Gløkner, J.-O. Odden, G. Halvorsen, and R. Tronstad, "LCA Comparison of the ELKEM Solar Metallurgical Route and Conventional Gas Routes to Solar Silicon," *23rd Eur. Photovolt. Sol. Energy Conf. Exhib.*, no. September, pp. 1225–1229, 2008.

[113] M. Schumann, T. Orellana Peres, and S. Riepe, "The solar cell wafering process," *Photovoltaics Int.*, vol. 5, p. 53, 2009.

[114] A. Masolin, "Fabrication and Characterization of Ultra-Thin Silicon Crystalline Wafers for Photovoltaic Applications using a Stress-Induced Lift-Off Method," 2012.

[115] T. Y. Wang, Y. C. Lin, C. Y. Tai, R. Sivakumar, D. K. Rai, and C. W. Lan, "A novel approach for recycling of kerf loss silicon from cutting slurry waste for solar cell applications," *J. Cryst. Growth*, vol. 310, no. 15, pp. 3403–3406, 2008.

[116] F. Henley, S. Kang, Z. Liu, L. Tian, J. Wang, and Y. L. Chow, "Kerf-free 20-150 μm c-Si wafering for thin PV manufacturing," *24th Eur. Photovolt. Sol. Energy Conf.*, no. September, pp. 886–890, 2009.

[117] F. J. Henley, "Kerf-free wafering: Technology overview and challenges for thin PV manufacturing," in *35th IEEE Photovoltaic Specialists Conference*, 2010, pp. 001184–001192.

[118] J. I. Bye, S. A. Jensen, F. Aalen, C. Rohr, Ø. Nielsen, B. Gäumann, J. Hodsden, and K. Lindemann, "Silicon Slicing with Diamond Wire for Commercial Production of PV Wafers," in *24th European photovoltaic solar energy conference*, 2015, pp. 1269–1272.

[119] M. Schumann, M. Singh, T. O. Pérez, and S. Riepe, "Reaching a kerf loss below 100 μm by optimizing the relation between wire thickness and abrasive size for multi-wire sawing," in *Proceedings of the 24th European Photovoltaic Solar Energy Conference*, 2009, pp.

1222–1227.

[120] D. Kray, M. Schumann, A. Eyer, G. P. Willeke, R. Kubler, J. Beinert, and G. Kleer, "Solar wafer slicing with loose and fixed grains," *Conf. Rec. 2006 IEEE 4th World Conf. Photovolt. Energy Conversion, WCPEC-4*, vol. 1, pp. 948–951, 2007.

[121] A. Bidiville, K. Wasmer, R. Kraft, and C. Ballif, "Diamond Wire-Sawn Silicon Wafers – from the Lab to the Cell Production," in *Proceedings of the 24th EU PV-SEC (No. PV-LAB-CONF-2010-026)*, 2009, no. September, pp. 1400–1405.

[122] J. I. Bye, L. Norheim, B. Holme, O. Nielsen, S. Steinsvik, S. A. Jensen, G. Fragiacomo, and I. Lombardi, "Industrialised Diamond Wire Wafer Slicing for High Efficiency Solar Cells," in *Proceedings of the 26th European photovoltaic solar energy conference*, 2011, pp. 956–960.

[123] M. J. Kerr, P. Campbell, and A. Cuevas, "Lifetime and efficiency limits of crystalline silicon solar cells," in *29th IEEE Photovoltaic Specialists Conference*, 2002, pp. 438–441.

[124] US Energy Information Administration (EIA), "Natural gas serves a small, but growing, portion of China's total energy demand," 2014. [Online]. Available: http://www.eia.gov/todayinenergy/detail.cfm?id=17591.

[125] M. Green, "Learning experience for thin-film solar modules: First Solar, Inc. case study," *Prog. Photovoltaics Res. …*, no. November 2010, pp. 498–500, 2011.

[126] EPA, "FACT SHEET: Clean Power Plan By The Numbers," 2015. [Online]. Available: https://www.epa.gov/cleanpowerplan/fact-sheet-clean-power-plan-numbers.

[127] NREL, "Renewable Electricity: Insights for the Coming Decade (No. NREL/TP-6A50-63604)," 2015.

[128] RenewEconomy, "Solar at grid parity in most of world by 2017," 2015. [Online]. Available: http://solarindustrymag.com/photovoltaic-grid-parity-expected-by-2017-in-us-china.

[129] Solar Industry, "Photovoltaic Grid Parity Expected By 2017 In U.S., China," 2012. [Online]. Available: http://solarindustrymag.com/photovoltaic-grid-parity-expected-by-2017-in-us-china.

[130] A. C. Goodrich, D. M. Powell, T. L. James, M. Woodhouse, and T. Buonassisi, "Assessing the drivers of regional trends in solar photovoltaic manufacturing," *Energy {&} Environ. Sci.*, vol. 6, p. 2811, 2013.

[131] L. Fabry and K. Hesse, "Crystalline Silicon Feedstock Preparation and Analysis," in *Advances in Photovoltaics:Part 1*, 2012, pp. 226–229.

[132] W. O. Filtvedt, A. Holt, P. A. Ramachandran, and M. C. Melaaen, "Chemical vapor deposition of silicon from silane: Review of growth mechanisms and modeling/scaleup of fluidized bed reactors," *Sol. Energy Mater. Sol. Cells*, vol. 107, pp. 188–200, 2012.

[133] J. Li, G. Chen, P. Zhang, W. Wang, and J. Duan, "Technical challenges and progress in fluidized bed chemical vapor deposition of polysilicon," *Chinese J. Chem. Eng.*, vol. 19, no. 5, pp. 747–753, 2011.

[134] K. Petter, Y. Ludwig, R. Bakowskie, M. Hlusiak, S. Diez, and L. Ritz, "Latest results on production of solar cells using umg-Si feedstock," in *25th European Photovoltaic Solar Energy Conference and Exhibition*, 2010, pp. 1624–1627.

[135] K. Peter, R. Kopecek, A. Soiland, and E. Enebakk, "Future potential for SoG-Si feedstock from the metallurgical process route," *Proc. 23rd Eur. Photovolt. Sol. Energy Conf.*, pp. 14–17, 2008.

[136] P. Preis, F. Buchholz, P. Diaz-Perez, J. Glatz-Reichenbach, C. Peter, S. Schmitt, J. Theobald, K. Peter, and A. K. S??iland, "Towards 20 % solar cell efficiency using silicon from metallurgical process route," *Energy Procedia*, vol. 55, pp. 589–595, 2014.

[137] D. Sarti and R. Einhaus, "Silicon feedstock for the multi-crystalline photovoltaic industry," *Sol. Energy Mater. Sol. Cells*, vol. 72, no. 1–4, pp. 27–40, 2002.

[138] S. Pizzini, "Towards solar grade silicon: Challenges and benefits for low cost photovoltaics," *Sol. Energy Mater. Sol. Cells*, vol. 94, no. 9, pp. 1528–1533, 2010.

[139] E. Van Kerschaver, K. Baert, and J. Poortmans, "Challenges in producing photovoltaic modules on thin wafers," *Photovoltaics Int. Technol. Resour. PV Prof.*, no. 4, pp. 64–67, 2009.

[140] X. Brun, "Analysis of Handling Stresses and Breakage of Thin Crystalline Silicon Wafers," 2008.

[141] C. a. Wolden, J. Kurtin, J. B. Baxter, I. Repins, S. E. Shaheen, J. T. Torvik, A. a. Rockett, V. M. Fthenakis, and E. S. Aydil, "Photovoltaic manufacturing: Present status, future prospects, and research needs," *J. Vac. Sci. Technol. A*, vol. 29, p. 030801, 2011.

CHAPTER 4

AN ANTICIPATORY APPROACH TO QUANTIFY ENERGETICS OF RECYCLING CDTE PHOTOVOLTAIC SYSTEMS

This chapter has been accepted for publication in the peer-reviewed *Progress in Photovoltaics: Research and Applications* and appears as accepted. The citation for the article is: Ravikumar, D., Sinha, P., Seager, T. P., & Fraser, M. P. (2016). An anticipatory approach to quantify energetics of recycling CdTe photovoltaic systems. Progress in Photovoltaics: Research and Applications, 24(5),735-746

Introduction

PV is an important technology for transitioning to a low carbon economy as solar energy offers the highest global technical potential for electricity generation among renewable energy sources [1]. To meet growing electricity demands and increase the environmental gains from PV systems, deployment needs to increase from gigawatt (GW) to terawatt (TW) scale. With the PV systems expected to reach EOL after typical operational lifetime of 30 years [2], TW scale deployments necessitate a corresponding increase in the scale of environmentally efficient PV recycling operations to meet existing and potential regulatory requirements [3][4], achieve manufacturer sustainability goals [5][6][7], minimize environmental and human health impacts of managing PV waste [8][9], and address potential material constraints [10][11][12]. The design of environmentally efficient PV recycling processes requires (i) quantifying the net environmental impacts of existing processes that recycle bulk and semiconductor materials in PV module, ES and BOS, (ii) identifying environmental hotspots in the existing recycling process for future improvements, and (iii)

optimally locating PV recycling facilities to minimize the transportation impacts of material flows.

Existing PV recycling operations manage EOL waste through two alternatives - low value recycling (LVR) and high value recycling (HVR) [13]. In LVR, the shredding, sorting and crushing processes are designed to recycle only the bulk materials including glass, aluminum and copper but not the semiconductor layer [13]. LVR will likely require less initial outlay of capital than HVR as recycling infrastructure for the bulk materials captured in LVR are likely already established whereas HVR may require novel processing of the specialized materials such as the semiconductor layer. In the absence of PV-specific treatment standards, LVR is therefore more likely to be adopted if it meets the regulatory requirements of the region in which the PV systems have to be recycled. HVR is preferred by First Solar, a leading PV recycler [14], as it separates the semiconductor material from the glass, prevents the contamination of the glass with semiconductor, ensures recovery of a greater percentage of the total system's mass, reduces abiotic resource depletion [15][16], and removes and contains potentially harmful substances (e.g. compounds of Pb, Cd, Se) that are common in commercial PV technologies.

The net environmental impact of HVR operations is the difference between the environmental burden and benefit of recycling materials from the module, ES and BOS. To the best knowledge of the authors there is no study that provides a comprehensive environmental analysis of recycling the entire PV system. Existing literature (i) assess the environmental performance of recovering materials from either only the module [17][18] [19] (ii) analyze the lifecycle environmental impacts of only the BOS and EOS [20][21], (iii) propose novel process improvements [22][23][24][25][26][27][28][29][30], (iv) present a

break-up of the module recycling energy requirements [31], and (v) analyze optimal plant locations for module recycling to minimize environmental and economic impacts [32][33].

By not including the BOS and ES and analyzing the environmental impacts of recycling only the module, these studies fail to assess the energy and transportation impacts of around 50% of the mass of the PV system (mass of BOS and ES). Moreover, existing PV recycling environmental impact assessments [17][18] are limited to a retrospective analysis of mature recycling processes. Given the temporal lag between manufacturing and installation of PV systems and the processing at EOL, a prospective analysis is necessary to identify environmental improvements for future recycling processes. Further, with large scale commercial recyclers identifying in-situ recycling as a promising strategy to reduce transportation impacts [14], there is a need to evaluate the environmental trade-offs between de-centralized in-situ recycling [34][35] and the existing strategy of transporting and recycling modules at centralized locations.

To address the above knowledge gaps, this paper presents an energy and material flow model (Figure 16) to analyze the energy burden and benefit of collecting, disassembling and recycling an entire CdTe PV system based on First Solar's recycling processes. The analysis is based on CdTe technology as it is the primary technology recycled by First Solar which operates the PV industry's largest commercial recycling plants with a capacity of around 25,000 metric tons (~200MWp) [14] of end of life and prompt scrap modules per year. The model disaggregates energy flows for recycling CdTe PV systems under multiple EOL scenarios and demonstrates the energy benefits of recycling bulk materials from the ES and BOS. Using an energetic hotspot analysis, this paper identifies significant recycling process parameters (Figure 21), which upon improvement; will reduce the energetic performance of future PV recycling processes. Further, through a frontier diagram (Figure

20), we depict the optimal recycling strategy that minimizes recycling energy by choosing between recycling PV systems partially or completely in a de-centralized facility and transporting and recycling the PV system in a centralized facility.

This paper focusses on the energy metric as it enables material flows to be compared with recycling energy based on the energy difference between producing materials from the primary and secondary sources. Energy impacts can be combined with data on the greenhouse gas (GHG) intensity for different primary energy mixes to calculate other environmental impacts like GHG emissions and global warming impact. Further, data is currently unavailable for other environmental metrics for all the CdTe PV recycling steps[18][17] and the model presented in this paper can be extended to quantify other environmental impact categories when this data, normalized to unit mass of the recycled material, is made available.

Methods

Energy and material flows for HVR of CdTe PV systems

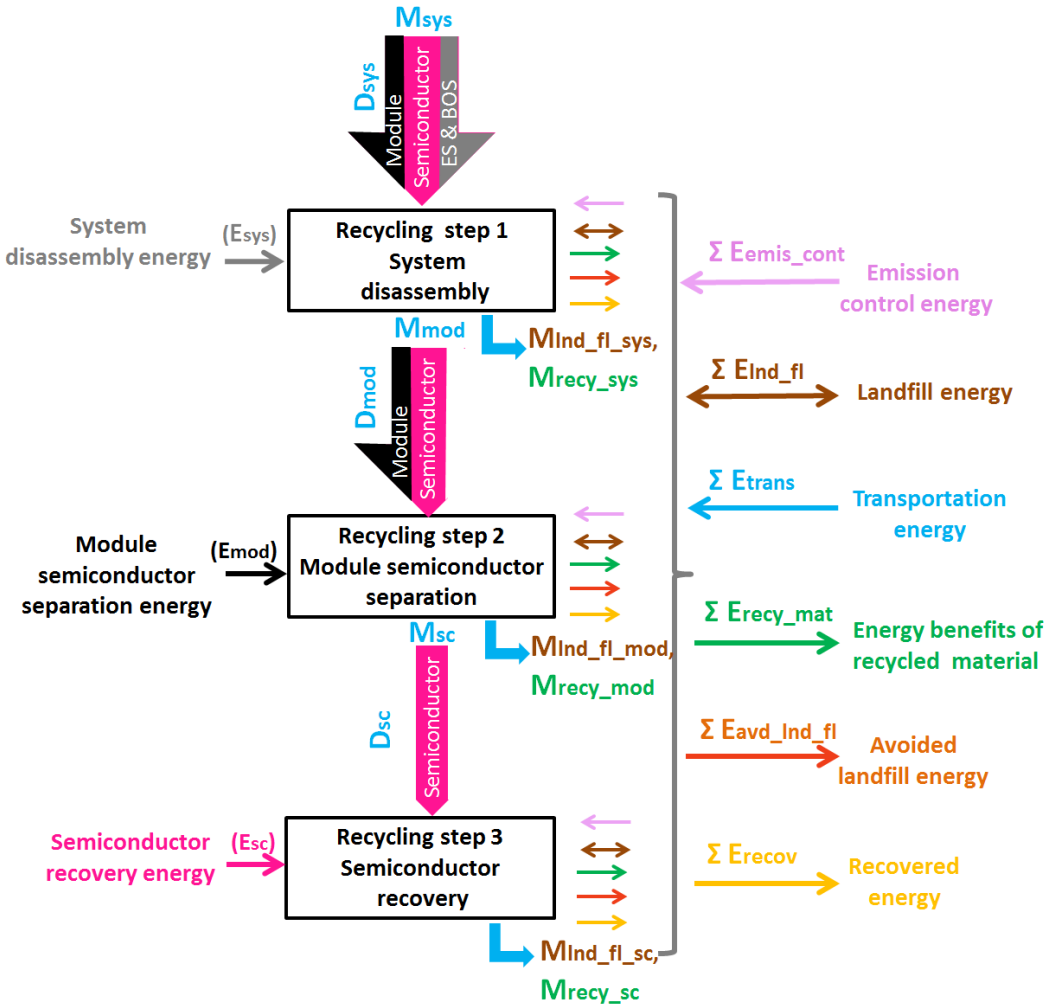

Figure 16 Energy and material flows for CdTe PV recycling.
Energy flows and material flows (thick arrows) for the three steps in HVR of CdTe PV systems. Energy used and saved is depicted by thin arrows directed towards and away from the recycling steps, respectively. Landfill energy is bidirectional as energy is used and recovered from landfill operations and incineration, respectively. Mass, energy and distance are represented by 'M, 'E' and 'D', respectively. Refer equation 1 to 7 for calculations of the energy flow depicted.

The material and energy flows for CdTe PV system recycling (Figure 16) are normalized to 1 m^2 of the module for utility scale deployment conditions and the scope of this analysis includes materials recovered from (i) PV modules (ii) mounting, cabling,

conduits and fittings, and concrete footing and pads for the BOS and (iii) inverters and transformers in the ES. The inventory data for BOS and ES is from [20] and [21] and literature sources for the material and energy flows described below are presented in section 1 in Appendix D.

The PV system (M_{sys} kg) is transported over a distance D_{sys} km from the deployment site to the disassembly site where the module is separated from the BOS and electrical systems in the system disassembly step (step 1). The materials recovered and recycled (M_{recy_sys}) consists of steel, aluminum and copper from the transformers and inverters and PVC, synthetic rubber (EPDM), HDPE and concrete from the remaining BOS. Based on a previous LCA of transformers [36], we assume that 90% of the mass of the transformer, inverter and BOS per m^2 of the PV module is recovered and the remaining is landfilled ($M_{lnd\_fl\_sys}$). The disassembled modules (M_{mod}) are transported over a distance D_{mod} km and subjected to mechanical and chemical processes in semiconductor separation step (step 2) to recover CdTe as unrefined semiconductor material (USM). The processes in step 2 are described in detail in [17]. Glass cullet (M_{recy_mod}) is recovered as a byproduct and is re-used in industrial and commercial applications and the remaining inert glass is landfilled ($M_{lnd\_fl\_mod}$) [18]. The recovery rates for the glass and semiconductor in the module is 90% and 95%, respectively [18]. The USM (M_{sc}) is transported over a distance D_{sc} km to be further refined in step 3. Solar grade cadmium and tellurium [18] is recovered in step 3 (M_{recy_sc}) and the residue from this recovery process is landfilled ($M_{lnd\_fl\_sc}$). Step 3 processes are described in [18] .

E_{emis_cont} is the energy used to control and treat emissions from the three recycling steps to meet regulatory requirements. Landfill energy requirements (E_{lnd_fl}) accounts for the energy required to separate metals and glass at the sorting site and the energy recovered from

incinerating the remaining materials. We assume transportation by a 20 metric ton truck with ultra-low sulfur diesel as fuel and the transportation energy (E_{trans}) is determined from the mass transported and the distance of transport. The materials recovered (M_{recy_sys}, M_{recy_mod}, M_{recy_sc}) from the 3 recycling steps save energy by avoiding landfill operations ($E_{avd\_lnd\_fl}$). The energy benefits of recycled materials (E_{recy_mat}) accounts for recovered materials displacing virgin material production and is the product of the mass of the material recovered and the difference between the energy intensity of producing the material through virgin and recycled routes. E_{recov} is the energy recovered from each of the recycling steps.

Calculating and allocating the net energy impacts of recycling

The total energy used for recycling end-of-life CdTe PV systems (E_{used}) is given by the sum of the energy required for recycling processes (E), controlling emissions (E_{emis_cont}), landfill processes (E_{lnd_fl}), and transportation (E_{trans}) of recovered PV system materials to facilities for the three recycling steps,

$$E_{used}=\left[\sum_{\substack{x=\text{ sys,}\\ \text{mod,sc}}}(E_x+ E_{emis\_cont\_x})\right]+E_{lnd\_fl}+E_{trans} \qquad 22$$

E_x and E_{emis_cont} for the three steps are based on literature reported values (section 1 in Appendix D). E_{lnd_fl} is given by

$$E_{lnd\_fl}=\sum_{\substack{x\ =\ \text{sys}\\ \text{mod,sc}}} M_{lnd\_fl\_x}\times[(E_{trk}\times D_{lnd\_fl}) + E_{lnd\_fl\_op} - E_{lnd\_fl\_inc}] \qquad 23$$

where, M_{lnd_fl} is the material landfilled. The energy intensity of transporting freight by truck (E_{trk}) over a distance (D_{lnd_fl}) to the landfill, energy used for landfill operations ($E_{lnd\_fl\_op}$) and energy recovered from incineration of materials at the landfill ($E_{lnd\_fl\_inc}$) are constant across the three recycling steps.

E_{trans} is determined by the product of the mass of materials (M), material recovery rate in each step (rr), distance over which the materials are transported (D) and E_{trk}

$$E_{trans} = \sum_{\substack{x = sys,\\ mod,sc}} M_x \times rr_x \times D_x \times E_{trk} \qquad 24$$

The total energy saved (E_{saved}) by recycling is given by

$$E_{saved} = E_{recy\_mat} + E_{avd\_lnd\_fl} + \sum_{\substack{x=sys,\\ mod,sc}} E_{recov\_x} \qquad 25$$

where, E_{recy_mat} is the energy benefits of recycling materials, $E_{avd\_lnd\_fl}$ is the energy saved when landfilling is avoided by recycling, and E_{recov} is the energy recovered from each recycling step.

$$E_{recy\_mat} = \left[\sum_{\substack{y=trn\_st,inv\_st,inv\_al,\\ bos\_st,bos\_al,bos\_cu,\\ bos\_pvc,bos\_hdpe,\\ bos\_epdm,bos\_conc}} (M_{recy\_sys\_y} * rr_{sys} * E_{sec\_prod\_bnf\_y}) \right] + \left[M_{recy\_mod\_glass} * rr_{mod} * E_{sec\_prod\_bnf\_glass} \right] + \left[\sum_{y=te,cd} M_{recy\_sc\_y} * rr_{sc} * E_{sec\_prod\_bnf\_y} \right]$$

26

where, M_{recy} is the mass of a particular material recycled (from the PV system, module and semiconductor) and $E_{sec\_prod\_bnf}$ is the energy difference between producing a material from virgin and secondary (recycled) sources (refer section 2 in Appendix D).

$E_{avd\_lnd\_fl}$ is given by

$$E_{avd\_lnd\_fl} = \left[\sum_{\substack{y=trn\_st,inv\_st,inv\_al,\\ bos\_st,bos\_al,bos\_cu,\\ bos\_pvc,bos\_hdpe,\\ bos\_epdm,bos\_conc}} (M_{recy\_sys\_y} * rr_{sys}) + (M_{recy\_mod\_glass} * rr_{mod}) + \sum_{y=te,cd} M_{recy\_sc\_y} * rr_{sc} \right] * \left[(E_{trk} * D_{lnd\_fl}) + E_{lnd\_fl\_op} \right]$$

27

The net energy impact (E_{net_imp}) of CdTe PV recycling is the difference between the energy used for recycling operations (equation 22) and energy saved through recycling (equation 25).

$$E_{net\_imp} = E_{used} - E_{saved} \qquad 28$$

Existing literature propose two main approaches to allocate the benefits of recycling (E_{net_imp}) i) end of life recycling (EOLR) allocation, and ii) recycled content (RC) or cut-off allocation [37][38][39][40]. In EOLR allocation, the benefit of EOL recycling is realized from recycled material displacing primary production. The environmental burdens and benefits of recycling are allocated to the product producing the EOL waste and the product's manufacturing burden is calculated assuming production from 100% primary material with no secondary content. In RC allocation, the benefit of recycled content is realized during manufacturing by calculating the manufacturing burdens for only the primary material used in the product. Also, burdens of recycling are not allocated to the product producing the EOL waste. We select the EOLR approach as it is recommended for recycled metals [40][41] which represent the largest share (by mass) of recovered materials and contribute the most to recycling energy benefits (steel, aluminum, copper and bulk material like glass in Figure 21). Further, by accounting for recycling benefits as the energetic difference between the primary and secondary production routes (Figure 1 in Appendix D), our results will not depend on any subsequent material purification required for secondary application. This subsequent purification is assumed to represent a common energy cost that is incurred irrespective of whether the metal is produced through the primary or secondary route.

Scenario Analysis

After reaching EOL due to breakage, premature failure or completion of 30 years of deployment, the PV system can be managed by (i) landfilling (ii) a combination of landfilling and recycling and (iii) recycling. The mass of the material recycled and landfilled in each of these methods determines the energy used and saved in recycling operations and energy impacts of transportation. For example, if the BOS components are landfilled and not recycled then energy required for landfill operations (equation 23) increases and the energy benefits of recycled materials and avoided landfill benefits decrease (equations 26 and 27). We create 3 groups with a total of 10 scenarios (Figure 17) with increasing magnitude of PV system mass being recycled and quantify the corresponding recycling and transportation energy impacts. For no recycling (NR) scenarios, only landfilling strategy is adopted and no mass is recycled. The medium recycling (MR) and high recycling (HR) scenarios use varying degrees of landfilling and recycling and 10 to 30 kg/m^2 and 30 to 40 kg/m^2 of the PV system mass is recycled, respectively. For example, HR3 belongs to "High recycling" group as 32 kg/m^2 of the module, BOS, inverter and transformer are recycled at the end of life and this is indicated by the green color for all the PV system components.

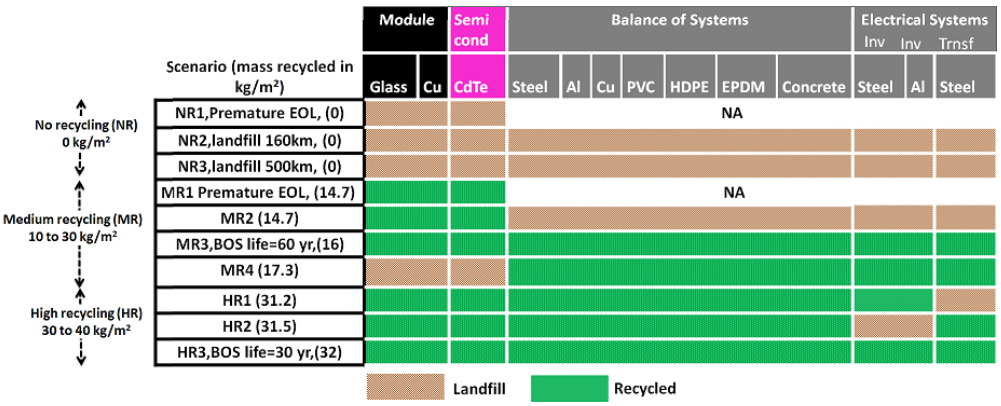

Figure 17 Recycling scenarios for CdTe PV systems.
Recycling scenarios and the corresponding end of life method for handling waste from the module, BOS, inverter and transformer. Recycling and material recovery is not applicable (NA) in NR1 and MR1 as the BOS components continue to be used at the deployment site when there is a premature end of life of modules. Inv-inverter, Trnsf-transformer.

NR1 and MR1 simulate a premature end of life when only the failed or damaged module at the deployment site or manufacturing location is landfilled or recycled, respectively. NR2 and HR3 represent no recycling and maximum recycling when all the PV system components are landfilled and recycled, respectively. NR3 is similar to NR2 and only the landfilling distance is changed from the default 160 km to 500 km identical to calculate the change E_{net_imp} when the transportation energy for landfilling increases. In MR3 we calculate the energy impact of recycling when the BOS life is extended from 30 to 60 years as recommended by the LCA guidelines for PV systems [2].In scenarios MR4, HR1 and HR2 we calculate the change in the net energy benefits when only the module, transformer and inverter are landfilled, respectively. Based on the mass of recycled materials, we calculate the energy impacts for each of the scenarios using equation 28.

Sensitivity analysis for process parameters and allocation method, centralized versus decentralized recycling, and uncertainty analysis

The sensitivity analysis identifies process parameters under the direct control of a recycler that, when improved, will increase the net recycling energy benefit the most for a given scenario. We select HR3 as the base scenario as it includes material flows and the corresponding recycling operations for all the three recycling steps. We increase and decrease each of the recycling process parameters (Figure 21) by 20% and calculate the corresponding variation in the net energy benefit for HR 3 from equation28. 20% is assumed to be a reasonable upper and lower bound as the recycling processes are mature and have been

standardized to handle 25,000 metric tons (~200MWp) [14] of end of life modules per year and will therefore show low variations. The higher the variation in the net energy benefit of recycling the greater is the significance of the process parameter in improving recycling energetics.

To analyze the sensitivity of the net energy impact calculations to the choice of the allocation method, we compare the net energy impact values when the EOLR and RC approach by using the cumulative energy demand (CED) metric.

$$\text{CED} = \text{manufacturing energy} + \text{recycling energy burden} - \text{recycling energy credit} \quad (29)$$

For EOLR, manufacturing energy is calculated assuming 100% virgin content and CED is calculated from equation 29 after accounting for the recycling energy credit and burden. Detailed calculations of recycling energy burden and recycling energy credit and the resulting CED value is explained for scenario H3 in section 7 in Appendix D. For RC, CED depends on only the manufacturing energy which is calculated for virgin raw materials required after accounting for recycled materials from the end of life. The recycling energy credit and burden are not considered for CED calculations.

Thus, using CED values calculated from the RC and EOLR approach, we can compare the impact of choice of allocation approach on the net energy benefits of PV recycling. CED increases when the allocation of recycling energy benefits decreases. Based on this CED metric, the sensitivity of the net energy impact calculations to the choice of the allocation method is calculated for four scenarios for the most and least recycling, BOS only recycling, and module only recycling (HR3, NR2, MR4 and MR2, respectively).

At end of life, some or all of the system material can be recovered in decentralized mobile units at the PV installation site or the system material can be transported to centralized sites where disaggregation and recycling can be accomplished at permanent facilities capturing economies of scale. For example, consider two options for separating and refining the semiconductor from the module. In the first option, the semiconductor material is separated from module glass at a mobile plant and then transported to a centralized facility where it is refined. In the second option, the semiconductor is separated from glass and refined at the mobile plant. The choice between recycling at a centralized or a decentralized location is an energetic trade-off between (i) transporting the EOL PV system components (with mass M_x, x = sys, mod, sc) over a distance (D km) and recycling it in the centralized refining facility and, (ii) recycling the PV system components in the decentralized plants. This energetic trade-off can be expressed as an energy penalty ($E_{penalty}$) that is incurred for recycling PV systems decentrally.

$$E_{penalty} = E_{decentral\_x} - [(D \times E_{trk} \times M_x) + E_x] \quad 30$$

where x = sys, mod, sc and E_x and $E_{decentral\_x}$ are the recycling energy requirements in the centralized and decentralized facilities, respectively. Refer Table 1 in Appendix D for values of M_x, E_x and E_{trk}. D is varied between 0 and 2500 km as transportation distances can vary significantly based on the site of deployment and location at which the recycling infrastructure exists. Decentralized recycling is energetically favorable if $E_{penalty} < 0$ as the energy required to transport and recycle a PV system in a centralized location exceeds that of decentralized recycling. Similarly, centralized recycling is favored when $E_{penalty} > 0$. Since the values of M_x, E_x and E_{trk} are known, $E_{penalty}$ depends only on the values of $E_{decentral\_x}$ and D.

Therefore, we can determine combinations of $E_{decentral\_x}$ and D for which decentralized recycling is favorable ($E_{penalty} < 0$) and centralized recycling is favorable ($E_{penalty} > 0$).

Literature values for the difference in energy between producing materials from the primary and secondary routes vary between an upper and lower bound ($E_{sec\_prod\_bnf}$ values in section 2 in Appendix D). The analysis assumes a point value for $E_{sec\_prod\_bnf}$ (equation 26) for each material based on the average of the upper and lower bounds to calculate net energy impact of recycling (equation28). The uncertainty analysis determines the sensitivity of the net energy impact calculations to the point value of $E_{sec\_prod\_bnf}$ for four dominant materials (by mass) – steel, aluminum, copper and glass (section 8 in Appendix D). The upper and lower bounds of $E_{sec\_prod\_bnf}$ for a particular material is incremented and decremented by 20% while keeping the $E_{sec\_prod\_bnf}$ for the other three materials fixed at the base point value. 10000 uniformly distributed random values of $E_{sec\_prod\_bnf}$ are generated between the newly incremented and decremented bounds for the particular material and the corresponding E_{net_imp} for each of these 10000 iterations is calculated using equation 28. The whisker plot of the 10000 E_{net_imp} values generated for each of the four materials is compared with a corresponding whisker plot for a base scenario (HR3).

Results

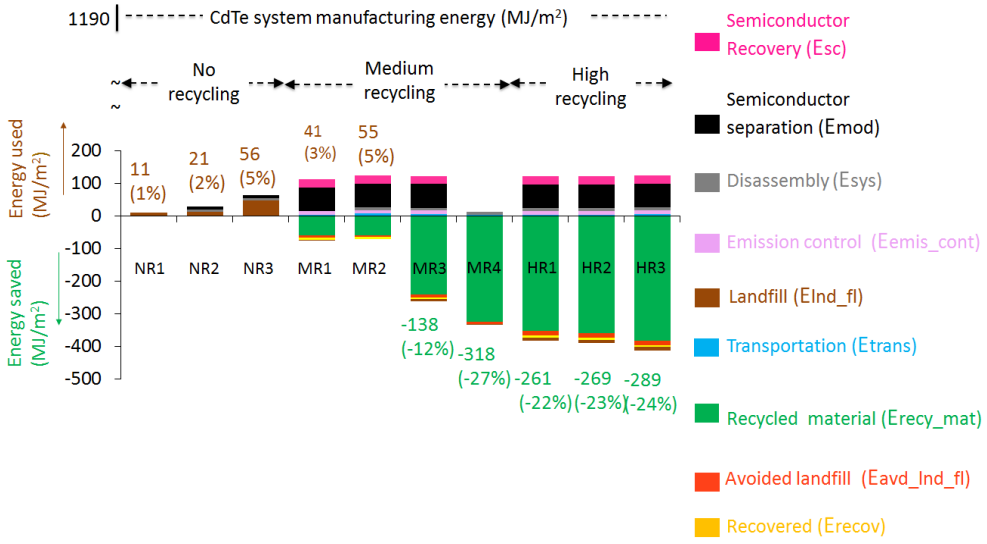

Figure 18 Net energy impact of CdTe PV system recycling.
Net energy impact of CdTe PV system recycling for ten scenarios in Table 2. Negative values in green indicate a net energy benefit (energy saved > energy used) and positive values in brown indicate that energy used exceeds energy saved. The parenthesis contain the net energy impact as a percentage of the current energy intensity of manufacturing CdTe PV systems which is 1190 MJ/m^2 (section 11 in Appendix D).

In Figure 18, the break-up of the energy used in recycling and the energy saved by recovering materials through recycling and avoiding landfill operations are represented above and below the x-axis, respectively. The results demonstrate that the energy benefits of recycling increases with the mass of the PV system recycled. For example in HR3, where the maximum mass is recycled (Table 5), the net energy benefit of recycling is 289 MJ per m^2 of the recycled CdTe system and this is 24% of the current energy intensity of manufacturing 1 m^2 of a CdTe PV system.

Table 5 Material recovery from CdTe PV system recycling.
Results for quantities (in kg per m^2) of PV system materials recovered by scenario. Recycling and material recovery is not applicable (NA) in NR1 and MR1 as the BOS components continue to be used at the deployment site when there is a premature end of life of modules.

	NR 1	NR 2	NR 3	MR 1	MR 2	MR 3	MR 4	HR 1	HR 2	HR 3
Glass	0	0	0	13.2	13.2	6.6	0	13.2	13.2	13.2
Te	0	0	0	0.008	0.008	0.004	0	0.008	0.008	0.008
Cd	0	0	0	0.007	0.007	0.004	0	0.007	0.007	0.007
Steel	NA	0	0	NA	0	5.4	10.8	10.8	10.8	10.8
Aluminum	NA	0	0	NA	0	0.3	0.3	0.3	0.3	0.3
Copper	NA	0	0	NA	0	0.4	0.8	0.8	0.8	0.8
PVC	NA	0	0	NA	0	0.02	0.04	0.04	0.04	0.04
HDPE	NA	0	0	NA	0	0.1	0.3	0.3	0.3	0.3
EPDM	NA	0	0	NA	0	0.03	0.06	0.06	0.06	0.06
Concrete	NA	0	0	NA	0	1.7	3.4	3.4	3.4	3.4
Total	0	0	0	13.2	13.2	14.5	15.6	28.8	28.8	28.8

Table 6 Definitions for all the acronyms

Abbreviation	Definition	Unit
sys	PV system components (Transformer, Inverter	-
mod	PV module	-
sc	Semiconductor material in the PV module(CdTe)	-
E_{used}	Total energy used for recycling end-of-life CdTe PV systems	MJ/ m^2
E	Energy required for recycling processes	MJ/ m^2
E_{emis_cont}	Energy for controlling emissions from recycling operations	MJ/ m^2
E_{lnd_fl}	Total energy for landfill processes	MJ/ m^2
E_{trans}	Energy for transportation	MJ/ m^2
M_{lnd_fl}	Material landfilled	kg/ m^2
D_{lnd_fl}	Distance to the landfill	km
E_{trk}	Energy intensity of transporting freight by truck	MJ/ m^2
$E_{lnd\_fl\_op}$	Energy used for landfill operations	MJ/ m^2
$E_{lnd\_fl\_inc}$	Energy recovered from incineration of materials at the landfill	MJ/ m^2
M	Mass of material (in the PV system, module and semiconductor)	kg/m^2
rr	Material recovery rate in each recycling step	%
D	Distance over which the materials are transported	km
E_{saved}	Total energy saved from recycling	MJ/ m^2

Abbreviation	Definition	Unit
E_{recy_mat}	Energy benefits of recycling materials	MJ/ m^2
$E_{avd\_lnd\_fl}$	Energy saved when landfilling is avoided by recycling	MJ/ m^2
E_{recov}	Energy recovered from each recycling step	MJ/ m^2
M_{recy}	Mass of material recycled (from the PV system, module and semiconductor)	kg/ m^2
$E_{sec\_prod\_bnf}$	Energy difference between producing a material from virgin and secondary (recycled) sources	MJ
E_{net_imp}	Net energy impact of recycling	MJ/ m^2
$E_{penalty}$	Energy penalty that is incurred for recycling PV systems decentrally	MJ/ m^2
$E_{decentral\_x}$	Recycling energy requirements in decentralized facilities	MJ/ m^2

To provide some perspective on the magnitude of the net energy benefit for HR3, it would result in a reduction in the energy payback time (EPBT) of the PV system comparable to increasing CdTe PV module conversion efficiency from its current average value of 14% to over 18.42% (for calculations refer section 4 in Appendix D) , which is the current medium-term (2016-2017) target for this technology [42]. Therefore, PV system recycling has the potential to improve the energy payback time of PV systems [43] as much as improved module conversion efficiency. MR4, HR1, HR2, and HR3 have the highest energy gains and the magnitude of the green bars is largely due to recycling of glass in PV modules and metals in the BOS, inverter and transformer (for a break-up of the energy gains of recycling materials refer section 6 in Appendix D). The advantages of PV system recycling is

further demonstrated in MR2 and NR2 where recycling energy benefits are reduced as the BOS and electrical systems are landfilled and therefore, energy gains from recycling materials is zero.

It should be noted that the magnitude of the net energy impact of scenarios MR2 and NR2 is small (<=5%) relative to the energy intensity of manufacturing CdTe PV systems. In the context of the uncertainty in this analysis (Figure 5 in Appendix D), the net energy impact of these scenarios is approximately neutral. However, these scenarios reflect differing approaches to waste management, with MR2 including PV module recycling and NR2 including PV module landfilling. The finding that these differing scenarios yield similar (approximately neutral) net energy impacts indicates an important limitation of this study, which focuses on the energy demand of PV system recycling. The motivation for PV recycling extends beyond energy demand to management of environmentally sensitive materials and recovery of critical materials. For example, Bergesen et al. [9] indicated that PV system recycling can achieve on the order of 50% reductions in life cycle carcinogenic emissions and metal depletion, and Held [17] indicated that PV module recycling can achieve on the order of 6-8% reductions in acidification, euthrophication, and photochemical ozone creation potential. Therefore, although MR2 and NR2 have similar net energy impacts, the broader life cycle impacts with regards to health and resource depletion should be considered when evaluating PV module recycling (MR2) versus landfilling (NR2). As shown in Table 5, MR2 includes recoverable quantities of 13.2 kg of glass, 0.008 kg of Te, and 0.007 kg of Cd per m^2 of system, whereas NR2 has no material recovery.

In NR3, as distances to landfills increase, the transportation energy of bulk materials in BOS, inverters and transformers to the landfill increases, though it is still relatively small

compared with the energy required to manufacture 1 m^2 of a CdTe PV system. Scenario MR3 demonstrates that recycling benefits decrease by 52% (MR3 versus HR3) when the BOS life is extended to 60 years as energy benefits are alocated equally over two installations of PV modules having a life of 30 years each. MR3 shows the net positive energy impact of recycling all materials in a PV system even after halving energy benefits of recovering BOS materials. For scenarios MR1 and NR1 that simulate premature end-of-life due to unanticipated breakage or failures at the manufacturing or deployment location, net energy impacts are similar and approximately neutral. As discussed above in the comparison of MR2 and NR2, the finding of similar net energy impacts for MR1 and NR1 again indicates a limitation of this study. In addition to considering energy impacts, the broader life cycle impacts with regards to health and resource depletion should be considered when evaluating PV module recycling (MR1) versus landfilling (NR1).

The results depicting sensitivity of net energy benefit calculations to the choice of allocation approach (Figure 19) shows that the CED in the EOLR approach is higher by 0.4 to 10.2% than the RC approach. The EOLR approach decreases the recycling benefits allocated to the PV system. Therefore, the results in Figure 18, calculated using the EOLR approach, represent the lower bound of the net recycling energy benefits allocated to the CdTe PV system.

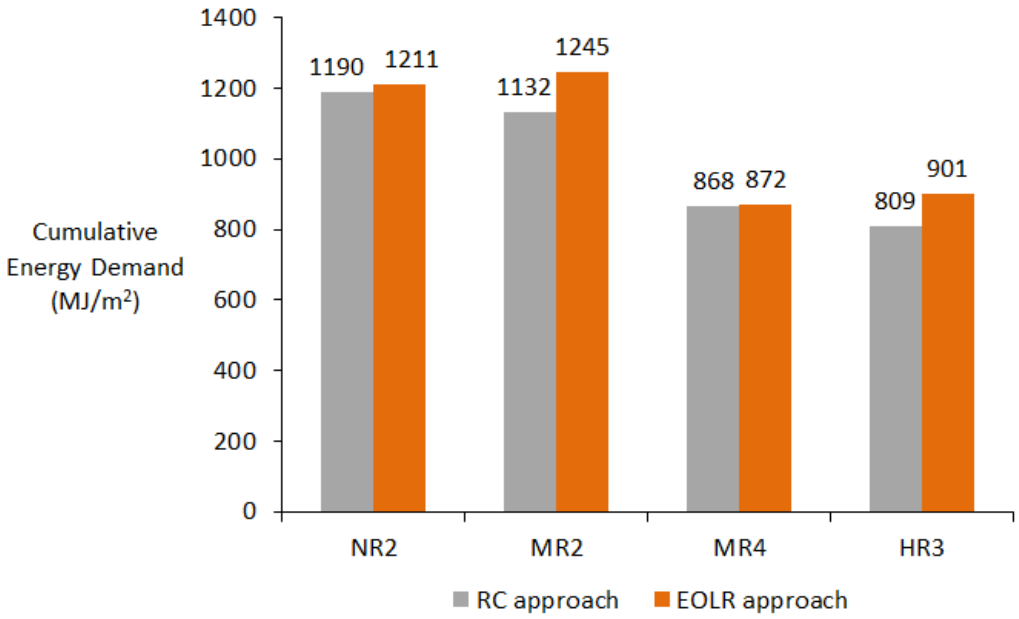

Figure 19. Allocation method and recycling net energy benefit calculations Cumulative energy demands across all four scenarios are comparable, regardless of whether the Recylced Content (RC) or End Of Life Recycling (EOLR) approaches are adopted.

The uncertainty analysis results (section 8 in Appendix D) demonstrate that net energy benefit calculation is most sensitive to $E_{sec\_prod\_bnf}$ values for steel. Even when lowest literature reported value for the recycling energy benefit of steel ($E_{sec\_prod\_bnf\_steel}$) is used, recycling offers a net benefit of around 10% (122 MJ/m^2 in Figure 5 in Appendix D) of the manufacturing energy requirements of 1190 MJ/m^2. The ES and BOS requirement per m^2 of the PV system are modeled based on utility scale deployments (3.5 MW and 550 MW_{AC} plants in [20] and [21]). This requirement may vary for non-utility scale deployments and this will change the magnitude of recycled material and the corresponding recycling energy benefits. The scenario and uncertainty analysis demonstrate that recycling of PV systems (module+ BOS+ES) and the credits earned through recycling these materials can reduce the cumulative energy demand of the PV system by 10 to 24% (137 MJ/m^2 in Figure 5 in

Appendix D and 289 MJ/m^2 for HR3 in Figure 18 in main paper, respectively) on a lifecycle basis.

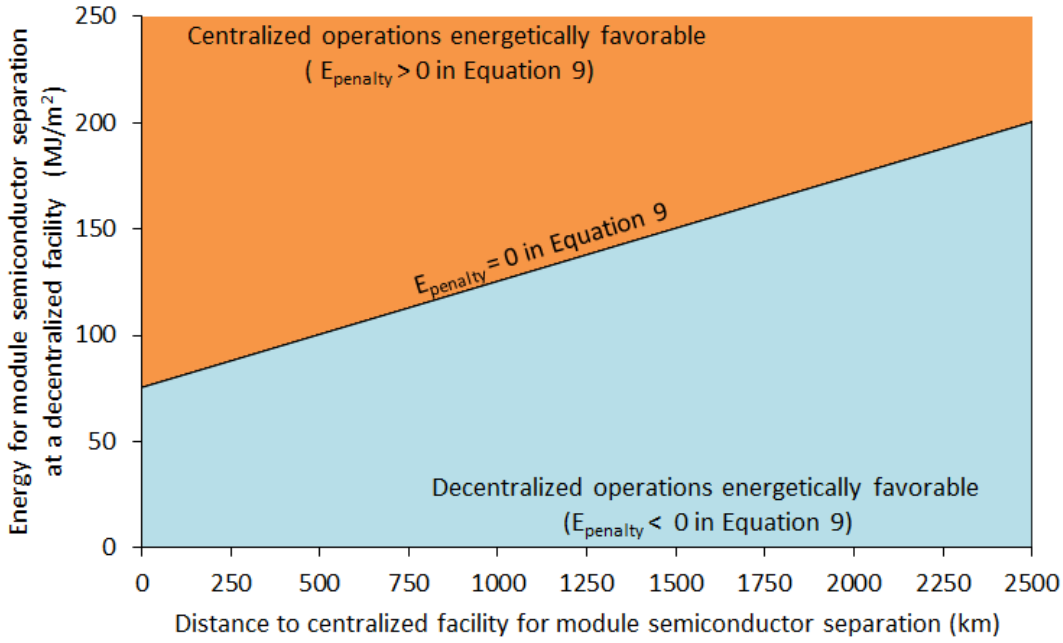

Figure 20 Energy impacts of centralized and decentralized recycling. Frontier diagram depicting two regions where centralized and decentralized facilities are favorable for module semiconductor separation (step 2). Decentralized recycling is favorable in the blue region where the combination of the distance to the centralized facility and the energy required at the decentralized facility result in a negative energy penalty ($E_{penalty}$ < 0 from equation 30). Similarly, centralized recycling is favored in the orange region when energy penalty of decentralization is positive.

Figure 20 in the main paper and Figure 6 in the Appendix D demonstrate that with increasing distances to the centralized location, in-situ mobile based operations that disassemble the system and separate the glass from the module is favored. This is due to the increase in energy impacts when bulk metals and glass in the PV system and module (33.98 and 16.66 kg/m^2) are transported over larger distances. Centralized operations are comparatively favorable for the semiconductor refining step (step 3 in Figure 16) even with increasing distances (figure 7 in Appendix D) because the transportation impact increase

insignificantly as the mass of unrefined USM transported for step 3 is only 0.06 kg/m^2. Decentralized refining of semiconductor will only be favorable if the energy requirements are lower than the current energy footprint in centralized facilities (E_{sc} = 26 MJ/m^2, refer Table 1 in Appendix D).

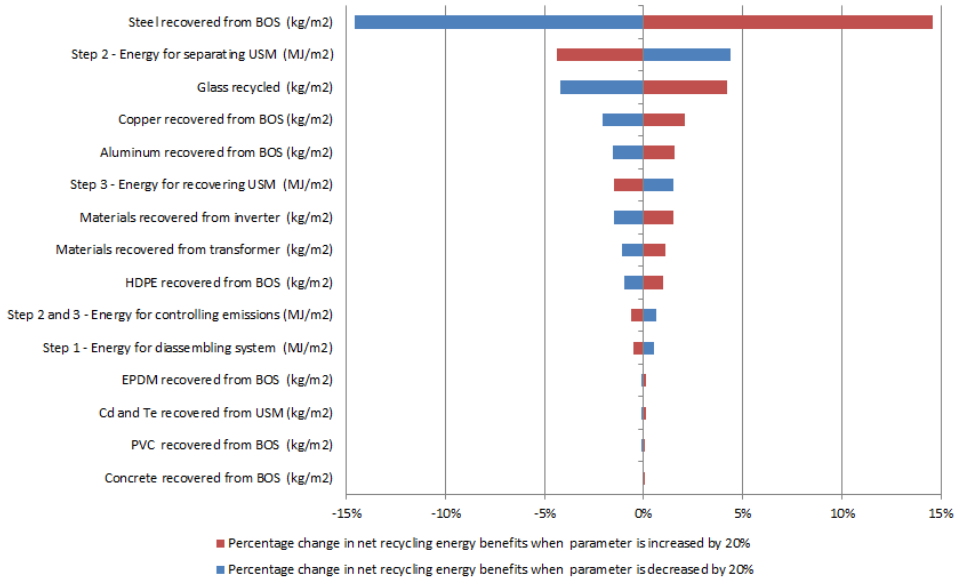

Figure 21 Sensitivity analysis of CdTe PV recycling energetics. Sensitivity of recycling energy benefits to parameters under the control of a recycler. The parameter is incremented and decremented by 20% and the horizontal bars depict the corresponding percentage change in recycling energy benefit from the base value in HR3.

In Figure 21, the net energy benefits of recycling is most sensitive to parameters with the widest bars and a recycler can identify strategies to improve these parameters to maximize the energy benefits of CdTe system recycling. Benefits can be maximized by increasing steel and glass recovery from module, BoS and the electrical components and reducing energy requirements for separation of unrefined semiconductor material (E_{mod} in step 2 in Figure 16).

Conclusion

The net energy impact analysis shows that 24% of the manufacturing energy of a CdTe PV system is recovered under conditions of maximum recycling (scenario HR3 in Figure 18). Further, these recycling energy benefits are conservative estimates as they are calculated using the EOLR allocation approach which lowers benefits by 0.5 to 10.2% when compared to the RC allocation approach (Figure 19). The uncertainty analysis (Figure 5 in Appendix D) shows that the calculation of the net energy impact is most sensitive to the difference between the energy intensity of primary and secondary pathways of steel production ($E_{sec\_prod\_bnf}$). Even when the conservative lower bound of literature reported values for $E_{sec\_prod\_bnf}$ is used, 10% of the manufacturing energy of CdTe PV systems is recovered through recycling (122 MJ/m^2 in Figure 5 in Appendix D).

An energy trade-off analysis between decentralized and centralized PV recycling operations (Figure 20 in main paper and Figure 6 in Appendix D) shows that, with increasing distances, decentralized operations are favorable as they minimize the transportation energy impacts of bulk materials processed during system disassembly and module semiconductor separation (steps 1 and 2 in Figure 16). Decentralization can include (i) leveraging the existing network of metal and glass recyclers and industries where recycled materials can be used as raw materials for subsequent processes [44][45], (ii) locating mobile recycling units for step 2 in the vicinity of disassembly centers or deployment sites. Centralized operations are favorable for semiconductor refining (Figure 6 in Appendix D) as transportation energy requirements for 0.06 kg/m^2 of the USM is negligible. The results on centralization and decentralization for the different PV recycling steps are relevant to current recycling operations where manufacturers are managing EOL PV systems based on recycling warranties at the time of purchase. In the future, these findings can inform policy on incentivizing optimal locations for recycling infrastructure to minimize environmental

impacts when small scale and third party recyclers are expected to play a larger role in PV recycling.

The sensitivity analysis results (Figure 21) reveals that a recycler can significantly increase the recycling energy benefits by reducing the energy footprint of the USM recovery process (E_{mod}). Approximately half of the USM separation energy is spent on removing or delaminating the ethylene vinyl acetate (EVA) encapsulant through mechanical processes [46] and reducing the energy for this process is a potential area for technical improvement [47]. Preliminary lab scale research has identified thermal processing [48], organic solvents[49], ultrasonic radiation [50], micro-emulsions [23] and cryogenic treatment[23]- as alternate methods for EVA removal. With current PV recycling studies using retrospective data based on commercially mature processes, methodological advances in impact assessments are required to analyze the energy and environmental impacts of adopting these alternate lab scale methods at an industrial scale. Recent studies on the anticipatory lifecycle assessment (a-LCA) framework [51][52] contain methodological advances to extrapolate lab scale data to a commercial scale and explore a prospective range of energy and environmental impacts for simulated scenarios. These a-LCA methods can be applied to lab scale data for alternate EVA removal methods and inform recyclers on favorable pathways to minimize the energy impacts and improve the environmental performance of future PV recycling.

Application of a similar approach can identify environmentally improved pathways for recycling c-Si PV systems which account for 90% of the global PV deployments [53] and will be the largest source of PV waste after an operational life span of 30 years. The first two steps of CdTe PV recycling (Figure 16) are applicable to c-Si systems as the components and bulk material contained in the BOS and ES of c-Si and CdTe PV systems are similar

[20][21]. Therefore, decentralization of recycling facilities, as demonstrated for CdTe PV recycling, will reduce transportation impacts of system disassembly and semiconductor module separation for c-Si PV recycling. The proposed a-LCA approach to evaluate environmental impacts of novel encapsulant removal methods for CdTe PV recycling is equally applicable to c-Si systems as EVA is the most common encapsulant in the PV industry [54]. Currently, 90% of the glass is recovered from CdTe PV modules [18] in step 2 and a similar recovery rate for bulk material from end of life c-Si PV systems will result in significant energy benefits. The energetics for the third step of recycling will be significantly different for c-Si systems as the mass of unrefined solar grade silicon (1.4 kg/m^2, refer section 10 in Appendix D) that will be transported for semiconductor recovery is higher than USM in CdTe PV recycling (0.06 kg/m^2, M_{sc} in Table 5 in Appendix D). Further, energy benefits derived from refining silicon in step 3 is higher compared to CdTe refining as the displaced primary process that produces solar grade silicon is energetically the most expensive for c-Si modules [55] and incurs high production losses of 40 -50 % during wafer slicing [56]. The corresponding values for energetic share in the module manufacturing process [31] and semiconductor manufacturing losses [57] are significantly lower for thin film CdTe PV systems.

Acknowledgements

This study is primarily supported by the National Science Foundation (NSF) and the Department of Energy (DOE) under NSF CA No.EEC-1041895 and 1140190. Any opinions, findings and conclusions or recommendations expressed in this material are those of the author and do not necessarily reflect those of NSF or DOE. We are thankful for the timely feedback and continued support from First Solar. The authors acknowledge the

support from B.A.Wender, Valentina Prado Lopez and other colleagues at the Quantum Energy and Sustainable Solar Technologies (QESST) center and members of the AWΣ studio at ASU. We thank the anonymous reviewers for their feedback which has helped improve this paper.

References

[1] O. Edenhofer, R. Pichs-Madruga, Y. Sokona, K. Seyboth, P. Matschoss, S. Kadner, T. Zwickel, P. Eickemeier, G. Hansen, S. Schlömer, and C. von Stechow, *IPCC, 2011: Summary for Policymakers. In: IPCC Special Report on Renewable Energy Sources and Climate Change Mitigation*. 2011.

[2] E. Alsema, D. Fraile, R. Frischknecht, V. Fthenakis, M. Held, H. . Kim, W. Pölz, M. Raugei, and M. de Wild Scholten, "Methodology guidelines on life cycle assessment of photovoltaic electricity," *IEA PVPS Rep.*, 2011.

[3] European Union, "Article 2(1)(a) in Directive 2012/19/EU of the European Parliament and of the Council on waste electrical and electronic equipment (WEEE)," 2012. [Online]. Available: http://eur-lex.europa.eu/LexUriServ/LexUriServ.do?uri=OJ:L:2012:197:FULL:EN:PDF.

[4] "Article 11.6, SB 1020 (California Photovoltaic Panel Collection and Recycling Act of 2014)," 2014. [Online]. Available: http://www.leginfo.ca.gov/pub/13-14/bill/sen/sb_1001-1050/sb_1020_bill_20140214_introduced.html.

[5] First Solar, "Sustainability Metrics," 2014. [Online]. Available: http://www.firstsolar.com/en/about-us/corporate-responsibility/sustainability-metrics.

[6] Trina Solar, "Sustainability," 2014. [Online]. Available: http://www.trinasolar.com/us/about-us/Sustainability.html.

[7] Yingli Solar, "Corporate Sustainability Report," 2013. [Online]. Available: http://www.yinglisolar.com/us/about/sustainability/.

[8] M. Raugei, M. Isasa, and P. F. Palmer, "Potential Cd emissions from end-of-life CdTe PV," *Int. J. Life Cycle Assess.*, vol. 17, no. 2, pp. 192–198, 2012.

[9] J. D. Bergesen, G. A. Heath, T. Gibon, and S. Suh, "Thin-film photovoltaic power generation offers decreasing greenhouse gas emissions and increasing environmental co-benefits in the long term.," *Environ. Sci. Technol.*, vol. 48, no. 16, pp. 9834–43, Aug. 2014.

[10] M. Marwede and A. Reller, "Future recycling flows of tellurium from cadmium telluride photovoltaic waste," *Resour. Conserv. Recycl.*, 2012.

[11] M. Redlinger, R. Eggert, and M. Woodhouse, "Evaluating the availability of gallium, indium, and tellurium from recycled photovoltaic modules," *Sol. Energy Mater. Sol. Cells*, vol. 138, pp. 58–71, 2015.

[12] V. Fthenakis, "Sustainability of photovoltaics: The case for thin-film solar cells," *Renew. Sustain. Energy Rev.*, vol. 13, no. 9, pp. 2746–2750, Dec. 2009.

[13] Bifa environmental Institute, "Eco-efficiency Analysis of Photovoltaic Modules," 2013.

[14] First Solar, "PV Recycling Policies and Technology," *IEA PVPS*, 2014.

[15] P. Sinha, M. J. de Wild-Scholten, Y. Matsuno, K. Brutsaert, and I. Soga, "Environmental benefits of a megasolar CdTe PV project in Japan," in *6th World Conference on Photovoltaic Energy Conversion*, 2014.

[16] P. Sinha, M. J. de Wild-Scholten, and L. Luckhurst, "Environmental Benefits of Solar Photovoltaics in South Africa," in *1st Africa Photovoltaic Solar Energy Conference Proceedings*, 2014.

[17] M. Held, "Life cycle assessment of CdTe module recycling," in *24th EU PVSEC Conference*, 2009, pp. 2370 – 2375.

[18] P. Sinha, M. Cossette, and J.-F. Menard, "End-of-life CdTe recycling with semiconductor refining," in *27th EU PVSEC*, 2012, pp. 24–28.

[19] A. Müller, K. Wambach, and E. Alsema, "Life Cycle Analysis of Solar Module Recycling Process," *Mater. Res. Soc. Symp. Proc.*, vol. 895, pp. 1–6, 2006.

[20] J. E. Mason, V. M. Fthenakis, T. Hansen, and H. C. Kim, "Energy payback and life-cycle CO2 emissions of the BOS in an optimized 3·5 MW PV installation," *Prog. Photovoltaics Res. Appl.*, vol. 14, no. 2, pp. 179–190, Mar. 2006.

[21] P. Sinha and M. de Wild-Scholten, "Life Cycle Assessment of Utility-Scale CdTe PV Balance of Systems," in *27th European Photovoltaic Solar Energy Conference*, 2012, pp. 4657 – 4660.

[22] W. Berger, F.-G. Simon, K. Weimann, and E. A. Alsema, "A novel approach for the recycling of thin film photovoltaic modules," *Resour. Conserv. Recycl.*, vol. 54, no. 10, pp. 711–718, Aug. 2010.

[23] M. Marwede, W. Berger, M. Schlummer, A. Mäurer, and A. Reller, "Recycling paths for thin-film chalcogenide photovoltaic waste – Current feasible processes," *Renew. Energy*, vol. 55, pp. 220–229, Jul. 2013.

[24] G. Granata, F. Pagnanelli, E. Moscardini, T. Havlik, and L. Toro, "Recycling of photovoltaic panels by physical operations," *Sol. Energy Mater. Sol. Cells*, vol. 123, pp. 239–248, Apr. 2014.

[25] G. Giacchetta, M. Leporini, and B. Marchetti, "Evaluation of the environmental benefits of new high value process for the management of the end of life of thin film photovoltaic modules," *J. Clean. Prod.*, vol. 51, pp. 214–224, Jul. 2013.

[26] J. B. Manuel Diequez Campo, Dieter Bonnet, Rainer Gegenwart, "Process for recycling CdTe/Cds thin film solar cell modules," US 6572782 B22003.

[27] P. Taylor and M. DeFilippo, "Process to recycle end of life CDTE modules and manufacturing scrap," US 8821711 B22014.

[28] V. Fthenakis and W. Wang, "extraction; leaching; cation exchange resins; for recycling photovoltaic devices," US 7731920 B22010.

[29] S. Kang, S. Yoo, J. Lee, B. Boo, and H. Ryu, "Experimental investigations for recycling of silicon and glass from waste photovoltaic modules," *Renew. Energy*, vol. 47, pp. 152–159, Nov. 2012.

[30] E. Klugmann-Radziemska and P. Ostrowski, "Chemical treatment of crystalline silicon solar cells as a method of recovering pure silicon from photovoltaic modules," *Renew. Energy*, vol. 35, no. 8, pp. 1751–1759, Aug. 2010.

[31] M. Held and R. Ilg, "Update of environmental indicators and energy payback time of CdTe PV systems in Europe," *Prog. Photovoltaics Res. Appl.*, vol. 19, no. January, pp. 614–626, 2011.

[32] J. K. Choi and V. Fthenakis, "Design and optimization of photovoltaics recycling infrastructure.," *Environ. Sci. Technol.*, vol. 44, no. 22, pp. 8678–83, Nov. 2010.

[33] J. K. Choi and V. Fthenakis, "Crystalline silicon photovoltaic recycling planning: Macro and micro perspectives," *J. Clean. Prod.*, vol. 66, pp. 443–449, 2014.

[34] V. Fthenakis, "End-of-life management and recycling of PV modules," *Energy Policy*, vol. 28, no. 2000, pp. 1051–1058, 2000.

[35] European Commission, "Photovoltaic panels Mobile Recycling Device (PV-MOREDE)," 2014. [Online]. Available: http://ec.europa.eu/environment/eco-innovation/projects/en/projects/pv-morede.

[36] R. S. Jorge, T. R. Hawkins, and E. G. Hertwich, "Life cycle assessment of electricity transmission and distribution—part 2: transformers and substation equipment," *Int. J. Life Cycle Assess.*, vol. 17, no. 2, pp. 184–191, Sep. 2011.

[37] R. Frischknecht, "LCI modelling approaches applied on recycling of materials in view of environmental sustainability, risk perception and eco-efficiency," *Int. J. Life Cycle Assess.*, vol. 15, no. 7, pp. 666–671, Jun. 2010.

[38] J. X. Johnson, C. A. McMillan, and G. A. Keoleian, "Evaluation of Life Cycle Assessment Recycling Allocation Methods," *J. Ind. Ecol.*, vol. 17, no. 5, pp. 700–711, Sep. 2013.

[39] A. Dubreuil, S. B. Young, J. Atherton, and T. P. Gloria, "Metals recycling maps and allocation procedures in life cycle assessment," *Int. J. Life Cycle Assess.*, vol. 15, no. 6, pp. 621–634, 2010.

[40] J. Atherton, "Declaration by the Metals Industry on Recycling Principles," *Int. J. Life Cycle Assess.*, vol. 12, no. 1, pp. 59–60, 2007.

[41] G. Bergsma and M. Sevenster, "End-of-life best approach for allocating recycling benefits in LCAs of metal packaging," 2013.

[42] R. Garabedian, "Technology Update," *First Sol. Anal. Meet.*, 2014.

[43] M. Goe and G. Gaustad, "Strengthening the case for recycling photovoltaics: An energy payback analysis," *Appl. Energy*, vol. 120, pp. 41–48, May 2014.

[44] K. Burrows and V. Fthenakis, "Glass needs for a growing photovoltaics industry," *Sol. Energy Mater. Sol. Cells*, vol. 132, pp. 455–459, 2015.

[45] J. M. Pearce, "Industrial symbiosis of very large-scale photovoltaic manufacturing," *Renew. Energy*, vol. 33, no. 5, pp. 1101–1108, 2008.

[46] First Solar, "Personal Communication," 2014.

[47] First Solar, "PV Recycling Policies and Technology," *IEA PVPS,* 2014.

[48] T. Wang, J. Hsiao, and C. Du, "Recycling of materials from silicon base solar cell module," *38th IEEE Photovolt. Spec. Conf.*, pp. 2355–2358, 2012.

[49] T. Doi, I. Tsuda, H. Unagida, A. Murata, K. Sakuta, and K. Kurokawa, "Experimental study on PV module recycling with organic solvent method," *Sol. Energy Mater. Sol. Cells*, vol. 67, no. 1–4, pp. 397–403, Mar. 2001.

[50] Y. Kim and J. Lee, "Dissolution of ethylene vinyl acetate in crystalline silicon PV modules using ultrasonic irradiation and organic solvent," *Sol. Energy Mater. Sol. Cells*, vol. 98, no. x, pp. 317–322, Mar. 2012.

[51] T. R. Dwarakanath, B. A. Wender, T. Seager, and M. P. Fraser, "Towards anticipatory life cycle assessment of photovoltaics," in *2013 IEEE 39th Photovoltaic Specialists Conference (PVSC)*, 2013, pp. 2392–2393.

[52] B. A. Wender, R. W. Foley, V. Prado-Lopez, D. Ravikumar, D. A. Eisenberg, T. A. Hottle, J. Sadowski, W. P. Flanagan, A. Fisher, L. Laurin, M. E. Bates, I. Linkov, T. P. Seager, M. P. Fraser, and D. H. Guston, "Illustrating Anticipatory Life Cycle Assessment for Emerging Photovoltaic Technologies.," *Environ. Sci. Technol.*, Sep. 2014.

[53] "Photovoltaics Report - Fraunhofer institute for solar energy systems." [Online]. Available: http://www.ise.fraunhofer.de/en/downloads-englisch/pdf-files-englisch/photovoltaics-report.pdf. [Accessed: 11-May-2014].

[54] NREL, "Module Encapsulation Materials, Processing and Testing," 2008. [Online]. Available: http://www.nrel.gov/docs/fy09osti/44666.pdf.

[55] N. Jungbluth, M. Tuchschmid, and M. de Wild-Scholten, "Life Cycle Assessment of Photovoltaics: Update of ecoinvent data v2. 0," *ESU-services Ltd., 2008*, pp. 1–22, 2008.

[56] T. Y. Wang, Y. C. Lin, C. Y. Tai, R. Sivakumar, D. K. Rai, and C. W. Lan, "A novel approach for recycling of kerf loss silicon from cutting slurry waste for solar cell applications," *J. Cryst. Growth*, vol. 310, no. 15, pp. 3403–3406, 2008.

[57] M. Woodhouse, A. Goodrich, R. Margolis, T. James, R. Dhere, T. Gessert, T. Barnes, R. Eggert, and D. Albin, "Perspectives on the pathways for cadmium telluride photovoltaic module manufacturers to address expected increases in the price for tellurium," *Sol. Energy Mater. Sol. Cells*, pp. 1–14, Apr. 2012.

Chapter 5

AN ANTICIPATORY LIFECYCLE ASSESSMENT OF NOVEL AND EXISTING CDTE PV MODULE RECYCLING PROCESSES

Introduction

Worldwide PV system deployments are increasing to reduce the reliance on electricity generated from greenhouse gas (GHG) intensive sources and meet climate goals. With these deployments expected to reach end of life (EOL) in 25 years, environmentally improved processes are required to recycle 78 million tons of projected PV waste in 2050 [1]. First Solar, the world's largest recycler, transports EOL PV systems from multiple deployment sites to centrally located recycling plants and recycles them through a combination of mechanical and chemical processes. Proposing and evaluating possible environmental improvements to existing recycling methods require a (1) quantification of energy and material flows and identifying environmental hotspots in existing operations that recycle the PV system (2) identifying novel recycling methods that can address the hotspots (3) evaluating the environmental trade-offs of replacing the incumbent recycling process with alternatives at a commercial scale. Recent research on the energetics of CdTe PV recycling shows that the mechanical shredding and hammering processes, required to weaken the ethylene vinyl acetate (EVA) encapsulant before recycling the module materials, accounts for around 50% of the energy footprint [2]. Replacing the mechanical processes with chemical or high temperature alternatives may offer potential environmental improvements. Also, adopting these alternatives in decentralized plants at the deployment site may be environmentally preferable to the current approach of transporting and recycling modules at centralized facilities.

Lifecycle assessment (LCA), the preferred framework for analyzing the environmental trade-offs between alternate choices, relies on inventory data gathered from commercial scale processes that have matured over a period of time and, therefore, is methodologically retrospective [3]. In contrast, the novel processes are studied at a lab or pilot scale and literature on these processes focus primarily on the feasibility of recovering materials from the EOL module and do not always report the material and energy inventory requirements. Recent studies on the elimination of the ethylene vinyl acetate (EVA) encapsulant using organic solvents and ultrasonic radiation [4], dissolution in organic solvents [5], pyrolysis [6][7] and a combination of thermal and physical processes[8] do not report the raw material requirements and energy used. Furthermore, studies reporting energy or material values for novel PV recycling methods contain significant uncertainty. For example, energy requirements for the thermal delamination of EVA per wafer vary significantly between 0.1 kWh [9] and 0.65 kWh [10]. Another study, exploring a combination of thermal and chemical processes for delamination, reported a value of 81.7 kWh/m^2 without disaggregating the energy between the thermal and chemical processes [11].

Also, prospective LCAs that evaluate an emerging technology and identify environmental hotspots for future improvements [12][13][14][15] may fail in a comparative context where the mutual differences in the environmental impacts of the alternatives and not the environmental hotspots of a particular alternative determine the environmental preferable alternative. For example, a recent study comparing five PV technologies[16] showed that the choice of CdTe as an environmentally preferable option over crystalline silicon technologies is driven by the mutual difference in the water depletion impact category. A prospective LCA, in this case, would have identified freshwater eutrophication as the environmental hotspot for future improvement. Also, by evaluating the environmental

hotspots without accounting for the relevant stakeholder inputs, prospective LCAs cannot guide an emerging technology towards an environmentally favorable trajectory in a specific decision context.

The lack of a comprehensive study that compares the environmental impacts of multiple CdTe PV recycling alternatives, unavailable or uncertain material and energy data for emerging PV recycling processes and the inherent methodological limitations in traditional and prospective LCA methods prevents PV recyclers from addressing three questions that can environmentally improve future CdTe PV recycling operations– (1) Do the alternative recycling methods at the lab scale environmentally outperform the incumbent process at the commercial scale? (2) What are the future research priorities to further reduce the environmental impact of the most environmentally promising PV recycling alternative? (3) Are the alternative methods operating in small-scale decentral plants environmentally preferable to transporting and recycling modules in centralized plants?

This study uses the Anticipatory LCA framework[17], a recent methodological innovation, to address these problematic aspects by stochastically comparing the environmental impacts of the incumbent and the alternatives for recycling CdTe PV modules, identifying the most environmentally promising pilot-scale recycling alternative for future commercialization, determining the uncertainties and stakeholder inputs that can impact the choice of this preferable alternative, identifying the environmental hotspots and prioritizing future research to address the hotspots and maximize the environmental benefit of commercializing the preferred alternative.

This study evaluates the environmental impact of four pilot-scale alternatives – thermal delamination of EVA [18], EVA dissolution by heating in an organic solvent [5], and EVA dissolution through probe [4] or bath sonication - to the incumbent mechanical

shredding and hammering process that eliminates the EVA encapsulant [19]. As an alternative to the incumbent leaching and precipitation process for the recovery of cadmium and tellurium [19], the environmental impacts of solvent extraction [20][21][22] and ion-exchange [23][24] are investigated. Energy and material inventory data for EVA elimination through - pyrolysis, dissolution by heating in an organic solvent and dissolution though sonication (probe and bath) - is gathered from laboratory experiments. Energy and material inventory data for EVA elimination in the incumbent commercial process [25] and recovery of cadmium and tellurium through - precipitation [25], solvent extraction (section 3 Appendix E), ion-exchange (section 1 Appendix E) - are determined from published literature. Based on different combinations of methods for EVA delamination and cadmium and tellurium recovery, seven CdTe PV recycling alternatives (Table 7) are compared for environmental impacts (Figure 22). The LCA software - SimaPro® [26] - is used to calculate the lognormal mean and standard deviation of the 18 environmental impact categories in ReCiPe impact assessment method [27] from the material and energy inventories for the seven recycling alternatives.

Using Stochastic Multi-attribute Assessment (SMAA) framework [28], this research stochastically generates values for the 18 environmental impact categories from the lognormally distributed mean and standard deviation, compares and outranks the values, and calculates an aggregated environmental score for each of the recycling alternatives. The aggregated environmental scores range between -1 (environmentally least favorable) and +1 (environmentally most favorable). To analyze the environmental trade-offs between decentralized and centralized recycling, the aggregated environmental scores of the most environmentally promising novel alternative operating in a decentralized and the centralized recycling plant are compared. To prioritize future research effort, the parameters that

significantly improve the environmental performance of the novel recycling methods at a commercial scale are identified through a global sensitivity analysis (GSA) [29].

Methods

Energy and material flows for the incumbent and emerging recycling processes

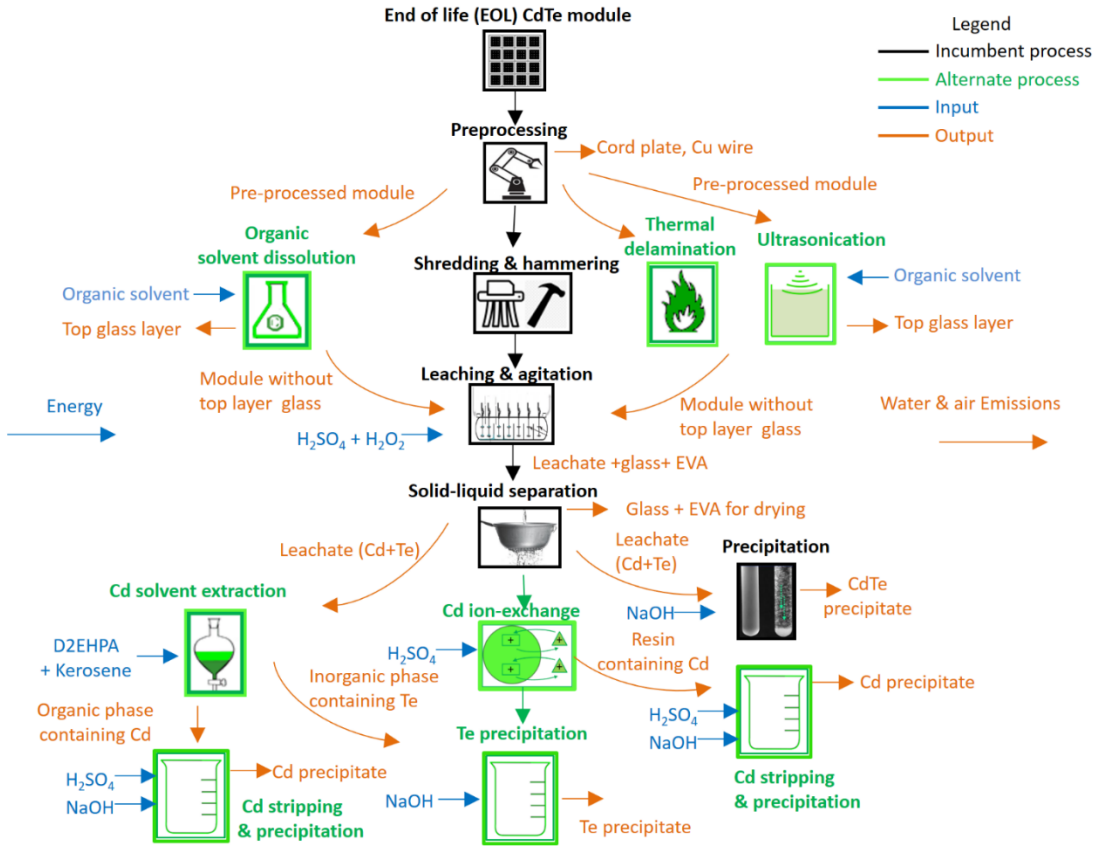

Figure 22 Material and energy flows for CdTe recycling alternatives.
Material and energy flows for the incumbent (black) and alternate (green) recycling processes considered in this research.

Figure 22 represents the material and energy flows for the incumbent CdTe PV recycling process consisting of EVA delamination (shredding and hammering) and the recovery of cadmium and tellurium (leaching & agitation, solid-liquid separation, precipitation) [25]. This study evaluates the environmental impacts of replacing the incumbent EVA delamination process with alternate methods (organic solvent dissolution/

ultrasonication/ thermal delamination), and cadmium and tellurium recovery methods (cadmium solvent extraction + cadmium stripping &precipitation + tellurium precipitation/ cadmium ion exchange + cadmium stripping & precipitation + tellurium precipitation). The functional unit for the comparative environmental impact assessment is 1 m^2 of an end-of-life CdTe PV module and the common outputs are cord plate, copper wiring, glass, and cadmium and tellurium precipitate. The feasibility and the energy and material requirements for the alternate EVA delamination methods are determined experimentally as there are no studies evaluating these processes for CdTe modules. The energy and material requirements for the incumbent process and alternative cadmium and tellurium recovery methods are calculated from published literature.

Incumbent CdTe PV recycling process

In the incumbent recycling process (black in Figure 22), the EOL module is preprocessed to remove the cord plate and copper wiring. The module is shred to large pieces and then hammered to 4-5 mm size pieces. The smaller size reduces the binding strength of the EVA encapsulant and exposes the CdTe layer to the leaching reactions (section 2 SI). Under acidic and oxidative conditions in the rotating leach drum, the CdTe layer is solubilized to Te^{4+} and Cd^{2+} after reacting with sulfuric acid and hydrogen peroxide [30][31]. The leachate is subsequently separated from the remaining glass particles in the solid-liquid separation step. After separation the leachate's pH is increased by adding sodium hydroxide to precipitate and recover the cadmium and tellurium in the form of a semiconductor cake. For the energy and material requirements of the incumbent CdTe PV recycling process refer section 4 of Appendix E.

Thermal delamination of EVA

This study experimentally determines the minimum time and energy requirements to completely delaminate glass samples by heating them to 500^{o}C in air. Previous studies report deacetylation and the formation of terminal alkenes at 360^{o}C and 480^{o}C, respectively [9][11][10][18][32]. 8x8 inch glass samples [33] were laminated with EVA [34] in a PV module laminator [35] and heated to 500^{o}C in a Vulcan 3-1750 box furnace [36] for T_{run} minutes. The furnace is then switched off and the sample is allowed to cool inside the closed furnace for T_{close} minutes as the residue from EVA heating combusts if the furnace is immediately opened after T_{run} minutes. The furnace is then opened and the delaminated sample is allowed to cool for T_{open} minutes as the glass cracks if the sample is removed immediately after opening the furnace. Complete delamination is confirmed through a mass-balance by weighing the sample before and after the thermal delamination. The energy required to run the furnace for T_{run} minutes is measured with an energy meter. The experimental runs, values for T_{run}, T_{close}, T_{open}, and the energy requirements are reported in section 6 of Appendix E.

Delaminating EVA by heating in an organic solvent

This study experimentally measures the energy, solvent volume and time required for delaminating 2x2 inch glass samples [33] laminated with EVA [34] in a PV module laminator [35] by heating in (1) o-dichlorobenzene(99.8% anhydrous, [37]) at 165^{o}C, (2) toluene(99.8% anhydrous, [38]) at 95^{o}C, and (3) trichloroethylene(>= 99%, [39]) at 70^{o}C. The temperatures chosen is 15^{o}C lower than the respective boiling points to prevent evaporation of the solvents. The samples are immersed in 300 ml of the solvent in a closed beaker and heated on a hot-plate until delamination. The energy required for heating is measured with an

energy meter. The experimental runs, delamination time, and energy requirements are reported in section 7 of Appendix E.

Delaminating EVA by sonicating in an organic solvent

This study experimentally measures the energy and time required for delaminating glass samples immersed in (1) o-dichlorobenzene (99.8% anhydrous, [37]), (2) toluene(99.8% anhydrous, [38]), and (3) trichloroethylene(>= 99%, [39]), and ultrasonicated with bath and probe sonicators. For the bath sonication, 2x2 inch glass samples [33] laminated with EVA [34] in a PV module laminator [35] are immersed in the solvent and the beaker was placed in a bath sonicator [40] containing water. The temperature during the bath sonication was set to the maximum allowed value of 60^{o}C.

For the probe sonication, 2x2 inch glass samples [33] laminated with EVA [34] in a PV module laminator [35] are immersed in the solvent and ultrasonicated with a probe tip. The probe sonicator is set to an alternate 3 minute on and off cycles to prevent over-heating of the probe tip. The solvent is not heated before sonication as heat is generated by the probe tip during sonication.

Extracting cadmium through ion exchange

Wang and Fthenakis experimentally investigated the feasibility of removing cadmium dissolved in an acidic solution (simulating the leachate from the solid-liquid separation in Figure 22) using Amberlyst 15 and DOWEX 50X8 [23], [24], [41]. The energy and material requirements for ion-exchange extraction of cadmium (section 1 Appendix E) is calculated from values reported in [23] which simulates the operational conditions similar to that of CdTe module recycling in the incumbent process.

Solvent extraction of cadmium

The cadmium from the leachate obtained from the solid-liquid separation in Figure 22 can be extracted into an organic phase using the extractant molecule di(2-ethylhexyl) Phosphoric Acid (D2EHPA) dissolved in kerosene. This study calculates the energy and material requirements of the solvent extraction of cadmium using D2EHPA as it is commonly used for extracting cadmium [20][21][22] and was evaluated in a pilot scale process for recycling CdTe module recycling [42]. The energy and material requirements for solvent extraction of cadmium is determined from literature and is detailed in section 3 of Appendix E.

Table 7 Summary of the seven CdTe recycling alternatives.
Summary of the seven CdTe recycling alternatives which are based on different combinations of methods for EVA delamination, and cadmium and tellurium recovery.

Sl No	Recycling alternative name	Recycling process for EVA delamination (refer Figure 22)	Recycling process for cadmium and tellurium recovery (refer Figure 22)
1	mech+leach+prcp (incumbent)	Shredding and hammering	Leaching and agitation+Solid liquid separation+Precipitation
2	thermal+leach+ion exch+prcp	Thermal delamination	Leaching and agitation+Solid liquid separation+Cd ion exchange+Te Precipitation+Cd stripping precipitation
3	thermal+leach+prcp	Thermal delamination	Leaching and agitation+Solid liquid separation+Precipitation
4	thermal+leach+solv ext+prcp	Thermal delamination	Leaching and agitation+Solid liquid separation+Cd solvent extraction+Te Precipitation+Cd stripping&precipitation
5	org solv+leach+ion exch+prcp	Organic solvent dissolution	Leaching and agitation+Solid liquid separation+Cd ion exchange+Te Precipitation+Cd stripping&precipitation
6	org solv+leach+prcp	Organic solvent dissolution	Leaching and agitation+Solid liquid separation+Precipitation
7	org solv+leach+solv ext+prcp	Organic solvent dissolution	Leaching and agitation+Solid liquid separation+Cd solvent extraction+Te Precipitation+Cd stripping&precipitation

Anticipatory LCA framework to evaluate and improve the environmental impact of CdTe PV recycling

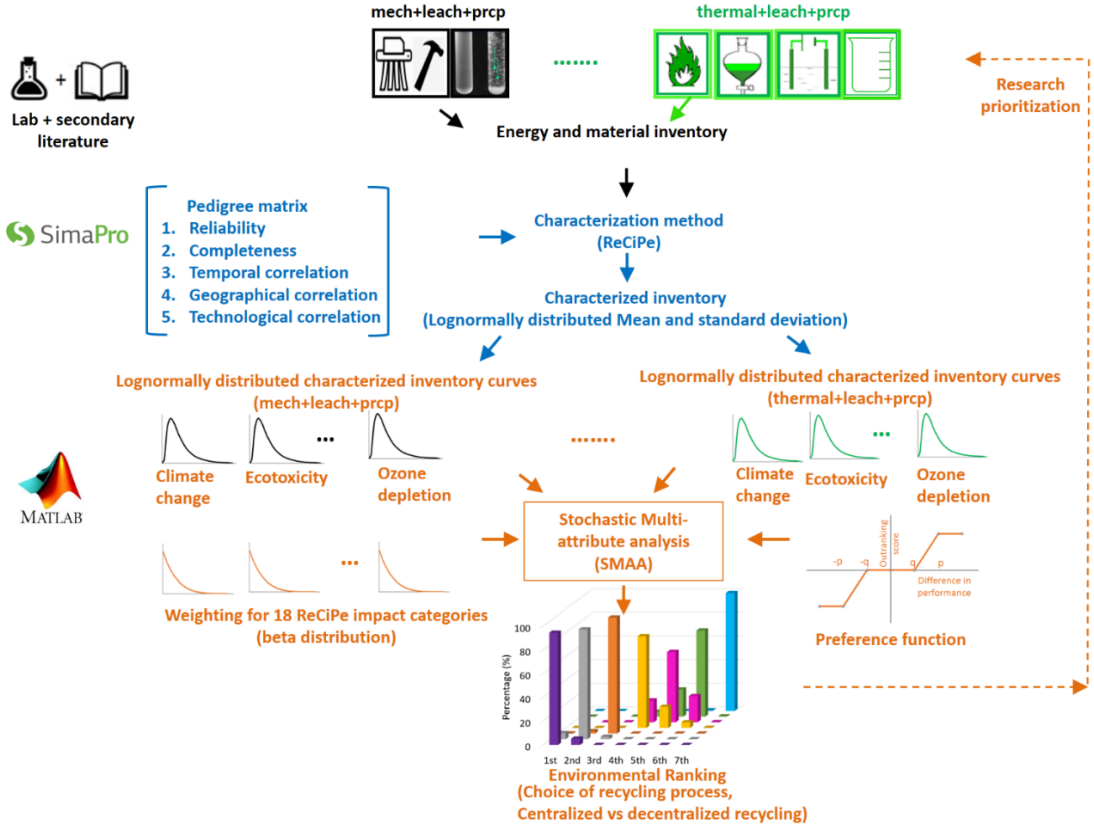

Figure 23 Anticipatory LCA framework for CdTe PV recycling.
Anticipatory LCA framework for comparing the environmental impacts of the seven CdTe PV recycling processes (Table 7). The incumbent method and the alternatives (Table 7) are depicted in black and green, respectively. The inventory requirements are collected from the laboratory experiments and secondary literature. SimaPro® is used to calculate the lognormally distributed mean and standard distribution for 18 environmental impact categories from the material and energy inventory (blue text). The pedigree matrix values accounts for the uncertainty in the inventory data. The SMAA method (implemented in MATLAB®) ranks the seven recycling alternatives by - using the preference function to outrank the stochastically generated values from the environmental impact distributions and aggregating the outranking scores using the weights for the environmental impact categories (orange text).

The anticipatory (aLCA) framework (Figure 23) compares the environmental performance of the incumbent CdTe PV recycling method with six novel alternatives (Table 7). Apart from the basic data uncertainty in the inventory values obtained from the

experiments and secondary literature, LCA inventory data includes five other uncertainties– reliability, completeness, temporal correlation, geographical correlation and technological correlation[43]. The lifecycle energy and material inventory from SimaPro (section 4 Appendix E) are collected from manufacturing locations that may not represent the environmental impacts of the actual inventory procured by PV recyclers. For example, the inventory data for sulfuric acid in SimaPro is based on European manufacturing conditions and a PV recycler in Malaysia may procure locally manufactured sulfuric acid. To account for this uncertainty, this study explores maximum and minimum range of five uncertainty parameters in the pedigree matrix (Figure 23) for all the inventory items in a recycling alternative. The uncertainty quantified in the pedigree matrix is combined with the basic uncertainty to get an overall uncertainty score for the inventory data ([44],[45]). After accounting for the overall uncertainty, the inventory data is multiplied by the single point characterization factors in ReCiPe midpoint heirarchist impact assessment method [27] to obtain the lognormally distributed mean and standard deviation for each of the 18 impact categories in ReCiPe. Since a total of seven PV recycling alternatives are evaluated, there are 7 sets of 18 means and standard distributions (section 8 Appendix E).

Using the mean and the standard deviations, 1000 values are stochastically generated for each of the 18 environmental impact categories for the 7 recycling alternatives. Based on a preference and an indifference threshold in a linear preference function (section 5 Appendix E), stochastic outranking converts the difference in the stochastically generated values in a particular impact category between two recycling methods into positive and negative outranking flows, ranging between 0 and 1. The positive and negative outranking flows (by impact category) for each recycling method are aggregated into a total positive and

negative flow using a weighting function (section 5 Appendix E). The weighting function assigns a weight to each environmental impact category based on the relative importance (as elicited from PV recycling stakeholders) or through a stochastic process. This study assigns weights stochastically to each of the 18 impact categories to explore the entire range of possibilities. The weights for the 18 impact categories will be a beta-distribution between 0 and 1 and the sum of all the weights is constrained to one.

The aggregated probabilistic environmental score for a recycling method is calculated by subtracting the total negative outranking flow from the total positive outranking flow (section 5 Appendix E). The net probabilistic environmental score ranges between -1 (environmentally least preferable) and 1 (environmentally most preferable). Based on the 1000 stochastic runs, each of the recycling alternatives will have 1000 aggregated environmental scores ranging between +1 and -1. The seven recycling alternatives are ranked between 1 (most environmentally favored) and 7 (least environmentally favored) in each of the 1000 runs and the percentage value for the number of times (out of a 1000) a recycling alternative obtains a particular rank is calculated.

To explore the full range of uncertainty in the material and energy inventory, the environmental rankings are calculated for both maximum and minimum uncertainty in the pedigree matrix.

Scenario analysis: centralized and decentralized recycling

The scenario analysis determines the environmentally favorable option between operating the most preferable recycling alternative in a decentralized and a centralized facility. In the centralized mode, the end-of-life PV modules are transported from the deployment site to an industrial-scale centralized recycling facility. The environmental trade-

off is between the burden of transporting end-of-life CdTe PV modules and the gains from operational efficiencies due to the economies of scale at the centralized recycling facility. In the decentralized mode, the end-of-life PV modules are recycled in a small-scale temporary facility located at the deployment site. The environmental trade-off is between the burden of lower operational efficiencies due to small-scale operations and the advantage of avoiding the transportation of end-of-life CdTe PV modules to the centralized facility.

To guide PV recyclers on the environmental trade-offs between pursuing R&D to further decrease the material and energy requirements in a centralized plant or investing in small-scale decentralized plants to avoid transportation burdens, this study environmentally compares and ranks centralized and decentralized recycling scenarios. To account for the higher operational efficiency with increasing the scale of operations from the baseline conidition, the material and energy inventory requirements in centralized recycling plants are assumed to be 15 and 30% lower than the baseline value. Similarly, for decentralized, small-scale recycling plants the inventory requirements are assumed to be 15 and 30% higher than the baseline coniditon to account for lower operational efficiencies. Additionally, a scenario with the centralized plant operating with 30% lower inventory requirements and electricity generated from PV systems is included in the scenario analysis. This scenario is assumed to represent the environmental best case with an inventory reduction through increased scale of operations and R&D, and an improvement in operations by shifting to PV electricity.

Beijing and California are chosen as PV deployment sites as they account for a significant share of the world-wide and US deployments, respectively [50][51]. Kuala Lumpur, Malaysia and Perrysburg, Ohio are chosen as the sites for centralized recycling as First Solar operates facilities at these locations. The assumptions for the shipping and the road transportation distances for centralized recycling are presented in section 9 of the

Appendix E. The environmental favorability is determined by ranking the aggregate probabilistic environmental scores (Figure 23) of the aforementioned centralized and decentralized recycling scenarios.

Global Sensitivity Analysis

The aggregate environmental score of a recycling alternative depends on (1) stochastically generated characterized inventory values in the 18 environmental impact categories for the particular alternative, (2) stochastically generated characterized inventory values in the 18 environmental impact categories for the 6 other recycling alternatives, and (3) the beta-normally distributed weights assigned to the 18 impact categories. Thus, the aggregate environmental score is dependent on a total of 144 input parameters.

To inform PV recyclers on the most significant parameters that can be addressed to further reduce the environmental impact of a particular recycling alternative, a global sensitivity analysis (GSA) [29] is performed. GSA is preferred as it accounts for the first and higher order interactions between the various input parameters when determining the sensitivity of the aggregated environmental score to a specific input parameter and is applicable to models with non-monotonic and non-linear relationships between the input and output parameters [46]. In the variance based GSA method that is implemented, a change in the most sensitive input parameter results in the greatest change in the variance of the aggregate environmental score. For a detailed quantitative discussion of variance based GSA refer [29], [47], [48]. The MATLAB® implementation of the variance based GSA is based on the approach presented in [49].

Results and Discussion

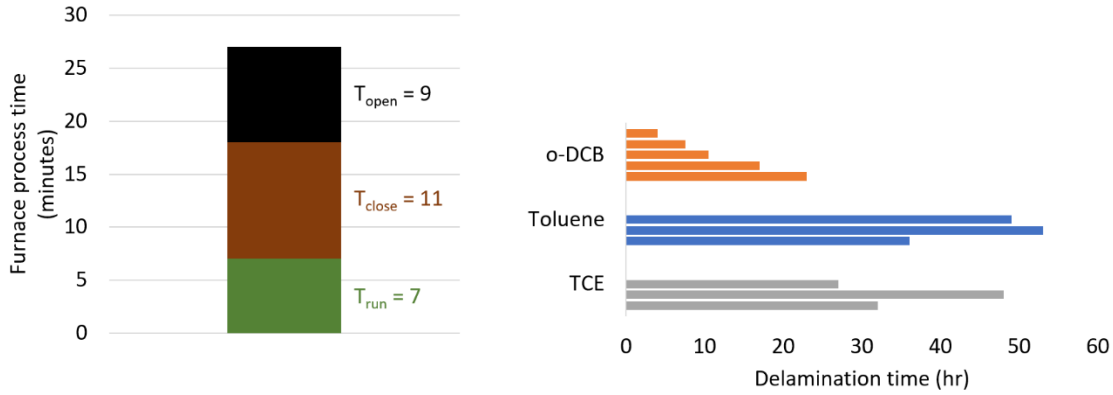

Figure 24 Process time for EVA elimination.
Process time for elimination of EVA by the thermal process (left) and heating in an organic solvent (right).

For the thermal delamination process, a minimum of 7 minutes (T_{run}) is required to delaminate the 8x8 inch samples and eliminate 100% of the EVA (section 6 Appendix E). Further, the sample is required to remain in the closed and switched-off furnace for a minimum of 11 minutes (T_{close}) to prevent the combustion of the residue from the melting of EVA. The sample is subsequently cooled for 9 minutes (T_{open}) by opening the furnace so that the temperature of the glass decreases from 500 to 220-280^{o}C to prevent the cracking (section 6 Appendix E). The total process time is 27 minutes and 0.48 kWh of electricity is consumed in the first 7 minutes to thermally delaminate 1 m^2 of the sample (section 6 Appendix E).

When the 2x2 glass samples laminated with EVA are heated in the organic solvents, delamination time for o-dcb, TCE and toluene are 4 to 23, 32 to 48, and 36 to 53 hours, respectively (section 7 Appendix E). The boiling point of o-dcb (180.5^{o}C) is greater than TCE (87.2^{o}C) or toluene (110.6^{o}C) and, therefore, a higher heating temperature with o-dcb results in a shorter delamination time. With PV recyclers preferring short process times for

recycling, only o-dcb is considered for the recycling alternatives that delaminate EVA by heating in an organic solvent ("org solv+leach+ion exch+prcp", "org solv+leach+prcp", and "org solv+leach+solv ext+prcp"). 6.8L of o-DCB and 5.4 to 36.7 kWh of electricity is required to delaminate 1 m^2 of the sample (section 7 Appendix E).

While a previous study reported the delamination of silicon PV modules with a Tedlar back-surface in 70 minutes[4], probe sonication failed to delaminate the 2x2 inch glass samples after 3 hours in o-dcb, TCE or toluene. The failure of probe sonicator to delaminate may be attributed to both the front and back surface of the sample being glass (as in commercially manufactured CdTe PV modules). Bath sonication failed to delaminate the 2x2 inch glass samples in 48 hours in o-DCB, TCE or toluene. Therefore, bath and probe sonication are not considered as possible alternatives to the incumbent shredding and hammering delamination process (Figure 22) and are not included in the environmental comparison with other recycling alternatives (Table 7).

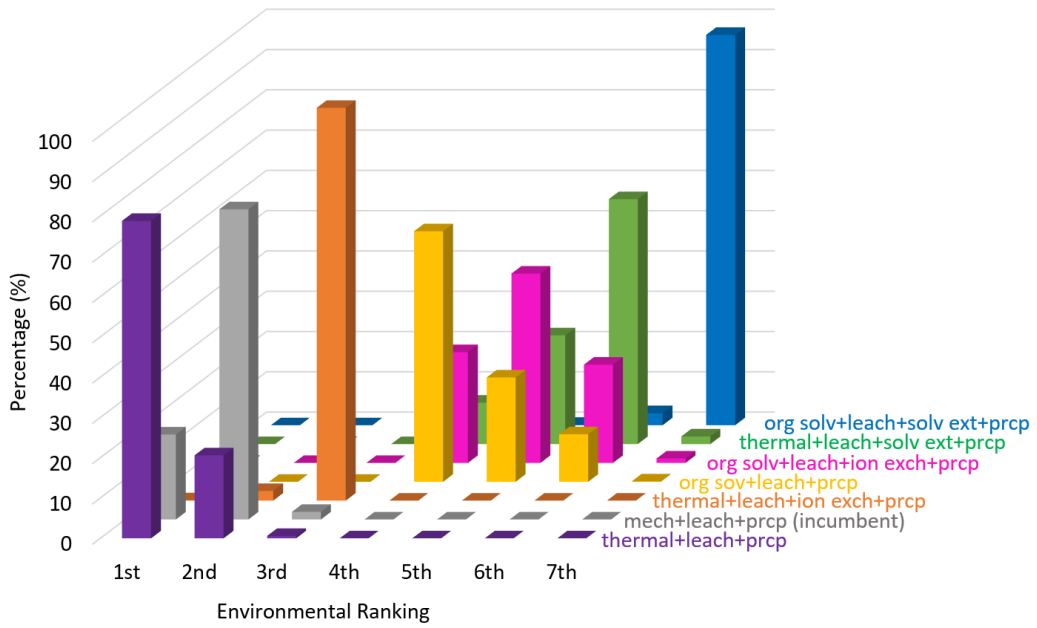

Figure 25 Environmental ranking for the CdTe PV recycling alternatives. Environmental rankings for the 7 recycling alternatives with rank 1 being most environmentally preferable. The rankings are calculated based on maximum uncertainty in the energy and material values in the pedigree matrix. The x-axis shows the ranks and the y-axis depicts the percentage value out of a 1000 runs that a particular recycling alternative obtains a rank.

The environmental rankings (Figure 25) demonstrate that the novel alternative "thermal+leach+prcp" is the most environmentally favored as it ranks first in 78% of the 1000 stochastic runs and the incumbent recycling method ("mech+leach+prcp") ranks second. Furthermore, when the minimum uncertainty for material and energy inventory values are selected in the pedigree matrix and the rankings are recalculated, the novel alternative "thermal+leach+prcp" is the most environmentally favored as it ranks first in 95% of the 1000 stochastic runs and the incumbent recycling method ("mech+leach+prcp") ranks second (section 12 Appendix E). The "thermal+leach+prcp" alternative is environmentally favored due to the lower energy requirements for thermal delamination

(0.48 kWh/m^2) when compared to mechanical shredding and hammering (2.2 kWh/m^2) to delaminate EVA in the incumbent process (section 4 Appendix E).

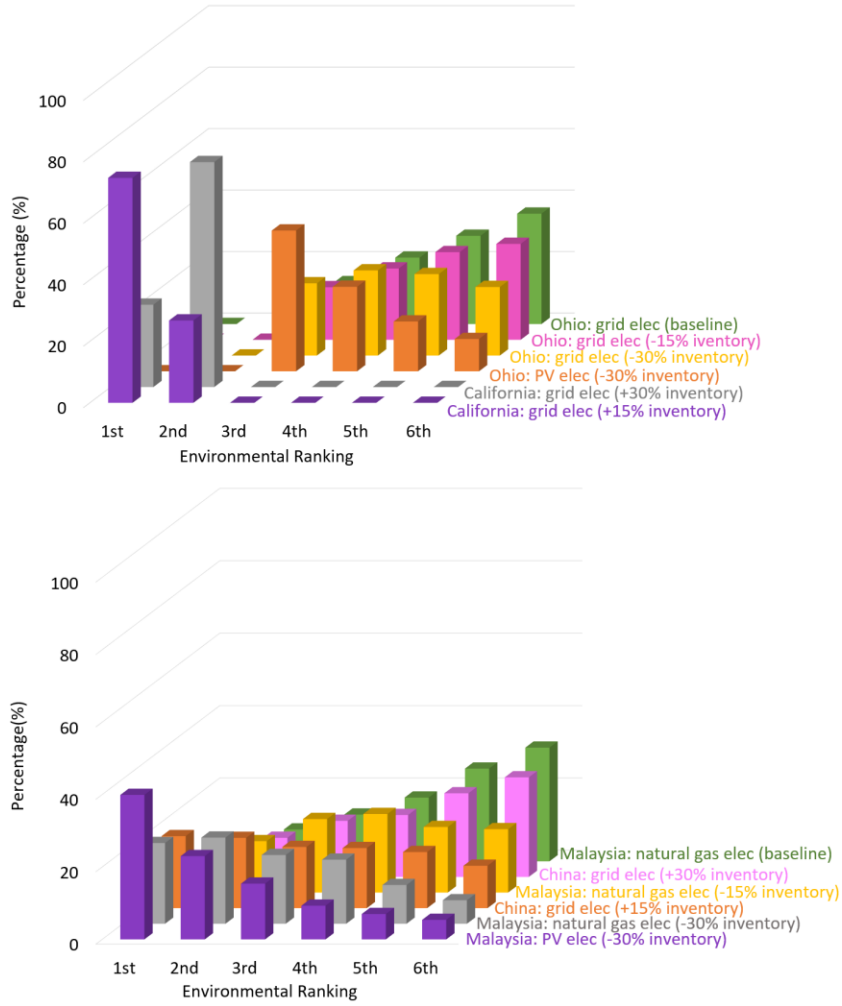

Figure 26 Environmental rankings for centralized and decentralized recycling. Environmental rankings when the "thermal+leach+prcp" recycling alternative is adopted in centralized and decentralized plants (rank 1 being the most environmentally favorable). The + and - percentage values represent the increased and decreased inventory requirements (compared to the baseline scenario) due to lower and higher operational efficiencies in decentralized and centralized plants, respectively. Decentralized recycling in California is environmentally preferable to centralized recycling in Ohio (top). Decentralized recycling in China environmentally outperforms the baseline scenario of centralized recycling in Malaysia only when the inventory requirementis less than 1.15 times the baseline value (bottom).

The results (Figure 26) show that decentral recycling of CdTe PV modules at the deployment site in California, with the most environmentally promising novel alternative "thermal+leach+prcp" (refer Figure 25), is environmentally preferable to recycling in centralized locations in Ohio and Malaysia, respectively. This due to the environmental burden of transporting spent CdTe PV modules by road from California to Ohio (100% of the total transportation share, section 9 Appendix E) outweighing the environmental benefit of increased operational efficiencies at the centralized plant at Ohio (due to economies of scale). For example, even with 30% lower inventory requirements than the baseline value and using PV electricity for centralized recycling operations, recycling decentrally in California with 90% increased inventory requirements is environmentally preferable (ranking of "Ohio PV elec -30% inventory" versus "California: grid elec +30% inventory").

Decentralized recycling in China is environmentally preferable to the baseline scenario of centralized recycling in Malaysia only when the inventory requirement is less than 1.15 times the baseline value ("China grid elec +15% inventory" outranks "Malaysia natural gas elec baseline"). If the inventory requirements in decentralized plants in China is greater than 1.15 times the baseline value, the difference in ranking with the baseline scenario is statistically insignificant (" China grid elec +30% inventory" versus "Malaysia natural gas elec baseline"). Furthermore, if the inventory requirements is 30% lower than baseline requirement and PV electricity is used for recycling operations, centralized recycling in Malysia outperforms decentralized recycling in China ("Malaysia PV elec -30% inventory" obtains rank one 40% of the times).

Comparing the results in the top and the bottom, we observe that environmentral rankings for decentralized recycling in China is less favorable than decentralized recycling in

California. This is because shipping, which accounts for 97% of the total transportation between China and Malaysia (in ton-km, section 9 Appendix E), has a lower environmental burden than road transportation which accounts for 100% of the total transportation between California and Ohio (section 13 Appendix E).

A possible approach to improve the environmental performance of decentral recycling in China is to replace carbon-intensive grid electricity with PV electricity for the decentral recycling processes. In this scenario, decentralized recycling in China is the environmentally preferred alternative only if the inventory requirements are within 1.3 times the baseline inventory requirements (in a centralized plant) (section 14 Appendix E). The results suggest that recyclers can improve the environmental performance of PV recycling by (1) locating centralized recycling plants in the vicinity of shipping ports to decrease the share of transportation by road (2) adopting decentralized recycling if transporting end-of-life modules to the nearest centralized plant involves a significant distance by road, and (3) utilizing carbon-efficient sources of electricity (e.g. photovoltaics) for centralized and decentralized recycling plant operations.

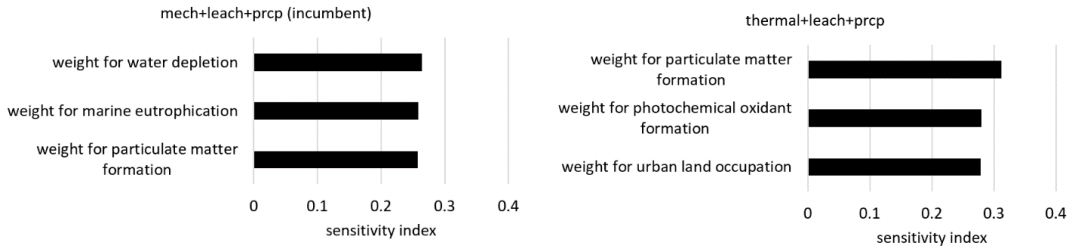

Figure 27 Global sensitivity analysis results (with weights).
Global sensitivity analysis results showing the values of the sensitivity indices for the three most significant input parameters (out of a total of 144 input parameters). The environmental ranking of the incumbent "mech+leach+prcp" (left) and the novel "thermal+leach+prcp" (right) recycling alternatives are most sensitive to the weights assigned to the three environmental impact categories.

The results from the GSA (Figure 27, left) demonstrate that beta-distributed random weights assigned to the water depletion, marine eutrophication, and particulate matter formation impact categories are the three most significant parameters (out of 144 input parameters) influencing the environmental ranking of the incumbent "mech+leach+prcp" alternative. Similarly, for the novel "thermal+leach+prcp" alternative (Figure 27, right), the weights assigned to the particulate matter formation, photochemical oxidant formation, and urban land occupation impact categories are the three most significant parameters. Furthermore, the ten most significant input parameters to influence the environmental rankings are all weights assigned to the environmental impact categories (section 11 Appendix E).

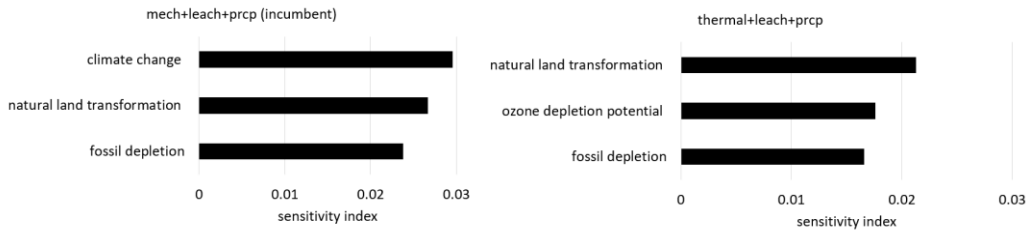

Figure 28 Global sensitivity analysis results (without weights).
Global sensitivity analysis results showing the values of the sensitivity indices for the three most significant environmental impact categories (out of a total of 126 impact cateogories) that influence the environmental ranking of the incumbent "mech+leach+prcp" (left) and the novel "thermal+leach+prcp" (right) alternatives. The weights are not included in the sensitivity analysis.

While demonstrating that dominance of the weights in determining the environmental rankings, the results in Figure 27 fail to identify uncertainties or hotspots in the recycling processes that PV recycling stakeholders can address in the future through research and development (R&D), and operational improvements. Therefore, this study repeats the GSA by including only the environmental impact categories and excluding the

weights. When the weights are excluded from the GSA, the results show that climate change, natural land transformation, and fossil depletion are the most significant environmental impact categories in the incumbent recycling process (Figure 28,left). Similarly, reducing the natural land transformation, ozone depletion potential and fossil depletion will further improve the environmental performance of the novel "thermal+leach+prcp" (Figure 28,right). These impact categories can be reduced if process improvements reduce the electricity used in the recycling operations (section 10 Appendix E). Furthermore, shifting to more carbon-efficient electricity sources (e.g. photovoltaics) can reduce the climate impacts of large scale PV recycling. It should be noted that the results in Figure 28 are specific to beta-randomly distributed weights for the impact categories and will change if the weighting method is modified.

The results from the a-LCA demonstrate the significance of eliciting inputs from various stakeholders (e.g. environmental engineers, regulatory authorities, recycling plant managers) on the most significant environmental impact categories (Figure 27) in a specific decision context and prioritize the R&D efforts towards addressing these environmental impacts. For example, stakeholders will assign a higher value to the weight for human toxicity than other impact categories in PV recycling markets with regulations sensitive to human toxicity. The a-LCA is then repeated to identify the recycling alternative with the least human toxicity impact and this can prioritize R&D efforts towards the addressing the significant environmental hotspots in the most preferable process. Furthermore, the results from the aLCA identify uncertainties in the lifecycle data of inventory items that significantly influence the environmental ranking (Figure 28). To improve decision making and identify the environmental preferable recycling alternative, research efforts should focus on

collecting and improving the upstream lifecycle data quality for these specific inventory items.

The environmental rankings (Figure 25) are based on the material and energy inputs and do not include the environmental burdens of emissions and emission control requirements for the recycling alternatives. Emission data at a commercial scale is only available for the incumbent process [25] and not the other recycling alternatives which operate only at the pilot-scale. For consistency in calculating the environmental rankings, the emissions are excluded for both the incumbent and novel alternatives. Furthermore, the "thermal+leach+prcp" alternative can emit volatile organic compounds (1-butene, ethylene, methane), carbon dioxide, carbon monoxide and methane [52]. The volatile organic emission control requirements which are implemented for the incumbent "mech+leach+prcp" process at a commercial scale are not included while calculating the environmental impacts. Therefore, assuming the same process is used to manage volatile organic emissions for the "thermal+leach+prcp" alternative and excluding them from the environmental impact calculations will not impact the relative environmental ranking of the two methods. Existing research also confirms the thermal stability of CdTe at the range of temperatures used in the thermal delamination process [53][54]. Therefore, the environmental burdens of cadmium and tellurium emissions from thermal delamination of EVA in CdTe PV modules are not included in this analysis.

The results presented in this research consider only the environmental impacts when ranking the recycling alternatives. The choice of a particular recycling alternative or a facility location strategy (decentralized versus centralized) is also influenced by economic and regulatory considerations. For example, when regulations do no permit end-of-life products containing cadmium to be transported to centralized recycling facilities across international

borders, recyclers have to manage the PV waste decentrally irrespective of the environmental and economic impacts. Further analysis on the economic, operational and regulatory aspects of PV recycling will complement this work on informing PV recycling stakeholders on the preferred recycling alternative and the location strategy.

CONCLUSION

The dominant approach to improve the environmental performance of PV systems is increasing the module efficiency and, therefore, the renewable electricity generated in the use phase. However, this approach fails to identify and address the potential environmental hotspots in PV manufacturing and recycling. This dissertation provides a compelling environmental rationale for an alternative strategy of improving the environmental performance of PV systems through improved manufacturing and recycling.

Chapter 2 identifies a methodological limitation in current PV LCAs which do not account for the time-sensitive climate impacts of manufacturing emissions that occur earlier than the emissions avoided in the use-phase. A framework with the CRF metric is presented to address this methodological limitation and account for the time-sensitive climate impacts of PV manufacturing emissions. The result show that the GHG payback time, the preferred environmental metric in PV LCAs, is always lower than the CRF payback-time of a PV system. GHG payback occurs when the mass of GHG avoided is equal to the GHG emitted and is insensitive to the timing and atmospheric residence time of emissions. CRF payback is sensitive to the magnitude and timing of emission and the residence time of GHG in the atmosphere. Therefore, early manufacturing emissions have a higher CRF impact than emissions avoided after deployment and this increases the CRF payback time. By not accounting for this time-sensitive climate impact of PV manufacturing emissions, current PV LCAs underestimate the environmental benefits from PV manufacturing emissions.

Chapter 3 further develops the findings in Chapter 2 which identifies CRF as the appropriate metric to quantify the time-sensitive climate impact of PV manufacturing emissions and prospectively evaluates strategies to decrease the climate impact of future PV manufacturing. The results show that GHG- intensity of the electricity used for PV

manufacturing has the most significant climate impact. This is the result of PV modules being predominantly manufactured in China with GHG-intense sources of electricity. The climate benefit of shifting to GHG-efficient electricity sources (e.g PV) for PV manufacturing is equivalent to increasing the module efficiency from the current commercial value of 17% to 21.7% and 16% to 18.7% for mono-Si and multi-Si modules, respectively. This equivalent module efficiency gain is significant as the module efficiency for crystalline silicon-PV technologies has increased annually by only 0.25% in the last twelve years.

To identify the environmental hotspots in PV recycling, Chapter 4 presents the first detailed energetic assessment of commercial-scale CdTe PV system recycling operations. The findings show that recovering and recycling the bulk materials (steel, aluminum, copper and glass) from end-of-life CdTe systems can reduce the lifecycle energy footprint of the CdTe PV system by approximately 24% of the energy required to manufacture the PV system. Furthermore, the process to eliminate the EVA polymer that encapsulates the module to recover the unrefined the semiconductor material is the most significant environmental hotspot.

To environmentally improve future PV recycling operations, Chapter 5 evaluates the environmental trade-off of replacing the hotspot identified in chapter 4 with novel pilot-scale recycling alternatives. Lifecycle assessment (LCA), the preferred framework to evaluate the environmental trade-offs between multiple alternatives, is methodologically retrospective by relying on inventory data gathered from commercial scale processes that have matured over time. In contrast, the existing research on the feasibility of novel pilot-scale processes do not always report the material and energy inventory requirements which is required for an LCA. Additionally, a limited number of studies adopt a prospective mode of LCA to evaluating an emerging technology by identifying environmental hotspots for future

improvements. This approach may fail in a comparative context where the environmental preferable choice is determined by the mutual differences in the environmental impacts of the alternatives and not the environmental hotspots of an alternative. Chapter 5 addresses these methodological shortcomings by using the anticipatory lifecycle assessment framework to evaluate the incumbent CdTe PV recycling process and 6 pilot-scale alternatives. The results show that thermally eliminating the EVA is environmentally the most favorable alternative to the incumbent mechanical process. Furthermore, when road is the dominant mode for transporting end-life modules to centralized recycling locations from the deployment site, recycling end-of-life modules decentrally in mobile plants near the deployment site is environmentally favorable. Centralized recycling is environmentally favorable if shipping is the dominant mode of transport. Additionally, the results show that the choice of the environmentally preferred alternative is most sensitive to the stakeholder inputs on the relative importance of the multiple environmental impact categories used to evaluate the alternatives. If the weights assigned to the environmental impact categories are excluded from the sensitivity analysis, the results show that the environmental performance of the incumbent recycling process and the thermal delamination alternative is most sensitive to the GHG intensity of the electricity for recycling operations. Therefore, apart from adopting the novel thermal delamination alternative, recyclers can further reduce the environmental impact of future recycling operations by using GHG-efficient sources of electricity.

This dissertation's findings on increasing the environmental benefits from PV systems through improved manufacturing and recycling are significant to stakeholders in the PV industry as PV manufacturing facilities that are expected to meet the terawatt-scale of global demand are increasingly shifting to GHG intensive manufacturing locations like

China. Furthermore, with a typical lifespan of twenty-five years, the rapid acceleration of PV installations post-2005 will contribute to a significant increase in end-of-life volumes over the next ten to 20 years. Identifying and implementing environmentally promising alternatives in present-day recycling plants at a smaller scale is operationally and economically preferable to modifying the recycling technology at a much larger scale in the future when end-of-life volumes are expected to increase.

REFERENCES

[1] International Renewable Energy Agency, "End of Life Management: Solar Photovoltaic Panels," 2016.

[2] D. Ravikumar, P. Sinha, T. Seager, and M. P. Fraser, "An anticipatory approach to quantify energetics of recycling CdTe photovoltaic systems," *Prog. Photovoltaics Res. Appl.*, 2015.

[3] B. a. Wender, R. W. Foley, T. a. Hottle, J. Sadowski, V. Prado-Lopez, D. a. Eisenberg, L. Laurin, and T. P. Seager, "Anticipatory life-cycle assessment for responsible research and innovation," *J. Responsible Innov.*, vol. 1, no. 2, pp. 200–207, 2014.

[4] Y. Kim and J. Lee, "Dissolution of ethylene vinyl acetate in crystalline silicon PV modules using ultrasonic irradiation and organic solvent," *Sol. Energy Mater. Sol. Cells*, vol. 98, no. x, pp. 317–322, Mar. 2012.

[5] T. Doi, I. Tsuda, H. Unagida, A. Murata, K. Sakuta, and K. Kurokawa, "Experimental study on PV module recycling with organic solvent method," *Sol. Energy Mater. Sol. Cells*, vol. 67, no. 1–4, pp. 397–403, Mar. 2001.

[6] P. Dias, S. Javimczik, M. Benevit, and H. Veit, "Recycling WEEE: Polymer characterization and pyrolysis study for waste of crystalline silicon photovoltaic modules," *Waste Manag.*, 2016.

[7] Z. De-wen, M. Born, and K. Wambachz, "Pyrolysis of EVA and its application in recycling of photovoltaic modules," *J. Environ. Sci.*, 2004.

[8] G. Granata, F. Pagnanelli, E. Moscardini, T. Havlik, and L. Toro, "Recycling of photovoltaic panels by physical operations," *Sol. Energy Mater. Sol. Cells*, vol. 123, pp. 239–248, Apr. 2014.

[9] L. Frisson, H. Hofkens, K. de Clercq, J. Nijs, and A. Geeroms, "Cost effective recycling of PV modules and the impact on environment, life cycle, energy payback time and cost," in *2nd World Conference on Photovoltaic Solar Technology*, 1998, pp. 2210–2213.

[10] L. Frisson, K. Lieten, T. Bruton, K. Declercq, J. Szlufcik, H. De Moor, M. Goris, A. Benali, and O. Aceves, "Recent improvements in industrial PV module recycling," in *16th European Photovoltaic Solar Energy Conference*, 2000.

[11] A. Müller, K. Wambach, and E. Alsema, "Life Cycle Analysis of Solar Module Recycling Process," *MRS Proc.*, vol. 895, no. August 2015, pp. 18–21, 2005.

[12] N. Jungbluth, "Life cycle assessment of crystalline photovoltaics in the Swiss ecoinvent database," *Prog. Photovoltaics Res. Appl.*, vol. 13, no. 5, pp. 429–446, Aug. 2005.

[13] N. Jungbluth, C. Bauer, R. Dones, and R. Frischknecht, "Life cycle assessment for emerging technologies: Case studies for photovoltaic and wind power," *Int. J. Life Cycle Assess.*, vol. 10, no. 1, pp. 24–34, 2005.

[14] A. Meijer, M. a. J. Huijbregts, J. J. Schermer, and L. Reijnders, "Life-cycle assessment of photovoltaic modules: Comparison of mc-Si, InGaP and InGaP/mc-Si solar modules," *Prog. Photovoltaics Res. Appl.*, vol. 11, no. 4, pp. 275–287, Jun. 2003.

[15] D. Ravikumar, T. P. Seager, M. V. Chester, and M. P. Fraser, "Intertemporal cumulative radiative forcing effects of photovoltaic deployments," *Environ. Sci. Technol.*, vol. 48, no. 17, pp. 10010–10018, 2014.

[16] V. Prado-lopez, B. A. Wender, T. P. Seager, L. Laurin, M. Chester, and E. Arslan, "Tradeoff Evaluation Improves comparative life cycle assessment A Photovoltaic Case Study," *J. Ind. Ecol.*, vol. 0, no. 0, pp. 1–9, 2015.

[17] B. a Wender, R. W. Foley, V. Prado-Lopez, D. Ravikumar, D. a Eisenberg, T. a Hottle, J. Sadowski, W. P. Flanagan, A. Fisher, L. Laurin, M. E. Bates, I. Linkov, T. P. Seager, M. P. Fraser, and D. H. Guston, "Illustrating anticipatory life cycle assessment for emerging photovoltaic technologies.," *Environ. Sci. Technol.*, vol. 48, no. 18, pp. 10531–8, Sep. 2014.

[18] M. L. Marín, a. Jiménez, J. López, and J. Vilaplana, "Thermal degradation of ethylene (vinyl acetate)," *J. Therm. Anal.*, vol. 47, no. 1, pp. 247–258, 1996.

[19] M. Held, "Life cycle assessment of CdTe module recycling," in *24th EU PVSEC Conference*, 2009, pp. 2370–2375.

[20] A. Babakhani, F. Rashchi, A. Zakeri, and E. Vahidi, "Selective separation of nickel and cadmium from sulfate solutions of spent nickel-cadmium batteries using mixtures of D2EHPA and Cyanex 302," *J. Power Sources*, vol. 247, pp. 127–133, 2014.

[21] Ehsan Vahidi et Al., "Modeling of synergistic effect of Cyanex 302 and D2EHPA on separation of nickel and cadmium from sulfate leach liquors of spent Ni–Cd batteries," *Eng. Technol.*, vol. 6, no. 12, p. 53, 2012.

[22] V. Kumar, M. Kumar, M. K. Jha, J. Jeong, and J. C. Lee, "Solvent extraction of cadmium from sulfate solution with di-(2-ethylhexyl) phosphoric acid diluted in kerosene," *Hydrometallurgy*, vol. 96, no. 3, pp. 230–234, 2009.

[23] W. Wang and V. Fthenakis, "Kinetics study on separation of cadmium from tellurium in acidic solution media using ion-exchange resins," *J. Hazard. Mater.*, vol. 125, no. 1–3, pp. 80–88, 2005.

[24] V. Fthenakis and W. Wang, "System and method for separating tellurium from cadmium waste," US7731920 B2, 2010.

[25] P. Sinha, M. Cossette, and J.-F. Ménard, "End-of-Life CdTe PV Recycling with Semiconductor Refining," in *PVSEC 2012*, pp. 8–11.

[26] PRe Consultants, "Simapro version 8.0.3.14," 2015. [Online]. Available: http://www.pre-sustainability.com/simapro.

[27] M. Goedkoop, R. Heijungs, M. Huijbregts, A. De Schryver, J. Struijs, and R. van Zelm, "ReCiPe 2008 - A life cycle impact assessment method which comprises harmonised category indicators at the midpoint and the endpoint level," 2013.

[28] V. Prado-Lopez, T. P. Seager, M. Chester, L. Laurin, M. Bernardo, and S. Tylock, "Stochastic multi-attribute analysis (SMAA) as an interpretation method for comparative life-cycle assessment (LCA)," *Int. J. Life Cycle Assess.*, vol. 19, no. 2, pp. 405–416, 2014.

[29] A. Saltelli, M. Ratto, T. Andres, J. C. Francesca Campolongo, D. Gatelli, M. Saisana, and S. Tarantola, "Global Sensitivity Analysis: The Primer," 2008, pp. 159–167.

[30] C. Zeng, A. Ramos-Ruiz, J. a. Field, and R. Sierra-Alvarez, "Cadmium telluride (CdTe) and cadmium selenide (CdSe) leaching behavior and surface chemistry in response to pH and O2," *J. Environ. Manage.*, vol. 154, pp. 78–85, 2015.

[31] M. Pourbaix, *Atlas of electrochemical equilibria in aqueous solutions*. 1974.

[32] B. J. McGrattan, "Examining the Decomposition of Ethylene-Vinyl Acetate Copolymers Using TG/GC/IR," *Appl. Spectrosc.*, vol. 48, no. 12, pp. 1472–1476, 1994.

[33] AGC Solar, "SOLITE™ - Extra Clear Patterned Glass For Solar Applications," 2016. [Online]. Available: http://www.agc-solar.com/agc-solar-products/patterned-glass/solite.html.

[34] Specialized Technology Resources, "EVA - STR Photocap15420P/UF," 2016. [Online]. Available: http://www.strsolar.com/UploadedFiles/Files/15420P_2015-01.pdf.

[35] NPC Incorporated, "Photovoltaic Module Laminator LM-110X 160-S."

[36] Vulcan, "Vulcan Box Furnace - Owner & Operator's Manual." [Online]. Available: http://www.coleparmer.com/Assets/manual_pdfs/33855-10.pdf.

[37] Sigma Aldrich, "1,2-Dichlorobenzene (99%, anhydrous)," 2016. [Online]. Available: http://www.sigmaaldrich.com/catalog/product/sial/240664?lang=en&region=US.

[38] Sigma Aldrich, "Toluene (99.8%, anhydrous)," 2016. [Online]. Available: http://www.sigmaaldrich.com/catalog/product/sial/244511?lang=en&region=US.

[39] Sigma Aldrich, "Trichloroethylene (>=99%)," 2016. [Online]. Available: http://www.sigmaaldrich.com/catalog/product/aldrich/133124?lang=en&region=US.

[40] Fisher Scientific, "FS60 Ultrasonic Cleaner." [Online]. Available: https://fscimage.fishersci.com/cmsassets/downloads/segment/Scientific/pdf/fisher_ultrasonic_cleaner_data.pdf?&storeId=10652.

[41] V. M. Fthenakis and W. Wang, "Extraction and separation of Cd and Te from cadmium telluride photovoltaic manufacturing scrap," *Prog. Photovoltaics Res. Appl.*, vol. 14, no. 4, pp. 363–371, 2006.

[42] A. Mezei, M. Ashbury, M. Canizares, R. Molnar, H. Given, A. Meader, K. Squires, F. Ojebuoboh, T. Jones, and W. Wang, "Hydrometallurgical recycling of the semiconductor material from photovoltaic materials—part II: metal recovery," in *Hydrometallurgy*, 2008, pp. 224–237.

[43] B. P. Weidema and M. S. Wesnæs, "Data quality management for life cycle inventories—an example of using data quality indicators," *J. Clean. Prod.*, vol. 4, no. 3–4, pp. 167–174, 1996.

[44] B. P. Weidema, C. Bauer, R. Hischier, T. Nemecek, J. Reinhard, C. O. Vadenbo, and G. Wernet, "Overview and methodology. Data quality guideline for the ecoinvent database version 3," *Ecoinvent Rep. 1(v3). St. Gall. ecoinvent Cent.*, pp. 70–78, 2013.

[45] S. Muller, P. Lesage, A. Ciroth, C. Mutel, B. P. Weidema, and R. Samson, "The application of the pedigree approach to the distributions foreseen in ecoinvent v3," *Int. J. Life Cycle Assess.*, 2014.

[46] X. Zhang, M. N. Trame, L. J. Lesko, and S. Schmidt, "Sobol Sensitivity Analysis : A Tool to Guide the Development and Evaluation of Systems Pharmacology Models," *CPT pharmacometrics Syst. Pharmacol.*, vol. 4, no. October 2014, pp. 1–4, 2015.

[47] A. Saltelli, "Global Sensitivity Analysis : An Introduction," in *4th International Conference on Sensitivity Analysis of Model Output (SAMO'04)*, 2004, pp. 27–43.

[48] A. Saltelli, P. Annoni, I. Azzini, F. Campolongo, M. Ratto, and S. Tarantola, "Variance based sensitivity analysis of model output. Design and estimator for the total sensitivity index," *Comput. Phys. Commun.*, vol. 181, no. 2, pp. 259–270, 2010.

[49] A. Saltelli, M. Ratto, T. Andres, J. C. Francesca Campolongo, D. Gatelli, M. Saisana, and S. Tarantola, "Global Sensitivity Analysis: The Primer," 2008, pp. 164–167.

[50] Fraunhofer Institute for Solar Energy Systems ISE, "Photovoltaics Report," no. August, p. 4, 2015.

[51] Solar Energy Industries Association (SEIA), "Solar Market Insight Report 2016 Q2,"

2016. [Online]. Available: http://www.seia.org/research-resources/solar-market-insight-report-2016-q2.

[52] M. B. Maurin, L. W. Dittert, and A. A. Hussain, "Thermogravimetric Analysis of Ethylene- vinyl Acetate Copolymers with Fourier Transform Infrared Analysis of the Pyrolysis Products," *Thermochim. Acta*, vol. 186, no. 1, pp. 97–102, 1991.

[53] V. M. Fthenakis, M. Fuhrmann, J. Heiser, a. Lanzirotti, J. Fitts, and W. Wang, "Emissions and encapsulation of cadmium in CdTe PV modules during fires," *Prog. Photovoltaics Res. Appl.*, vol. 13, no. 8, pp. 713–723, Dec. 2005.

[54] European Chemicals Agency (ECHA), "Cadmium telluride," 2010. [Online]. Available: https://www.echa.europa.eu/en/web/guest/registration-dossier/-/registered-dossier/12227/4/3.

APPENDIX A

A. PREVIOUSLY PUBLISHED MATERIAL AND CO-AUTHOR PERMISSION

Chapter 2 was published in *Environmental Science & Technology* and appears as published. The citation for the article is: Ravikumar, D., Seager, T. P., Chester, M. V., & Fraser, M. P. (2014). Intertemporal cumulative radiative forcing effects of photovoltaic deployments. *Environmental Science & Technology*, 48(17),10010-10018.

Chapter 4 has been published in *Progress in Photovoltaics: Research and Applications* and appears as published. The citation for the article is: Ravikumar, D., Sinha, P., Seager, T. P., & Fraser, M. P. (2016). An anticipatory approach to quantify energetics of recycling CdTe photovoltaic systems. *Progress in Photovoltaics: Research and Applications*, 24(5),735-746.

All co-authors have granted their permission for the use of this material in this dissertation.

APPENDIX B

B. SUPPORTING INFORMATION FOR CHAPTER 2

1. Calculation of Radiative Efficiencies and CRF impacts

The radiative forcing calculations in the model are performed for emissions measured in kilograms. Therefore, to convert radiative efficiency values from W m^{-2} ppb^{-1} to W m^{-2} kg^{-1} they are multiplied by $(Ma/Mi)*(10^9/Tm)$[1] where,

- Ma is the mean molecular weight of air (28.97 kg $kmol^{-1}$)
- Mi is the molecular weight of the GHG species (kg)
- Tm is the total mass of the atmosphere(5.1352×10^{18}kg) [1]

A	B	C	D
GHG	Molecular mass Mi (kg $kmol^{-1}$)	Radiative efficiency aghg (W m^{-2} ppb^{-1}) [1,2]	Radiative efficiency aghg (W m^{-2} kg^{-1})
CO2	44.01	1.37E-05	1.75E-15
CH4	16.04	3.7E-04	1.30E-13
HFC-152a	66.05	9E-02	7.68E-12
SF6	146.06	5.2E-01	2.00E-11

Table S8 Radiative Efficiencies for CO2, CH4, HFC-152a, SF6.

The time sensitive CRF impact of CO_2 emissions for a ten year horizon is tabulated in Table S9.

A	B	C	D	E
Atmospheric residence time (years)	CO_2 remaining in the atmosphere (kg)	Radiative Forcing (W m^{-2})	CRF impact 'kt'(W m^{-2} yr)	kt allocated to CO_2 emitted in year
1	8.75E-01	1.50E-15	1.50E-15	10
2	8.11E-01	1.39E-15	2.89E-15	9
3	7.74E-01	1.32E-15	4.21E-15	8
4	7.49E-01	1.28E-15	5.50E-15	7
5	7.29E-01	1.25E-15	6.75E-15	6
6	7.13E-01	1.22E-15	7.97E-15	5
7	6.98E-01	1.19E-15	9.17E-15	4
8	6.84E-01	1.17E-15	1.03E-14	3
9	6.71E-01	1.15E-15	1.14E-14	2
10	6.58E-01	1.12E-15	1.26E-14	1

Table S9 Calculation of CRF impacts for 1 kg of CO_2 emitted for each year between year 1 and 10. The CRF impacts are measured over a 10 year period.

Column B values are calculated by substituting 't' (in equation 2 in main paper) with the corresponding Column A values. Column C values are calculated by multiplying the corresponding column B values by a_{co2}, the radiative efficiency of CO_2 (column D in Table S8). Column D values are the cumulative sum of column C values until that year. The CRF impact of 'm' kg of CO_2 emitted in year 'n' (column E) is calculated by multiplying 'm' by the corresponding value in column D. For example if 5 kg of CO_2 is emitted in year 4 the CRF impact is 5*9.17E-15 (row 7 in column D).

The CRF impacts for CH_4, HFC-152a, SF_6 emissions are similarly calculated in Table S10, Table S11 and Table S12, respectively. Column B values in the following 3 tables are calculated using equation 3 from the main paper and perturbation time (τ) values of 12, 1.4 and 3200 years for CH_4, HFC-152a and SF_6 , respectively [2].

A	B	C	D	E
Atmospheric residence time (years)	CH_4 remaining in the atmosphere (kg)	Radiative Forcing (W m^{-2})	CRF impact 'kt'(W m^{-2} yr)	kt allocated to CH_4 emitted in year
1	9.20E-01	1.68E-13	1.68E-13	10
2	8.46E-01	1.55E-13	3.23E-13	9
3	7.79E-01	1.42E-13	4.65E-13	8
4	7.17E-01	1.31E-13	5.96E-13	7
5	6.59E-01	1.20E-13	7.17E-13	6
6	6.07E-01	1.11E-13	8.27E-13	5
7	5.58E-01	1.02E-13	9.29E-13	4
8	5.13E-01	9.38E-14	1.02E-12	3
9	4.72E-01	8.63E-14	1.11E-12	2
10	4.35E-01	7.94E-14	1.19E-12	1

Table S10 Calculation of CRF impacts for 1 kg of CH_4 emitted for each year between year 1 and 10. The CRF impacts are measured over a 10 year period. Column C values are multiplied by a factor of 1.4 (only in this table) to account for the indirect impacts of methane emissions on ozone and stratospheric water vapor concentrations [3]

A	B	C	D	E
Atmospheric residence time (years)	HFC-152a remaining in the atmosphere (kg)	Radiative Forcing (W m^{-2})	CRF impact 'kt'(W m^{-2} yr)	kt allocated to HFC-152a emitted in year
1	4.90E-01	3.76E-12	3.76E-12	10
2	2.40E-01	1.84E-12	5.60E-12	9
3	1.17E-01	9.01E-13	6.50E-12	8
4	5.74E-02	4.41E-13	6.94E-12	7
5	2.81E-02	2.16E-13	7.16E-12	6
6	1.38E-02	1.06E-13	7.26E-12	5
7	6.74E-03	5.17E-14	7.32E-12	4
8	3.30E-03	2.53E-14	7.34E-12	3
9	1.61E-03	1.24E-14	7.35E-12	2
10	7.90E-04	6.07E-15	7.36E-12	1

Table S11 Calculation of CRF impacts for 1 kg of HFC-152a emitted for each year between year 1 and 10. The CRF impacts are measured over a 10 year period.

A	B	C	D	E
Atmospheric residence time (years)	SF_6 remaining in the atmosphere (kg)	Radiative Forcing (W m^{-2})	CRF impact 'kt'(W m^{-2} yr)	kt allocated to SF_6 emitted in year
1	9.99E-01	2.01E-11	2.01E-11	10
2	9.99E-01	2.01E-11	4.02E-11	9
3	9.99E-01	2.01E-11	6.03E-11	8
4	9.98E-01	2.01E-11	8.03E-11	7
5	9.98E-01	2.01E-11	1E-10	6
6	9.98E-01	2.01E-11	1.2E-10	5
7	9.98E-01	2.01E-11	1.41E-10	4
8	9.97E-01	2.00E-11	1.61E-10	3
9	9.97E-01	2.00E-11	1.81E-10	2
10	9.97E-01	2.00E-11	2.01E-10	1

Table S12 Calculation of CRF impacts for 1 kg of SF_6 emitted for each year between year 1 and 10. The CRF impacts are measured over a 10 year period.

2. Data Assumptions for the Optimization Framework

China is assumed to be the manufacturing location for monocrystalline Silicon (mSi) and polycrystalline Si (pSi) modules as around 60% of the world's Si PV modules are manufactured in China and 11 among the top 15 PV module manufacturers are in China [4]. First Solar is the only thin film PV manufacturer in the top 10 PV manufacturers worldwide [5]. Malaysia is assumed to be the manufacturing location for CdTe modules as 70% of First Solar's modules are produced in Malaysia [6]. The degradation in the module performance over time is assumed to be 0.7%/year [7]. The following values are used in the optimization framework

Parameter	Value	Equation in the main paper using this parameter	Source
MCIchina mono Si in 2011	2,870,000 (grams CO_2e /kWp)	4	[7].
MCIchina poly Si in 2011	1,590,000 (grams CO_2e /kWp)	4	[7]
MCImalayisa CdTe in 2011	498,000 (grams CO_2e /kWp)	4	[7] has reported a value of 630,000 g/ kWp based on manufacturing conditions in China. This value is multiplied by a ratio of the current grid mixes in Malaysia (909 g/kWh from [8]) and China (1,148 g/kWh from [8]) as CdTe is assumed to be manufactured in Malaysia.
DGI California 2007	481 (CO_2e g/kWh)	5,6	[8]
DGI Wyoming 2007	1,105 (CO_2e g/kWh)	5,6	[8]
pr	0.75	5,6	[9]
Irr California	2,000 (kwh/m^2 /year)	5,6	[10]
Irr Wyoming	1,700 (kwh/m^2 /year)	5,6	[10]
op	.1	5,6	[11]
tl	.07	5,6	[12]

Table S13 Values of parameters used for optimizing PV deployment strategy for minimal CRF impacts

The CO_2e emissions per kWh of electricity produced in California and Wyoming have not shown a consistent trend from 2001 to 2009 [13]. An annual decrease of 2% is assumed for the period from 2007 to 2016. This annual decrease is comparable to the 17% GHG emission reductions mandated by the American Climate and Energy Security Act for the period between 2005 and 2020 [14].

3. PV technology improvements

As PV technology improves, manufacturing GHG emissions (MCI) decrease over time. The base value for MCI is assumed to be in the year 2011 (Table S13). MCI value in year 't' (MCIt) is (i) directly proportional to the manufacturing energy (MEt) used to manufacture the PV module (MJ/m^2) and, (ii) inversely proportional to the module efficiency (efft) as increasing module efficiencies reduce material and manufacturing energy requirement which decreases manufacturing GHG emissions. Thus, the MCIt value for any year 't' between 2007 and 2017 is modelled by the equation,

$$MCI_t = MCI_{2011} \times (ME_t/ME_{2011}) \times (eff_{2011}/eff_t) \qquad \text{(SI 1)}$$

ME values for mSi, pSi and CdTe were 6200 (including 500 MJ for the module frame in 2000 [15]), 3700 (in 2005 [16]) and 1200 MJ/ m^2 (in 2005 [16]),respectively. These values decreased to 4697 (in 2011 [7]), 2624 (in 2011 [7]) and 940 MJ/ m^2 (in 2011 [7]), respectively. Based on this, ME is assumed to decrease annually by 2.5%, 5.5% and 4% for mSi, pSi and CdTe, respectively.

Module efficiency values for mSi and pSi in 2007 were 13.7% and 13.1% and increased to 15.1% and 14.7% in 2012, respectively [7]. Therefore, module efficiency is

assumed to increase annually by 2% and 1.5% for mSi and pSi, respectively. CdTe module efficiencies between 2007 and 2017 were based on data from de Wild-Scholten [7].

Based on these assumptions and equation (SI 1) the MCI values for mSi, pSi and CdTe are shown in Table S14, Table S15 and Table S16, respectively.

Year	Module efficiency (%)	Manufacturing energy ME (MJ/ m^2)	Manufacturing emissions MCI (CO_2e g/kWp)
2007	13.7	5198	3,430,873
2008	13.9	5068	3,296,970
2009	13.9	4941	3,214,546
2010	14.4	4817	3,025,356
2011 (base year)	14.8	4697	2,870,000
2012	15.1	4580	2,742,656
2013	15.4	4465	2,621,656
2014	15.7	4353	2,505,995
2015	16.0	4245	2,395,436
2016	16.3	4139	2,289,755
2017	16.7	4035	2,188,737

Table S14 Technology improvements (decreasing MCI) for mSi modules

Year	Module efficiency (%)	Manufacturing energy ME (MJ/ m^2)	Manufacturing emissions MCI (CO_2e g/kWp)
2007	13.1	3290	2,145,941
2008	13.3	3109	1,997,419
2009	13.5	2938	1,859,597
2010	13.7	2777	1,731,665
2011 (base year)	14.1	2624	1,590,000
2012	14.7	2480	1,441,221
2013	14.9	2343	1,341,827
2014	15.1	2214	1,249,287
2015	15.4	2093	1,163,129
2016	15.6	1978	1,082,914
2017	15.8	1869	1,008,230

Table S15 Technology improvements (decreasing MCI) for pSi modules

Year	Module efficiency (%)	Manufacturing energy ME (MJ/ m^2)	Manufacturing emissions MCI (CO_2e g/kWp)
2007	10.4	1106	670,900
2008	10.7	1062	626,006
2009	11	1019	584,576
2010	11.3	978	546,294
2011 (base year)	11.9	939	498,000
2012	12.7	902	447,965
2013	13.1	866	416,915
2014	14.2	831	369,234
2015	15.6	798	322,654
2016	16.6	766	291,088
2017	17.1	735	271,274

Table S16 Technology improvements (decreasing MCI) for CdTe modules

4. Optimal Deployment Strategy for California and Wyoming

Optimization was carried out in Matlab using the Global Optimization Toolbox.

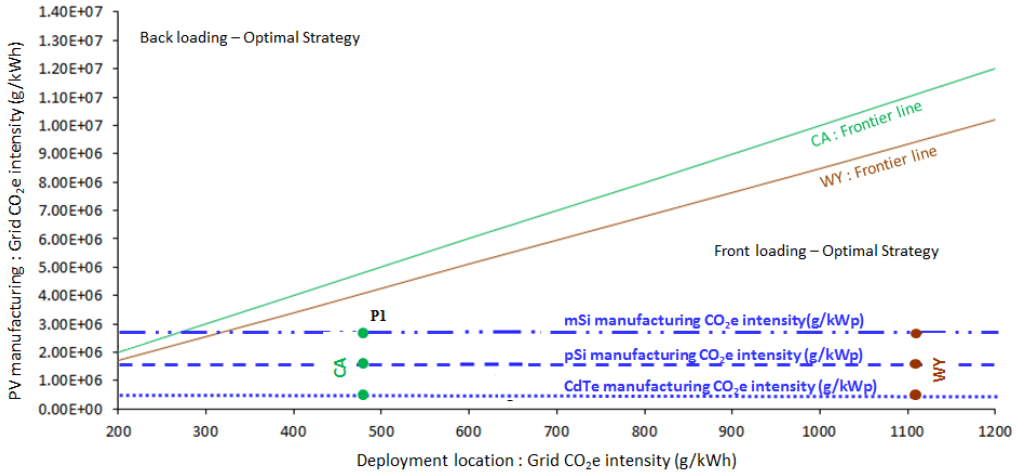

Figure S29 Optimal PV deployment strategy for minimized CRF impact. The Y-axis represents the CO_2e intensity (g/kWp) of manufacturing PV modules and X-axis represents the grid CO_2e intensity (g/kWh) at the deployment location. Frontier lines separate the plot into two optimal deployment strategy zones. The optimal deployment strategy is decided by plotting the CO_2e intensity of manufacturing energy (Y value) and the grid CO_2e intensity at the deployment location (X value) on the graph. If the plotted point is above the frontier line then back loading is the optimal strategy else front loading is the optimal strategy. The three blue lines depict the CO_2e intensity of manufacturing mSi, pSi (in China) and CdTe (in Malaysia). For example, consider a scenario where PV targets in California are met by importing only mSi modules from China. The intersection is at the point 'P1'. The frontier line for this scenario is the solid green line. This corresponds to a front loading strategy as this point lies below the solid green frontier line. Front loading is the optimal strategy for modules manufactured in China (mSi and pSi) or Malaysia (CdTe) are deployed in California or Wyoming. These are depicted by the six points.

Since mSi and CdTe represent the most and least GHG intensive PV systems to manufacture, respectively, the CO_2 intensity of manufacturing a PV deployment mix that relies on all the three technologies will be represented by a horizontal line lying between the blue lines for mSi and CdTe. Front loading will be the preferred strategy across the two states for any technology mix since the PV manufacturing GHG intensity line for the technology mix will lie below the blue line for mSi. The

frontier line for California is above that of Wyoming as the solar irradiation in California is higher (Table S13) and this increases the PV electricity generation and the grid electricity CO_2 that is displaced. Therefore, for the same PV capacity that is deployed, the probability of Front Loading being the favorable strategy in California is higher when compared to Wyoming. This is reflected in the increased area covered by the front loading region for California when compared to Wyoming.

5. GHG and CRF payback times in California and Wyoming for all scenarios

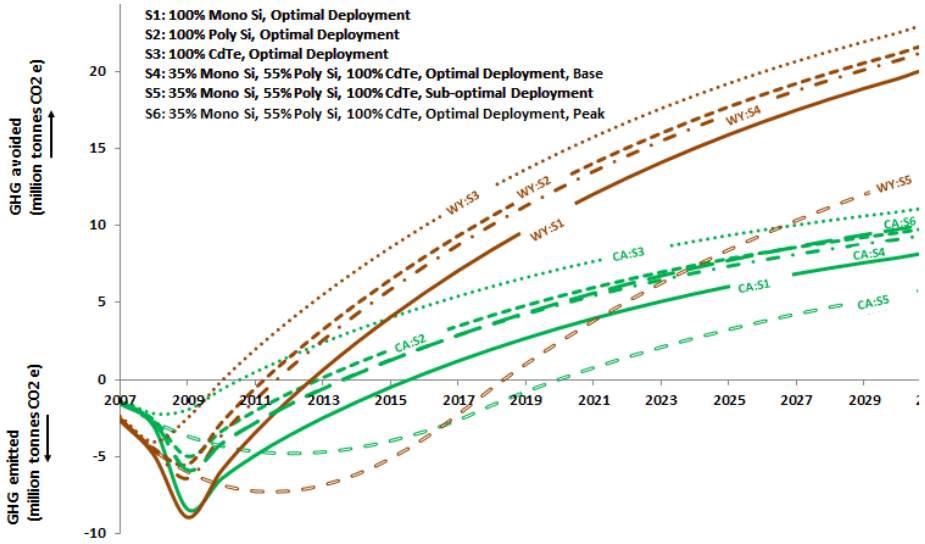

Figure S30 GHG payback times for all scenarios in CA (green) and WY(brown). In optimal deployment, 81MW and 169 MW are deployed in 2007 and 2008 and the remaining capacity of 1689 MW is deployed in 2009. For sub-optimal deployment, 81MW and 169 MW are deployed in 2007 and 2008 and the remaining capacity of 1689 MW is equally deployed between 2009 and 2016.

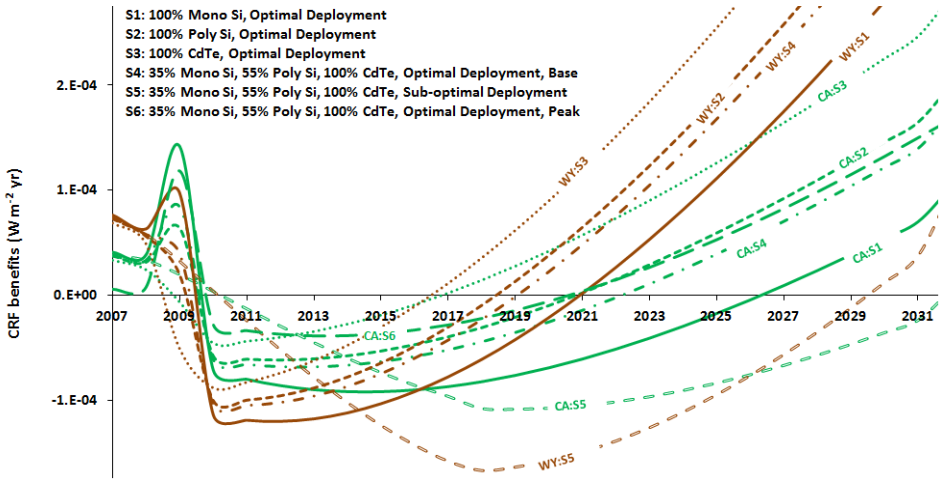

Figure S31 CRF payback times for all scenarios in CA and WY. Optimal deployment and sub-optimal deployments are the same as in Figure S30. CRF impacts of manufacturing emissions and emissions due to the continued reliance on fossil fuels (for sub-optimal deployment) represent PV CRF costs. The CRF impacts avoided when PV electricity offsets grid electricity represent the CRF benefits. If the curve is below the X axis then CRF costs exceed CRF benefits of deploying the PV module and if the curve is above the X axis then CRF benefits exceed CRF costs.

6. CRF impacts of SO2 and NO_x emissions

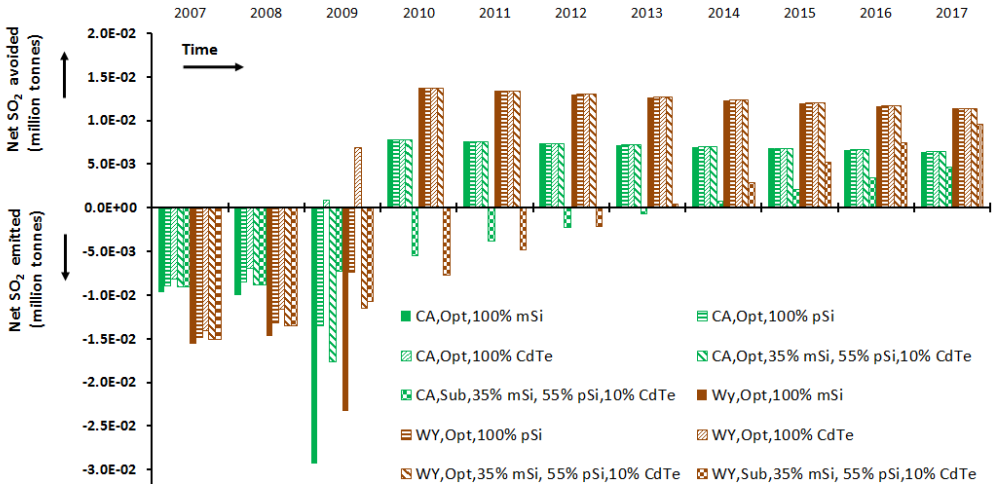

Figure S32 Net SO_2 emitted during PV manufacturing in China/Malaysia and avoided during deployments in California/Wyoming. Annual capacity additions for Optimal (Opt) and sub-optimal (Sub) scenarios are explained in Figure S30.

The SO_2 emitted during PV manufacturing and avoided at the deployment location are determined by multiplying the CO_2 emissions (per kWh electricity used and avoided) by the ratio of SO_2 and CO_2 emitted per kWh for grid electricity in China, Wyoming, California. This ratio is 0.0082 (for China), 0.0069 (for Wyoming) and 0.0086 (for California). ((i) Electricity mix/CN U, (ii) eGrid, RMPA, 2008/RNA U, and (iii) eGrid, CAMX, 2008/RNA U in Simapro).

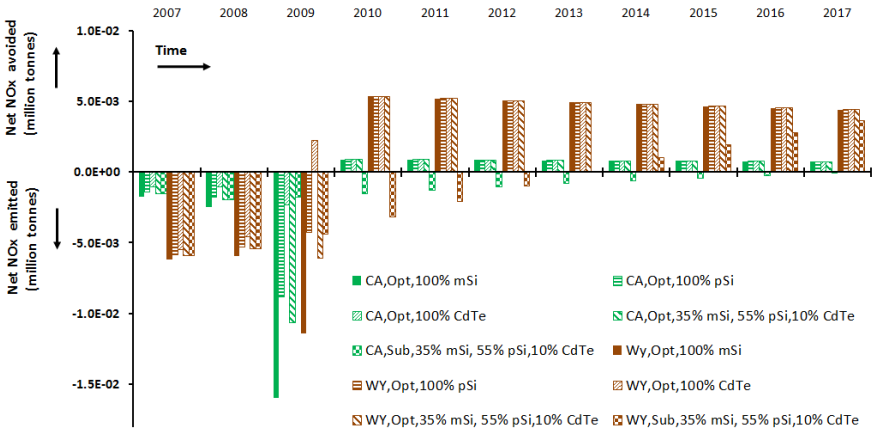

Figure S33 Net NO_x emissions over the PV manufacturing and use-phase. Net emission calculations are the same as in Figure S32.

The method for calculating NO_x emitted during PV manufacturing and avoided at the deployment location is identical to net SO_2 emission calculations. The NO_x / CO_2 ratio per kWh of grid electricity is 0.0037 in China, 0.0027 in Wyoming and 0.001 in California ((i) Electricity mix/CN U , (ii) eGrid, RMPA, 2008/RNA U, and (iii) eGrid, CAMX, 2008/RNA U in Simapro).

Emission	Global mean annual radiative forcing (W m^{-2})	Global mean annual emissions	Radiative Efficiency (W m^{-2} kg^{-1})
NO_x	-0.15 [17]	48.8 Tg [18]	-3.07E-12
SO_2	-0.4 [17]	100 Tg SO_2 [19]	-4E-12

Table S17 Radiative efficiency for NO_x and SO_2. The negative sign indicates a net cooling impact.

7. SimaPro model to disaggregate emissions reported in CO_2e into a GHG inventory for mSi, pSi and CdTe manufacturing

The steps to model mSi and pSi manufacturing in China using SimaPro are shown in Table S18 and Table S19. SimaPro defaults to a European grid mix for each step and this was replaced with a Chinese grid mix (Electricity mix/CN U in the SimaPro database) to simulate PV manufacturing in China. The GHG inventory for CdTe manufacturing (modeled in Table S20) was calculated using the Chinese grid mix which was then multiplied by a ratio of the current grid mixes in Malaysia (909 g/kWh [8]) and China (1148 g/kWh [8]).

SimaPro Process	Description	Inventory Amount per kWp	Assumptions based on the SimaPro database
MG-silicon, at plant/NO U	Gate to gate inventory for production of MG-silicon from silica sand including materials, energy use, wastes and air emissions.	5.73 kg	1 kg of solar grade Silicon requires 1.13 kg of MG-Silicon. Therefore, 5.07 kg requires 5.73 kg of MG-Silicon.
Silicon, solar grade, modified Siemens process, at plant/RER U	Gate to gate inventory for the production of high purity polycrystalline silicon from MG-silicon in actual processes.	5.07 kg	1 kg of CZ single crystalline silicon requires 1.07 kg of solar grade Silicon. Therefore, 4.74 kg requires 5.07 kg of solar grade Silicon.
CZ single crystalline silicon, photovoltaics, at plant/RER U	Gate to gate inventory for an improved Czochralski process.	4.74 kg	1 m^2 of mSi wafer requires 1.0748 kg of CZ single crystalline silicon. Therefore, 4.41 m^2 requires 4.74 kg of CZ single crystalline silicon.
Single-Si wafer, photovoltaics, at plant/RER U	Sawing and cleaning of wafers.	4.41 m^2	1 m^2 of mSi PV cell requires 1.06 m^2 of mSi wafer. Therefore, 4.16 m^2 requires 4.41 m^2 of mSi wafer.
Photovoltaic cell, single-Si, at plant/RER U	Cleaning, damage etching, texture etching, covering of backside, phosphor dotation, phosphor glass etching, printing of contacts, cleaning and quality testing.	4.16 m^2	1 m^2 of mSi wafer PV panel requires 0.93241 m^2 of mSi PV cells. Therefore, 4.46 m^2 requires 4.16 m^2 of mSi PV cells.
Photovoltaic panel, single-Si wafer	Production of the cell matrix, cutting of foils and washing of glass, production of laminate, isolation. Aluminum frame of the panel. Disposal after end of life.	4.46 m^2	1 m^2 of a mSi PV panel has a rated capacity of 224 Wp. Therefore, 1 kWp requires 4.46 m^2 of mSi panel.

Table S18 SimaPro model to disaggregate CO_2e into a GHG inventory when a 1 kWp mSi module is manufactured in China

SimaPro Process	Description	Inventory Amount per kWp	Assumptions based on the SimaPro database
MG-silicon, at plant/NOU	Gate to gate inventory for production of MG-silicon from silica sand including materials, energy use, wastes and air emissions.	6.91 kg	1 kg of solar grade Silicon requires 1.13 kg of MG-Silicon. Therefore, 6.12 kg requires 6.91 kg of MG-Silicon.
Silicon, solar grade, modified Siemens process, at plant/RERU	Gate to gate inventory for the production of high purity polycrystalline silicon from MG-silicon in actual processes.	6.12 kg	1 kg of a multi-Si cast requires 1.14 kg of solar grade Silicon. Therefore, 5.37 kg requires 6.12 kg of solar grade Silicon.
Silicon, multi-Si, casted, at plant/RERU	Purified silicon is melted in cast in a graphite box. Than edges are sliced and blocks are sawn.	5.37 kg	1 m^2 of a multi-Si wafer requires 1.14 kg of multi-Si cast. Therefore, 4.71 m^2 requires 5.37 kg of multi-Si cast.
Multi-Si wafer, at plant/RERU	Sawing and cleaning of wafers. The process data includes electricity use, water and working material consumption.	4.71 m^2	1 m^2 of a pSi PV cell requires 1.06 $m^2$of multi-Si wafer. Therefore, 4.44 m^2 requires 4.71 m^2 of multi-Si wafer.
Photovoltaic cell, multi-Si, at plant/RERU	Cleaning, damage etching, texture etching, covering of backside, phosphor dotation, phosphor glass etching, printing of contacts, cleaning and quality testing.	4.44 m^2	1 m^2 of a pSi panel requires 0.93241 m^2 of pSi PV cell. Therefore, 4.76 m^2 requires 4.44 m^2 of pSi PV cells.
Photovoltaic panel, multi-Si, at plant/RER/IU	Production of the cell matrix, cutting of foils and washing of glass, production of laminate, isolation. Aluminium frame of the panel. Disposal after end of life.	4.76 m^2	1 m^2 of a pSi panel has a rated capacity of 210 Wp. Therefore, 1 kWp requires 4.76 m^2 of pSi panel.

Table S19 SimaPro model used to disaggregate CO_2e into a GHG inventory when a 1 kWp pSi module is manufactured in China

SimaPro Process	Description	Inventory Amount per kWp	Assumptions based on the SimaPro database
Cadmium telluride, semiconductor-grade, at plant/US U		0.66 kg	Each module requires 0.043 kg of CdTe semiconductor; therefore, 15.38 modules require 0.66 kg.
Photovoltaic laminate, CdTe, at plant/DE/I	Electricity including overhead operations and office use, materials, transport of materials, infrastructure. Module processing includes film deposition, etching, cleaning and module assembly. Disposal after end of life.	15.38 modules	Each module has a rated capacity of 65Wp. Therefore, 1 kWp requires 15.38 modules.

Table S20 SimaPro model to disaggregate CO_2e into GHG inventory when a 1 kWp CdTe module is manufactured in Malaysia

The disaggregated GWP_{100} inventory for manufacturing 1 kWp of mSi modules based on the SimaPro model (Table S18) is shown in column B in Table S21. Column D is calculated by

$$(MCI_{\text{china mono Si}} \times GHG_{gwp\%})/GHG_{gwp100} \quad \text{(SI 2)}$$

where, GHGgwp% = Column B value, GHGgwp100 = Column C value. Based on the emission mass in column D the 10 year CRF value is calculated as explained in the introduction section in the main paper. Similar calculations are performed for pSi (Table S22) and CdTe (Table S23) modules.

A	B	C	D	E
GHG	% of total GWP_{100}	GWP_{100}	Emission mass (grams)	% of 10 Year CRF
Carbon dioxide, fossil	8.39E+01	1	2.41E+08	6.25E+01
Methane, fossil	1.25E+01	25	1.43E+06	3.48E+01
Sulfur hexafluoride	1.63E+00	22800	2.05E+02	8.06E-01
Ethane, 1,1-difluoro-, HFC-152a	1.24E-01	124	2.88E+03	6.09E-01
Methane, chlorodifluoro-, HCFC-22	1.32E-01	1810	2.10E+02	3.65E-01
Methane, tetrafluoro-, CFC-14	6.87E-01	7390	2.67E+02	3.36E-01
Dinitrogen monoxide	4.28E-01	298	4.13E+03	3.01E-01
Ethane, hexafluoro-, HFC-116	3.83E-01	12200	9.02E+01	1.88E-01
Methane, trifluoro-, HFC-23	6.85E-02	14800	1.33E+01	3.93E-02
Ethane, 1,1,1,2-tetrafluoro-, HFC-134a	9.07E-03	1430	1.82E+01	2.26E-02
Methane, dichlorodifluoro-, CFC-12	1.93E-02	10900	5.09E+00	1.42E-02
Methane, tetrachloro-, CFC-10	4.00E-03	1400	8.20E+00	6.38E-03
Chloroform	6.61E-04	31	6.12E+01	3.19E-03
Methane, bromochlorodifluoro-, Halon 1211	2.71E-04	1890	4.11E-01	6.15E-04
Methane, bromotrifluoro-, Halon 1301	5.39E-04	7140	2.17E-01	4.78E-04
Ethane, 1,2-dichloro-1,1,2,2-tetrafluoro-, CFC-114	5.66E-04	10000	1.62E-01	3.21E-04
Methane, trichlorofluoro-, CFC-11	1.12E-04	4750	6.78E-02	1.23E-04
Methane, monochloro-, R-40	9.56E-06	13	2.11E+00	4.63E-05
Methane, dichloro-, HCC-30	5.61E-06	8.7	1.85E+00	2.75E-05
Methane, dichlorofluoro-, HCFC-21	2.20E-06	151	4.18E-02	1.07E-05
Ethane, 1,1,1-trichloro-, HCFC-140	8.86E-08	146	1.74E-03	3.76E-07
Ethane, 1,1,2-trichloro-1,2,2-trifluoro-, CFC-113	3.89E-09	6130	1.82E-06	3.05E-10
Methane, bromo-, Halon 1001	4.25E-14	5	2.44E-08	1.99E-13

Table S21 Disaggregating CO_2e values into a GHG inventory for manufacturing a 1 kWp mSi module.

A	B	C	D	E
GHG	% contribution to total GWP_{100}	GWP_{100}	Emission mass (grams)	% contribution to 10 Year CRF
Carbon dioxide, fossil	8.37E+01	1	1.33E+06	6.17E+01
Methane, fossil	1.23E+01	25	7.82E+03	3.40E+01
Sulfur hexafluoride	1.89E+00	22800	1.32E+00	1.30E+00
Ethane, 1,1-difluoro-, HFC-152a	1.49E-01	124	1.91E+01	1.01E+00
Methane, chlorodifluoro-, HCFC-22	1.59E-01	1810	1.39E+00	6.06E-01
Methane, tetrafluoro-, CFC-14	8.25E-01	7390	1.77E+00	5.59E-01
Dinitrogen monoxide	3.88E-01	298	2.06E+01	3.78E-01
Ethane, hexafluoro-, HFC-116	4.60E-01	12200	5.99E-01	3.13E-01
Methane, trifluoro-, HFC-23	8.23E-02	14800	8.83E-02	6.53E-02
Ethane, 1,1,1,2-tetrafluoro-, HFC-134a	1.09E-02	1430	1.20E-01	3.75E-02
Methane, dichlorodifluoro-, CFC-12	2.32E-02	10900	3.38E-02	2.36E-02
Methane, tetrachloro-, CFC-10	4.91E-03	1400	5.56E-02	1.08E-02
Chloroform	7.93E-04	31	4.06E-01	5.30E-03
Methane, bromochlorodifluoro-, Halon 1211	2.60E-04	1890	2.18E-03	8.17E-04
Methane, bromotrifluoro-, Halon 1301	5.94E-04	7140	1.32E-03	7.30E-04
Ethane, 1,2-dichloro-1,1,2,2-tetrafluoro-, CFC-114	6.10E-04	10000	9.68E-04	4.79E-04
Methane, trichlorofluoro-, CFC-11	1.35E-04	4750	4.50E-04	2.04E-04
Methane, monochloro-, R-40	1.15E-05	13	1.40E-02	7.71E-05
Methane, dichloro-, HCC-30	6.74E-06	8.7	1.23E-02	4.58E-05
Methane, dichlorofluoro-, HCFC-21	2.64E-06	151	2.77E-04	1.78E-05
Ethane, 1,1,1-trichloro-, HCFC-140	1.06E-07	146	1.15E-05	6.23E-07
Ethane, 1,1,2-trichloro-1,2,2-trifluoro-, CFC-113	4.75E-09	6130	1.23E-08	5.16E-10
Methane, bromo-, Halon 1001	5.10E-14	5	1.62E-10	3.32E-13

Table S22 Disaggregating CO_2e values into a GHG inventory for manufacturing a 1 kWp pSi module.

A	B	C	D	E
GHG	Percentage of GWP_{100}	GWP_{100}	Percentage of 10 Year CRF	Emission mass (grams)
Carbon dioxide	88.6%	1	70.12%	441,228
Methane	9.92%	25	29.37%	1,976
Other GHGs	1.48%	-	0.51%	-

Table S23 Disaggregating CO_2e values into a GHG inventory for manufacturing a 1 kWp CdTe module.

8. SimaPro model to disaggregate emissions reported in CO_2e into a GHG inventory for electricity generation in California and Wyoming

A	B	C	D	E
GHG	% contribution to total GWP_{100}	GWP_{100}	Emission mass (kg)	% contribution to 10 Year CRF
Carbon dioxide, fossil	8.83E+01	1	0.388552	70.4338
Methane	9.78E+00	25	0.001722	29.22909
Dinitrogen monoxide	4.47E-01	298	6.6E-06	0.337086
Methane, dichloro-, HCC-30	3.00E-06	8.7	1.52E-09	1.58E-05
Methane, dichlorodifluoro-, CFC-12	4.99E-07	10900	2.01E-13	3.93E-07
Methane, monochloro-, R-40	1.15E-08	13	3.88E-12	5.95E-08
Ethane, 1,1,1-trichloro-, HCFC-140	1.03E-08	146	3.09E-13	4.66E-08
Methane, tetrachloro-, CFC-10	6.40E-09	1400	2.01E-14	1.09E-08
Chloroform	3.04E-09	31	4.32E-13	1.57E-08
Methane, bromo-, Halon 1001	1.33E-09	5	1.17E-12	6.69E-09

Table S24 Disaggregating CO_2e values into a GHG inventory for 1 kWh of California's electricity mix. Calculations for column D and E values are the same as in Table S21

This study considers only two GHGs - CO_2, CH_4 – for CRF calculations for electricity displaced in California as they contribute 98% and 99.6% of the GWP_{100} inventory and the 10 year CRF impact, respectively (Table S24).

A	B	C	D	E
GHG	% contribution to total GWP_{100}	GWP_{100}	Emission mass (kg)	% contribution to 10 Year CRF
Carbon dioxide, fossil	9.47E+01	1	0.88142	8.34E+01
Methane	5.00E+00	25	0.001862	1.65E+01
Dinitrogen monoxide	2.35E-01	298	2.22E-06	5.91E-02
Methane, dichloro-, HCC-30	7.10E-02	8.7	5.05E-08	2.74E-04
Methane, dichlorodifluoro-, CFC-12	4.72E-05	10900	7.69E-13	7.83E-07
Methane, monochloro-, R-40	9.01E-07	13	3.82E-11	3.06E-07
Ethane, 1,1,1-trichloro-, HCFC-140	5.33E-08	146	2.06E-12	1.62E-07
Chloroform	3.24E-08	31	3.47E-12	6.60E-08
Methane, tetrachloro-, CFC-10	1.42E-08	1400	9.41E-14	2.67E-08
Methane, bromo-, Halon 1001	1.16E-08	5	1.15E-11	3.44E-08

Table S25 Disaggregating CO_2e values into a GHG inventory for 1 kWh of Wyoming's electricity mix. Calculations for column D and E values are the same as in Table S21

This study considers only two GHGs - CO_2, CH_4 – for the CRF calculations for the electricity displaced in Wyoming as they contribute 99% of the GWP_{100} inventory and the 10 year CRF impact (Table S25).

9. Sensitivity of CRF calculations to IPCC's uncertainty range for radiative efficiencies of GHGs

Gas (IPCC radiative efficiency uncertainty range)	Radiative Efficiency – Base value ($W\ m^{-2}\ kg^{-1}$)	Radiative Efficiency - Upper limit value ($W\ m^{-2}\ kg^{-1}$)	Radiative Efficiency - Lower limit value ($W\ m^{-2}\ kg^{-1}$)
CO_2 (+/- 10%)	1.75E-15	1.92E-15	1.57E-15
CH_4 (+/- 17%)	1.30E-13	1.52E-13	1.07E-13
HFC 152a (+/- 10%)	7.68E-12	8.44 E-12	6.91 E-12
SF_6 (+/- 10%)	2.00E-11	2.20E-11	1.80E-11
SO_2 (+/- 50%)	-4E-12	-2E-12	-6E-12
NO_x (+ 116/- 124%)	-3.07E-12	4.91E-13	-6.88E-12

Table S26 Upper and lower limits for radiative efficiencies of GHGs based on IPCC estimates [20]

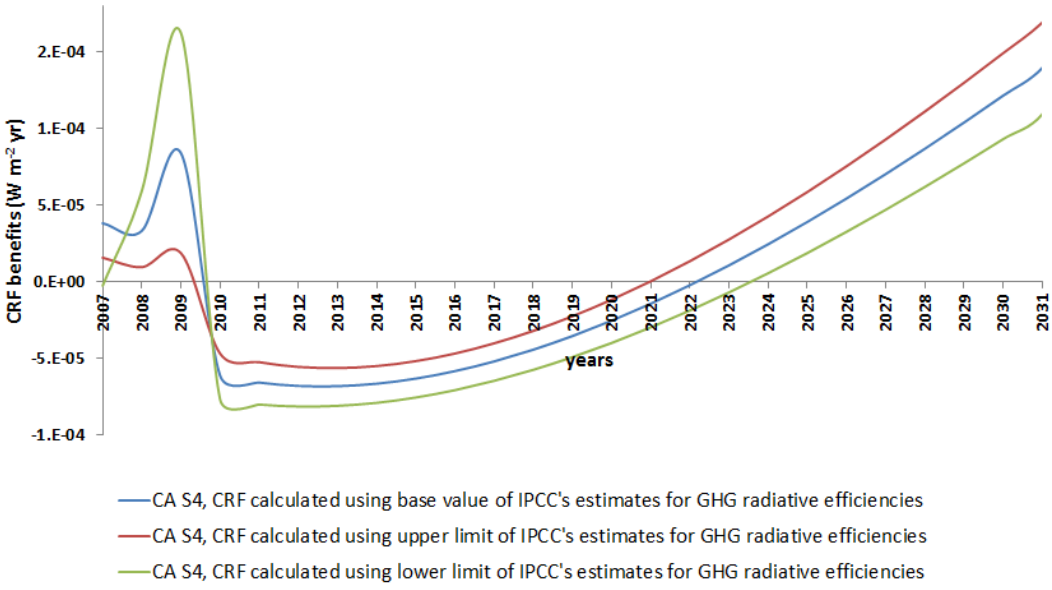

Figure S34 Change in CRF and CRF payback times when the radiative efficiency of GHGs are varied between IPCC's upper and lower limits. CRF impacts of manufacturing emissions and emissions due to the continued reliance on fossil fuels (for sub-optimal deployment) represent PV CRF costs. The CRF impacts avoided when PV electricity offsets grid electricity represent the CRF benefits. If the curve is below the X axis then CRF costs exceed CRF benefits of deploying the PV module and if the curve is above the X axis then CRF benefits exceed CRF costs. All the CRF calculations are performed for scenario CA: S4 (refer Figure S31). The CRF impacts in 2017 and 2031 are greater and lesser than the base scenario by 22% when using the upper and lower radiative efficiency estimates, respectively.

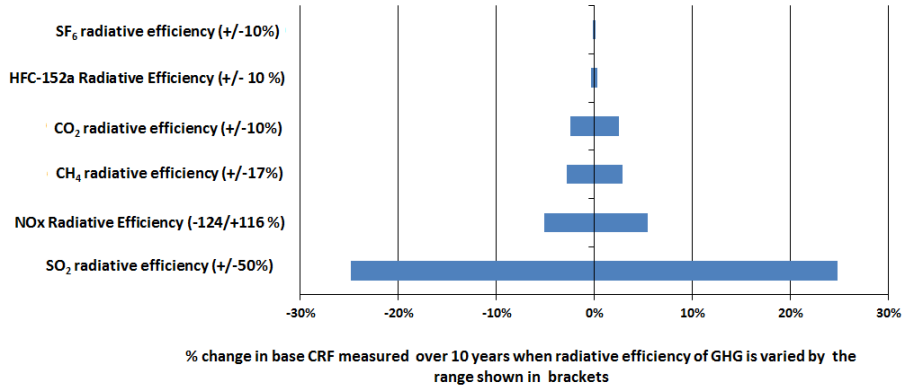

Figure S35 The graph depicts percentage change in CRF (measured in 2017) from the base condition when radiative efficiencies of emissions are varied by a range established by IPCC[20] (shown in brackets). The base scenario's CRF value is represented by the vertical line passing through zero and is identical to the base scenario in Figure 6 in the main paper.

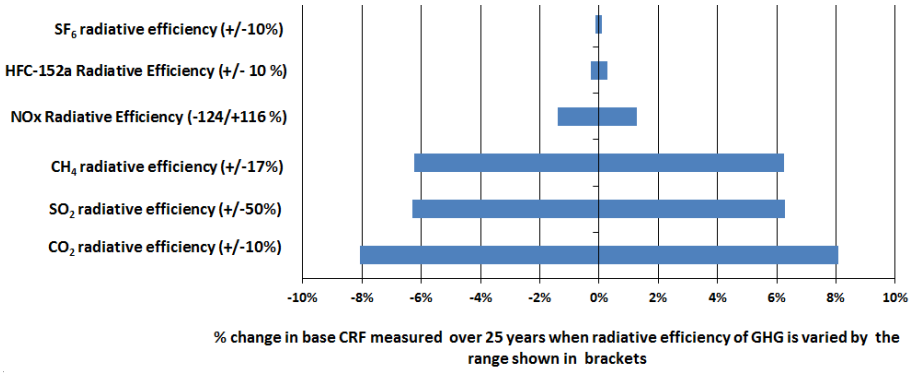

Figure S36 Calculations in Figure S35 are repeated for a 25 year time period.

Among the gases considered, CRF impacts are the most sensitive to radiative efficiency of SO_2 over a 10 year period (Figure S35) and CO_2 over a 25 year period (Figure S36).

10. Acronym List

Acronym	Expansion	Units
$aGHG_t$	GHG emissions avoided in year 't' at the deployment location	grams
a_{ghg}	Radiative efficiency of a GHG	watts m^{-2} kg^{-1}
apd	annual performance degradation for the PV module	%/year
$bGHG_t$	GHG emissions due to BLS in year 't' at the deployment location	grams
BLS	Back loading strategy	
C	Total policy target	kW_p
CA	California	
CdTe	cadmium telluride	
CO_2e	CO_2 equivalent	
CRF	Cumulative Radiative Forcing	W m^{-2} yr
CRF_{av}	CRF benefit due to avoided GHG emissions	W m^{-2} yr
CRF_{bl}	CRF due to back loading	W m^{-2} yr
CRF_{mnf}	CRF due to PV manufacturing GHG emissions	W m^{-2} yr
DGI_t	CO_{2e} intensity of the grid (base load), at the deployment location in the year 't'	CO_{2e} g/kWh
CSI	California Solar Initiative	
eff_t	PV module efficiency in the year 't'	%
EPBT	Energy payback time	years
FLS	Front loading strategy	
GHG	Greenhouse gas	
IPCC	Intergovernmental Panel on Climate Change	
Irr	Annual average solar irradiation at the deployment location	kWh/m^2/year
k_t	CRF impact of one kg of a GHG depending on the year of emission over a ten year period	W m^{-2} yr
kW	Kilowatts	
LCA	Life Cycle Assessment	
M_a	Mean molecular mass of air	kg $kmol^{-1}$
MCI_{t_i}	CO_{2e} intensity of the manufactured PV technology 'i' in the year 't'	CO_{2e} g/kW_p
$MCI_{china\ mono\ Si}$	CO_{2e} intensity of the mono Si PV manufactured in China	CO_{2e} g/kW_p
$MCI_{china\ poly\ Si}$	CO_{2e} intensity of the poly Si PV manufactured in China	CO_{2e} g/kW_p

Acronym	Expansion	Units
$MCI_{malayisa\ CdTe}$	CO_{2e} intensity of the CdTe PV manufactured in Malaysia	CO_{2e} g/kW_p
$mGHG_t$	PV manufacturing GHG emissions in year 't'	grams
ME	Manufacturing energy embedded in the PV module	MJ/m^2
M_i	molecular weight of the GHG species	kg $kmol^{-1}$
mSi	mono-Silicon	
MW	Megawatts	
op	Ratio of energy spent on the operations and maintenance of the PV module to the total energy generated by the PV module	
opt	Optimal PV deployment strategy	
pr	Performance ratio, the ratio between the AC power generated to the rated DC power	
pSi	poly Silicon	
PV	Photovoltaics	
S1	PV deployment Scenario 1. PV targets met using a 100% mSi mix.	
S2	PV deployment Scenario 2. PV targets met using a 100% pSi mix.	
S3	PV deployment Scenario 3. PV targets met using a 100% CdTe mix.	
S4	PV deployment Scenario 4. PV targets met using a 35% mSi, 55% pSi and 10% CdTe mix. Optimal deployment	
S5	PV deployment Scenario 5. PV targets met using a 35% mSi, 55% pSi and 10% CdTe mix. Sub-optimal deployment	
SI	Supplementary information	
Sub	Sub-optimal PV deployment strategy	
tl	transmissions losses during electricity distribution	%
T_m	Total mass of the atmosphere	kg
TH	Time period for CRF calculation	years
W_{t_i}	Capacity of a particular PV technology 'i' deployed in the year 't'	kW_p
WY	Wyoming	
τ	Perturbation time	years

Table 27 Acronym list

REFERENCES

1.Stocker, T. F., Dahe, Q., & Plattner, G. K *IPCC Fifth Assessment Report - Climate Change 2013: The Physical Science Basis (Chapter 8 Supplementary Information Section 8.SM.11.3)*; 2013.

2.Pachauri, R. R., A. IPCC fourth assessment report (Table 2.14). http://www.ipcc.ch/publications_and_data/ar4/wg1/en/ch2s2-10-2.html.

3.Stocker, T. F., Dahe, Q., & Plattner, G. K, IPCC Fifth Assessment Report - Climate Change 2013: The Physical Science Basis (Chapter 8 Supplementary Information Section 8.SM.11.3.2). **2013**.

4.Green Tech Media,GTM Research: Yingli Gains Crown as Top Producer in a 36 GW Global PV Market. http://www.greentechmedia.com/articles/read/Yingli-Gains-Crown-As-Top-Producer-in-a-36-GW-Global-PV-Market.

5.PVTECH Top 10 PV module suppliers in 2012. http://www.pv-tech.org/guest_blog/top_10_pv_module_suppliers_in_2012.

6.Personal Communication with First Solar. 2013.

7.Wild-Scholten, M. J. M. d., Energy payback time and carbon footprint of commercial photovoltaic systems. *Solar Energy Materials and Solar Cells* **2013,** *119*, 296-305.

8.Simparo, Grid CO2 intensity as reported by Simparo. **2013**.

9.Fthenakis, V.; Frischknecht, R.; Raugei, M.; Kim, H.; Alsema, E.; Held, M.; de Wild-Scholten, M., Methodology guidelines on life cycle assessment of photovoltaic electricity. *IEA PVPS Task* **2011,** *12*.

10.NREL National Solar Radiation Data Base - Class I locations. http://rredc.nrel.gov/solar/old_data/nsrdb/1991-2010/hourly/list_by_state.html#C.

11.FirstSolar *Life Cycle Carbon Impacts of Utility Scale Photovoltaic Projects*; 2011.

12.EIA Transmission and Distribution losses in the United States. http://www.eia.gov/tools/faqs/how-much-electricity-lost-transmission-and-distribution-united-states.

13.DOE, U. State Electrcity Profiles. http://www.eia.gov/electricity/state/.

14.EPA *EPA Analysis of the American Clean Energy and Security Act of 2009*; 2009.

15.Alsema, E., Energy pay-back time and CO2 emissions of PV systems. *Progress in photovoltaics: research and applications* **2000,** *8* (1), 17-25.

16.Fthenakis, V.; Kim, H.; Held, M.; Raugei, M.; Krones, J. In *Update of PV energy payback times and life-cycle greenhouse gas emissions*, 24th European Photovoltaic Solar Energy Conference and Exhibition, 2009; pp 21-25.

17.Stocker, T. F.; Dahe, Q.; Plattner, G.-K., Climate Change 2013: The Physical Science Basis (Chapter 8 Supplementary Information, Table 8.SM.6) *Working Group I Contribution to the Fifth Assessment Report of the Intergovernmental Panel on Climate Change. Summary for Policymakers (IPCC, 2013)* **2013**.

18.Stocker, T. F.; Dahe, Q.; Plattner, G.-K., Climate Change 2013: The Physical Science Basis (Chapter 6, Table 6.9). *Working Group I Contribution to the Fifth Assessment Report of the Intergovernmental Panel on Climate Change. Summary for Policymakers (IPCC, 2013)* **2013**.

19.Klimont, Z.; Smith, S. J.; Cofala, J., The last decade of global anthropogenic sulfur dioxide: 2000–2011 emissions (Supplementary Information Table S-1). *Environmental Research Letters* **2013,** *8* (1), 014003.

20.Myhre, G., D. Shindell, F.-M. Bréon, W. Collins, J. Fuglestvedt, J. Huang, D. Koch, J.-F. Lamarque, D. Lee, B. Mendoza, T. Nakajima, A. Robock, G. Stephens, T. Takemura and H. Zhang, Anthropogenic and Natural Radiative Forcing Supplementary Material. In: Climate Change 2013: The Physical Science Basis. Contribution of Working Group I to the Fifth Assessment Report of the Intergovernmental Panel on Climate Change (Table 8.SM.7). **2013**.

APPENDIX C

C. SUPPORTING INFORMATION FOR CHAPTER 3

S1 Data for PV manufacturing experience curve

Table 28 List of abbreviations and modeling parameters with assumed values and references

Sl No	Year	Technology	Energy	Unit	Comments	Considered for analysis?	Reason for not considering	Source	Section referred to in source
1	1998	Multi Si	4200	MJ/m²	Energy value includes silicon winning and purification, silicon wafer production, cell/module processing, module encapsulation materials, overhead operations and equipment manufacturing.	Yes		E.A Alsema, E Nieuwlaar, Energy viability of photovoltaic systems, Energy Policy, Volume 28, Issue 14, November 2000, Pages 999-1010	Table 1
2	1998	amorphous Si	1100	MJ/m²	Energy value includes cell material, cell/module processing, module encapsulation materials, overhead operations and equipment manufacturing.	Yes		E.A Alsema, E Nieuwlaar, Energy viability of photovoltaic systems, Energy Policy, Volume 28, Issue 14, November 2000, Pages 999-1010	Table 2
3	2000	Other non a-si TF PV		MJ/m²		No	Only Mono Si, Multi Si, CdTe, amorphous Si is considered in this analysis	E.A Alsema, E Nieuwlaar, Energy viability of photovoltaic systems, Energy Policy, Volume 28, Issue 14, November 2000, Pages 999-1010,	
4	1992	amorphous Si	1584	MJ/m²	Energy value includes cell material, encapsulation material, direct processes, ancillary processing. For consistency with other literature reported values, we have not included 396 MJ/m2 for capital equipment.	Yes		Erik Alsema, Energy requirements of thin-film solar cell modules—a review, Renewable and Sustainable Energy Reviews, Volume 2, Issue 4, 1 December 1998, Pages 387-415	Table 2
5	1993	amorphous Si	1446	MJ/m²	Energy value includes cell material, encapsulation material, processing direct, ancillary processing. For consistency with other literature	No	Duplicate value. This study refers to value	Erik Alsema, Energy requirements of thin-film solar cell modules—a review, Renewable and	Table 2

Sl No	Year	Technology	Energy	Unit	Comments	Considered for analysis?	Reason for not considering	Source	Section referred to in source
					reported values, we have not included 443 MJ/m2 for capital equipment.		published in Sl No 206.	Sustainable Energy Reviews, Volume 2, Issue 4, 1 December 1998, Pages 387-415	
6	1991	amorphous Si	708	MJ/m²	Quoted in paper based on older study.	No	Duplicate value. This study refers to value published in Sl No 107.	Erik Alsema, Energy requirements of thin-film solar cell modules—a review, Renewable and Sustainable Energy Reviews, Volume 2, Issue 4, 1 December 1998, Pages 387-415	Table 2
7	1992	amorphous Si	983	MJ/m²	Energy value includes cell material, encapsulation material, processing direct, ancillary processing.	Yes		Erik Alsema, Energy requirements of thin-film solar cell modules—a review, Renewable and Sustainable Energy Reviews, Volume 2, Issue 4, 1 December 1998, Pages 387-415	Table 2
8	1995	amorphous Si	1345	MJ/m²	Energy value includes cell material, encapsulation material, processing direct, ancillary processing. For consistency with other literature reported values, we have not included 9 MJ/m2 for capital equipment.	Yes		Erik Alsema, Energy requirements of thin-film solar cell modules—a review, Renewable and Sustainable Energy Reviews, Volume 2, Issue 4, 1 December 1998, Pages 387-415	Table 2
9	1996/ 1997	amorphous Si	881-1130	MJ/m²	Energy value includes input materials and manufacturing.	No	Duplicate value. This study refers to value published in Sl No 131.	Erik Alsema, Energy requirements of thin-film solar cell modules—a review, Renewable and Sustainable Energy Reviews, Volume 2, Issue 4, 1 December 1998, Pages 387-415	Table 2
10	1994	CdTe	938	MJ/m²	Energy value includes material and manufacturing. For consistency with	No	Duplicate value. This	Erik Alsema, Energy requirements of thin-	Table 2

Sl No	Year	Technology	Energy	Unit	Comments	Considered for analysis?	Reason for not considering	Source	Section referred to in source
					other literature reported values, we have not included 54 MJ/m2 for capital equipment.		study refers to value published in Sl No 156.	film solar cell modules—a review, Renewable and Sustainable Energy Reviews, Volume 2, Issue 4, 1 December 1998, Pages 387-415	
11	1995	CdTe	642	MJ/m²	This is for worst case. Energy value includes direct and indirect process requirements and input materials. For consistency with other literature reported values, we have not included 446 MJ/m2 for capital	No	Duplicate value. This study refers to value published in Sl No 209.	Erik Alsema, Energy requirements of thin-film solar cell modules—a review, Renewable and Sustainable Energy Reviews, Volume 2, Issue 4, 1 December 1998, Pages 387-415	Table 2
12	1993	CdTe	1415	MJ/m²	Energy value includes cell material, encapsulation material, direct processes, ancillary processing.	Yes		Erik Alsema, Energy requirements of thin-film solar cell modules—a review, Renewable and Sustainable Energy Reviews, Volume 2, Issue 4, 1 December 1998, Pages 387-415	Table 2
13	1998	CdTe	520-880	MJ/m²	Energy value includes cell material, substrate+encapsulation material, processing direct, processing ancillary. For consistency with other literature reported values, we have not included capital equipment of 100-200 MJ/m2.	No	Author estimates based on previously reported literature values and not actual industry data.	Erik Alsema, Energy requirements of thin-film solar cell modules—a review, Renewable and Sustainable Energy Reviews, Volume 2, Issue 4, 1 December 1998, Pages 387-415	Table 4
14	1998	CdTe	690-1070	MJ/m²	Energy value includes cell material, substrate+encapsulation material, processing direct, processing ancillary. For consistency with other literature reported values, we have not included capital equipment of 100-200 MJ/m2.	No	Author estimates based on previousy reported literature values and not	Erik Alsema, Energy requirements of thin-film solar cell modules—a review, Renewable and Sustainable Energy Reviews, Volume 2,	Table 4

Sl No	Year	Technology	Energy	Unit	Comments	Considered for analysis?	Reason for not considering	Source	Section referred to in source
							actual industry data.	Issue 4, 1 December 1998, Pages 387-415	
15	1998	amorphous Si	670-1090	MJ/m²	Energy value includes cell material, substrate+encapsulation material, processing direct, processing ancillary. For consistency with other literature reported values, we have not included capital equipment of 100-200 MJ/m2.	No	Author estimates based on previously reported literature values and not actual industry data.	Erik Alsema, Energy requirements of thin-film solar cell modules—a review, Renewable and Sustainable Energy Reviews, Volume 2, Issue 4, 1 December 1998, Pages 387-415	Table 4
16	1998	amorphous Si	840-1280	MJ/m²	Energy value includes cell material, substrate+encapsulation material, processing direct, processing ancillary. For consistency with other literature reported values, we have not included capital equipment of 100-200 MJ/m2.	No	Author estimates based on previously reported literature values and not actual industry data.	Erik Alsema, Energy requirements of thin-film solar cell modules—a review, Renewable and Sustainable Energy Reviews, Volume 2, Issue 4, 1 December 1998, Pages 387-415	Table 4
17	2000	Mono Si	5700	MJ/m²	Energy value includes Si Production, purification,crystallization, wafering, cell Processing, module assembly	No	Author estimates based on previously reported literature values and not actual industry data.	Energy pay-back time and CO2 emissions of PV systems E. A. Alsema* - Progress in Photovoltaics: Research and Applications Volume 8, Issue 1, pages 17–25, January/February 2000	Table 1
18	2000	Multi Si	4200	MJ/m²	Energy value includes Si Production, purification,crystallization, wafering, cell Processing, module assembly	No	Author estimates based on previously reported literature values and not actual industry data.	Energy pay-back time and CO2 emissions of PV systems E. A. Alsema* - Progress in Photovoltaics: Research and Applications Volume 8, Issue 1, pages 17–25, January/February 2000	Table 1

Sl No	Year	Technology	Energy	Unit	Comments	Considered for analysis?	Reason for not considering	Source	Section referred to in source
19	2000	amorphous Si	1050	MJ/m²	Energy value includes cell material, substrate and encapsulation, cell/module processing and overhead operations. For consistency with other literature reported values, we have not included capital equipment of 150 MJ/m2.	No	Author estimates based on previously reported literature values and not actual industry data.	Energy pay-back time and CO2 emissions of PV systems E. A. Alsema* - Progress in Photovoltaics: Research and Applications Volume 8, Issue 1, pages 17–25, January/February 2000	Table 3
20	2006	CdTe	1200	MJ/m²	Energy value includes materials and manufacturing	No	Duplicate value. This study refers to value published in Sl No 150.	UPDATE OF PV ENERGY PAYBACK TIMES AND LIFE-CYCLE GREENHOUSE GAS EMISSIONS - 24th European Photovoltaic Solar Energy Conference, 21-25 September 2009, Hamburg, Germany V. Fthenakis, H.C. Kim, M. Held, M. Raugei and J. Krones	Table 1
21	2009	CdTe	966	MJ/m²	Energy value includes materials and manufacturing	Yes		UPDATE OF PV ENERGY PAYBACK TIMES AND LIFE-CYCLE GREENHOUSE GAS EMISSIONS - 24th European Photovoltaic Solar Energy Conference, 21-25 September 2009, Hamburg, Germany V. Fthenakis, H.C. Kim, M. Held, M. Raugei and J. Krones	Table 1

Sl No	Year	Technology	Energy	Unit	Comments	Considered for analysis?	Reason for not considering	Source	Section referred to in source
22	2009	CdTe	853	MJ/m²	Energy value includes materials and manufacturing. Based on actual industrial data.	Yes		UPDATE OF PV ENERGY PAYBACK TIMES AND LIFE-CYCLE GREENHOUSE GAS EMISSIONS - 24th European Photovoltaic Solar Energy Conference, 21-25 September 2009, Hamburg, Germany V. Fthenakis, H.C. Kim, M. Held, M. Raugei and J. Krones	Table 1
23	2009	CdTe	802	MJ/m²	Energy value includes materials and manufacturing	No	Duplicate value. This study refers to value published in Sl No 155.	UPDATE OF PV ENERGY PAYBACK TIMES AND LIFE-CYCLE GREENHOUSE GAS EMISSIONS - 24th European Photovoltaic Solar Energy Conference, 21-25 September 2009, Hamburg, Germany V. Fthenakis, H.C. Kim, M. Held, M. Raugei and J. Krones	Table 1
24	2006	Mono Si	5000	MJ/m²	Energy value includes materials and manufacturing. Based on actual industrial data.	Yes		UPDATE OF PV ENERGY PAYBACK TIMES AND LIFE-CYCLE GREENHOUSE GAS EMISSIONS - 24th European Photovoltaic Solar Energy Conference, 21-25 September 2009, Hamburg, Germany	Table 2

Sl No	Year	Technology	Energy	Unit	Comments	Considered for analysis?	Reason for not considering	Source	Section referred to in source
								V. Fthenakis, H.C. Kim, M. Held, M. Raugei and J. Krones	
25	2008	Mono Si	2900	MJ/m²	Energy value includes materials and manufacturing. Based on actual industrial data.	No	Duplicate value. This study refers to value published in Sl No 49.	UPDATE OF PV ENERGY PAYBACK TIMES AND LIFE-CYCLE GREENHOUSE GAS EMISSIONS - 24th European Photovoltaic Solar Energy Conference, 21-25 September 2009, Hamburg, Germany V. Fthenakis, H.C. Kim, M. Held, M. Raugei and J. Krones	Table 2
26	2005	Multi Si	3700	MJ/m²	Energy value includes materials and manufacturing. Based on actual industrial data.	Yes		UPDATE OF PV ENERGY PAYBACK TIMES AND LIFE-CYCLE GREENHOUSE GAS EMISSIONS - 24th European Photovoltaic Solar Energy Conference, 21-25 September 2009, Hamburg, Germany V. Fthenakis, H.C. Kim, M. Held, M. Raugei and J. Krones	Table 2
27	2007	Multi Si	2700	MJ/m²	Energy value includes materials and manufacturing. Based on actual industrial data.	No	Duplicate value. This study refers to value published in Sl No 50.	UPDATE OF PV ENERGY PAYBACK TIMES AND LIFE-CYCLE GREENHOUSE GAS EMISSIONS - 24th European Photovoltaic Solar Energy Conference,	Table 2

Sl No	Year	Technology	Energy	Unit	Comments	Considered for analysis?	Reason for not considering	Source	Section referred to in source
								21-25 September 2009, Hamburg, Germany V. Fthenakis, H.C. Kim, M. Held, M. Raugei and J. Krones	
28	2005	Ribbon Si	2300	MJ/m²	Energy value includes materials and manufacturing. Based on actual industrial data.	No	This study only considers mono Si, multi Si, CdTe, a Si	UPDATE OF PV ENERGY PAYBACK TIMES AND LIFE-CYCLE GREENHOUSE GAS EMISSIONS - 24th European Photovoltaic Solar Energy Conference, 21-25 September 2009, Hamburg, Germany V. Fthenakis, H.C. Kim, M. Held, M. Raugei and J. Krones	Table 2
29	2009	Ribbon Si	1550	MJ/m²	Energy value includes materials and manufacturing. Based on actual industrial data.	No	This study only considers mono Si, multi Si, CdTe, a Si	UPDATE OF PV ENERGY PAYBACK TIMES AND LIFE-CYCLE GREENHOUSE GAS EMISSIONS - 24th European Photovoltaic Solar Energy Conference, 21-25 September 2009, Hamburg, Germany V. Fthenakis, H.C. Kim, M. Held, M. Raugei and J. Krones	Table 2
30	2008	CdTe	750	MJ/m²	Energy value includes materials and manufacturing. Based on actual industrial data.	Yes		Update of environmental indicators and energy payback time of CdTe PV systems in Europe - Michael	Figure 3

Sl No	Year	Technology	Energy	Unit	Comments	Considered for analysis?	Reason for not considering	Source	Section referred to in source
								Held*, Robert Ilg - Progress in Photovoltaics: Research and Applications Volume 19, Issue 5, pages 614–626, August 2011	
31	2006	CdTe	664	MJ/m²	Energy value includes materials and manufacturing. Based on actual industrial data.	No	Duplicate value. This study refers to value published in Sl No 150.	V.M. Fthenakis, H.C. Kim, Photovoltaics: Life-cycle analyses, Solar Energy, Volume 85, Issue 8, August 2011, Pages 1609-1628	Table 1
32	2006	Mono Si	3534	MJ/m²	Energy value includes materials and manufacturing. Based on actual industrial data.	No	Duplicate value. The author updates the original value published in Sl No 65 to reflect improvements in 2006.	V.M. Fthenakis, H.C. Kim, Photovoltaics: Life-cycle analyses, Solar Energy, Volume 85, Issue 8, August 2011, Pages 1609-1628	Table 1
33	2006	Multi Si	3098	MJ/m²	Energy value includes materials and manufacturing. Based on actual industrial data.	No	Duplicate value. The author updates the original value published in Sl No 174 to reflect improvements in 2006.	V.M. Fthenakis, H.C. Kim, Photovoltaics: Life-cycle analyses, Solar Energy, Volume 85, Issue 8, August 2011, Pages 1609-1628	Table 1
34	1999	Multi Si	4200	MJ/m²	Energy value includes frame, module assembly, cell production, ingot+wafer, Si feedstock	No	Duplicate value. This study refers to the estimates published in Sl No 18.	Alsema, EA and de Wild-Scholten, MJ,The real environmental impacts of crystalline silicon PV modules: an analysis based on	Figure 5

Sl No	Year	Technology	Energy	Unit	Comments	Considered for analysis?	Reason for not considering	Source	Section referred to in source
								up-to-date manufacturers data, 2005	
35	1999	Mono Si	6000	MJ/m²	Energy value includes frame, module assembly, cell production, ingot+wafer, Si feedstock	No	Duplicate value. This study refers to the estimates published in Sl No 17.	Alsema, EA and de Wild-Scholten, MJ,The real environmental impacts of crystalline silicon PV modules: an analysis based on up-to-date manufacturers data, 2005	Figure 5
36	2004	Multi Si	3408	MJ/m²	Energy value includes frame, module assembly, cell production, ingot+wafer, Si feedstock. Based on actual manufacturing data.	Yes		Alsema, EA and de Wild-Scholten, MJ,The real environmental impacts of crystalline silicon PV modules: an analysis based on up-to-date manufacturers data, 2005	Figure 5
37	2004	Mono Si	4794	MJ/m²	Energy value includes frame, module assembly, cell production, ingot+wafer, Si feedstock. Based on actual manufacturing data.	Yes		Alsema, EA and de Wild-Scholten, MJ,The real environmental impacts of crystalline silicon PV modules: an analysis based on up-to-date manufacturers data, 2005	Figure 5
38	1998	Multi Si	3254	MJ/m²	Energy value includes Si production process, casting and cutting, cell production, module assembly and others at a production scale of 10MW per year. The original data reported in the paper (3534 mj/m2) includes the frame for 280 mj/m2 (see "A life-cycle analysis on thin-film CdS/CdTe PV	No	The material inventory and energy values are author estimates and not based on actual manufacturing data.	Kato, K. and Murata, A. and Sakuta, K., Energy pay-back time and life-cycle CO2 emission of residential PV power system with silicon PV module,1998	Table 2

Sl No	Year	Technology	Energy	Unit	Comments	Considered for analysis?	Reason for not considering	Source	Section referred to in source
					modules" from the same authors). This frame energy value is deducted.				
39	1998	Multi Si	3100	MJ/m²	Energy value includes Si production process, casting and cutting, cell production, module assembly and others at a production scale of 30MW per year.The original data reported in the paper (3380 mj/m2) includes the frame for 280 mj/m2 (see "A life-cycle analysis on thin-film CdS/CdTe PV modules" from the same authors). This frame energy value is deducted.	No	The material inventory and energy values are author estimates and not based on actual manufacturing data.	Kato, K. and Murata, A. and Sakuta, K., Energy pay-back time and life-cycle CO2 emission of residential PV power system with silicon PV module,1998	Table 2
40	1998	Multi Si	1987	MJ/m²	Energy value includes Si production process, casting and cutting, cell production, module assembly and others at a production scale of 100MW per year.The original data reported in the paper (2267 mj/m2) includes the frame for 280 mj/m2 (see "A life-cycle analysis on thin-film CdS/CdTe PV modules" from the same authors). This frame energy value is deducted.	No	The material inventory and energy values are author estimates and not based on actual manufacturing data.	Kato, K. and Murata, A. and Sakuta, K., Energy pay-back time and life-cycle CO2 emission of residential PV power system with silicon PV module,1998	Table 2
41	1998	amorphous Si	1363	MJ/m²	Energy value includes cell production, module assembly and others at a production scale of 10MW per year.The original data reported in the paper (1643 mj/m2) includes the frame for 280 mj/m2 (see "A life-cycle analysis on thin-film CdS/CdTe PV modules" from the same authors). This frame energy value is deducted.	No	The material inventory and energy values are author estimates and not based on actual manufacturing data.	Kato, K. and Murata, A. and Sakuta, K., Energy pay-back time and life-cycle CO2 emission of residential PV power system with silicon PV module,1998	Table 3
42	1998	amorphous Si	1307	MJ/m²	Energy value includes cell production, module assembly and others at a production scale of 30MW per year. The original data reported in the paper (1587 mj/m2) includes the frame for 280 mj/m2 (see "A life-cycle analysis on thin-film CdS/CdTe PV modules" from the same authors). This frame energy value is deducted.	No	The material inventory and energy values are author estimates and not based on actual manufacturing data.	Kato, K. and Murata, A. and Sakuta, K., Energy pay-back time and life-cycle CO2 emission of residential PV power system with silicon PV module,1998	Table 3

Sl No	Year	Technology	Energy	Unit	Comments	Considered for analysis?	Reason for not considering	Source	Section referred to in source
43	1998	amorphous Si	898	MJ/m²	Energy value includes cell production, module assembly and others at a production scale of 100MW per year. The original data reported in the paper (1178 mj/m2) includes the frame for 280 mj/m2 (see "A life-cycle analysis on thin-film CdS/CdTe PV modules" from the same authors). This frame energy value is deducted.	No	The material inventory and energy values are author estimates and not based on actual manufacturing data.	Kato, K. and Murata, A. and Sakuta, K., Energy pay-back time and life-cycle CO2 emission of residential PV power system with silicon PV module,1998	Table 3
44	2001	CdTe	1523	MJ/m²	Energy value includes cell production, module assembly and others at a production scale of 10MW per year.The original data reported in the paper (1803 mj/m2) includes the frame for 280 mj/m2. This frame energy value is deducted.	No	The material inventory and energy values are author estimates and not based on actual manufacturing data.	Kato, K. and Hibino, T. and Komoto, K. and Ihara, S. and Yamamoto, S. and Fujihara, H., A life-cycle analysis on thin-film CdS/CdTe PV modules,2001	Table 2
45	2001	CdTe	1234	MJ/m²	Energy value includes cell production, module assembly and others at a production scale of 30MW per year. The original data reported in the paper (1514 mj/m2) includes the frame for 280 mj/m2. This frame energy value is deducted.	No	The material inventory and energy values are author estimates and not based on actual manufacturing data.	Kato, K. and Hibino, T. and Komoto, K. and Ihara, S. and Yamamoto, S. and Fujihara, H., A life-cycle analysis on thin-film CdS/CdTe PV modules,2001	Table 2
46	2001	CdTe	992	MJ/m²	Energy value includes cell production, module assembly and others at a production scale of 100MW per year. The original data reported in the paper (1272 mj/m2) includes the frame for 280 mj/m2. This frame energy value is deducted.	No	The material inventory and energy values are author estimates and not based on actual manufacturing data.	Kato, K. and Hibino, T. and Komoto, K. and Ihara, S. and Yamamoto, S. and Fujihara, H., A life-cycle analysis on thin-film CdS/CdTe PV modules,2001	Table 2
47	2005	Multi Si	3727	MJ/m²	Energy value includes Si feedstock,ingot and wafer, cell production, module assembly	No	Duplicate value. This study refers to the estimates published in Sl No 174.	Alsema, E., & de Wild, M. J. (2005, January). Environmental impact of crystalline silicon photovoltaic	Figure 3

Sl No	Year	Technology	Energy	Unit	Comments	Considered for analysis?	Reason for not considering	Source	Section referred to in source
								module production. In *MRS Proceedings* (Vol. 895, pp. 0895-G03). Cambridge University Press.	
48	1999	Mono Si	7000	MJ/m²	Energy value includes materials and processes for Ingot, wafer, cells and module. The reported values is 5598 kWh/kWp including the frame. Without the energy values for frame (324 kWh/kWp) we get 5274 kWh/kWp. This value corresponds to the SP75 module and 1 m2 of a module contains 118 Wp (http://www.abcsolar.com/pdf/sp75.pdf). Converting the energy value to a m2 basis we get 622 kWh per m2 and this corresponds to 7000 MJ/m2 (using a grid factor of 0.32 and conversion factor of 3.6 between MJ and kWh). This study reports actual manufacturing data.	No	Duplicate value. This study refers to the estimates published in Sl No 104.	Knapp, Karl, and Theresa Jester. "An empirical perspective on the energy payback time for photovoltaic modules." PROCEEDINGS OF THE SOLAR CONFERENCE. AMERICAN SOLAR ENERGY SOCIETY; AMERICAN INSTITUTE OF ARCHITECTS, 2000.	Slide 9
49	2008	Mono Si	2860	MJ/m²	Energy value includes materials and manufacturing. Based on actual industrial data.	Yes		Mariska de Wild-Scholten,Energy payback time of photovoltaic modules and systems,2009	Slide 9
50	2007	Multi Si	2699	MJ/m²	Energy value includes materials and manufacturing. Based on actual industrial data.	Yes		Mariska de Wild-Scholten,Energy payback time of photovoltaic modules and systems,2009	Slide 9
51	2008	amorphous Si	989	MJ/m²	Energy value includes materials and manufacturing. Based on actual industrial data.	Yes		Mariska de Wild-Scholten,Energy payback time of photovoltaic modules and systems,2009	Slide 9
52	2008	amorphous Si	866	MJ/m²	Energy value includes materials and manufacturing. Based on actual industrial data.	Yes		Mariska de Wild-Scholten,Energy payback time of	Slide 9

Sl No	Year	Technology	Energy	Unit	Comments	Considered for analysis?	Reason for not considering	Source	Section referred to in source
								photovoltaic modules and systems,2009	
53	2009	CdTe	811	MJ/m²	Energy value includes materials and manufacturing. Based on actual industrial data.	Yes		Mariska de Wild-Scholten,Energy payback time of photovoltaic modules and systems,2009	Slide 9
54	1998	Mono Si	6000	MJ/m²	This is for the "low scenario".Energy value includes Si production, purification and crystallization, wafering, cell processing and module assembly.	No	The reported values are assumptions based on values reported in previous studies and not actual production data.	Alsema, E. A., Frankl, P., & Kato, K. (1998, July). Energy pay-back time of photovoltaic energy systems: present status and prospects. In 2nd World Conference on photovoltaic solar energy conversion, Vienna (pp. 6-10).	Table 1
54	1998	Mono Si	13900	MJ/m²	This is for the "high scenario".Energy value includes Si production, purification and crystallization, wafering, cell processing and module assembly.	No	The reported values are assumptions based on values reported in previous studies and not actual production data.	Alsema, E. A., Frankl, P., & Kato, K. (1998, July). Energy pay-back time of photovoltaic energy systems: present status and prospects. In 2nd World Conference on photovoltaic solar energy conversion, Vienna (pp. 6-10).	Table 1
55	1998	amorphous Si	1050	MJ/m²	Energy value include cell material, substrate and encapsulation, cell/module processing, overhead operations. For consistency with other literature reported values, we have not included capital equipment of 150 MJ/m2.	No	The reported values are assumptions based on values reported in previous studies and not actual production data.	Alsema, E. A., Frankl, P., & Kato, K. (1998, July). Energy pay-back time of photovoltaic energy systems: present status and prospects. In 2nd World Conference on photovoltaic solar	Table 3

Sl No	Year	Technology	Energy	Unit	Comments	Considered for analysis?	Reason for not considering	Source	Section referred to in source
								energy conversion, Vienna (pp. 6-10).	
56	1995	Multi Si	2916	MJ/m²	This is for worst case. Energy value includes direct and indirect process requirements and input materials. For consistency with other literature reported values, we have not included 576 MJ/m2 for investments.	No	The reported values are assumptions based on values reported in previous studies and not actual production data.	Phylipsen, G. J. M., & Alsema, E. A. (1995). Environmental life-cycle assessment of multicrystalline silicon solar cell modules (NOVEM Report 95057). Netherlands Agency for Energy and the Environment: The Hague, The Netherlands.	Table 4.3
57	1995	Multi Si	1296	MJ/m²	This is for base case. Energy value includes direct and indirect process requirements and input materials. For consistency with other literature reported values, we have not included 144 MJ/m2 for investments.	No	The reported values are assumptions based on values reported in previous studies and not actual production data.	Phylipsen, G. J. M., & Alsema, E. A. (1995). Environmental life-cycle assessment of multicrystalline silicon solar cell modules (NOVEM Report 95057). Netherlands Agency for Energy and the Environment: The Hague, The Netherlands.	Table 4.3
58	1995	Multi Si	576	MJ/m²	This is for best case. Energy value includes direct and indirect process requirements and input materials. For consistency with other literature reported values, we have not included 72 MJ/m2 for investments.	No	The reported values are assumptions based on values reported in previous studies and not actual production data.	Phylipsen, G. J. M., & Alsema, E. A. (1995). Environmental life-cycle assessment of multicrystalline silicon solar cell modules (NOVEM Report 95057). Netherlands Agency for Energy and the Environment: The Hague, The Netherlands.	Table 4.3

Sl No	Year	Technology	Energy	Unit	Comments	Considered for analysis?	Reason for not considering	Source	Section referred to in source
59	1998	Mono Si	15524	MJ/m²	Energy value includes metal grade Si production, poly Si production, Czochralski Si and wafer production, cell production and module assembly	No	The reported values are assumptions based on values reported in previous studies and not actual production data.	Kato, K., Murata, A., & Sakuta, K. (1998). Energy pay- back time and life- cycle CO2 emission of residential PV power system with silicon PV module. Progress in Photovoltaics: Research and Applications, 6(2), 105-115.	Table 5
60	1998	Mono Si	11673	MJ/m²	Energy value includes metal grade Si production, poly Si production, Czochralski Si and wafer production, cell production and module assembly	No	The reported values are assumptions based on values reported in previous studies and not actual production data.	Kato, K., Murata, A., & Sakuta, K. (1998). Energy pay- back time and life- cycle CO2 emission of residential PV power system with silicon PV module. Progress in Photovoltaics: Research and Applications, 6(2), 105-115.	Table 5
61	1998	Mono Si	4159	MJ/m²	Energy value includes metal grade Si production, poly Si production, Czochralski Si and wafer production, cell production and module assembly	No	The reported values are assumptions based on values reported in previous studies and not actual production data.	Kato, K., Murata, A., & Sakuta, K. (1998). Energy pay- back time and life- cycle CO2 emission of residential PV power system with silicon PV module. Progress in Photovoltaics: Research and Applications, 6(2), 105-115.	Table 5
62	1999	amorphous Si	1456	MJ/m²	Energy value includes cell production, module assembly, overhead at a 10MW per year production scale.The original data reported in the paper (1731 mj/m2) includes the frame for 275	No	The material inventory and energy values are author estimates and not based on	Kato, K., Hibino, T., Komoto, K., Ihara, S., Yamamoto, S., & Fujihara, H. (2001). A life-cycle analysis on thin-film CdS/CdTe	Figure 4

Sl No	Year	Technology	Energy	Unit	Comments	Considered for analysis?	Reason for not considering	Source	Section referred to in source
					mj/m2. This frame energy value is deducted.		actual manufacturing data.	PV modules. Solar Energy Materials and Solar Cells, 67(1), 279-287.	
63	1999	amorphous Si	1406	MJ/m²	Energy value includes cell production, module assembly, overhead at a 30MW per year production scale.The original data reported in the paper (1681 mj/m2) includes the frame for 275 mj/m2. This frame energy value is deducted.	No	The material inventory and energy values are author estimates and not based on actual manufacturing data.	Kato, K., Hibino, T., Komoto, K., Ihara, S., Yamamoto, S., & Fujihara, H. (2001). A life-cycle analysis on thin-film CdS/CdTe PV modules. Solar Energy Materials and Solar Cells, 67(1), 279-287.	Figure 4
64	1999	amorphous Si	961	MJ/m²	Energy value includes cell production, module assembly, overhead at a 100MW per year production scale.The original data reported in the paper (1236 mj/m2) includes the frame for 275 mj/m2. This frame energy value is deducted.	No	The material inventory and energy values are author estimates and not based on actual manufacturing data.	Kato, K., Hibino, T., Komoto, K., Ihara, S., Yamamoto, S., & Fujihara, H. (2001). A life-cycle analysis on thin-film CdS/CdTe PV modules. Solar Energy Materials and Solar Cells, 67(1), 279-287.	Figure 4
65	2005	Mono Si	5016	MJ/m²	Energy value includes materials and manufacturing. Based on actual industrial data.	Yes		Alsema, E., & de Wild, M. J. (2005, January). Environmental impact of crystalline silicon photovoltaic module production. In *MRS Proceedings* (Vol. 895, pp. 0895-G03). Cambridge University Press.	Figure 3
66	1998	Multi Si	4200	MJ/m²	This is for the "low scenario".Energy value includes Si production, Si purification and crystallization, wafering, cell processing, module assembly.	No	The reported values are assumptions based on values reported in	Alsema, E. "Energy requirements and CO2 mitigation potential of PV systems." Photovoltaics and the	Table 1

Sl No	Year	Technology	Energy	Unit	Comments	Considered for analysis?	Reason for not considering	Source	Section referred to in source
							previous studies and not actual production data.	Environment 1999 (1998).	
67	1998	Mono Si	6000	MJ/m²	This is for the "low scenario".Energy value includes Si production, Si purification and crystallization, wafering, cell processing, module assembly.	No	The reported values are assumptions based on values reported in previous studies and not actual production data.	Alsema, E. "Energy requirements and CO2 mitigation potential of PV systems." Photovoltaics and the Environment 1999 (1998).	Table 1
68	1998	amorphous Si	1050	MJ/m²	Energy value includes cell material, substrate and encapsulation, cell/module processing, overhead operations. For consistency with other literature reported values, we have not included capital equipment of 150 MJ/m2.	No	The reported values are assumptions based on values reported in previous studies and not actual production data.	Alsema, E. "Energy requirements and CO2 mitigation potential of PV systems." Photovoltaics and the Environment 1999 (1998).	Table 3
69	2006	Multi Si	3245	MJ/m²	Energy value includes Si feedstock, ingot, wafer, cell production and module assembly. Data based on actual production data.	Yes		Alsema, E. A., de Wild-Scholten, M. J., & Fthenakis, V. M. (2006, September). Environmental impacts of PV electricity generation-a critical comparison of energy supply options. In *21st European photovoltaic solar energy conference, Dresden, Germany* (Vol. 3201).	Figure 2

Sl No	Year	Technology	Energy	Unit	Comments	Considered for analysis?	Reason for not considering	Source	Section referred to in source
70	2006	Multi Si	2916	MJ/m²	Energy value includes Si feedstock, ingot, wafer, cell production and module assembly. Data based on actual production data.	Yes		Alsema, E. A., & de Wild-Schoten, M. J. (2007, September). Reduction of the environmental impacts in crystalline silicon module manufacturing. In 22nd European Photovoltaic Solar Energy Conference (pp. 829-836). WIP-Renewable Energies.	Figure 2
71	2006	Mono Si	3680	MJ/m²	Energy value includes Si feedstock, ingot, wafer, cell production and module assembly. Data based on actual production data.	Yes		Alsema, E. A., & de Wild-Schoten, M. J. (2007, September). Reduction of the environmental impacts in crystalline silicon module manufacturing. In 22nd European Photovoltaic Solar Energy Conference (pp. 829-836). WIP-Renewable Energies.	Figure 2
72	2006	CdTe	684	MJ/m²	Energy value includes material and processes for laminate production. Efficiency used in the study is 9% and this multiplied by 7600 MJ/kWp value reported. Based on actual production data.	Yes		Raugei, Marco; Bargigli, Silvia; Ulgiati, Sergio Life cycle assessment and energy pay-back time of advanced photovoltaic modules: CdTe and CIS compared to poly-Si	Figure 5
73	2006	Multi Si	9716	MJ/m²	This data assumes that electronic grade silicon is used to manufacture the multi Si module and the entire energetic burden of electronic grade silicon is allocated to the PV module.	No	This value does not include actual industrial data for upstream	Raugei, Marco; Bargigli, Silvia; Ulgiati, Sergio Life cycle assessment and energy pay-back time of advanced	Figure 5

Sl No	Year	Technology	Energy	Unit	Comments	Considered for analysis?	Reason for not considering	Source	Section referred to in source
							silicon purification.	photovoltaic modules: CdTe and CIS compared to poly-Si	
74	2006	Multi Si	3542	MJ/m²	This data assumes that electronic grade silicon is used to manufacture the multi Si module and 30% of the energetic burden of electronic grade silicon is allocated to the PV module.	No	This value does not include actual industrial data for upstream silicon purification.	Raugei, Marco; Bargigli, Silvia; Ulgiati, Sergio Life cycle assessment and energy pay-back time of advanced photovoltaic modules: CdTe and CIS compared to poly-Si	Figure 5
75	2006	Multi Si	3584	MJ/m²	Energy value includes frame, module assembly, cell production, ingot+wafer, Si feedstock. Based on actual manufacturing data.	No	Duplicate value. This study refers to the estimates published in Sl No 36.	Raugei, Marco; Bargigli, Silvia; Ulgiati, Sergio Life cycle assessment and energy pay-back time of advanced photovoltaic modules: CdTe and CIS compared to poly-Si	Figure 5
76	2006	CdTe	684	MJ/m²	Energy value includes material and processes for laminate production. Efficiency used in the study is 9% and this multiplied by 7600 MJ/kWp value reported. Based on actual production data.	No	Duplicate value. This study refers to the estimates published in Sl No 72.	Azzopardi, B; Mutale, J Life cycle analysis for future photovoltaic systems using hybrid solar cells	Figure 1
77	2001	Multi Si	5150	MJ/m²	Energy value includes Si feedstock, ingot, wafer, cell production and module assembly. Based on actual production data and secondary literature reported values.	No	This value does not include actual industrial data for upstream silicon purification.	Riccardo Battisti, Annalisa Corrado, Evaluation of technical improvements of photovoltaic systems through life cycle assessment methodology	Figure 4
78	2008	Multi Si	1442	MJ/m²	Energy value of 177 kWh for 1.38 m2 and this includes materials and manufacturing. Converting kWh to MJ	No	Energy values are not based on actual	Botsaris, P N; Filippidou, F, Estimation of the	Table 6

Sl No	Year	Technology	Energy	Unit	Comments	Considered for analysis?	Reason for not considering	Source	Section referred to in source
					and normalizing to an area of 1 m2 we get 1442		production data but calculated using the CES EduPack 2008, Granta software.	Energy Payback Time (EPR) of a PV Module Installed in North–Eastern Greece	
79	1998	Multi Si	4200	MJ/m²	Energy value includes silicon winning and purification, silicon wafer production, cell/module processing, module encapsulation materials, overhead operations and equipment manufacturing.	No	Duplicate value. This study refers to the estimates published in Sl No 1	Jose L. Bernal-Agustın*, Rodolfo Dufo-Lopez, Economical and environmental analysis of grid connected photovoltaic systems in Spain.	Table 1
80	1998	amorphous Si	1050	MJ/m²	Energy value include cell material, substrate and encapsulation, cell/module processing, overhead operations.	No	Duplicate value. This study refers to the estimates published in Sl No 55.	Jose L. Bernal-Agustın*, Rodolfo Dufo-Lopez, Economical and environmental analysis of grid connected photovoltaic systems in Spain.	Table 1
81	1998	Mono Si	9950	MJ/m²	Energy value includes Si production, purification and crystallization, wafering, cell processing and module assembly.	No	Author has taken the average of the values reported in Sl no 54 - Alsema, E. A., Frankl, P., & Kato, K. (1998, July). Energy pay-back time of photovoltaic energy systems: present status and prospects.	Bizzarri, G., and G. L. Morini. "A Life Cycle Analysis of roof integrated photovoltaic systems." *International journal of environmental technology and management* 7.1-2 (2007): 134-146.	Table 5

Sl No	Year	Technology	Energy	Unit	Comments	Considered for analysis?	Reason for not considering	Source	Section referred to in source
							In 2nd World Conference on photovoltaic solar energy conversion, Vienna (pp. 6-10).		
82	1998	Multi Si	7898	MJ/m²	This scenario is the same as sl no 89,90. Data was averaged over the range reported in Sl no 89,90	No	Author has taken the average of the values reported in Sl no 54 - Alsema, E. A., Frankl, P., & Kato, K. (1998, July). Energy pay-back time of photovoltaic energy systems: present status and prospects. In 2nd World Conference on photovoltaic solar energy conversion, Vienna (pp. 6-10).	Bizzarri, G., and G. L. Morini. "A Life Cycle Analysis of roof integrated photovoltaic systems." *International journal of environmental technology and management* 7.1-2 (2007): 134-146.	Table 5
83	1988	Mono Si	8285	MJ/m²	Energy value includes Si purification, Si wafer and cell production and module production with frame. Based on actual production data and we deduct 700 mj/m2 for the frame. Since this study was published in 1988 we assume an extra 200 mj/m2 for the frame when compared to 500 mj/m2 assumed in a later study ,"Energy pay-back time and	Yes		Hagedorn, G. (1989). Hidden energy in solar cells and photovoltaic power stations. In 9th European Photovoltaic Solar Energy Conference (p. 542).	Section 7.1.1

Sl No	Year	Technology	Energy	Unit	Comments	Considered for analysis?	Reason for not considering	Source	Section referred to in source
					CO2 emissions of PV systems", published in year 2000.				
84	1988	Multi Si	6446	MJ/m²	Energy value includes Si purification, Si wafer and cell production and module production with frame. Based on actual production data and we deduct 700 mj/m2 for the frame. Since this study was published in 1988 we assume an extra 200 mj/m2 for the frame when compared to 500 mj/m2 assumed in a later study ,"Energy pay-back time and CO2 emissions of PV systems", published in year 2000.	Yes		Hagedorn, G. (1989). Hidden energy in solar cells and photovoltaic power stations. In 9th European Photovoltaic Solar Energy Conference (p. 542).	Section 7.1.2
85	1988	amorphous Si	1785	MJ/m²	Energy value includes module production	No	Not based on actual production data	Hagedorn, G. (1989). Hidden energy in solar cells and photovoltaic power stations. In 9th European Photovoltaic Solar Energy Conference (p. 542).	Section 7.2
86	1988	Mono Si	6260	MJ/m²	Energy value includes Si purification, Si wafer and cell production and module production without frame.	No	Not based on actual production data and represents improved manufacturing in the future.	Hagedorn, G. (1989). Hidden energy in solar cells and photovoltaic power stations. In 9th European Photovoltaic Solar Energy Conference (p. 542).	Section 7.1.1
87	1988	Multi Si	3575	MJ/m²	Energy value includes Si purification, Si wafer and cell production and module production without frame.	No	Not based on actual production data and represents improved manufacturing in the future.	Hagedorn, G. (1989). Hidden energy in solar cells and photovoltaic power stations. In 9th European Photovoltaic Solar Energy Conference (p. 542).	Section 7.1.2

Sl No	Year	Technology	Energy	Unit	Comments	Considered for analysis?	Reason for not considering	Source	Section referred to in source
88	1988	amorphous Si	1573	MJ/m²	Energy value includes module production	No	Not based on actual production data	Hagedorn, G. (1989). Hidden energy in solar cells and photovoltaic power stations. In 9th European Photovoltaic Solar Energy Conference (p. 542).	Section 7.2
89	1998	Multi Si	4200	MJ/m²	This is for the "low scenario".Energy value includes Si production, Si purification and crystallization, wafering, cell processing, module assembly.	No	The reported values are assumptions based on values reported in previous studies and not actual production data.	Alsema, EA and Frankl, P. and Kato, K.,Energy pay-back time of photovoltaic energy systems: present status and prospects,1998	Table 1
90	1998	Multi Si	11600	MJ/m²	This is for the "high scenario".Energy value includes Si production, Si purification and crystallization, wafering, cell processing, module assembly.	No	The reported values are assumptions based on values reported in previous studies and not actual production data.	Alsema, EA and Frankl, P. and Kato, K.,Energy pay-back time of photovoltaic energy systems: present status and prospects,1998	Table 1
91	2000	Mono Si	5700	MJ/m²	Energy value includes Si Production, purification,crystallization, wafering, cell Processing, module assembly	No	Duplicate value. This study refers to the estimates published in Sl No 17.	García-Valverde, R., Miguel, C., Martínez-Béjar, R., & Urbina, A. (2009). Life cycle assessment study of a 4.2 kW p stand-alone photovoltaic system. *Solar Energy*, *83*(9), 1434-1445.	Section 3.2.1.1
92	1998	Multi Si	2044	MJ/m²	Energy value includes Si production process, casting and cutting, cell	No	Duplicate value. This	Ito, M., Kato, K., Komoto, K.,	Table 4

Sl No	Year	Technology	Energy	Unit	Comments	Considered for analysis?	Reason for not considering	Source	Section referred to in source
					production, module assembly and others at a production scale of 100MW per year		study refers to the estimates published in Sl No 40.	Kichimi, T., & Kurokawa, K. (2008). A comparative study on cost and life-cycle analysis for 100 MW very large- scale PV (VLS- PV) systems in deserts using m- Si, a- Si, CdTe, and CIS modules. Progress in Photovoltaics: research and applications, 16(1), 17-30.	
93	2000	amorphous Si	1202	MJ/m²	Energy value includes cell production, module assembly and others at a production scale of 100MW per year.	No	Not based on actual production data. The authors mention that this value represents an update of the value reported in sl no 43	Ito, M., Kato, K., Komoto, K., Kichimi, T., & Kurokawa, K. (2008). A comparative study on cost and life-cycle analysis for 100 MW very large- scale PV (VLS- PV) systems in deserts using m- Si, a- Si, CdTe, and CIS modules. Progress in Photovoltaics: research and applications, 16(1), 17-30.	Table 4
94	2000	CdTe	918	MJ/m²	Energy value includes cell production, module assembly and others at a production scale of 100MW per year.	No	Not based on actual production data. The authors mention that this value represents an update of the	Ito, M., Kato, K., Komoto, K., Kichimi, T., & Kurokawa, K. (2008). A comparative study on cost and life-cycle analysis for 100 MW very large- scale PV (VLS- PV) systems in deserts	Table 4

Sl No	Year	Technology	Energy	Unit	Comments	Considered for analysis?	Reason for not considering	Source	Section referred to in source
							value reported in sl no 46	using m- Si, a- Si, CdTe, and CIS modules. Progress in Photovoltaics: research and applications, 16(1), 17-30.	
95	2006	Multi Si	2300	MJ/m²	1494 Mj per panel of area 0.65 m2. Energy value includes Si Production, purification,crystallization, wafering, cell Processing, module assembly	No	Not based on actual production data. The authors estimate the value from commonly used industrial processes.	Stoppato, A. (2008). Life cycle assessment of photovoltaic electricity generation. Energy, 33(2), 224-232.	Section 4
96	2009	Mono Si	3986	MJ/m²	Energy value includes Si production process, casting and cutting, cell production, module assembly	No	Author estimates not based on actual production data.	Ito, Masakazu, et al. "A comparative study on life cycle analysis of 20 different PV modules installed at the Hokuto mega-solar plant." Progress in Photovoltaics: Research and Applications 19.7 (2011): 878-886.	Table 3
97	2009	Multi Si	2737	MJ/m²	Energy value includes Si production process, casting and cutting, cell production, module assembly	No	Author estimates not based on actual production data.	Ito, Masakazu, et al. "A comparative study on life cycle analysis of 20 different PV modules installed at the Hokuto mega-solar plant." Progress in Photovoltaics: Research and Applications 19.7 (2011): 878-886.	Table 3
98	2001	amorphous Si	1202	MJ/m²	Energy value includes cell production, module assembly and others at a production scale of 100MW per year.	No	Author estimates not based on	Ito, Masakazu, et al. "A comparative study on life cycle analysis	Table 3

Sl No	Year	Technology	Energy	Unit	Comments	Considered for analysis?	Reason for not considering	Source	Section referred to in source
							actual production data. Duplicate value. This study refers to the estimates published in Sl No 93.	of 20 different PV modules installed at the Hokuto mega-solar plant." Progress in Photovoltaics: Research and Applications 19.7 (2011): 878-886.	
99	2009	Multi Si	19712	GJ/MW	Energy value includes mining, manufacturing, transport, construction, transmission, operation.	No	Data given in GJ/MW without module efficiency values. Therefore, we cannot convert this to a MJ/m2 value. Further the LCA data referred to by the authors is the same as the study in Sl No 95 to 98	Ito, Masakazu, Keiichi Komoto, and Kosuke Kurokawa. "Life-cycle analyses of very-large scale PV systems using six types of PV modules." Current Applied Physics 10.2 (2010): S271-S273.	Figure 2
100	2009	Mono Si	28119	GJ/MW	Energy value includes mining, manufacturing, transport, construction, transmission, operation.	No	Data given in GJ/MW without module efficiency values. Therefore, we cannot convert this to a MJ/m2 value. Further the LCA data referred to by the authors is the same as	Ito, Masakazu, Keiichi Komoto, and Kosuke Kurokawa. "Life-cycle analyses of very-large scale PV systems using six types of PV modules." Current Applied Physics 10.2 (2010): S271-S273.	Figure 2

Sl No	Year	Technology	Energy	Unit	Comments	Considered for analysis?	Reason for not considering	Source	Section referred to in source
							the study in Sl No 95 to 98		
101	2009	amorphous Si	14181	GJ/MW	Energy value includes mining, manufacturing, transport, construction, transmission, operation.	No	Data given in GJ/MW without module efficiency values. Therefore, we cannot convert this to a MJ/m2 value. Further the LCA data referred to by the authors is the same as the study in Sl No 95 to 98	Ito, Masakazu, Keiichi Komoto, and Kosuke Kurokawa. "Life-cycle analyses of very-large scale PV systems using six types of PV modules." Current Applied Physics 10.2 (2010): S271-S273.	Figure 2
102	2009	CdTe	14181	GJ/MW	Energy value includes mining, manufacturing, transport, construction, transmission, operation.	No	Data given in GJ/MW without module efficiency values. Therefore, we cannot convert this to a MJ/m2 value.	Ito, Masakazu, Keiichi Komoto, and Kosuke Kurokawa. "Life-cycle analyses of very-large scale PV systems using six types of PV modules." Current Applied Physics 10.2 (2010): S271-S273.	Figure 2
103	1999	Mono Si	7000	MJ/m^2	Energy value includes materials and processes for Ingot, wafer, cells and module. The reported values is 5598 kWh/kWp including the frame. Without the energy values for frame (324 kWh/kWp) we get 5274 kWh/kWp. This value corresponds to the SP75 module and 1 m2 of a module contains 118 Wp (http://www.abcsolar.com/pdf/sp75.pdf). Converting the energy value to a m2 basis we get 622 kWh per m2 and	No	Duplicate value. This study refers to the estimates published in Sl No 104.	Knapp, Karl E., and Theresa L. Jester. "Initial empirical results for the energy payback time of photovoltaic modules." Proceedings of 16th European PVSEC, Glasgow, Scotland (2000): 2053-2056.	Table 1

Sl No	Year	Technology	Energy	Unit	Comments	Considered for analysis?	Reason for not considering	Source	Section referred to in source
					this corresponds to 7000 MJ/m2 (using a grid factor of 0.32 and conversion factor of 3.6 between MJ and kWh).				
104	1999	Mono Si	7000	MJ/m^2	Energy value includes materials and processes for Ingot, wafer, cells and module. The reported values is 5598 kWh/kWp including the frame. Without the energy values for frame (324 kWh/kWp) we get 5274 kWh/kWp. This value corresponds to the SP75 module and 1 m2 of a module contains 118 Wp (http://www.abcsolar.com/pdf/sp75.pdf). Converting the energy value to a m2 basis we get 622 kWh per m2 and this corresponds to 7000 MJ/m2 (using a grid factor of 0.32 and conversion factor of 3.6 between MJ and kWh). This study reports actual manufacturing data.	Yes		Knapp, K., & Jester, T. (2001). Empirical investigation of the energy payback time for photovoltaic modules. Solar Energy, 71(3), 165-172.	Table 1
105	1999	Mono Si	7000	MJ/m^2	Energy value includes materials and processes for Ingot, wafer, cells and module. The reported values is 5598 kWh/kWp including the frame. Without the energy values for frame (324 kWh/kWp) we get 5274 kWh/kWp. This value corresponds to the SP75 module and 1 m2 of a module contains 118 Wp (http://www.abcsolar.com/pdf/sp75.pdf). Converting the energy value to a m2 basis we get 622 kWh per m2 and this corresponds to 7000 MJ/m2 (using a grid factor of 0.32 and conversion factor of 3.6 between MJ and kWh).	No	Duplicate value. This study refers to the estimates published in Sl No 103.	Kannan, R., Leong, K. C., Osman, R., Ho, H. K., & Tso, C. P. (2006). Life cycle assessment study of solar PV systems: an example of a 2.7 kW p distributed solar PV system in Singapore. Solar energy, 80(5), 555-563.	Section 4.2
106	1991	Multi Si	5456	MJ/m^2	The value reported is 235 kWh/m2. However, this does not include the purification of metal grade silicon to poly silicon as the author assumes poly silicon is got from electronic industry off specs. 1.16 kg/m2 of purified silicon is required. To account for this	Yes		Palz, W., & Zibetta, H. (1991). Energy pay-back time of photovoltaic modules. International Journal	Table 1

Sl No	Year	Technology	Energy	Unit	Comments	Considered for analysis?	Reason for not considering	Source	Section referred to in source
					we include 250 kWh/kg refining energy that is reported in "EG-Silicon" section in "Hagedorn, G. (1989). Hidden energy in solar cells and photovoltaic power stations. In 9th European Photovoltaic Solar Energy Conference (p. 542).". We select this study as it is the closest in time with the Palz and Zibetta study. Energy value includes Silicon purification, cutting, wafering, cell preparation, encapsulation materials and process and indirect processes.			of Solar Energy, 10(3-4), 211-216.	
107	1991	amorphous Si	774	MJ/m²	Energy value includes glass substrate, SnO2 layer, laser cutting, a-Si deposition, Al deposition, encapsulation, raw materials, indirect processes.	Yes		Palz, W., & Zibetta, H. (1991). Energy pay-back time of photovoltaic modules. International Journal of Solar Energy, 10(3-4), 211-216.	Table 3
108	2005	Mono Si	3444	MJ/m²	The study reports 24.6 GJ/kWp and this is converted to 3444 MJ/m2 based on the efficiency of 14% (140 Wp per m2). This study reports actual manufacturing data. Energy value includes materials and processes for Si Ingot, wafer, cells and module production.	Yes		Jungbluth, N., Tuchschmid, M., & de Wild-Scholten, M. (2008). Life Cycle Assessment of Photovoltaics: update of ecoinvent data V2. 0. ESU-services Ltd.	Figure 5
109	2005	Multi Si	2640	MJ/m²	The study reports 20 GJ/kWp and this is converted to 2640 MJ/m2 based on the efficiency of 13.2% (132 Wp per m2). This study reports actual manufacturing data. Energy value includes materials and processes for Si Ingot, wafer, cells and module production.	Yes		Jungbluth, N., Tuchschmid, M., & de Wild-Scholten, M. (2008). Life Cycle Assessment of Photovoltaics: update of ecoinvent data V2. 0. ESU-services Ltd.	Figure 5
110	2005	CdTe	1036	MJ/m²	The study reports 14.6 GJ/kWp and this is converted to 1036 MJ/m2 based on the efficiency of 7.1% (71 Wp per m2). This study reports actual manufacturing data.	Yes		Jungbluth, N., Tuchschmid, M., & de Wild-Scholten, M. (2008). Life Cycle Assessment of	Figure 5

Sl No	Year	Technology	Energy	Unit	Comments	Considered for analysis?	Reason for not considering	Source	Section referred to in source
								Photovoltaics: update of ecoinvent data V2. 0. ESU-services Ltd.	
111	2005	amorphous Si	1150	MJ/m²	The study reports 17.7 GJ/kWp and this is converted to 1150 MJ/m2 based on the efficiency of 6.5% (65 Wp per m2).	No	This study refers to the estimates published in Sl No 179 and 180	Jungbluth, N., Tuchschmid, M., & de Wild-Scholten, M. (2008). Life Cycle Assessment of Photovoltaics: update of ecoinvent data V2. 0. ESU-services Ltd.	Figure 5
112	2011	Mono Si	3592	MJ/m²	Energy value includes Si feedstock, ingot and cell production, module production. Based on actual manufacturing data. Assumes electricity used for manufacturing is based on UCTE (continental Europe) grid mix.	Yes		de Wild-Scholten, M. M. (2013). Energy payback time and carbon footprint of commercial photovoltaic systems. Solar Energy Materials and Solar Cells, 119, 296-305.	Table 1 (page 298)
113	2011	Mono Si	4406	MJ/m²	Energy value includes Si feedstock, ingot and cell production, module production. Based on actual manufacturing data. Assumes electricity used for manufacturing is based on the grid mix in China.	Yes		de Wild-Scholten, M. M. (2013). Energy payback time and carbon footprint of commercial photovoltaic systems. Solar Energy Materials and Solar Cells, 119, 296-305.	Table 1 (page 298)
114	2011	Multi Si	1934	MJ/m²	Energy value includes Si feedstock, ingot and cell production, module production. Based on actual manufacturing data. Assumes electricity used for manufacturing is based on UCTE (continental Europe) grid mix.	Yes		de Wild-Scholten, M. M. (2013). Energy payback time and carbon footprint of commercial photovoltaic systems. Solar Energy Materials and Solar Cells, 119, 296-305.	Table 1 (page 298)
115	2011	Multi Si	2370	MJ/m²	Energy value includes Si feedstock, ingot and cell production, module production. Based on actual manufacturing data. Assumes electricity	Yes		de Wild-Scholten, M. M. (2013). Energy payback time and carbon footprint of	Table 1 (page 298)

Sl No	Year	Technology	Energy	Unit	Comments	Considered for analysis?	Reason for not considering	Source	Section referred to in source
					used for manufacturing is based on the grid mix in China.			commercial photovoltaic systems. Solar Energy Materials and Solar Cells, 119, 296-305.	
116	2008	amorphous Si	1060	MJ/m²	Energy value includes module production. Based on actual manufacturing data. Assumes electricity used for manufacturing is based on UCTE (continental Europe) grid mix.	Yes		de Wild-Scholten, M. M. (2013). Energy payback time and carbon footprint of commercial photovoltaic systems. Solar Energy Materials and Solar Cells, 119, 296-305.	Table 1 (page 298)
117	2008	amorphous Si	1050	MJ/m²	Energy value includes module production. Based on actual manufacturing data. Assumes electricity used for manufacturing is based on UCTE (continental Europe) grid mix.	Yes		de Wild-Scholten, M. M. (2013). Energy payback time and carbon footprint of commercial photovoltaic systems. Solar Energy Materials and Solar Cells, 119, 296-305.	Table 1 (page 301)
118	2010	CdTe	752	MJ/m²	Energy value includes module production. Based on actual manufacturing data. Assumes electricity used for manufacturing is based on UCTE (continental Europe) grid mix.	Yes		de Wild-Scholten, M. M. (2013). Energy payback time and carbon footprint of commercial photovoltaic systems. Solar Energy Materials and Solar Cells, 119, 296-305.	Table 1 (page 301)
119	2010	CdTe	745	MJ/m²	Energy value includes module production. Based on actual manufacturing data. Assumes electricity used for manufacturing is based on UCTE (continental Europe) grid mix.	Yes		de Wild-Scholten, M. M. (2013). Energy payback time and carbon footprint of commercial photovoltaic systems. Solar Energy Materials and Solar Cells, 119, 296-305.	Table 1 (page 301)

Sl No	Year	Technology	Energy	Unit	Comments	Considered for analysis?	Reason for not considering	Source	Section referred to in source
120	1998	Mono Si	5045	MJ/m²	Energy value includes Si feedstock, ingot and cell production, module production. See "calculations" tab on how the energy valued is determined. Based on actual manufacturing data.	Yes		Dones, R., & Frischknecht, R. (1998). Life-cycle assessment of photovoltaic systems: results of Swiss studies on energy chains. Progress in Photovoltaics Research and Applications, 6(2), 117-125.	Table 1 and Figure 1
121	1998	Multi Si	6203	MJ/m²	Energy value includes Si feedstock, ingot and cell production, module production. See "calculations" tab on how the energy valued is determined. Based on actual manufacturing data.	Yes		Dones, R., & Frischknecht, R. (1998). Life-cycle assessment of photovoltaic systems: results of Swiss studies on energy chains. Progress in Photovoltaics Research and Applications, 6(2), 117-125.	Table 1 and Figure 1
122	2000	Mono Si	3426	MJ/m²	Energy value includes Si feedstock, ingot and cell production, module production. See "calculations" tab on how the energy valued is determined.	No	This study updates Sl No 120 for technological imprvements and is not based on actual manufacturing data.	Jungbluth, N. (2005). Life cycle assessment of crystalline photovoltaics in the Swiss ecoinvent database. *Progress in Photovoltaics: Research and Applications*, *13*(5), 429-446.	Table 4
123	2000	Multi Si	1965	MJ/m²	Energy value includes Si feedstock, ingot and cell production, module production. See "calculations" tab on how the energy valued is determined.	No	This study updates Sl No 121 for technological imprvements and is not based on actual	Jungbluth, N. (2005). Life cycle assessment of crystalline photovoltaics in the Swiss ecoinvent database. *Progress in Photovoltaics: Research*	Table 4

Sl No	Year	Technology	Energy	Unit	Comments	Considered for analysis?	Reason for not considering	Source	Section referred to in source
							manufacturing data.	*and Applications*, *13*(5), 429-446.	
124	1989	Mono Si	8120	MJ/m²	Energy value includes Si purification, Si wafer and cell production and module production with frame. Based on actual production data and we deduct 700 mj/m2 for the frame. Since this study was published in 1988 we assume an extra 200 mj/m2 for the frame when compared to 500 mj/m2 assumed in a later study ,"Energy pay-back time and CO2 emissions of PV systems", published in year 2000.	No	Duplicate value. This study refers to the estimates published in Sl No 83.	Schaefer, H., & Hagedorn, G. (1992). Hidden energy and correlated environmental characteristics of PV power generation. Renewable Energy, 2(2), 159-166.	Table 1
125	1989	Multi Si	6428	MJ/m²	Energy value includes Si purification, Si wafer and cell production and module production with frame. Based on actual production data and we deduct 700 mj/m2 for the frame. Since this study was published in 1988 we assume an extra 200 mj/m2 for the frame when compared to 500 mj/m2 assumed in a later study ,"Energy pay-back time and CO2 emissions of PV systems", published in year 2000.	No	Duplicate value. This study refers to the estimates published in Sl No 84.	Schaefer, H., & Hagedorn, G. (1992). Hidden energy and correlated environmental characteristics of PV power generation. Renewable Energy, 2(2), 159-166.	Table 1
126	1989	amorphous Si	1028	MJ/m²	Energy value includes module production	No	Duplicate value. This study refers to the estimates published in Sl No 85.	Schaefer, H., & Hagedorn, G. (1992). Hidden energy and correlated environmental characteristics of PV power generation. Renewable Energy, 2(2), 159-166.	Table 1
127	1989	Mono Si	6138	MJ/m²	Energy value includes Si purification, Si wafer and cell production and module production without frame.	No	Duplicate value. This study refers to the estimates published in Sl No 86.	Schaefer, H., & Hagedorn, G. (1992). Hidden energy and correlated environmental characteristics of PV power generation. Renewable Energy, 2(2), 159-166.	Table 1

Sl No	Year	Technology	Energy	Unit	Comments	Considered for analysis?	Reason for not considering	Source	Section referred to in source
128	1989	Multi Si	3645	MJ/m²	Energy value includes Si purification, Si wafer and cell production and module production without frame.	No	Duplicate value. This study refers to the estimates published in Sl No 87.	Schaefer, H., & Hagedorn, G. (1992). Hidden energy and correlated environmental characteristics of PV power generation. Renewable Energy, 2(2), 159-166.	Table 1
129	1989	amorphous Si	1584	MJ/m²	Energy value includes module production	No	Duplicate value. This study refers to the estimates published in Sl No 88.	Schaefer, H., & Hagedorn, G. (1992). Hidden energy and correlated environmental characteristics of PV power generation. Renewable Energy, 2(2), 159-166.	Table 1
130	1999	Mono Si	7000	MJ/m²	Energy value includes materials and processes for Ingot, wafer, cells and module. The reported values is 5598 kWh/kWp including the frame. Without the energy values for frame (324 kWh/kWp) we get 5274 kWh/kWp. This value corresponds to the SP75 module and 1 m2 of a module contains 118 Wp (http://www.abcsolar.com/pdf/sp75.pdf). Converting the energy value to a m2 basis we get 622 kWh per m2 and this corresponds to 7000 MJ/m2 (using a grid factor of 0.32 and conversion factor of 3.6 between MJ and kWh).	No	Duplicate value. This study refers to the estimates published in Sl No 104.	Knapp, K. E., Jester, T. L., & Mihaiik, G. B. (2000). Energy balances for photovoltaic modules: status and prospects. In Photovoltaic Specialists Conference, 2000. Conference Record of the Twenty-Eighth IEEE (pp. 1450-1455). IEEE.	Figure 2
131	1997	amorphous Si	895	MJ/m²	Module dimension is 0.1194 m * 0.34 m and the corresponding energy requirement is 366.7 MJ. Energy value includes input materials and manufacturing.	Yes		Keoleian, G. A. and Lewis, G. McD. (1997), Application of life-cycle energy analysis to photovoltaic module design. Prog. Photovolt: Res. Appl., 5: 287–300.	"Energy Analysis" subsection under "Results and Discussion"

Sl No	Year	Technology	Energy	Unit	Comments	Considered for analysis?	Reason for not considering	Source	Section referred to in source
132	2011	Mono Si	5572	MJ/m²	Boundary is unclear as the authors don't mention if they include the frame, BOS or not	No	This study refers to the ecoinvent report for PV manufacturing inventory and is not based on actual manufacturing data	Laleman, R., Albrecht, J., & Dewulf, J. (2011). Life cycle analysis to estimate the environmental impact of residential photovoltaic systems in regions with a low solar irradiation. Renewable and Sustainable Energy Reviews, 15(1), 267-281.	Figure 1
133	2011	Multi Si	4700	MJ/m²	Boundary is unclear as the authors don't mention if they include the frame, BOS or not	No	This study refers to the ecoinvent report for PV manufacturing inventory and is not based on actual manufacturing data	Laleman, R., Albrecht, J., & Dewulf, J. (2011). Life cycle analysis to estimate the environmental impact of residential photovoltaic systems in regions with a low solar irradiation. Renewable and Sustainable Energy Reviews, 15(1), 267-281.	Figure 1
134	2011	amorphous Si	2064	MJ/m²	Boundary is unclear as the authors don't mention if they include the frame, BOS or not	No	This study refers to the ecoinvent report for PV manufacturing inventory and is not based on actual manufacturing data	Laleman, R., Albrecht, J., & Dewulf, J. (2011). Life cycle analysis to estimate the environmental impact of residential photovoltaic systems in regions with a low solar irradiation. Renewable and Sustainable Energy Reviews, 15(1), 267-281.	Figure 1

Sl No	Year	Technology	Energy	Unit	Comments	Considered for analysis?	Reason for not considering	Source	Section referred to in source
135	2011	CdTe	2233	MJ/m²	Boundary is unclear as the authors don't mention if they include the frame, BOS or not	No	This study refers to the ecoinvent report for PV manufacturing inventory and is not based on actual manufacturing data	Laleman, R., Albrecht, J., & Dewulf, J. (2011). Life cycle analysis to estimate the environmental impact of residential photovoltaic systems in regions with a low solar irradiation. Renewable and Sustainable Energy Reviews, 15(1), 267-281.	Figure 1
136	2004	Mono Si	7174	MJ/m²	Author does not mention explicitly whether frame is included in this energy value that accounts for the manufacturing processes and materials required to produce the PV module. We assume the embodied energy includes a frame and therefore deduct a value of 150 MJ/m2 for frame based on a similar study (Sl no 71) published during the same time.	No	Energy values are determined by reviewing existing literature and not based on actual manufacturing data.	Gürzenich, D., & Wagner, H. J. (2004). Cumulative energy demand and cumulative emissions of photovoltaics production in Europe. Energy, 29(12), 2297-2303.	Table 3
137	2004	Multi Si	2588	MJ/m²	Author does not mention explicitly whether frame is included in this energy value that accounts for the manufacturing processes and materials required to produce the PV module. We assume the embodied energy includes a frame and therefore deduct a value of 150 MJ/m2 for frame based on a similar study (Sl no 71) published during the same time.	No	Energy values are determined by reviewing existing literature and not based on actual manufacturing data.	Gürzenich, D., & Wagner, H. J. (2004). Cumulative energy demand and cumulative emissions of photovoltaics production in Europe. Energy, 29(12), 2297-2303.	Table 3
138	2004	amorphous Si	1576	MJ/m²	Energy value includes manufacturing processes and materials required to produce the PV module	No	Energy values are determined by reviewing existing literature and not based on actual	Gürzenich, D., & Wagner, H. J. (2004). Cumulative energy demand and cumulative emissions of photovoltaics production in	Table 3

Sl No	Year	Technology	Energy	Unit	Comments	Considered for analysis?	Reason for not considering	Source	Section referred to in source
							manufacturing data.	Europe. Energy, 29(12), 2297-2303.	
139	2008	Mono Si	3528	MJ/m²	Energy value includes Silicon purification and processing, silicon ingot slicing and module fabrication.	No	Energy values are determined by reviewing existing literature and not based on actual manufacturing data.	Estimation of the energetic Cucchiella, F., & D'Adamo, I. (2012). Estimation of the energetic and environmental impacts of a roof-mounted building-integrated photovoltaic systems. Renewable and Sustainable Energy Reviews, 16(7), 5245-5259.and environmental impacts of a roof-mounted building-integrated photovoltaic systems	Table 8
140	2004	Mono Si	3513	MJ/m²	Energy value includes Silicon purification and processing, silicon ingot slicing and module fabrication.	No	Energy values are determined by reviewing existing literature and not based on actual manufacturing data.	Estimation of the energetic Cucchiella, F., & D'Adamo, I. (2012). Estimation of the energetic and environmental impacts of a roof-mounted building-integrated photovoltaic systems. Renewable and Sustainable Energy Reviews, 16(7), 5245-5259.and environmental impacts of a roof-mounted building-integrated photovoltaic systems	Table 8

Sl No	Year	Technology	Energy	Unit	Comments	Considered for analysis?	Reason for not considering	Source	Section referred to in source
141	2011	Mono Si	3513	MJ/m²	Energy value includes Silicon purification and processing, silicon ingot slicing and module fabrication.	No	Energy values are determined by reviewing existing literature and not based on actual manufacturing data.	Estimation of the energetic Cucchiella, F., & D'Adamo, I. (2012). Estimation of the energetic and environmental impacts of a roof-mounted building-integrated photovoltaic systems. Renewable and Sustainable Energy Reviews, 16(7), 5245-5259.and environmental impacts of a roof-mounted building-integrated photovoltaic systems	Table 8
142	2012	Mono Si	5670	MJ/m²	Energy value includes Silicon purification and processing, silicon ingot slicing and module fabrication.	No	Energy values are determined by reviewing existing literature and not based on actual manufacturing data.	Estimation of the energetic Cucchiella, F., & D'Adamo, I. (2012). Estimation of the energetic and environmental impacts of a roof-mounted building-integrated photovoltaic systems. Renewable and Sustainable Energy Reviews, 16(7), 5245-5259.and environmental impacts of a roof-mounted building-integrated photovoltaic systems	Table 9
143	2012	Multi Si	4720	MJ/m²	Energy value includes Silicon purification and processing, silicon ingot slicing and module fabrication.	No	Energy values are determined by reviewing	Estimation of the energetic Cucchiella, F., & D'Adamo, I. (2012). Estimation of	Table 9

Sl No	Year	Technology	Energy	Unit	Comments	Considered for analysis?	Reason for not considering	Source	Section referred to in source
							existing literature and not based on actual manufacturing data.	the energetic and environmental impacts of a roof-mounted building-integrated photovoltaic systems. Renewable and Sustainable Energy Reviews, 16(7), 5245-5259.and environmental impacts of a roof-mounted building-integrated photovoltaic systems	
144	2012	CdTe	2200	MJ/m²	Energy value includes module manufacturing.	No	Energy values are determined by reviewing existing literature and not based on actual manufacturing data.	Estimation of the energetic Cucchiella, F., & D'Adamo, I. (2012). Estimation of the energetic and environmental impacts of a roof-mounted building-integrated photovoltaic systems. Renewable and Sustainable Energy Reviews, 16(7), 5245-5259.and environmental impacts of a roof-mounted building-integrated photovoltaic systems	Table 9
145	2000	Mono Si	3426	MJ/m²	Energy value includes Si feedstock, ingot and cell production, module production. See "calculations" tab on how the energy valued is determined.	No	Duplicate value. This study refers to the estimates published in Sl No 122.	Dones, R., Bauer, C., Bolliger, R., Burger, B., Faist Emmenegger, M., Frischknecht, R., ... & Tuchschmid, M. (2007). Life cycle inventories of energy	Table 12.2

Sl No	Year	Technology	Energy	Unit	Comments	Considered for analysis?	Reason for not considering	Source	Section referred to in source
								systems: results for current systems in Switzerland and other UCTE countries. Ecoinvent report, 5(5).	
146	2008	Multi Si	1912	MJ/m²	Energy value includes material and manufacture and excludes transportation and use.	No	Not based on actual manufacturing data and is based on source in Sl No 78.	Filippidou, F., Botsaris, P. N., Angelakoglou, K., & Gaidajis, G. (2010). A comparative analysis of a cdte and a poly-Si photovoltaic module installed in North Eastern Greece1. Applied Solar Energy, 46(3), 182-191.	Table 6
147	1998	CdTe	937	MJ/m²	Energy value includes material and manufacturing and excludes transportation and use.	No	Duplicate value. This study refers to the estimates published in Sl No 10.	Filippidou, F., Botsaris, P. N., Angelakoglou, K., & Gaidajis, G. (2010). A comparative analysis of a cdte and a poly-Si photovoltaic module installed in North Eastern Greece1. Applied Solar Energy, 46(3), 182-191.	Table 5
148	1995	Mono Si	13685	MJ/m²	Energy value includes module manufacturing.	No	The author refers to a source which is in Italian. Further the boundary conditions and the processes included in this energy calculation	Frankl, P., Masini, A., Gamberale, M. and Toccaceli, D. (1998), Simplified life-cycle analysis of PV systems in buildings: present situation and future trends. Prog. Photovolt: Res. Appl., 6: 137–146	Table 3

Sl No	Year	Technology	Energy	Unit	Comments	Considered for analysis?	Reason for not considering	Source	Section referred to in source
							cannot be verified from this paper and the mass based allocation of the energy impacts of producing electronic grade silicon between the PV and the electronic industries has not be explained in detail.		
149	1995	Multi Si	16394	MJ/m²	Energy value includes module manufacturing.	No	The author refers to a source which is in Italian. Further the boundary conditions and the processes included in this energy calculation cannot be verified from this paper and the mass based allocation of the energy impacts of producing electronic grade silicon between the	Frankl, P., Masini, A., Gamberale, M. and Toccaceli, D. (1998), Simplified life-cycle analysis of PV systems in buildings: present situation and future trends. Prog. Photovolt: Res. Appl., 6: 137–146	Table 3

Sl No	Year	Technology	Energy	Unit	Comments	Considered for analysis?	Reason for not considering	Source	Section referred to in source
							PV and the electronic industries has not be explained in detail.		
150	2005	CdTe	1200	MJ/m²	Energy value includes material and manufacturing.	Yes		Fthenakis, V., & Kim, H. C. (2005, January). Energy use and greenhouse gas emissions in the life cycle of CdTe photovoltaics. In MRS Proceedings (Vol. 895, pp. 0895-G03). Cambridge University Press.	Table 2
151	2005	Multi Si	3940	MJ/m²	Energy value includes Si feedstock,ingot and wafer, cell production, module assembly.	No	Duplicate value. This study refers to the estimates published in Sl No 47. Sl 47 has the embodied energy of frame deducted where as this paper reports values with the frame	Fthenakis, V. M., & Kim, H. C. (2007). Greenhouse-gas emissions from solar electric-and nuclear power: A life-cycle study. Energy Policy, 35(4), 2549-2557.	Section 3
152	2006	CdTe	1200	MJ/m²	Energy value includes material and manufacturing for module production.	Yes	Authors refer "Fthenakis, V.M., Kim, H.C., 2006. Life cycle energy use and greenhouse gas emissions embedded in	Fthenakis, V. M., & Kim, H. C. (2007). Greenhouse-gas emissions from solar electric-and nuclear power: A life-cycle study. Energy Policy, 35(4), 2549-2557.	Section 3

Sl No	Year	Technology	Energy	Unit	Comments	Considered for analysis?	Reason for not considering	Source	Section referred to in source
							electricity generated by thin film CdTe photovoltaics. Material Research Society Symposium Proceedings' which we were not able to locate. Therefore, we use this data point		
153	2011	Multi Si	4256	MJ/m²	Energy value includes Si feedstock,ingot and wafer, cell production, module assembly. Based on actual manufacturing data.	Yes		Fthenakis, V., Betita, R., Shields, M., Vinje, R., & Blunden, J. (2012). Life cycle analysis of high-performance monocrystalline silicon photovoltaic systems: energy payback times and net energy production value. In 27th European Photovoltaic Solar Energy Conference and Exhibition.	Table 4
154	2000	Mono Si	5700	MJ/m²	Energy value includes Si Production, purification,crystallization, wafering, cell Processing, module assembly	No	Duplicate value. This study uses the same data as used in Sl No 17.	García-Valverde, R., Miguel, C., Martínez-Béjar, R., & Urbina, A. (2009). Life cycle assessment study of a 4.2 kW p stand-alone photovoltaic system. Solar Energy, 83(9), 1434-1445.	Section 3.2.1.1

Sl No	Year	Technology	Energy	Unit	Comments	Considered for analysis?	Reason for not considering	Source	Section referred to in source
155	2008	CdTe	806	MJ/m²	Energy value includes material and manufacturing and is based on actual industrial production.	Yes		Held, M., & Ilg, R. (2008). Life Cycle Assessment (LCA) of CdTe thin film modules and Material Flow Analysis of cadmium within EU27'. In 23rd European Photovoltaic Solar Energy Conference (EU PVSEC) (Vol. 10).	Figure 2
156	1994	CdTe	938	MJ/m²	Energy value includes material and manufacturing. For consistency with other literature reported values, we have not included 54 MJ/m2 for capital equipment.	No	Not based on actual manufacturing data	Hynes, K. M., Baumann, A. E., & Hill, R. (1994). An assessment of the environmental impacts on thin film cadmium telluride modules based on life cycle analysis. In 1994 IEEE first world conference on photovoltaic energy conversion: Conference record of the twenty fourth IEEE photovoltaic specialists conference--1994. Volume 1.	Table 2
157	1994	CdTe	1142	MJ/m²	Energy value includes material and manufacturing. For consistency with other literature reported values, we have not included 46 MJ/m2 for capital equipment.	No	Not based on actual manufacturing data	Hynes, K. M., Baumann, A. E., & Hill, R. (1994). An assessment of the environmental impacts on thin film cadmium telluride modules based on life cycle analysis. In 1994 IEEE first world	Table 2

Sl No	Year	Technology	Energy	Unit	Comments	Considered for analysis?	Reason for not considering	Source	Section referred to in source
								conference on photovoltaic energy conversion: Conference record of the twenty fourth IEEE photovoltaic specialists conference--1994. Volume 1.	
158	1998	Multi Si	2044	MJ/m²	Energy value includes Si production process, casting and cutting, cell production, module assembly and others at a production scale of 100MW per year	No	Duplicate value. This study uses the same data as used in Sl No 92.	Ito, M., Kato, K., Komoto, K., Kichimi, T., Sugihara, H., & Kurokawa, K. (2003, May). An analysis of variation of very large-scale PV (VLS-PV) systems in the world deserts. In Photovoltaic Energy Conversion, 2003. Proceedings of 3rd World Conference on (Vol. 3, pp. 2809-2814). IEEE.	Table 6
159	2000	Mono Si	3426	MJ/m²	Energy value includes Si feedstock, ingot and cell production, module production.	No	Duplicate value. This study uses the same data as used in Sl No 122.	Jungbluth, N., Bauer, C., Dones, R., & Frischknecht, R. (2005). Life cycle assessment for emerging technologies: case studies for photovoltaic and wind power (11 pp). The International Journal of Life Cycle Assessment, 10(1), 24-34.	Table 4
160	2000	Multi Si	1965	MJ/m²	Energy value includes Si feedstock, ingot and cell production, module production.	No	Duplicate value. This study uses the same data as	Jungbluth, N., Bauer, C., Dones, R., & Frischknecht, R. (2005). Life cycle	Table 4

Sl No	Year	Technology	Energy	Unit	Comments	Considered for analysis?	Reason for not considering	Source	Section referred to in source
							used in Sl No 123.	assessment for emerging technologies: case studies for photovoltaic and wind power (11 pp). The International Journal of Life Cycle Assessment, 10(1), 24-34.	
161	2006	Mono Si	3513	MJ/m²	Energy value includes Si purification and processing, cell fabrication and module assembly	No	Based on previously published literature values	Nawaz, I., & Tiwari, G. N. (2006). Embodied energy analysis of photovoltaic (PV) system based on macro-and micro-level. Energy Policy, 34(17), 3144-3152.	Table 3
162	2009	Mono Si	4284	MJ/m²	Based on review of previous literature. Do not use this.	No	Based on previously published literature values	Kaldellis, J. K., Zafirakis, D., & Kondili, E. (2009). Optimum autonomous stand-alone photovoltaic system design on the basis of energy pay-back analysis. Energy, 34(9), 1187-1198.	Table 1
163	2009	Multi Si	3276	MJ/m²	Based on review of previous literature. Do not use this.	No	Based on previously published literature values	Kaldellis, J. K., Zafirakis, D., & Kondili, E. (2009). Optimum autonomous stand-alone photovoltaic system design on the basis of energy pay-back analysis. Energy, 34(9), 1187-1198.	Table 1
164	2009	CdTe	1360	MJ/m²	Based on review of previous literature. Do not use this.	No	Based on previously published	Kaldellis, J. K., Zafirakis, D., & Kondili, E. (2009).	Table 1

Sl No	Year	Technology	Energy	Unit	Comments	Considered for analysis?	Reason for not considering	Source	Section referred to in source
							literature values	Optimum autonomous stand-alone photovoltaic system design on the basis of energy pay-back analysis. Energy, 34(9), 1187-1198.	
165	2009	amorphous Si	957	MJ/m²	Based on review of previous literature. Do not use this.	No	Based on previously published literature values	Kaldellis, J. K., Zafirakis, D., & Kondili, E. (2009). Optimum autonomous stand-alone photovoltaic system design on the basis of energy pay-back analysis. Energy, 34(9), 1187-1198.	Table 1
166	2013	CdTe	495	MJ/m²	Based on actual production data. Energy value includes module manufacturing.	Yes		Kim, H., Cha, K., Fthenakis, V. M., Sinha, P., & Hur, T. (2014). Life cycle assessment of cadmium telluride photovoltaic (CdTe PV) systems. Solar Energy, 103, 78-88.	Section 4.3
167	1990	Mono Si	9618	MJ/m²	Boundary assumptions is not mentioned.	No	Author has not metnioned the boundary assumptions and not provided the source for the embodied energy values.	Kreith, F., Norton, P., & Brown, D. (1990). A comparison of CO 2 emissions from fossil and solar power plants in the United States. Energy, 15(12), 1181-1198.	Table 6
168	2006	Mono Si	3513	MJ/m²	Energy value includes Si purification and processing, cell fabrication and module assembly	No	Duplicate value. This study uses the same data as used in Sl No 161.	Li, D. H. W., Chow, S. K. H., & Lee, E. W. M. (2013). An analysis of a medium size grid-connected building integrated	Section 4

Sl No	Year	Technology	Energy	Unit	Comments	Considered for analysis?	Reason for not considering	Source	Section referred to in source
								photovoltaic (BIPV) system using measured data. Energy and Buildings, 60, 383-387.	
169	2006	Mono Si	3513	MJ/m²	Energy value includes Si purification and processing, cell fabrication and module assembly	No	Duplicate value. This study uses the same data as used in Sl No 161.	Lu, L., & Yang, H. X. (2010). Environmental payback time analysis of a roof-mounted building-integrated photovoltaic (BIPV) system in Hong Kong. Applied Energy, 87(12), 3625-3631.	Section 3.1
170	1997	amorphous Si	782	MJ/m²	Energy value includes input materials and manufacturing.	No	Not based on actual manufacturing data and is based on source in Sl No 131.	Meier, P. J. (2002). Life-cycle assessment of electricity generation systems and applications for climate change policy analysis. University of Wisconsin--Madison. Chicago	Table B3
171	1997	amorphous Si	782	MJ/m²	Energy value includes input materials and manufacturing.	No	Not based on actual manufacturing data and is based on source in Sl No 131.	Meier PJ, Kulcinski. Life-Cycle Energy Costs and Greenhouse Gas Emissions for Building-Integrated Photovoltaics. 2002.	Table in page A2
172	1998	Mono Si	3804	MJ/m²	Energy value includes input materials and manufacturing.	No	Not based on actual manufacturing data and calculated from published literature values	Meijer, A., Huijbregts, M. A. J., Schermer, J. J., & Reijnders, L. (2003). Life- cycle assessment of photovoltaic modules: Comparison of mc- Si, InGaP and InGaP/mc- Si solar	Table 2 (page 282)

Sl No	Year	Technology	Energy	Unit	Comments	Considered for analysis?	Reason for not considering	Source	Section referred to in source
								modules. Progress in Photovoltaics: Research and Applications, 11(4), 275-287.	
173	2004	Multi Si	4000	MJ/m²	Energy value includes Si purification and processing, cell fabrication and module assembly	No	Not based on actual manufacturing data and is based on source in Sl No 174.	Müller, A., Wambach, K., & Alsema, E. (2005, January). Life Cycle Analysis of solar module recycling process. In MRS Proceedings (Vol. 895, pp. 0895-G03). Cambridge University Press.	Table 1
174	2004	Multi Si	3706	MJ/m²	Energy value includes materials and manufacturing. Based on actual industrial data.	Yes		Alsema, E., & de Wild, M. J. (2005, January). Environmental impact of crystalline silicon photovoltaic module production. In *MRS Proceedings* (Vol. 895, pp. 0895-G03). Cambridge University Press.	Figure 3
175	2005	Mono Si	4050	MJ/m²	Energy value includes processes and materials for the PV module. 180 kWh thermal for 160 m2.	No	Not based on actual manufacturing data and calculated from published literature values	Muneer, T., Younes, S., Lambert, N., & Kubie, J. (2006). Life cycle assessment of a medium-sized photovoltaic facility at a high latitude location. Proceedings of the Institution of Mechanical Engineers, Part A: Journal of Power and Energy, 220(6), 517-524.	Table 2

Sl No	Year	Technology	Energy	Unit	Comments	Considered for analysis?	Reason for not considering	Source	Section referred to in source
176	1998	Multi Si	4200	MJ/m²	Energy value includes silicon winning and purification, silicon wafer production, cell/module processing, module encapsulation materials, overhead operations and equipment manufacturing.	No	Duplicate value. This study refers to the estimates published in Sl No 1	Pacca, S. A. (2003). Global warming effect applied to electricity generation technologies (Doctoral dissertation, University of California, Berkeley).	Table 10
177	1998	amorphous Si	1200	MJ/m²	Energy value includes cell material, cell/module processing, module encapsulation materials, overhead operations and equipment manufacturing.	No	Duplicate value. This study refers to the estimates published in Sl No 2	Pacca, S. A. (2003). Global warming effect applied to electricity generation technologies (Doctoral dissertation, University of California, Berkeley).	Table 10
178	1998	Multi Si	4435	MJ/m²	Energy value includes direct and indirect process requirements and input materials.	No	Duplicate value. This study refers to the estimates published in Sl No 1 and 56-58.	Pacca, S., Sivaraman, D., & Keoleian, G. A. (2006). Life cycle assessment of the 33 kW photovoltaic system on the Dana building at the University of Michigan: thin film laminates, multi-crystalline modules, and balance of system components. University of Michigan.	Table 12
179	2006	amorphous Si	861	MJ/m²	Energy value includes the production of the module. Based on actual production data.	Yes		Pacca, S., Sivaraman, D., & Keoleian, G. A. (2006). Life cycle assessment of the 33 kW photovoltaic system on the Dana building at the University of Michigan: thin film	Table 12. Energy and material inventory aspects are explained on page 27.

Sl No	Year	Technology	Energy	Unit	Comments	Considered for analysis?	Reason for not considering	Source	Section referred to in source
								laminates, multi-crystalline modules, and balance of system components. University of Michigan.	
180	2006	amorphous Si	834	MJ/m²	Energy value includes the production of the module. Based on actual production data.	Yes		Pacca, S., Sivaraman, D., & Keoleian, G. A. (2006). Life cycle assessment of the 33 kW photovoltaic system on the Dana building at the University of Michigan: thin film laminates, multi-crystalline modules, and balance of system components. University of Michigan.	Table 12. Energy and material inventory aspects are explained on page 27.
181	1998	Multi Si	4435	MJ/m²	Energy value includes direct and indirect process requirements and input materials.	No	Duplicate value. This study refers to the estimates published in Sl No 178	Pacca, S., Sivaraman, D., & Keoleian, G. A. (2007). Parameters affecting the life cycle performance of PV technologies and systems. Energy Policy, 35(6), 3316-3326.	Section 3.3
182	2006	amorphous Si	861	MJ/m²	Energy value includes the production of the module.	No	Duplicate value. This study refers to the estimates published in Sl No 179	Pacca, S., Sivaraman, D., & Keoleian, G. A. (2007). Parameters affecting the life cycle performance of PV technologies and systems. Energy Policy, 35(6), 3316-3326.	Section 3.3
183	2000	Multi Si	3560	MJ/m²	Energy value includes Si purification, cell processing and module assembly	No	Not based on actual manufacturing	Pehnt, M., Bubenzer, A., & Räuber, A. (2003). Life cycle	Table 4.2

Sl No	Year	Technology	Energy	Unit	Comments	Considered for analysis?	Reason for not considering	Source	Section referred to in source
							data. Author calculates the value by averaging previously published literature values.	assessment of photovoltaic systems—trying to fight deep-seated prejudices. In Photovoltaics Guidebook for Decision-Makers (pp. 179-213). Springer Berlin Heidelberg.	
184	2005	Mono Si	4950	MJ/m²	Energy value includes materials and manufacturing.	No	Duplicate value. This study refers to the estimates published in Sl No 65	Perpiñan, O., Lorenzo, E., Castro, M. A., & Eyras, R. (2009). Energy payback time of grid connected PV systems: comparison between tracking and fixed systems. Progress in Photovoltaics: Research and Applications, 17(2), 137-147.	Table 2
185	1993	Mono Si	6675	MJ/m²	Energy value includes Si purification and processing, cell fabrication and module assembly. Based on actual production data	Yes		Prakash, R., & Bansal, N. K. (1995). Energy analysis of solar photovoltaic module production in India. *Energy Sources*, *17*(6), 605-613.	Refer "Module Production" section
186	1993	Mono Si	6461	MJ/m²	Energy value includes Si purification and processing, cell fabrication and module assembly.	No	Not using this value as it is based on a 3 month industrial shift where as Sl No 185 (in the same study) is for a longer observation	Prakash, R., & Bansal, N. K. (1995). Energy analysis of solar photovoltaic module production in India. *Energy Sources*, *17*(6), 605-613.	Refer "Module Production" section

Sl No	Year	Technology	Energy	Unit	Comments	Considered for analysis?	Reason for not considering	Source	Section referred to in source
							period of 9 months.		
187	2000	amorphous Si	1190	MJ/m²	Energy value includes cell material, substrate and encapsulation, cell/module processing and overhead operations.	No	Not based on actual manufacturing data but derived from literature value in Sl No 19	Sherwani, A. F., & Usmani, J. A. (2011). Life cycle assessment of 50 kW p grid connected solar photovoltaic (SPV) system in India. International Journal of Energy & Environment, 2(1).	Table 4
188	2011	Multi Si	2783	MJ/m²	Energy value includes materials and processing of PV module.	No	Not based on actual manufacturing data and is based on published literature values	Sumper, A., Robledo-García, M., Villafáfila-Robles, R., Bergas-Jané, J., & Andrés-Peiró, J. (2011). Life-cycle assessment of a photovoltaic system in Catalonia (Spain). Renewable and Sustainable Energy Reviews, 15(8), 3888-3896.	Table 3
189	2006	Mono Si	3513	MJ/m²	Energy value includes Si purification and processing, cell fabrication and module assembly	No	Duplicate value. This study refers to the estimates published in Sl No 161	Tiwari, A., Barnwal, P., Sandhu, G. S., & Sodha, M. S. (2009). Energy metrics analysis of hybrid–photovoltaic (PV) modules. Applied Energy, 86(12), 2615-2625.	Table 8
190	2005	Multi Si	3043	MJ/m²	Energy value includes materials and processing of PV module.	No	Not based on actual manufacturing data and is based on data from the Simapro software	Tripanagnostopoulos, Y., Souliotis, M., Battisti, R., & Corrado, A. (2005). Energy, cost and LCA results of PV and hybrid PV/T solar systems. Progress in	Table 4

Sl No	Year	Technology	Energy	Unit	Comments	Considered for analysis?	Reason for not considering	Source	Section referred to in source
								Photovoltaics: Research and applications, 13(3), 235-250.	
191	2005	Multi Si	2683	MJ/m²	Energy value includes materials and processing of PV module.	No	Not based on actual manufacturing data and is based on data from the Simapro software	Tripanagnostopoulos, Y., Souliotis, M., Battisti, R., & Corrado, A. (2006). Performance, cost and life- cycle assessment study of hybrid PVT/AIR solar systems. Progress in Photovoltaics: Research and applications, 14(1), 65-76.	Table 3
192	2006	Mono Si	5264	MJ/m²	Energy value includes Si purification and processing, sawing, wafering, cell fabrication and module assembly. kWh/m2 value is converted to MJ/m2 using a grid factor of 0.32 and conversion factor of 3.6 between MJ and kWh.	No	Not based on actual manufacturing data and is based on published literature values	Williams, T., Guice, J., & Coyle, J. (2006, May). Strengthening the Environmental Case for Photovoltaics: A Life-Cycle Analysis. In Photovoltaic Energy Conversion, Conference Record of the 2006 IEEE 4th World Conference on (Vol. 2, pp. 2509-2512). IEEE. Chicago	Figure 1
193	2006	Mono Si	5264	MJ/m²	Energy value includes Si purification and processing, sawing, wafering, cell fabrication and module assembly. kWh/m2 value is converted to MJ/m2 using a grid factor of 0.32 and conversion factor of 3.6 between MJ and kWh.	No	Not based on actual manufacturing data and is based on published literature values	Williams, T., Guice, J., & Coyle, J. (2006, May). Strengthening the Environmental Case for Photovoltaics: A Life-Cycle Analysis. In Photovoltaic Energy Conversion,	Figure 1

Sl No	Year	Technology	Energy	Unit	Comments	Considered for analysis?	Reason for not considering	Source	Section referred to in source
								Conference Record of the 2006 IEEE 4th World Conference on (Vol. 2, pp. 2509-2512). IEEE. Chicago	
194	2006	Multi Si	4704	MJ/m²	Energy value includes Si purification and processing, sawing, wafering, cell fabrication and module assembly. kWh/m2 value is converted to MJ/m2 using a grid factor of 0.32 and conversion factor of 3.6 between MJ and kWh.	No	Not based on actual manufacturing data and is based on published literature values	Williams, T., Guice, J., & Coyle, J. (2006, May). Strengthening the Environmental Case for Photovoltaics: A Life-Cycle Analysis. In Photovoltaic Energy Conversion, Conference Record of the 2006 IEEE 4th World Conference on (Vol. 2, pp. 2509-2512). IEEE. Chicago	Figure 1
195	2006	Multi Si	5040	MJ/m²	Energy value includes Si purification and processing, sawing, wafering, cell fabrication and module assembly. kWh/m2 value is converted to MJ/m2 using a grid factor of 0.32 and conversion factor of 3.6 between MJ and kWh.	No	Not based on actual manufacturing data and is based on published literature values	Williams, T., Guice, J., & Coyle, J. (2006, May). Strengthening the Environmental Case for Photovoltaics: A Life-Cycle Analysis. In Photovoltaic Energy Conversion, Conference Record of the 2006 IEEE 4th World Conference on (Vol. 2, pp. 2509-2512). IEEE. Chicago	Figure 1
196	2006	Multi Si	4928	MJ/m²	Energy value includes Si purification and processing, sawing, wafering, cell fabrication and module assembly. kWh/m2 value is converted to MJ/m2 using a grid factor of 0.32 and	No	Not based on actual manufacturing data and is based on published	Williams, T., Guice, J., & Coyle, J. (2006, May). Strengthening the Environmental Case for Photovoltaics: A Life-	Figure 1

Sl No	Year	Technology	Energy	Unit	Comments	Considered for analysis?	Reason for not considering	Source	Section referred to in source
					conversion factor of 3.6 between MJ and kWh.		literature values	Cycle Analysis. In Photovoltaic Energy Conversion, Conference Record of the 2006 IEEE 4th World Conference on (Vol. 2, pp. 2509-2512). IEEE. Chicago	
197	2006	Multi Si	4928	MJ/m²	Energy value includes Si purification and processing, sawing, wafering, cell fabrication and module assembly. kWh/m2 value is converted to MJ/m2 using a grid factor of 0.32 and conversion factor of 3.6 between MJ and kWh.	No	Not based on actual manufacturing data and is based on published literature values	Williams, T., Guice, J., & Coyle, J. (2006, May). Strengthening the Environmental Case for Photovoltaics: A Life-Cycle Analysis. In Photovoltaic Energy Conversion, Conference Record of the 2006 IEEE 4th World Conference on (Vol. 2, pp. 2509-2512). IEEE. Chicago	Figure 1
198	1988	Mono Si	8285	MJ/m²	Energy value includes Si purification, Si wafer and cell production and module production with frame.	No	Duplicate value. This study refers to value published in Sl No 83.	Wilson, R., & Young, A. (1996). The embodied energy payback period of photovoltaic installations applied to buildings in the UK. Building and environment, 31(4), 299-305.	Table 1
199	2005	Mono Si	5016	MJ/m²	Energy value includes materials and manufacturing. Based on actual industrial data.	No	Duplicate value. This study refers to value published in Sl No 65.	Alsema, E., de Wild-Scholten, M. J. Environmental impacts of crystalline silicon photovoltaic module production. 13th CIRP International	Figure 3

Sl No	Year	Technology	Energy	Unit	Comments	Considered for analysis?	Reason for not considering	Source	Section referred to in source
								Conference on Life Cycle Engineering ; Leuven, Belgium, 31 May-2 June, 2006	
200	2004	Multi Si	3706	MJ/m²	Energy value includes materials and manufacturing. Based on actual industrial data.	No	Duplicate value. This study refers to value published in Sl No 174	Alsema, E., de Wild-Scholten, M. J. Environmental impacts of crystalline silicon photovoltaic module production. 13th CIRP International Conference on Life Cycle Engineering ; Leuven, Belgium, 31 May-2 June, 2006	Figure 3
201	2006	Multi Si	3240	MJ/m²	Energy value includes Si feedstock, ingot+wafer, cell production and module assembly.	No	Authors have modified previously published literature values to account for technological improvements in the PV manufacturing process.	Alsema, E. A., de Wild-Scholten, M. J., & Fthenakis, V. M. (2006, September). Environmental impacts of PV electricity generation-a critical comparison of energy supply options. In 21st European photovoltaic solar energy conference, Dresden, Germany (Vol. 3201).	Figure 2
202	2007	Multi Si	2580	MJ/m2	Energy value includes Si feedstock, ingot+wafer, cell production and module assembly.	No	Authors have modified previously data published in Sl 201 to account for technological improvements in the PV manufacturing process.	Zhai, P., & Williams, E. D. (2010). Dynamic hybrid life cycle assessment of energy and carbon of multicrystalline silicon photovoltaic systems.*Environmental science & technology*, *44*(20), 7950-7955.	Table 2

Sl No	Year	Technology	Energy	Unit	Comments	Considered for analysis?	Reason for not considering	Source	Section referred to in source
203	1995	Multi Si	2916	MJ/m²	This is for worst case. Energy value includes direct and indirect process requirements and input materials. For consistency with other literature reported values, we have not included 576 MJ/m2 for investments.	No	Values are the same as in Sl No 56	Alsema, Erik A. Environmental aspects of solar cell modules. Summary report. Rijksuniversiteit Utrecht (Netherlands). Dept. of Science, Technology and Society, 1996.	Table 4.1
204	1995	Multi Si	1296	MJ/m²	This is for base case. Energy value includes direct and indirect process requirements and input materials. For consistency with other literature reported values, we have not included 144 MJ/m2 for investments.	No	Values are the same as in Sl No 57	Alsema, Erik A. Environmental aspects of solar cell modules. Summary report. Rijksuniversiteit Utrecht (Netherlands). Dept. of Science, Technology and Society, 1996.	Table 4.1
205	1995	Multi Si	576	MJ/m²	This is for best case. Energy value includes direct and indirect process requirements and input materials. For consistency with other literature reported values, we have not included 72 MJ/m2 for investments.	No	Values are the same as in Sl No 58	Alsema, Erik A. Environmental aspects of solar cell modules. Summary report. Rijksuniversiteit Utrecht (Netherlands). Dept. of Science, Technology and Society, 1996.	Table 4.1
206	1995	amorphous Si	1447	MJ/m²	This is for worst case. Energy value includes direct and indirect process requirements and input materials. For consistency with other literature reported values, we have not included 443 MJ/m2 for investments.	No	The reported values are assumptions based on values reported in previous studies and not actual	Alsema, Erik A. Environmental aspects of solar cell modules. Summary report. Rijksuniversiteit Utrecht (Netherlands). Dept. of Science,	Table 4.2

Sl No	Year	Technology	Energy	Unit	Comments	Considered for analysis?	Reason for not considering	Source	Section referred to in source
							production data.	Technology and Society, 1996.	
207	1995	amorphous Si	580	MJ/m²	This is for base case. Energy value includes direct and indirect process requirements and input materials. For consistency with other literature reported values, we have not included 227 MJ/m2 for investments.	No	The reported values are assumptions based on values reported in previous studies and not actual production data.	Alsema, Erik A. Environmental aspects of solar cell modules. Summary report. Rijksuniversiteit Utrecht (Netherlands). Dept. of Science, Technology and Society, 1996.	Table 4.2
208	1995	amorphous Si	400	MJ/m²	This is for best case. Energy value includes direct and indirect process requirements and input materials. For consistency with other literature reported values, we have not included 137 MJ/m2 for investments.	No	The reported values are assumptions based on values reported in previous studies and not actual production data.	Alsema, Erik A. Environmental aspects of solar cell modules. Summary report. Rijksuniversiteit Utrecht (Netherlands). Dept. of Science, Technology and Society, 1996.	Table 4.2
209	1995	CdTe	637	MJ/m²	This is for worst case. Energy value includes direct and indirect process requirements and input materials. For consistency with other literature reported values, we have not included 446 MJ/m2 for capital	No	The reported values are assumptions based on values reported in previous studies and not actual production data.	Alsema, Erik A. Environmental aspects of solar cell modules. Summary report. Rijksuniversiteit Utrecht (Netherlands). Dept. of Science, Technology and Society, 1996.	Table 4.3
210	1995	CdTe	504	MJ/m²	This is for base case. Energy value includes direct and indirect process requirements and input materials. For consistency with other literature reported values, we have not included 122 MJ/m2 for capital	No	The reported values are assumptions based on values reported in previous	Alsema, Erik A. Environmental aspects of solar cell modules. Summary report. Rijksuniversiteit Utrecht	Table 4.3

Sl No	Year	Technology	Energy	Unit	Comments	Considered for analysis?	Reason for not considering	Source	Section referred to in source
							studies and not actual production data.	(Netherlands). Dept. of Science, Technology and Society, 1996.	
211	1995	CdTe	407	MJ/m²	This is for best case. Energy value includes direct and indirect process requirements and input materials. For consistency with other literature reported values, we have not included 40 MJ/m2 for capital	No	The reported values are assumptions based on values reported in previous studies and not actual production data.	Alsema, Erik A. Environmental aspects of solar cell modules. Summary report. Rijksuniversiteit Utrecht (Netherlands). Dept. of Science, Technology and Society, 1996.	Table 4.3
212	1998	Multi Si	11600	MJ/m²	This is for the "high scenario". Energy value includes Si production, Si purification and crystallization, wafering, cell processing, module assembly.	No	The reported values are assumptions based on values reported in previous studies and not actual production data.	Alsema, E. "Energy requirements and CO2 mitigation potential of PV systems." Photovoltaics and the Environment 1999 (1998).	Table 1
213	1998	Mono Si	13900	MJ/m²	This is for the "high scenario". Energy value includes Si production, Si purification and crystallization, wafering, cell processing, module assembly.	No	The reported values are assumptions based on values reported in previous studies and not actual production data.	Alsema, E. "Energy requirements and CO2 mitigation potential of PV systems." Photovoltaics and the Environment 1999 (1998).	Table 1
214	2008	CdTe	750	MJ/m²	Energy value includes materials and manufacturing. Based on actual industrial data.	No	This study reports 1190 MJ/m2 for the entire CdTe PV	Ravikumar, D., Sinha, P., Seager, T. P., & Fraser, M. P. (2015). An anticipatory approach to quantify	Figure 3

Sl No	Year	Technology	Energy	Unit	Comments	Considered for analysis?	Reason for not considering	Source	Section referred to in source
							system and includes the 750 Mj/m2 of the CdTe module reported in Sl no 30.	energetics of recycling CdTe photovoltaic systems. Progress in Photovoltaics: Research and Applications.	

S2 Abbreviation list and parameter values

Table 29 List of abbreviations and modeling parameters with assumed values and references

Term	Unit	Value	Explanation	Comment/Source
RE_{CO2}	$Wm^{-2}kg^{-1}$	1.75e-15	Radiative efficiency of CO_2	(1)
RE_{CH4}	$Wm^{-2}kg^{-1}$	1.30e-13	Radiative efficiency of CH_4	(1)
CRF_{bnf}	$Wm^{-2}yr$		CRF benefit after PV installation	Used in Equation 4 main paper
CRF_{avd}	$Wm^{-2}yr$		CRF impact of GHGs avoided after PV installation	Used in Equation 4 main paper
CRF_{mnf}	$Wm^{-2}yr$		CRF impact of PV manufacturing GHGs	Used in Equation 4 main paper

Term	Unit	Value	Explanation	Comment/Source
avd_{ghg}	g		GHGs avoided after PV installation	Used in Equation 5 main paper
deply_gGHG_kWh	g/kWh		GHG intensity of the grid electricity displaced by the PV system at the deployment location	Used in Equation 6 main paper
deply_gCO_2_kWh_CA	g/kWh	389	CO_2 intensity of the grid electricity displaced by the PV system at California	(2)
deply_gCH_4_kWh_CA	g/kWh	1.96	CH_4 intensity of the grid electricity displaced by the	(2)

Term	Unit	Value	Explanation	Comment/Source
			PV system at California	
deply_gCO_2_kWh_WY	g/kWh	881	CO_2 intensity of the grid electricity displaced by the PV system at Wyoming	(2)
deply_gCH_4_kWh_WY	g/kWh	1.86	CH_4 intensity of the grid electricity displaced by the PV system at Wyoming	(2)
kWp_m^2	kW/m^2		peak watts per m^2 of the PV module	Used in Equation 6 main paper
kWp_m^2_mono_si	kW/m^2	0.17	peak watts per m^2 of the mono-Si PV module	Based on 17% efficiency value reported by commercial

Term	Unit	Value	Explanation	Comment/Source
				manufacturer (3)
kWp_m^2_multi_si	kW/m^2	0.16	peak watts per m^2 of the multi-Si PV module	Based on 16% efficiency value reported by commercial manufacturers in (4)(5)
irrd	kWh m^{-2} yr^{-1}		Annual solar irradiation	Used in Equation 6 main paper
Irrd_CA	kWh m^{-2} yr^{-1}	2000	Annual solar irradiation in California	(6)
Irrd_WY	kWh m^{-2} yr^{-1}	1700	Annual solar irradiation in Wyoming	(6)
perf_rat	No unit	0.75	Ratio of the AC to DC power generated by the PV system	Used in Equation 6 main paper. Value from (7)

Term	Unit	Value	Explanation	Comment/Source
perf_deg	%	0.7	Annual performance degradation of the PV module	Used in Equation 6 main paper. Value from (8)
mnf_{ghg}	g/kWh		GHG intensity of electricity used for PV manufacturing	Used in Equation 7 main paper.
mnf_{china_CO2}	g/kWh	955	CO_2 intensity of electricity used for PV manufacturing in China	Used in Equation 7 main paper. Value from (2)
mnf_{china_CH4}	g/kWh	6.44	CH_4 intensity of electricity used for PV manufacturing in China	Used in Equation 7 main paper. Value from (2)
fdstk_kWh	kWh/m^2		Electricity required to purify the silicon	Used in Equation 8 main paper.

Term	Unit	Value	Explanation	Comment/Source
			feedstock per m^2 of the module.	
non_fdstk_kWh	kWh/m^2		Electricity required for non-feedstock processes per m^2 of the module	Used in Equation 8 main paper.
fdstk_kWh_multiSi	kWh/m^2	92.1	Electricity required to purify silicon feedstock for 1 m^2 of the multi-silicon PV module	Used in Equation 9 main paper. Value from (8)
fdstk_kWh_monoSi	kWh/m^2	175.37	Electricity required to purify silicon feedstock for 1 m^2 of the mono-silicon PV module	Used in Equation 9 main paper. Value from (8)

Term	Unit	Value	Explanation	Comment/Source
non_fdstk_kWh_multiSi	kWh/m^2	115.78	Electricity required for non-feedstock processes per m^2 of the multi-Si module	Used in Equation 8 main paper. Value from (8)
non_fdstk_kWh_monoSi	kWh/m^2	211	Electricity required for non-feedstock processes per m^2 of the mono-Si module	Used in Equation 8 main paper. Value from (8)
Ingot_wafer_kWh_multiSi	kWh/m^2	55.87	Electricity required for ingot and wafer processing (non-feedstock process) per m^2 of the multi-Si module	Used in Figure 3 main paper. Value from (8)

Term	Unit	Value	Explanation	Comment/Source
lamination_kWh_multiSi	kWh/m^2	39.47	Electricity required for lamination (non-feedstock process) per m^2 of the multi-Si module	Used in Figure 3 main paper. Value from (8)
cell_kWh_multiSi	kWh/m^2	20.4	Electricity required for cell processing (non-feedstock process) per m^2 of the multi-Si module	Used in Figure 3 main paper. Value from (8)

S3 CO_2 intensity of PV electricity

The electricity produced by 1 m^2 of a PV system over a 25-year lifetime is given by

$$pv\_elec = \sum_{t=1}^{25} kWp\_m^2 \times irrd \times perf\_rat \times (1\text{-}perf\_deg)^t \qquad S2$$

where kWp_m^2 is the peak wattage in (kW) per m^2 of the PV module, irrd is the annual solar irradiation (kWh m^{-2} yr^{-1}) at the deployment location, perf_rat (performance ratio) is the ratio of the AC to DC power generated by the PV system and perf_deg is the annual performance degradation of the PV module (%).

The values for kWp_m^2, perf_rat and perf_deg are given in Table 29. Based on the daily average solar irradiation value of 4.03 kWh/m^2 (9), we assume an annual average value of 1500 kWh/m^2 for irrd in China.

The manufacturing GHG emissions for 1m^2 of a PV module is given by

$$pv\_mnf\_CO_2 = (fdstk\_kWh\_multiSi + non\_fdstk\_kWh\_multiSi) \times mnf_{china\_CO2} \qquad S3$$

The values for the terms in equation S3 are given in Table 29.

For a PV system manufactured and installed in china, the CO_2 intensity of PV electricity is a ratio of $PV\_mnf\_CO_2$ and PV_elec (equations S3 and S2) and is equal to 51 g/kWh.

S4 CRF hotspot analysis: parameters and baseline values

Table 30 Baseline value of parameters used in the scenario analysis in the main paper

Term	Unit	Value	Explanation	Comment/Reference
mnf_{china_CO2}	g/kWh	955	CO_2 intensity of electricity used for PV manufacturing in China	Value from (2)
mnf_{china_CH4}	g/kWh	6.44	CH_4 intensity of electricity used for PV manufacturing in China	Value from (2)
Ingot_wafer_kWh_multiSi	kWh/m^2	55.87	Electricity required for ingot and wafer processing (non-feedstock process) per m^2 of the multi-Si module	Value from (8)
lamination_kWh_multiSi	kWh/m^2	39.47	Electricity required for lamination (non-feedstock process) per m^2 of the multi-Si module	Value from (8)

cell_kWh_multi Si	kWh/m^2	20.4	Electricity required for cell processing (non-feedstock process) per m^2 of the multi-Si module	Value from (8)
fdstk_kWh_mult iSi	kWh/kg	147.37	Electricity required to purify 1 kg of solar-grade silicon feedstock for the multi-silicon PV module	Ratio of feedstock energy intensity value of 92.1 kWh/m^2 and feedstock material intensity value of 0.625 kg/m^2. Values from (8)
fdstk_kWh_mult iSi	Kg/m^2	0.625	Solar-grade silicon feedstock material intensity for 1m^2 of the multi-silicon PV module	Value from (8)

S5 Equivalence between a decrease in solar-grade silicon energy/feedstock intensity and an increase in module efficiency

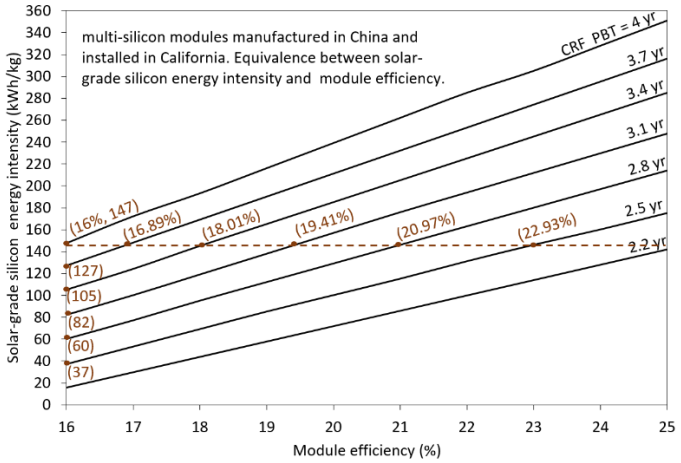

Figure 37 CRF payback time (PBT) equivalence between module efficiency improvements and reduction in solar-grade energy intensity for poly-silicon modules manufactured in China and installed in California.

In Figure 37, the dotted horizontal line and the y-axis intersect the CRF PBT equivalence lines at multiples module efficiency and feedstock energy intensity values. As explained in the main paper, the CRF PBT can be reduced from 4 to 3.7 years by decreasing the feedstock energy intensity from 147 to 127 kWh kg^{-1} or increasing the module efficiency from 16 to 16.89%. This corresponds to an equivalence ratio of 22.47 kWh kg^{-1} per unit percentage increase in module efficiency (20 kWh kg^{-1}/0.89%). Similar equivalence ratios between the feedstock energy intensity and the module efficiency values are calculated by moving horizontally and vertically between pairs of CRF PBT lines. The mean of all the calculated equivalence ratios is 16.93 kWh kg^{-1} per unit increase in module efficiency percentage. Similar equivalence values for mono-Si and multi-Si modules manufactured in China and deployed in Wyoming and California are tabulated in Table 4 and Table 5.

Table 31 Equivalence between solar-grade silicon energy intensity (kWh/kg) and unit increase in module efficiency (%) for mono and poly-Si modules manufactured in China and installed in California and Wyoming

Scenario	Equivalence between energy intensity (kWh/kg) and unit increase in module efficiency (%)	Reference Figure
multi-Si manufactured in China, Installed in California	16.93	Figure 37
multi-Si manufactured in China, Installed in Wyoming	16.02	Figure 3
mono-Si manufactured in China, Installed in California	17.19	Figure 5
mono-Si manufactured in China, Installed in Wyoming	15.59	Figure 7

Table 32 Equivalence between solar-grade silicon feedstock intensity (kg/m^2) and a unit increase in module efficiency (%) for mono and poly-Si modules manufactured in China and installed in California and Wyoming

Scenario	Equivalence between feedstock intensity (kg m^{-2}) and unit increase in module efficiency (%)	Reference figure
multi-Si manufactured in China, Installed in California	0.065	Figure 2
multi-Si manufactured in China, Installed in Wyoming	0.069	Figure 4
mono-Si manufactured in China, Installed in California	0.128	Figure 6
mono-Si manufactured in China, Installed in Wyoming	0.119	Figure 8

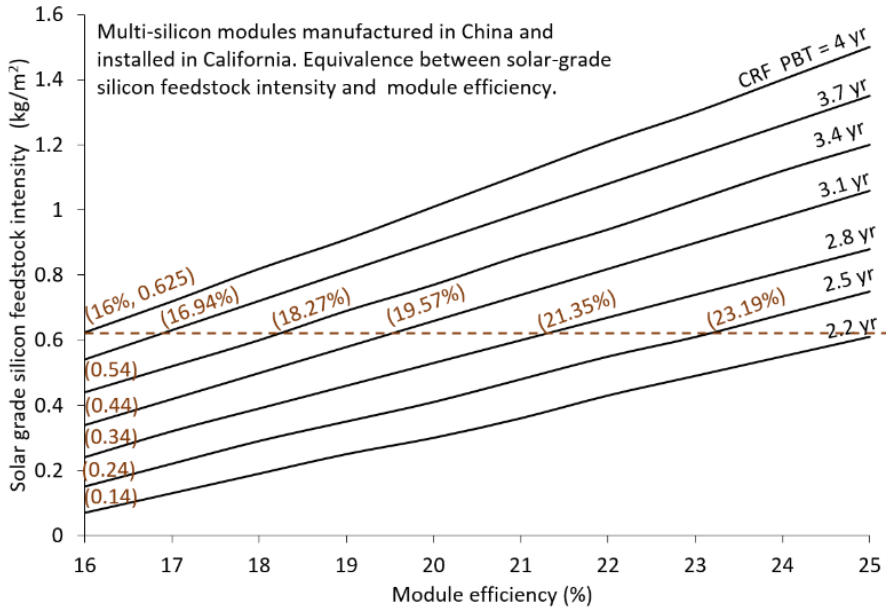

Figure 38 CRF payback time (PBT) equivalence between an increase in module efficiency and reduction in solar-grade feedstock intensity for poly-silicon modules manufactured in China and installed in California.

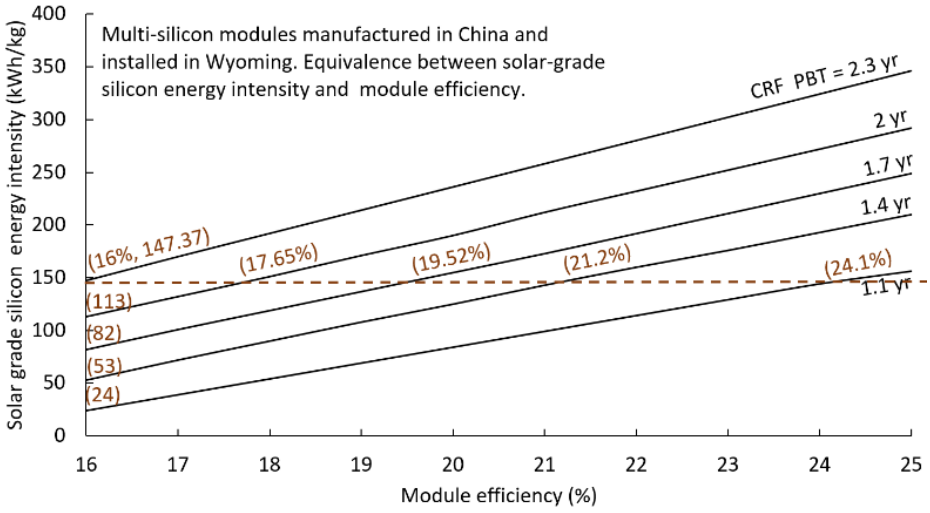

Figure 39 CRF payback time (PBT) equivalence between an increase in module efficiency and reduction in solar-grade energy intensity for poly-silicon modules manufactured in China and installed in Wyoming.

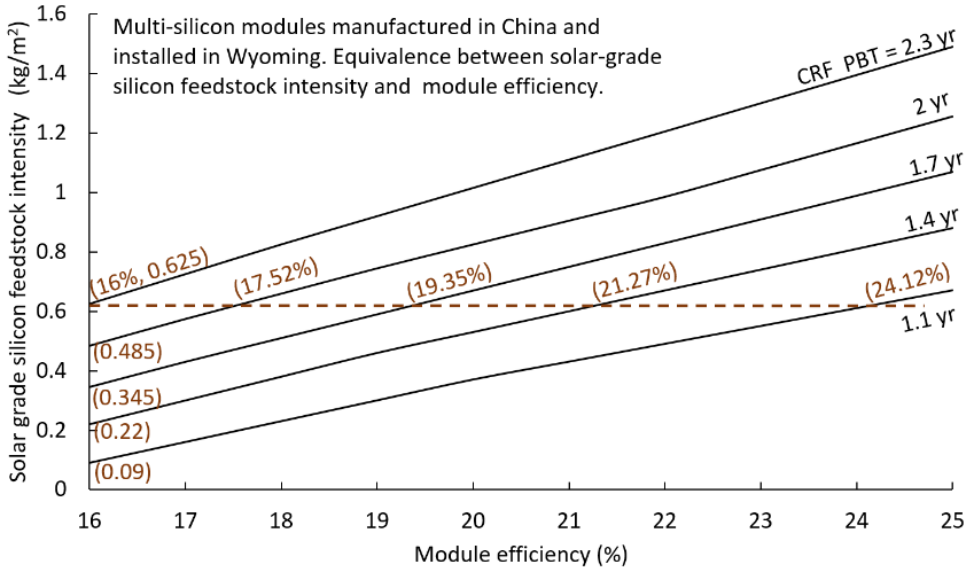

Figure 40 CRF payback time (PBT) equivalence between an increase in module efficiency and reduction in solar-grade feedstock intensity for poly-silicon modules manufactured in China and installed in Wyoming.

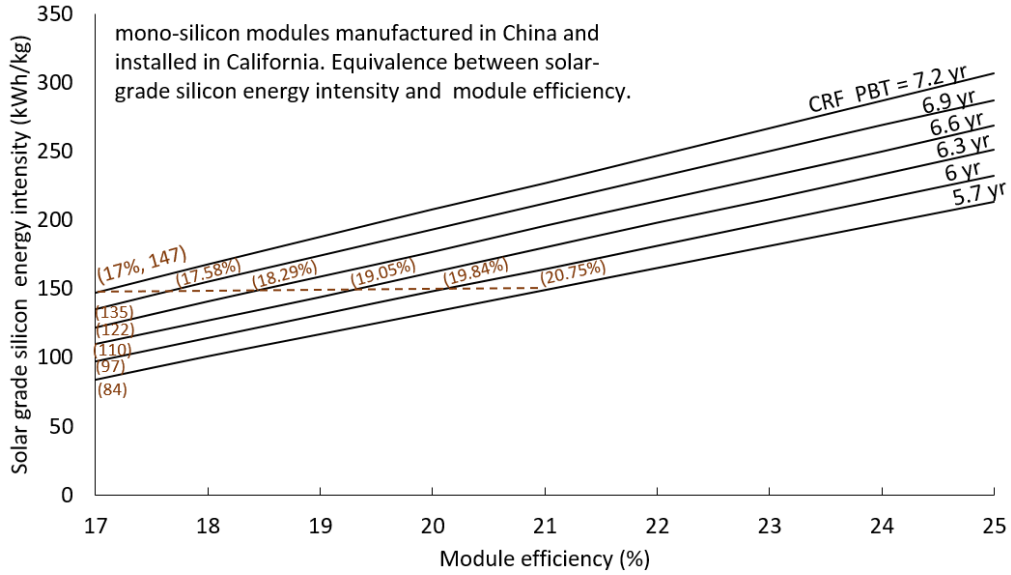

Figure 41 CRF payback time (PBT) equivalence between an increase in module efficiency and reduction in solar-grade energy intensity for mono-silicon modules manufactured in China and installed in California.

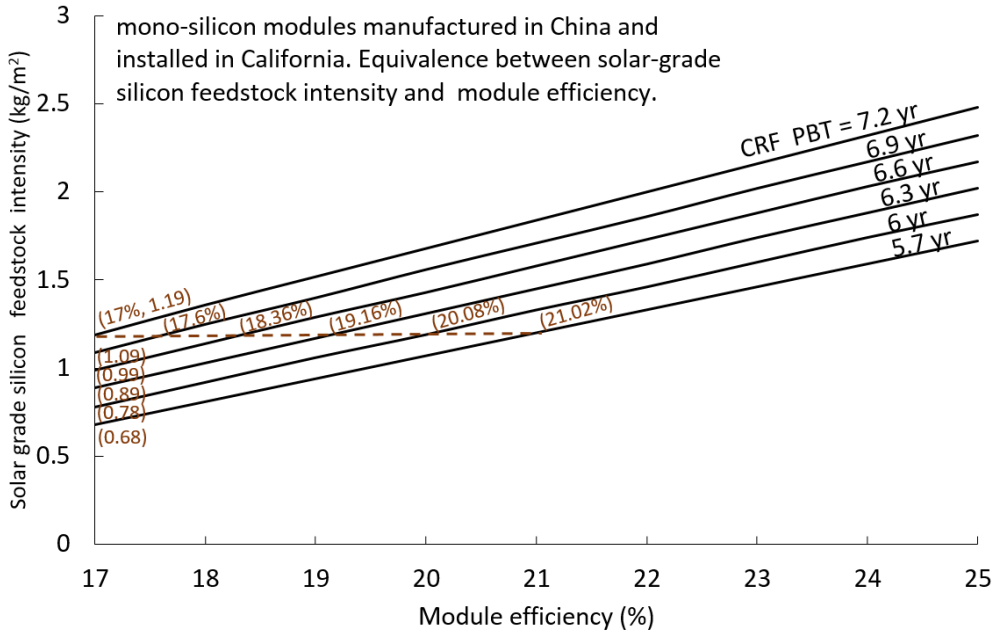

Figure 42 CRF payback time (PBT) equivalence between an increase in module efficiency and reduction in solar-grade feedstock intensity for mono-silicon modules manufactured in China and installed in California.

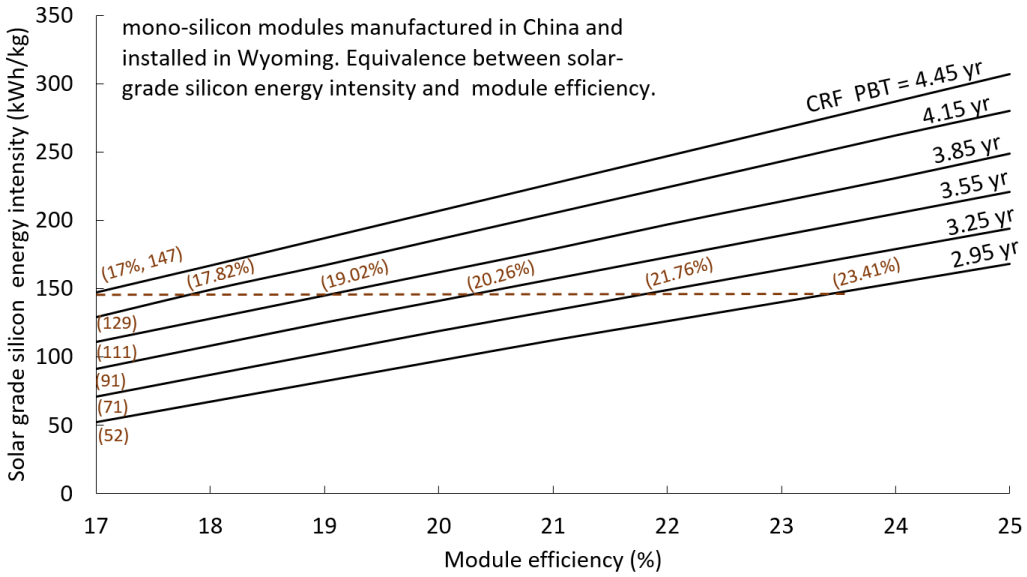

Figure 43 CRF payback time (PBT) equivalence between an increase in module efficiency and reduction in solar-grade energy intensity for mono-silicon modules manufactured in China and installed in Wyoming.

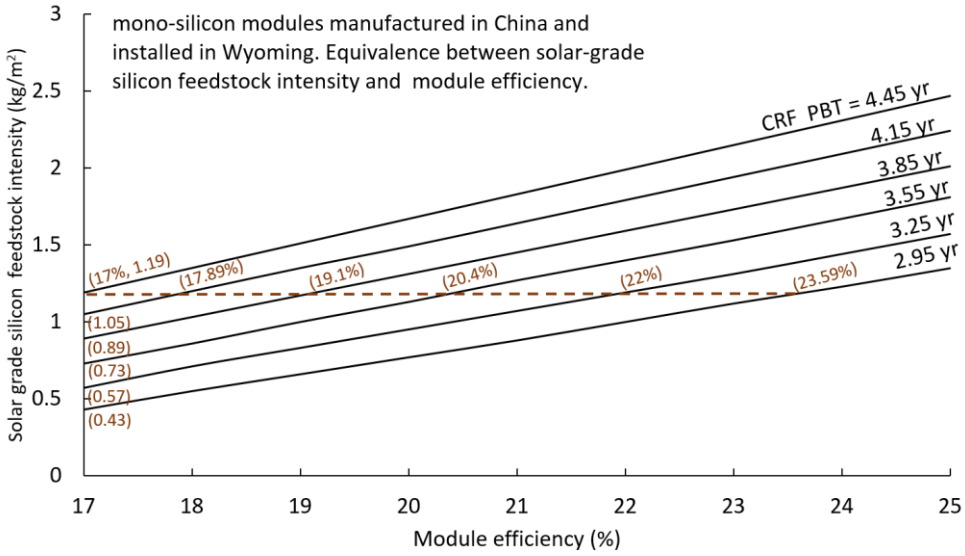

Figure 44 CRF payback time (PBT) equivalence between an increase in module efficiency and reduction in solar-grade feedstock intensity for mono-silicon modules manufactured in China and installed in Wyoming.

S6 Equivalent increase in module efficiency by addressing CRF hotspots in manufacturing processes

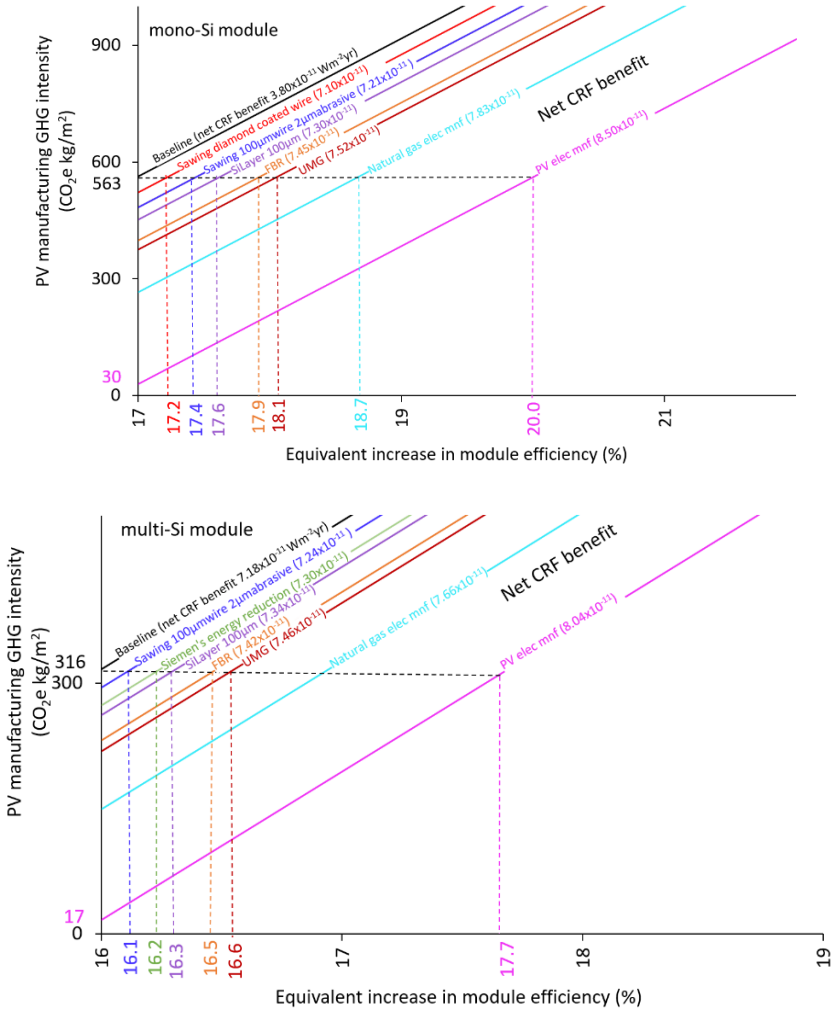

Figure 45 The equivalence in the CRF benefits between addressing PV manufacturing hotspots (Figure *14*) and an increase in module efficiency for mono-Si (upper plot) and multi-Si (lower plot) modules manufactured in China and deployed in Wyoming. The manufacturing improvement that addresses the hotspot is accounted for by lowering the manufacturing GHG intensity (y-axis). The equivalent increase in module efficiency is determined by projecting the difference between the CRF benefit equivalence lines of the improved manufacturing and baseline scenario on to the x-axis.

S7 Growth in commercial multi-silicon module efficiency

The commercial module efficiency in 2004 was 13.2% (10) and has increased to 16.7% in 2016 (4)(5). This corresponds to an annual increment of 0.25% per year from 2004 to 2016.

S8 Kerf loss and silicon feedstock requirement

The solar-grade silicon feedstock in $1m^2$ of a multi-silicon PV wafer is 0.625 kg (8). The typical thickness of the silicon wafer is 180 μm and the volume is $180x10^{-6}$ m^3 (8). Based on the density of silicon (2330 kg/m^3), the mass of solar-grade silicon contained in 180 $x10^{-6}$ m^3 of the multi-silicon wafer is 0.41 kg and, therefore, the kerf-loss is 0.2 kg/m^2 (0.625-0.41) or 33%.

If the kerf loss is decreased by 50% ("mwss_wire_abrasive_reduced_diameter" scenario in the main paper) or by 25% ("diamond_coated_wire_saw" scenario in the main paper), the new feedstock requirement will be 0.52 kg or 0.57 kg per m^2 respectively.

S9 Difference between GHG and CRF metrics

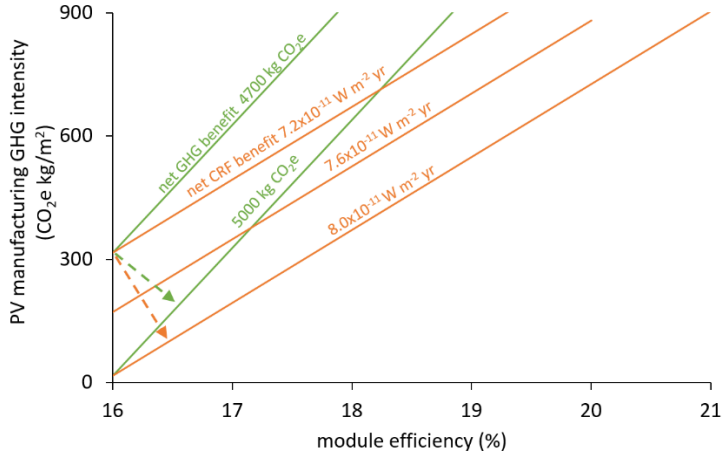

Figure 46 Difference in the climate benefit of improved PV manufacturing as measured by the net GHG and net CRF benefits for multi-Si modules manufactured in China and deployed in Wyoming. The green and orange lines represent combinations of PV manufacturing GHG intensity and module efficiency that result in the same net GHG and net CRF benefit over the 25-year lifespan of a module, respectively. A reduction in the GHG intensity of PV manufacturing from 314 to 17 kg CO_2e/m^2 increases the net GHG benefit by only 6% (4700 to 5000 kg CO_2e) when compared to 11% increase in the net CRF benefit ($7.2x10^{-11}$ to $8.0x10^{-11}$ $Wm^{-2}yr$)

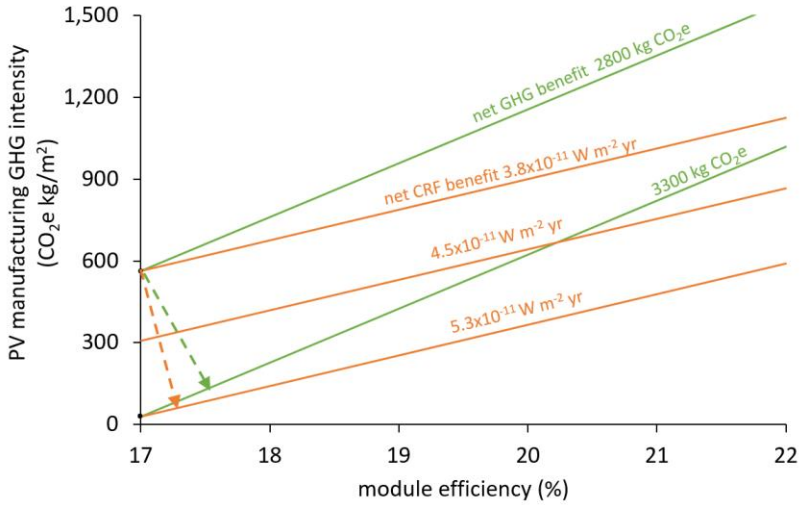

Figure 47 Difference in the climate benefit of improved PV manufacturing as measured by the net GHG and net CRF benefits for mono-Si modules manufactured in China and deployed in California. The green and orange lines represent combinations of PV manufacturing GHG intensity and module efficiency that result in the same net GHG and net CRF benefit over the 25-year lifespan of a module, respectively. A reduction in the GHG intensity of PV manufacturing from 563 (current state of manufacturing) to 30 kg CO_2e/m^2 (using PV electricity for PV

manufacturing) increases the net GHG benefit by only 18% (2800 to 3300 kg CO_2e) when compared to 39% increase in the net CRF benefit ($3.8x10^{-11}$ to $5.3x10^{-11}$ $Wm^{-2}yr$)

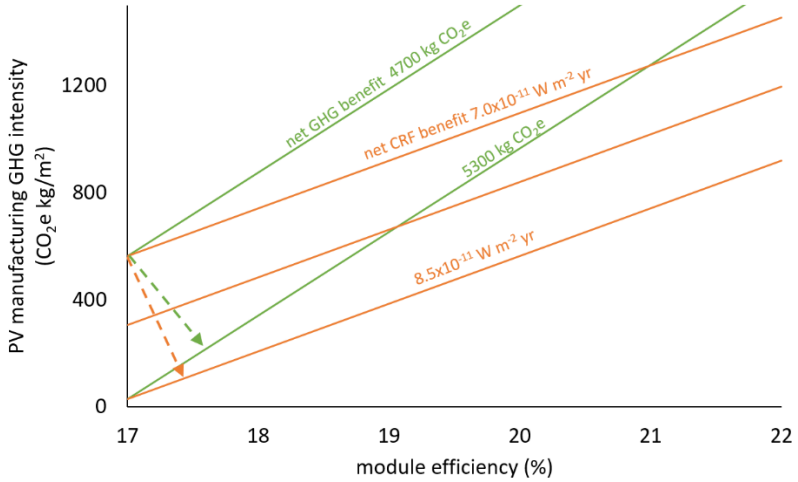

Figure 48 Difference in the climate benefit of improved PV manufacturing as measured by the net GHG and net CRF benefits for mono-Si modules manufactured in China and deployed in Wyoming. The green and orange lines represent combinations of PV manufacturing GHG intensity and module efficiency that result in the same net GHG and net CRF benefit over the 25-year lifespan of a module, respectively. A reduction in the GHG intensity of PV manufacturing from 563 (current state of manufacturing) to 30 kg CO_2e/m^2 (using PV electricity for PV manufacturing) increases the net GHG benefit by only 13% (4700 to 5300 kg CO_2e) when compared to 21% increase in the net CRF benefit ($7.0x10^{-11}$ to $8.5x10^{-11}$ $Wm^{-2}yr$)

S10 CRF Hotspot analysis

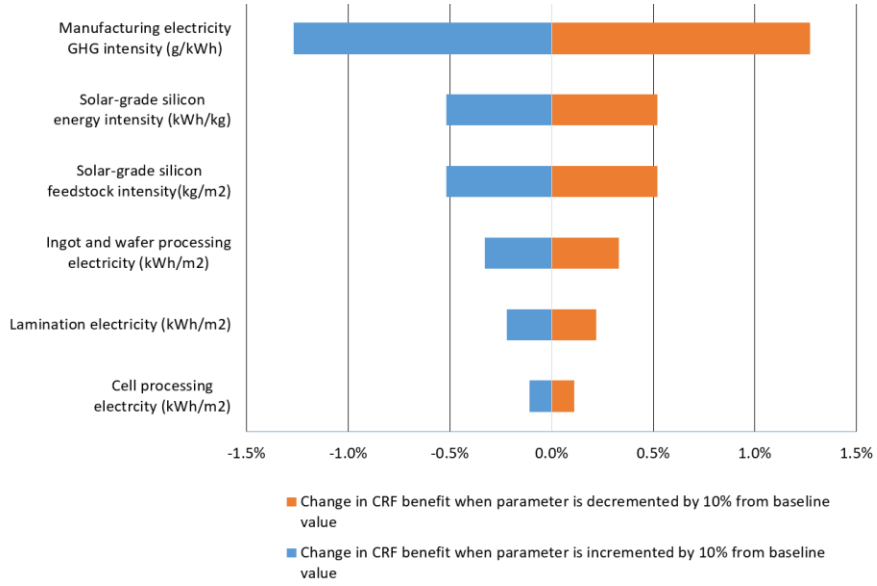

Figure 49 CRF hotspots multi-silicon PV modules manufactured in China and deployed in Wyoming. The width of the bars indicate the percentage change in the CRF benefit of the baseline scenario when a parameter in the manufacturing process is incremented and decremented by 10%. The widest bars correspond to the PV manufacturing process parameters with the highest CRF impacts.

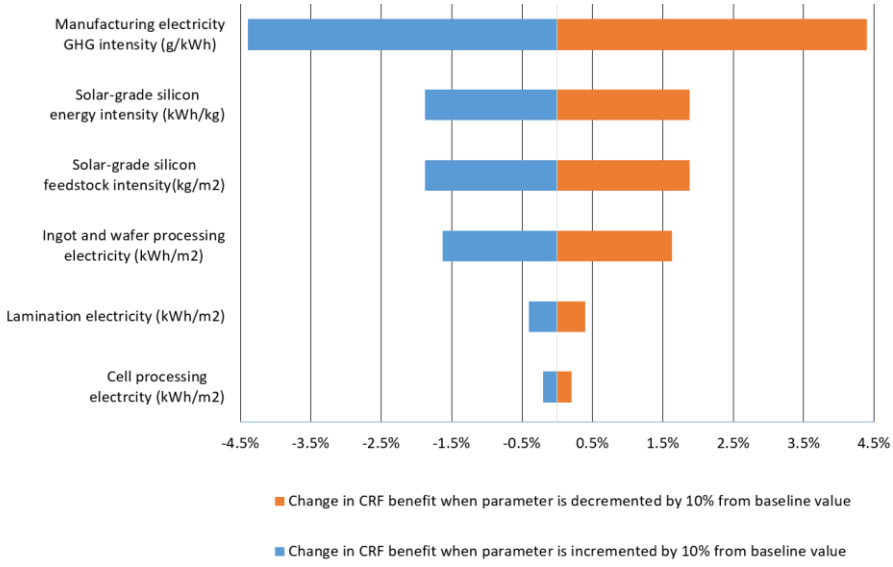

Figure 50 CRF hotspots mono-silicon PV modules manufactured in China and deployed in California. The width of the bars indicate the percentage change in the CRF benefit of the baseline scenario when a parameter in the manufacturing process is incremented and decremented by 10%. The widest bars correspond to the PV manufacturing process parameters with the highest CRF impacts.

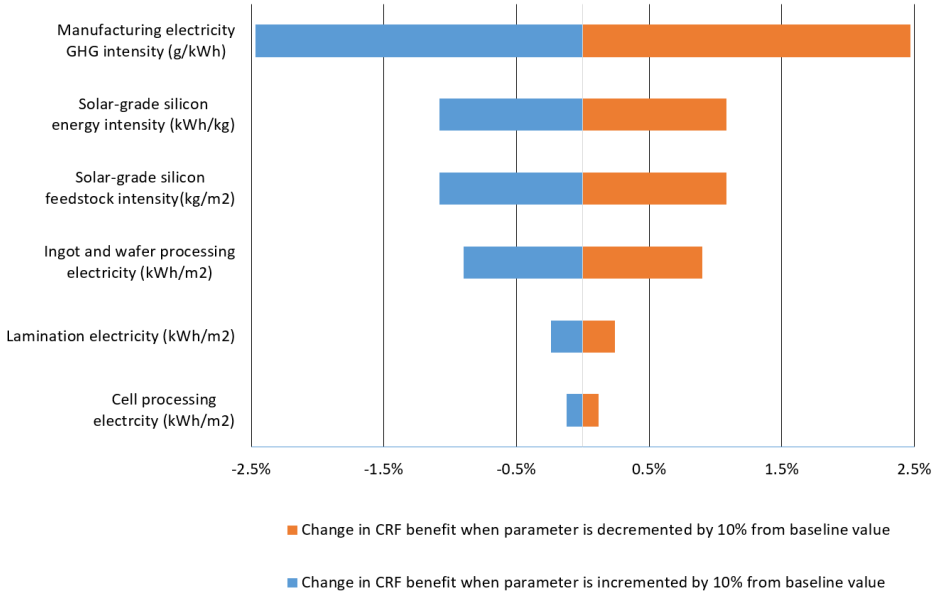

Figure 51 CRF hotspots mono-silicon PV modules manufactured in China and deployed in Wyoming. The width of the bars indicate the percentage change in the CRF benefit of the baseline scenario when a parameter in the manufacturing process is incremented and decremented by 10%. The widest bars correspond to the PV manufacturing process parameters with the highest CRF impacts.

References

1. Ravikumar D, Seager TP, Chester M V, Fraser MP. Intertemporal Cumulative Radiative Forcing Effects of Photovoltaic Deployments. Environ Sci Technol. 2014;48(17):10010–8.

2. SimaPro version 8.03. Grid GHG intensity as reported by SimaPro. 2014;

3. Yingli Solar. Monocrystalline Solar Panels [Internet]. 2015 [cited 2016 Jan 1]. Available from: http://www.yinglisolar.com/us/products/monocrystalline/

4. Trina Solar. DUOMAX Series Dual Glass Module [Internet]. 2016 [cited 2016 Jan 1]. Available from: http://www.trinasolar.com/us/product/PDG5.html

5. Yingli Solar. Multicrystalline Solar Panels [Internet]. 2016 [cited 2016 Jan 1]. Available from: http://www.yinglisolar.com/us/products/multicrystalline/

6. NREL. National Solar Radiation Data Base - Class I locations [Internet]. [cited 2016 Jan 1]. Available from: http://rredc.nrel.gov/solar/old_data/nsrdb/1991-2010/hourly/list_by_state.html#C

7. Alsema E, Fraile D, Frischknecht R, Fthenakis V, Held M, Kim HC, et al. Methodology guidelines on life cycle assessment of photovoltaic electricity. IEA PVPS Rep [Internet]. 2011 [cited 2014 Dec 25]; Available from: http://www.seas.columbia.edu/clca/IEA_Task12_LCA_Guidelines_12_1_11_Latest.pdf

8. De Wild-Scholten MJ. Energy payback time and carbon footprint of commercial photovoltaic systems. Sol Energy Mater Sol Cells [Internet]. Elsevier; 2013;119:296–305. Available from: http://dx.doi.org/10.1016/j.solmat.2013.08.037

9. Department of Energy. Solar: monthly and annual average direct normal (DNI) GIS data at 40km resolution for China from NREL [Internet]. 2015. Available from: http://catalog.data.gov/dataset/solar-monthly-and-annual-average-direct-normal-dni-gis-data-at-40km-resolution-for-china-f-e67c1

10. Alsema E, Mar. Environmental impacts of crystalline silicon photovoltaic module production. MRS Proc. 2005;895:0895–G03.

APPENDIX D

D. SUPPORTING INFORMATION FOR CHAPTER 4

1. Values for energy inputs and material and energy recovered

Table 33 Values for energy inputs and material and energy recovered

Step1 - System disassembly			
Label	Description	Value	Source
Esys	Primary energy for disassembling PV system (step 1)	8.52 MJ/m²	Refer section 2 in SI
Msys	Material transported from deployment site to step 1 location	33.98 kg/ m²	Sum of electrical systems and BOS (RM1 to RM10) and the module which weighs 16.66 kg/ m²
Dsys	Distance between deployment site and step 1 location	50 km	Assumption
rr_{sys}	Material recovery rate from BOS, inverter and transformer	0.9	[1]
Mrecy_sys_trn_st	Steel content in transformer	0.82 kg/m²	[2]
Mrecy_sys_inv_st	Steel content in inverter	0.37 kg/m²	[2]
Mrecy_sys_inv_al	Aluminum content in inverter	0.11 kg/m²	[2]
Mrecy_sys_bos_st	Steel content in BOS	10.83 kg/m²	[3]
Mrecy_sys_ bos_al	Aluminum content in BOS	0.17 kg/m²	[3]
Mrecy_sys_bos_cu	Copper content in BOS	0.88 kg/m²	[3]
Mrecy_sys_bos_pvc	PVC content in BOS	0.04 kg/m²	[3]
Mrecy_sys_bos_hdpe	HDPE content in BOS	0.28 kg/m²	[3]
Mrecy_sys_bos_epdm	EPDM content in BOS	0.06 kg/m²	[3]
Mrecy_sys_bos_conc	Concrete content in BOS	3.74 kg/m²	[3]
Mlnd_fl_sys	Land filled material	1.73 kg/m²	Refer section 2 in SI
Eemis_cont_sys	Primary energy used for controlling emissions	0/m²	Assumed that there is no emission in step 1 while dismantling the PV system.
Erecov_sys	Energy recovered from waste incineration	0 MJ/m²	Assumed that there is no energy recovered from the PV system disassembly step

Step2 - Module semiconductor separation			
Emod	Primary energy for USM separation (step 2)	72.9 MJ/m^2	Based on a personal communication from First Solar, we allocate 90% of the 81 MJ/ m^2 reported in [4] to Emod
Mmod	Module material transported from step 1 to 2	16.66 kg/m^2	Module weight.
Dmod	Distance between step 1 and 2 locations	50 km	Assumption
rr_{mod}	Material recovery rate from module	0.9	[5]
Eemis_cont_mod	Primary energy used for controlling emissions	8.1 MJ/m^2	Based on a personal communication from First Solar, we allocate 10% of the 81 MJ/ m^2 reported in [4] to Eemis_cont_mod
Erecov_mod	Energy recovered from waste incineration	5.6 MJ/m^2	[4]
Mrecy_mod_glass	Glass cullet content in module	14.7 kg/m^2	90% of module glass recovered [5]
Mlnd_fl_mod	Land filled material	0.13 kg/m^2	Refer section 2 in SI
Step 3- Semiconductor recovery			
Esc	Primary energy for USM recovery (step 3)	25.3 MJ/m^2	Based on a personal communication from First Solar, we allocate 90% of the 28 MJ/ m^2 reported in [5] to Esc
Msc	Unrefined semiconductor material transported from step 2 to 3	0.06 kg/m^2	Refer section 5 in SI.

Dsc	Distance between step 2 and 3 locations	50 km	Assumption
Eemis_cont_sc	Primary energy used for controlling emissions	2.8 MJ/m^2	Based on a personal communication from First Solar, we allocate 10% of the 28 MJ/ m^2 reported in [5] to Eemis_cont_sc
rr_{sc}	Material recovery rate CdTe	0.95	[5]
Mrecy_sc_te	Te content in semiconductor material	0.009 kg/m^2	95% of module CdTe recovered [4]
Mrecy_sc_cd	Cd content in semiconductor material	0.008 kg/m^2	95% of module CdTe recovered [4]
Mlnd_fl_sc	Land filled material	0.043 kg/m^2	Refer section 5 in SI
Common parameters across the three steps			
Esec_prod_bnf_inv_st, Esec_prod_bnf_trn_st, Esec_prod_bnf_bos_st	Energy benefit of recycling secondary steel recovered from the inverter, transformer and BOS	22.06 MJ/kg	Refer section 2 in SI
Esec_prod_bnf_inv_al	Energy benefit of recycling aluminum recovered from the inverter	151 MJ/kg	Refer section 2 in SI
Esec_prod_bnf_bos_cu	Energy benefit of recycling copper recovered from the BOS	38.85 MJ/kg	Refer section 2 in SI
Esec_prod_bnf_glass	Energy benefit of producing glass cullet from secondary sources	4.3 MJ/kg	Refer section 2 in SI
Esec_prod_bnf_te	Energy benefit of producing tellurium from secondary sources	127 MJ/kg	Refer section 2 in SI
Esec_prod_bnf_cd	Energy benefit of producing cadmium from secondary sources	60 MJ/kg	Refer section 2 in SI
Esec_prod_bnf_bos_hdpe	Energy benefit of recycling high-density polyethylene (HDPE) recovered from the BOS	55.7MJ/kg	Refer section 2 in SI

Esec_prod_bnf_bos_pvc	Energy benefit of recycling PVC recovered from the BOS	33.6 MJ/kg	Refer section 2 in SI
Esec_prod_bnf_bos_epdm	Energy recovered from synthetic rubber (EPDM) content of BOS	31.8 MJ/kg	Refer section 2 in SI
Esec_prod_bnf_bos_conc	Energy benefit of recycling concrete recovered from the BOS	-0.22 MJ/kg	Refer section 2 in SI
Etrk	Energy intensity of transportation by truck	0.003 MJ per kg km	Refer section 2 in SI
Elnd_fl_op	Energy required for landfill operations	0.32 MJ/kg	Refer section 2 in SI
Elnd_fl_inc	Electricity recovered from landfill incineration	7.14 MJ/kg	Refer section 2 in SI
Dlnd_fl	Distance to landfill	160 km	Assumption based on the landfill distance used in an LCA of PV BOS [2]

2. **Methodology and data sources for calculating the energy benefits of material recycling**

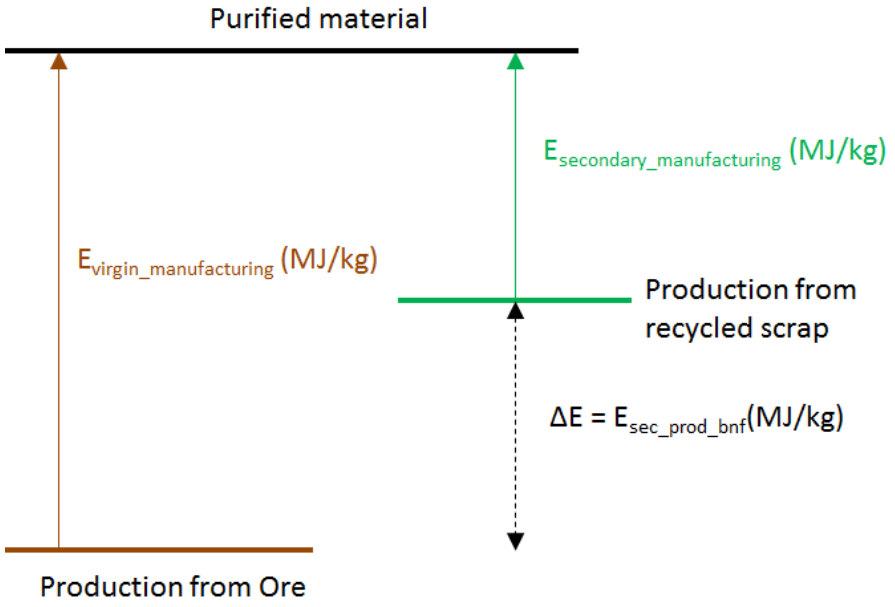

Figure 52 Conceptual representation of the calculation of energy benefits of material recycling ($E_{sec\_prod\_bnf}$) which is the difference between energy intensity of manufacturing the material from virgin and secondary sources.

The estimated difference between the primary and secondary manufacturing pathways for steel is 22.06 MJ/kg which is the mean of:

- 53 MJ/kg (difference between scenario 'b' and 'c' in [6])
- 7.6 MJ/kg (mean of the values – 3.2, 9.7, 10 - in Table 6 [7])
- 14.7 MJ/kg (difference between 18.99 million and 5.01 MBtu/ton mentioned in page 3-53 in [8])
- 13 MJ/kg (slide 7 in [9]).

For copper we calculate the difference between the energy footprints of the primary and secondary pathways from the second figure in page 12 in [10]. The energy requirement for the primary pathways range between 33 MJ/kg (3% Cu ore) to 57.3 MJ/kg (3% Cu ore) and the secondary pathway has a value of 6.3 MJ/kg. Thus, the net energy benefits of recycling copper ranges between 26.7 and 51 MJ/kg and we use a mean value of 38.85 MJ/kg.

Corresponding values for aluminum are 148 [11], 144 [12], 162 MJ/kg [13], and we use a mean of 151 MJ/kg.

1 kg of glass cullet, when used in glass production, displaces 1.2 kg of virgin raw material which would have required 2.7 MJ/kg [14] of production energy. Also, each kg of glass cullet reduces the manufacturing energy of glass by 1.6 MJ (mean of 1.3 to 1.9 MJ/kg glass cullet reported in [15]) as process temperatures in the production furnace are lowered. Thus, by displacing virgin raw materials and reducing glass manufacturing energy requirements, every kg of glass cullet recovered from a PV module results in a total energetic benefit of 4.3 MJ.

The recycling energy benefits for tellurium and cadmium are calculated by assuming they displace the energy required for virgin production. The energy for producing virgin tellurium is 10.9 kWh/kg [16] and this accounts for tellurium purification from anode slimes that is collected during copper extraction. The equivalent primary energy value is 127 MJ/kg (using an electricity grid factor of 0.31). The corresponding value for cadmium is 60 MJ/kg [16].

The energy required to manufacture virgin HDPE is 35.8 million Btu per 1000 pounds (last section in Table 3-2 in [17]).The corresponding values for recycled HDPE range between 3.72 and 19.9 million Btu per 1000 pounds and we assume a mean of 11.81 Btu per 1000 pounds. Thus, the mean of the difference between virgin and recycled energy requirements is 55.7 MJ/kg (after converting from Btu per 1000 pounds to MJ/kg).

For PVC, the energy difference between virgin and recycled manufacturing routes is 33.6 MJ/kg based on the difference between the "All Energy Resources" value for the "PVC conventional route" and "Vinyloop" columns in annex 7 in [18].

As there was no LCA study or data available for the energy benefits of recycling synthetic rubber (EPDM) we assume that energy is recovered through the combustion of the EPDM present in the BOS. We approximate this by considering a similar process of combustion of spent rubber tires. The energy recovered from the combustion of spent rubber tires is 31.8 MJ/kg which is the mean of

- 32.6 MJ/kg reported for "Rubber, 5 cm w/o metal " in Table in [19]
- 31.4 "Scrap tires" in Table 1 in [20]
- 31.5 MJ/kg (mean of the range of 28 to 35 MJ/kg in page 16-7 [21])

We assume the concrete in the BOS will be recycled as aggregate and literature shows that recycled aggregate is energetically more expensive than conventional aggregate [22][23]. 1 m^3 of natural aggregate concrete (NAC) and recycled aggregate concrete (RAC) weigh 2194 kgs (315 kg cement + 1879 kg of natural aggregate) and 2046 kgs (330 kg cement + 1716 kg of natural aggregate), respectively (Table 5 in [23]). The corresponding energy requirements are 1570.42 and 1922.62 MJ/ m^3 (Table 10 in [23]) therefore the energy intensity is 0.71 and 0.93 MJ/kg.

The energy intensity of truck freight ranges from 2.5 (USA specific values in Figure 7 in [24]) to 3.5 MJ per ton-km (North America specific values in Figure 6.4 in [25]) and we assume a mean of 3 MJ per ton-km.

For energy spent on landfill operations (LFO) we assume a value of 0.32 MJ/kg ("Energy production and use" bar for the "RDF production and combustion" scenario in figure 5 in [26]).

7.14 MJ of electricity is recovered per kg of landfill incineration (LFI) and this is a mean of

- 5.38 MJ/kg ("Energy production and use" bar for the "RDF production and combustion" scenario in figure 5 in [26]).
- 8.9 MJ/kg, the primary energy equivalent of 0.767 kWh/kg (gross electricity output for scenario 2 in Table 1 in [27]). We use a grid factor of 0.31.

3. Energy required for disassembling a PV system

As there is no data available on the energy required to disassemble a PV system, we assume that the PV system disassembly energy is equal to the energy required to install the PV system. 0.2 kg of diesel is required to install 1 m^2 of a CdTe PV system [28] and we convert this to a primary energy value of 8.52 MJ/ m^2 using the lower heating value (129488 Btu/gallon) and fuel density value (3.206 kg/gallon) of low sulphur diesel provided in [29].

4. Reduction in cumulative energy demand (CED) through recycling and PV module efficiency improvements

Energy payback time (EPBT) is the ratio of the energy required to manufacture the CdTe PV system and the annual energy produced by the CdTe PV system [30]. EPBT can be reduced by either decreasing the manufacturing energy or increasing the annual energy produced by the CdTe PV system through module efficiency improvements. Decreasing CED by 289 MJ through recycling (Table 34) or increasing the efficiency of CdTe PV module from 14 to 18.9% (Table 35) reduces the EPBT to 0.41 years.

Table 34 Reduction in EPBT through recycling

Energy input				
Parameter description	Parameter label	Calculation	Parameter value	Source
CdTe PV system CED(MJ/ m^2)	A		1190	[31]
% reduction in CED through recycling	B		24%	289 MJ of energy saved in scenario HR3 in Figure 3 in main paper
Net CdTe PV system CED (MJ/ m^2)	C	a*(1-b)	904	
Efficiency module (%)	D		14	[32]
Peak watts per m^2 (Wp/ m^2)	E	d*10. Assuming 14% module efficiency is based on standard test conditions of 1000 w/m^2	140	
CdTe PV system CED (MJ/kWp)	F	c/(e/1000)	6460	
Energy output				
Irradiation (kWh/ m^2/yr)	G		1800	Average southern European irradiation conditions [31]

AC to DC conversion or Performance ratio	H		0.8	Ground mount values in [30]
Generated electricity (kWh/kWp/yr)	I	g*h	1440	
Primary energy equivalent of electricity generated (MJ/kWh)	J	1 kWh = 3.6 MJ and we use a grid efficiency factor of 0.31	11.41	
Avoided energy (MJ/kWp/yr)	K	i*j	16425	
Energy payback time (EPBT)				
EPBT (yr)		f/k	0.39	

Table 35 Reduction in EPBT through module efficiency improvements

Energy input				
Parameter description	Parameter label	Calculation	Parameter value	Source
CdTe PV system CED (MJ/ m^2)	A		1190	[31]
Efficiency module (%)	B		18.42	
Peak watts per m^2 (Wp/ m^2)	C	b*10. Assuming 18.9% module efficiency is based on standard test conditions of 1000 w/m^2	184.2	
CdTe PV system CED (MJ/kWp)	D	a/(c/1000)	6460	
Energy output				
Irradiation (kWh/ m^2/yr)	G		1800	Average southern European irradiation conditions [31]
AC to DC conversion or performance ratio	H		0.8	Ground mount values in [30]
Generated electricity (kWh/kWp/yr)	I	g*h	1440	
Primary energy equivalent of electricity generated (MJ/kWh)	J	1 kWh = 3.6 MJ and we use a grid efficiency factor of 0.31	11.41	

Avoided energy (MJ/kWp/yr)	K	i*j	16425	
Energy payback time (EPBT)				
EPBT (yr)		f/k	0.39	

5. Residue content in a CdTe module after USM refining

The density of CdTe is 5860 kg/ m^3 and a 1 m^2 module with a 3μm thick CdTe layer contains 0.018 kg of CdTe. 16.5 m^2 of a module is processed to recover 1 kg of USM [5] so processing 1 m^2 of a module results in 0.06 kg of USM. Therefore, 1 m^2 of a module will have a residue content of 0.043 kg after 95% of the CdTe is recovered and refined (0.06-(0.95*0.018)).

6. **Split of the energy benefits of recycled materials for HR 3 scenario**

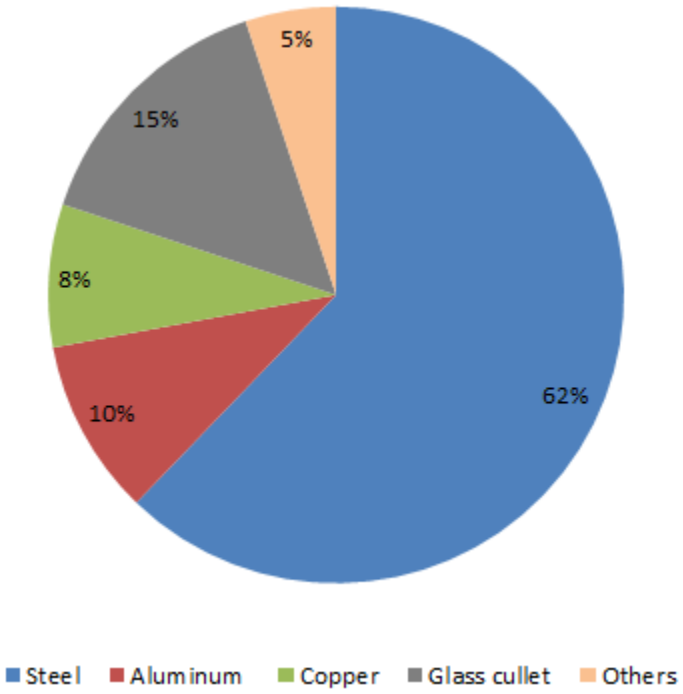

Figure 53 Split of the energy benefits of recycled materials for HR 3 scenario. The total energy benefit of recycled materials, represented by the entire pie chart, corresponds to the green bar for HR 3 in Figure 3 in the main paper

7. Sensitivity of recycling energy benefits to allocation method

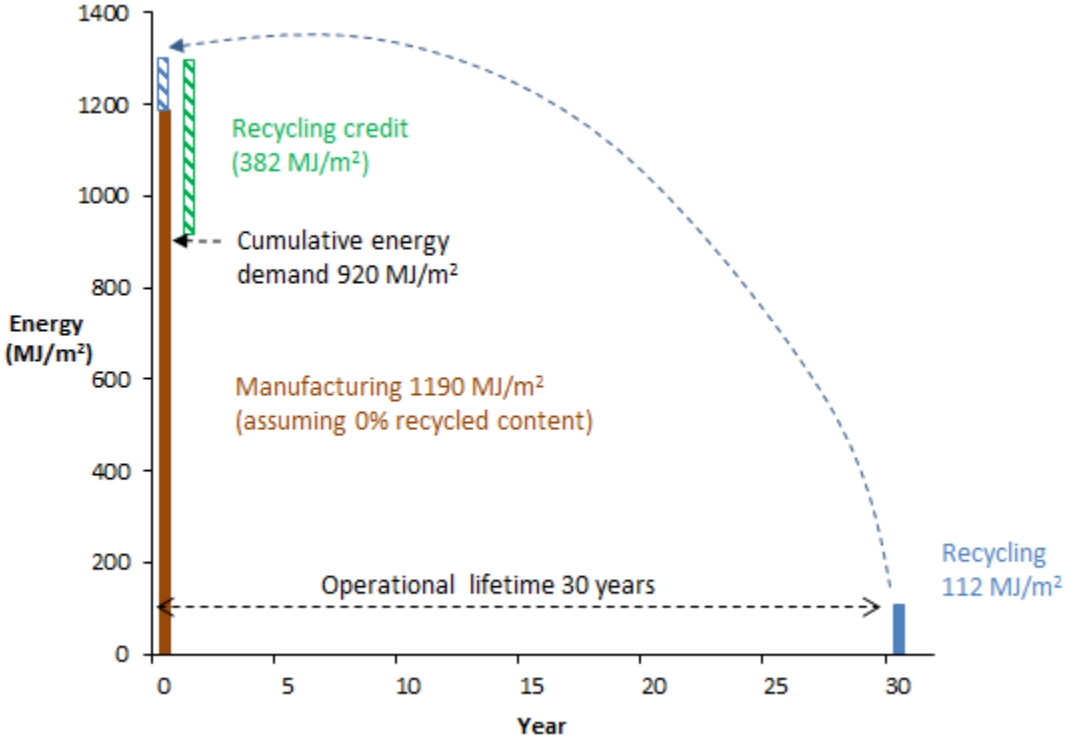

Figure 54 EOLR approach to allocate benefits of PV system recycling and calculating the CED.

The manufacturing energy (brown) is calculated assuming 100% virgin content and this value is 1190 MJ/m^2 (section 11 in SI). The recycling energy burden (blue) includes the transportation, recycling processes, emission control and landfilling (equation 1 in main paper). The recycling credit (green), 382 MJ/m^2, is the sum of the values calculated in the column on the right in Table 36. The CED using EOLR allocation is 920 MJ/m^2 (from Equation 8 in main paper).

Table 36 Calculations for recycling credit

Material	90% recovery of quantities reported in kg/m^2 in Table 1 (assuming 90% recovery rate for BOS materials and module glass and 95% for CdTe)	Energy saved through recycling in MJ/kg from Table 1	Energy benefit of recycling material in MJ/m^2 (product of values in the previous two columns)
Steel	10.82 (sum of steel from inverter, transformer and BOS)	22.06	238.7
Aluminum	0.25	151	37.9
Cu	0.79	38.85	30.8
Glass cullet	13.23	4.3	56.9
CdTe	0.017	127 for Te and 60 for Cd	1.4 (after splitting the mass of CdTe using the stoichiometric mass ratio of Cd and Te)
HDPE	0.26	55.7	14.4
PVC	0.04	33.6	1.3
EPDM	0.06	31.8	1.8
Concrete	3.37	-0.22	-0.7

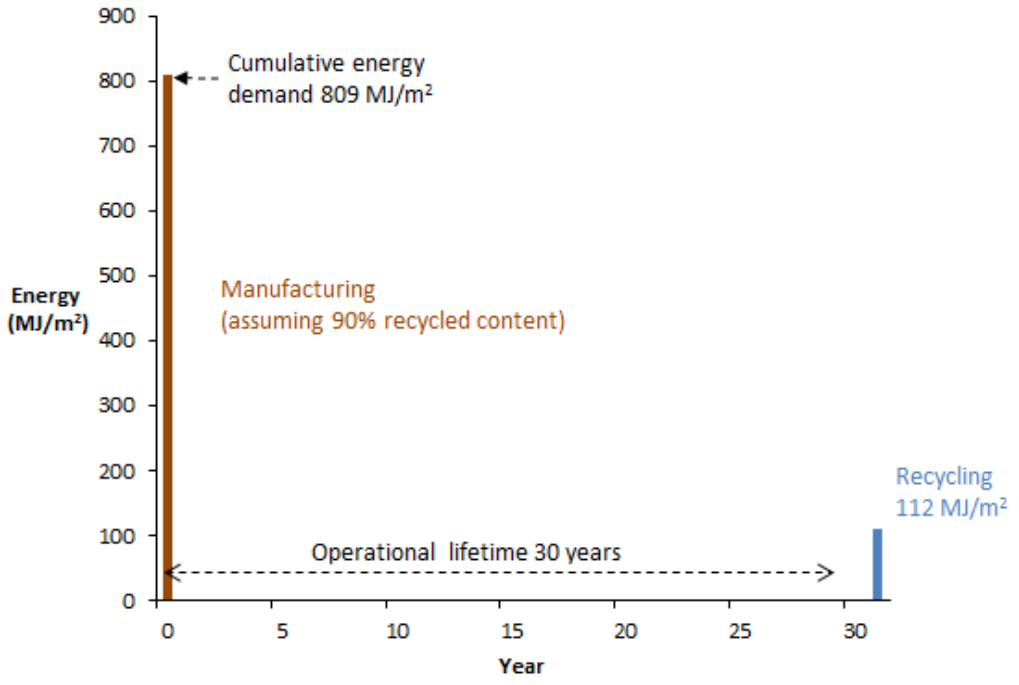

Figure 55 Recycled content (RC) approach to allocate the benefits of PV recycling and calculating CED.

The manufacturing energy (brown) is calculated assuming 100% recycled content and the recycling energy burden (blue) and credits are not considered as part of calculations in the RC approach. We get 809 MJ/m^2 after the energy benefits of 90% recycling (sum of the last column in Table 36) is subtracted from 1190 MJ/m^2 (section 11 in SI) which is the manufacturing energy assuming 100% virgin contents.

Using the same approach we calculate CED using RC and EOLR for scenarios NR2, MR2 and MR4.

8. Flowchart and results for uncertainty analysis

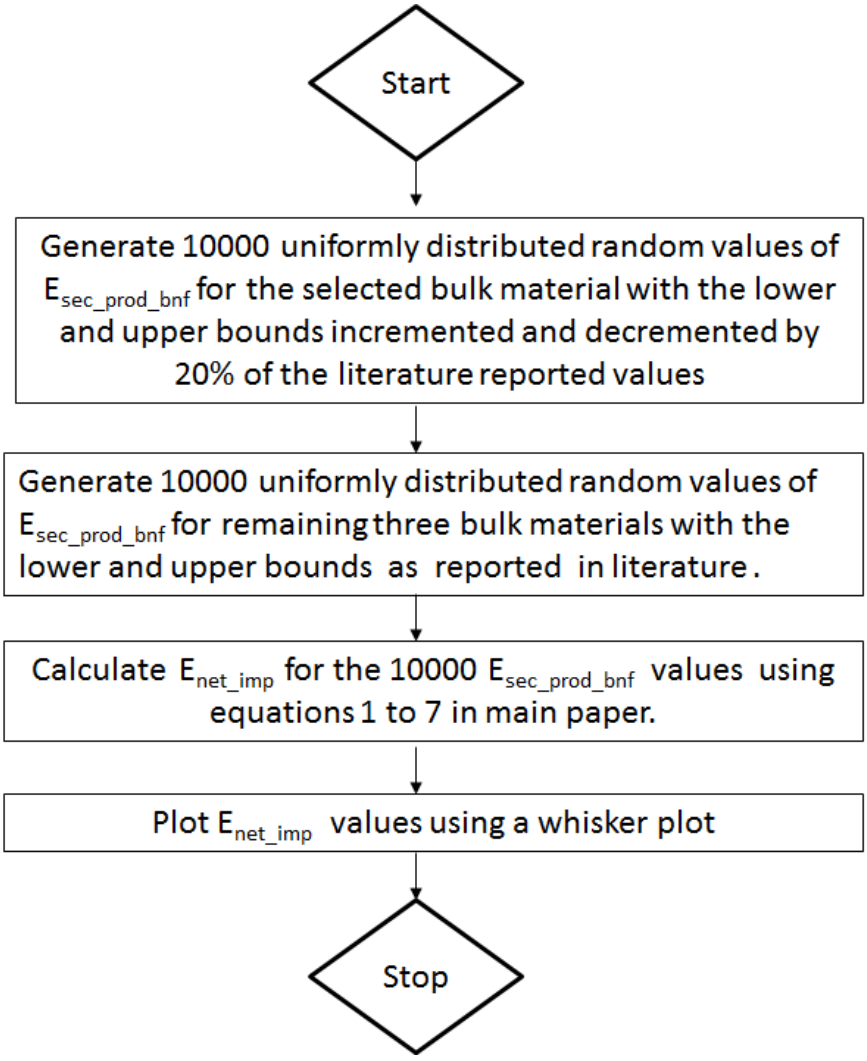

Figure 56 Flowchart for calculating and plotting the sensitivity of net energy impact of recycling (E_{net_imp}) to values assumed for energy benefits of recycling materials ($E_{sec\_prod\_bnf}$). The literature values for lower and upper bounds of $E_{sec\_prod\_bnf}$ is reported in section 2 in SI. This flowchart is run for the four bulk materials (steel, aluminum, copper, and glass) and results are compared with the base scenario HR3 in Figure 6 in SI.

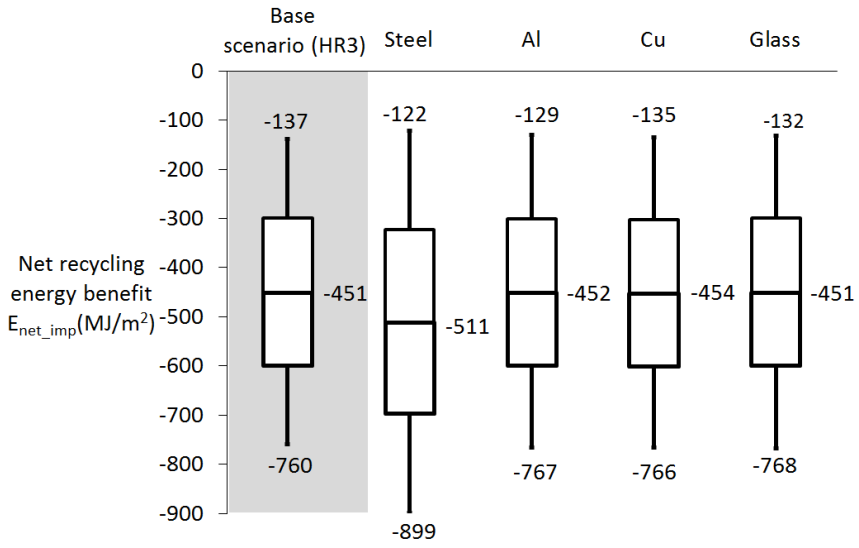

Figure 57 Uncertainty in net recycling energy benefit calculations (E_{net_imp} in equation 7 in main paper) to $E_{sec\_prod\_bnf}$ values for the four dominant materials (by mass) in a CdTe PV system. The simulations were run 10,000 times and the box and whisker plots depict the minimum, median and maximum values for the calculated net energy benefit.

Figure 57 demonstrates that net energy benefit calculation is most sensitive to $E_{sec\_prod\_bnf}$ values for steel as the maximum value and the median of steel vary the most when compared to the base scenario. The distribution of net energy benefits shows the maximum variation between -899 and -122 MJ/m^2 when the $E_{sec\_prod\_bnf}$ values of steel are varied between the modified upper and lower bounds. Corresponding values for the base HR 3 scenario and other materials show a smaller variation between -760 and -137 MJ/m^2.

9. **Optimal recycling plant location for system disassembly (step 1) and semiconductor refining (step 3)**

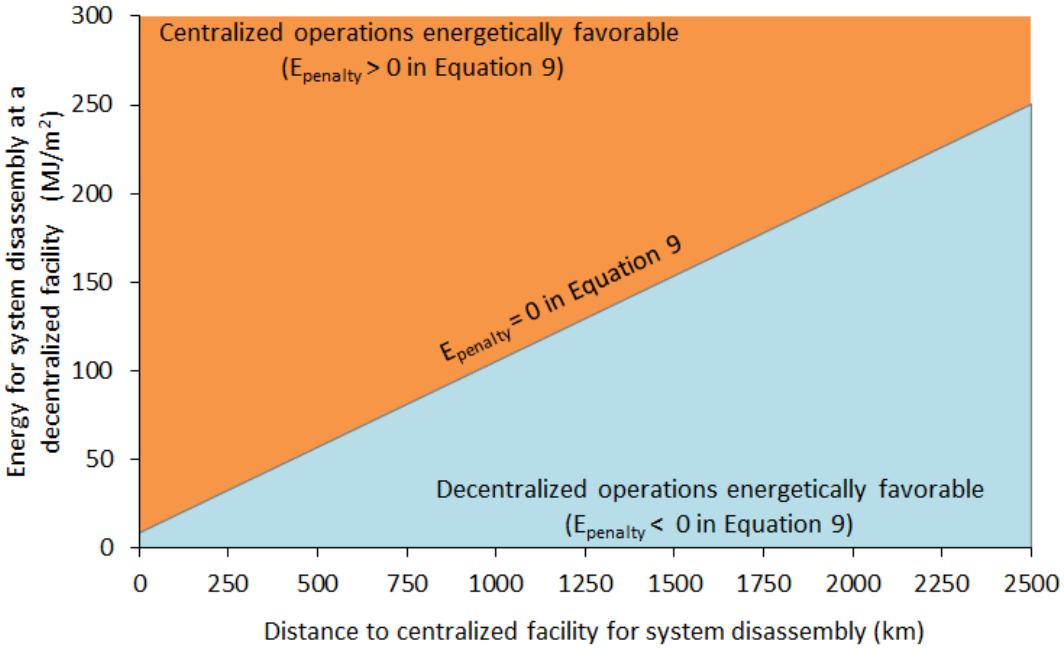

Figure 58 Frontier diagram depicting two regions where centralized and decentralized facilities are favorable for system disassembly (step 1 in figure 1 in main paper). Decentralized recycling is favorable in the blue region where the combination of the distance to the centralized facility and the energy required at the decentralized facility result in a negative energy penalty ($E_{penalty} < 0$ from equation 9 in main paper). Similarly, centralized recycling is favored in the orange region when energy penalty of decentralization is positive.

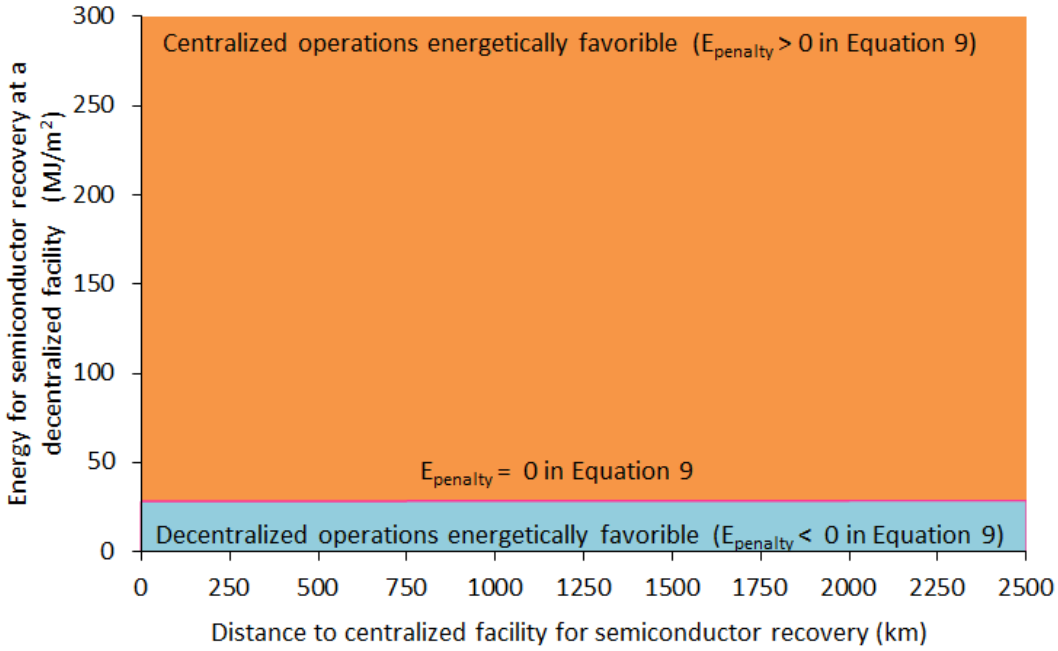

Figure 59 Frontier diagram depicting two regions where centralized and decentralized facilities are favorable for semiconductor recovery (step 3 in figure 1 in main paper). Decentralized recycling is favorable in the blue region where the combination of the distance to the centralized facility and the energy required at the decentralized facility result in a negative energy penalty ($E_{penalty} < 0$ from equation 9 in main paper). Similarly, centralized recycling is favored in the orange region when energy penalty of decentralization is positive.

10. Mass of unrefined solar grade silicon per m^2 of a crystalline silicon module

Table 4 in [33] reports a purified silicon use of 9.8 g/W_p and a panel area of 20.8 $m^2/3kW_p$ in 2007. Based on these values, the mass of unrefined solar grade silicon is 1.4 kg/m^2. This is a conservative estimate as it accounts for only the purified content and not impurities that will be part of the recovered solar grade silicon (from step 2) and transported to the location of step 3.

11. Manufacturing energy for 1 m^2 of a CdTe PV system

The total lifecycle energy of 1270 MJ/m^2 is reported for a CdTe PV system in Table III in [31] and this includes the 81 MJ/m^2 of energy for EOL processing. After excluding the EOL energy component which is accounted for in the energy flow model (Figure 1 in main paper), the manufacturing energy for 1 m^2 of a CdTe PV system is 1190 MJ/m^2.

References

[1] R. S. Jorge, T. R. Hawkins, and E. G. Hertwich, "Life cycle assessment of electricity transmission and distribution—part 2: transformers and substation equipment," *Int. J. Life Cycle Assess.*, vol. 17, no. 2, pp. 184–191, Sep. 2011.

[2] J. E. Mason, V. M. Fthenakis, T. Hansen, and H. C. Kim, "Energy payback and life-cycle CO2 emissions of the BOS in an optimized 3·5 MW PV installation," *Prog. Photovoltaics Res. Appl.*, vol. 14, no. 2, pp. 179–190, Mar. 2006.

[3] P. Sinha and M. de Wild-Scholten, "Life Cycle Assessment of Utility-Scale CdTe PV Balance of Systems," in *27th European Photovoltaic Solar Energy Conference*, 2012, pp. 4657 – 4660.

[4] M. Held, "Life cycle assessment of CdTe module recycling," in *24th EU PVSEC Conference*, 2009, pp. 2370 – 2375.

[5] P. Sinha, M. Cossette, and J.-F. Menard, "End-of-life CdTe recycling with semiconductor refining," in *27th EU PVSEC*, 2012, pp. 24–28.

[6] J. Johnson, B. K. Reck, T. Wang, and T. E. Graedel, "The energy benefit of stainless steel recycling," *Energy Policy*, vol. 36, no. 1, pp. 181–192, Jan. 2008.

[7] World Steel Association, *Life cycle inventory study for steel products*.

[8] EPA, "Energy Trends in Selected Manufacturing Sectors: Opportunities and Challenges for Environmentally Preferable Energy Outcomes," no. March, 2007.

[9] Clare Broadbent, "End-of-life recycling and disposal: essential to any LCA study," in *LCA XI*, 2011.

[10] Bureau of International Recycling, "Report on the Environmental Benefits of Recycling," *2008*.

[11] PE Americas, "Life cycle impact assessment of aluminum beverage cans," *Prep. Alum. Assoc.*, 2010.

[12] Aluminum Association, "Aluminum: The element of sustainability," 2011.

[13] Global Aluminium Recycling Committee, "Global aluminium recycling: a cornerstone of sustainable development," 2006.

[14] R. F. Cook, "The collection and recycling of waste glass (cullet) in glass container manufacture," *Conserv. Recycl.*, vol. 2, no. March, pp. 59–69, 1978.

[15] A. W. Larsen, H. Merrild, and T. H. Christensen, "Recycling of glass: accounting of greenhouse gases and global warming contributions.," *Waste Manag. Res.*, vol. 27, no. 8, pp. 754–62, Nov. 2009.

[16] M. Classen et al, "Life Cycle Inventories of Metals. Final report ecoinvent data v2.1, No 10.," *Eco Inven.*, 2009.

[17] Franklin Associates, A divsion of ERG, "Lifecycle inventory of 100% postconsumer HDPE and PET recycled resin from post consumer containers and packaging," 2010.

[18] Solvay Group and VinylLoop Ferrara SpA, "The VinyLoop Eco-Footprint - Benchmarking the environmental impact of PVC compound recycled in the VinylLoop process with PVC compound produced in the coventional route," no. February, 2012.

[19] T. Amari, N. J. Themelis, and I. K. Wernick, "Resource recovery from used rubber tires," *Resour. Policy*, vol. 25, no. 3, pp. 179–188, Sep. 1999.

[20] E. Laboy-Nieves, "Energy Recovery from Scrap Tires: A Sustainable Option for Small Islands like Puerto Rico," *Sustainability*, vol. 6, no. 5, pp. 3105–3121, May 2014.

[21] US DoT Federal Highway Administration, "User Guidelines for Waste and Byproduct Materials in Pavement Construction," *Publication Number: FHWA-RD-97-148*, 2012. [Online]. Available: http://www.fhwa.dot.gov/publications/research/infrastructure/structures/97148/st1.cfm.

[22] M. Weil, "Closed-loop recycling of construction and demolition waste in Germany in view of stricter environmental threshold values," *Waste Manag. Res.*, vol. 24, no. 3, pp. 197–206, Jun. 2006.

[23] S. Marinković, V. Radonjanin, M. Malešev, and I. Ignjatović, "Comparative environmental assessment of natural and recycled aggregate concrete.," *Waste Manag.*, vol. 30, no. 11, pp. 2255–64, Nov. 2010.

[24] J. Eom, L. Schipper, and L. Thompson, "We keep on truckin': Trends in freight energy use and carbon emissions in 11 IEA countries," *Energy Policy*, vol. 45, pp. 327–341, Jun. 2012.

[25] International Energy Agency, "Transport Energy and CO2: Moving Towards Sustainability," OECD Publishing, 2009.

[26] U. Arena, M. . Mastellone, and F. Perugini, "The environmental performance of alternative solid waste management options: a life cycle assessment study," *Chem. Eng. J.*, vol. 96, no. 1–3, pp. 207–222, Dec. 2003.

[27] F. Cherubini, S. Bargigli, and S. Ulgiati, "Life cycle assessment (LCA) of waste management strategies: Landfilling, sorting plant and incineration," *Energy*, vol. 34, no. 12, pp. 2116–2123, Dec. 2009.

[28] First Solar, "Personal Communication," 2014.

[29] Argonne National Laboratory, "The Greenhouse Gases, Regulated Emissions, and Energy Use in Transportation (GREET) Model: Version 2.," 2014.

[30] E. Alsema, D. Fraile, R. Frischknecht, V. Fthenakis, M. Held, H. . Kim, W. Pölz, M. Raugei, and M. de Wild Scholten, "Methodology guidelines on life cycle assessment of photovoltaic electricity," *IEA PVPS Rep.*, 2011.

[31] M. Held and R. Ilg, "Update of environmental indicators and energy payback time of CdTe PV systems in Europe," *Prog. Photovoltaics Res. Appl.*, vol. 19, no. January, pp. 614–626, 2011.

[32] First Solar, "Key Quarterly Financial Data, Feb 2015," 2015.

[33] N. Jungbluth, M. Tuchschmid, and M. de Wild-Scholten, "Life Cycle Assessment of Photovoltaics: Update of ecoinvent data v2. 0," *ESU-services Ltd., 2008*, pp. 1–22, 2008.

APPENDIX E
E. SUPPORTING INFORMATION FOR CHAPTER 5

1. Cadmium ion-exchange material usage efficiency

The theoretical dry capacity for Amberlyst 15 is 4.7 meq/g [1][2] which corresponds to 263 mg of cadmium per mg of Amberlyst 15. Therefore, to extract 7.74 gram of cadmium contained in 1 m^2 of a CdTe module (see section 2 SI), 0.029 gram of the resin is required.

Wang and Fthenakis experimentally investigated the feasibility of removing cadmium dissolved in acidic solution (0.5M H_2SO_4 similar to acidic leachate during recycling operations) using Amberlyst 15 and DOWEX 50X8 ([2]–[4]). The ion-exchange resin requirements is determined from [3] as it simulates the separation of cadmium from a leachate operational conditions encountered in actual CdTe module recycling. An extraction of 33 mg of cadmium per gram of Amberlyst-15 was reported [3] and, therefore, 234g of Amberlyst 15 is required to extract 7.74g of cadmium in 1 m^2 of the module (section 2 SI).

As there is no study reporting the energy requirement for ion exchange extraction of cadmium, we estimate a value based on ion exchange systems used in water treatment plants. The energy requirement ranges between 1.2 and 5.5 x 10^{-5} kWh per liter of water treated [5][6] and a mid-point value of 3.35 x 10^{-5} kWh per liter is assumed. Fthenakis and Wang's study on CdTe PV recycling successfully recovered cadmium from a leachate with a cadmium concentration of 942 ppm (0.942 g/l) [3]. Therefore, to recover 7.7g of cadmium from 1 m^2 of a CdTe module, 8.2 liters of leachate needs to be treated with an ion exchange resin and this requires 27.5 x 10^{-5} kWh.

After the ion exchange treatment of the leachate, the cadmium in the saturated resin is eluted into a solution by washing with 1 to 5 bed volumes of 5M sulfuric acid [2] and we assume mid-point value of 2.5 bed volumes. This corresponds to 20.5 liters of 5M sulfuric

acid or 10052 g of sulfuric acid per m^2 of the PV module as a total bed volume of 8.2 liters of leachate per m^2 of the PV module is treated with ion exchange resins.

The eluted cadmium is precipitated using 33 grams of NaOH. This value of 33g is obtained by splitting a total of 100 grams of NaOH used to precipitate both cadmium and tellurium in equations 3 and in section 2 of the SI in the corresponding stoichiometric ratio of 2:4. Similarly, the tellurium remaining in the leachate (after cadmium is separated through ion exchange) is recovered by precipitating with 67g of NaOH.

2. Cadmium and tellurium in 1 m^2 of a CdTe PV module and leaching and precipitation reactions

Table 37 CdTe and CdS content in 1 m^2 of a CdTe module

Compound	Layer thickness (t)	Density (d)	Mass (1 m^2 x t x d)	Moles
CdTe	3 x 10^{-6} m	5.86 x 10^6 g/ m^3	18 g	7.5 x 10^{-2} moles
CdS	6 x 10^{-8} m [7]	4.82 x 10^6 g/ m^3	0.29 g	2 x 10^{-3} moles

Based on the atomic masses, the 18 grams of CdTe in 1 m^2 of the module consists of 10.26 grams (0.08 moles) and 7.74 grams (0.069 moles) of tellurium and cadmium, respectively.

The oxidative leaching of CdTe, as explained in the main paper, is represented by the following reactions

$$CdTe + 3H_2O_2 + 3H_2SO_4 \rightleftharpoons CdSO_{4(aq)} + 6H_2O + Te(SO_4)_{2\,(aq)} \quad 4$$

$$CdS + H_2O_2 + H_2SO_4 \rightleftharpoons CdSO_{4(aq)} + 2H_2O + S_{(s)} \quad 5$$

The precipitation of Cd and Te from the leachate, as explained in the main paper, is given by

$$CdSO_{4(aq)} + 2NaOH \rightleftharpoons Cd(OH)_{2(s)} + Na_2SO_{4\,(aq)} \quad 6$$

$$Te(SO_4)_{2(aq)} + 4NaOH \rightleftharpoons TeO_{2(s)} + 2Na_2SO_{4\,(aq)} + 2H_2O \quad 7$$

3. Material requirements for solvent extraction of cadmium

At a pilot scale, four contacting stages of leaching is required to extract 99.995% cadmium from an acidic leachate which is chemically similar to the leachate processed in commercial operations [8]. In each stage, 10% D2EHPA (by volume) in four liters of an organic diluent (kerosene) is mixed with 1 liter of aqueous leachate containing 10 grams of cadmium. Based on a 0.965 g/mL density value for D2EHPA [9], the 1600 mL of D2EHPA required for the four stages corresponds to a mass of 1544 grams. Normalizing this to the 7.74 g of cadmium contained in 1 m^2 of the PV module (section 2 in SI), the pilot scale D2EHPA requirement is 1195 grams/m^2. This study assumes kerosene as the organic diluent in which D2EHPA is dissolved as it was previously used in the solvent extraction of cadmium [10][11][12]. In each of the four extraction stages for 10 grams of cadmium, kerosene constitutes 90% by volume of the 4 liters of organic diluent and this corresponds to a total volume of 14400 mL. Normalizing this to the 7.74 g of cadmium contained in 1 m^2 of the PV module (section 2), the pilot scale kerosene requirements (per m^2) is 11145 mL or 11.8 kg (using a density value of 0.82 kg/cm^3 for kerosene).

A previous study reported the use of sulfuric acid (180 g/l) to strip cadmium from the loaded organic phase consisting of kerosene and D2EHPA with a 1:1 volumetric ratio of sulfuric acid and the organic phase [11]. Therefore, 16 liters of 180 g/l sulfuric acid is

required for 16 liters of the organic phase used for solvent extraction of cadmium from 1 m^2 of a CdTe PV module (4 stages each with 4 liters of kerosene containing D2EHPA). This corresponds to 2880 g of sulfuric acid.

The cadmium stripped through sulfuric acid is precipitated using NaOH. By splitting the total of 100g of NaOH (Alternative 1 in Table 38 in SI) required to precipitate both cadmium and tellurium in the stoichiometric ratio of 2:4 (equations 6 and in section 2 of SI), the NaOH required to precipitate only cadmium is calculated as 33g. Similarly, the tellurium, remaining in the leachate after cadmium is separated through solvent extraction, is recovered by precipitating with 67g of NaOH.

As there is no study reporting the energy requirement for solvent extraction of cadmium, we use a value of 0.5 kWh per liter of the aqueous phase (leachate containing the cadmium) based on a previous study on the solvent extraction of rare earth elements [13]. With four liters of the aqueous phase, 2 kWh of electricity is required.

4. Material and energy requirements for the seven CdTe PV recycling alternatives

Table 38 Material and energy requirements for the seven CdTe PV recycling alternatives and the corresponding SimaPro dataset used to determine the ReCiPe environmental impact categories.

Recycling Method	Inventory item	Requirement per m^2 [source]	SimaPro dataset
Alternative 1 (Incumbent): mech+leach+prcp (incumbent)	electricity for mechanical stripping and crushing of CdTe PV module	2.2 kWh. We assume 50% of the energy reported in Table 1 in [14] is required for the mechanical stripping and crushing. The remaining 50% is required for the leaching process. Based on First Solar's current recycling operations in Malaysia, electricity is sourced from captive natural gas plants.	Electricity, high voltage {MY}| electricity production, natural gas, at conventional power plant | Alloc Def, U
	electricity for leaching process	2.2 kWh. We assume 50% of the energy reported in Table 1 in [14] is required for the leaching process. The remaining 50% is required for the mechanical stripping and crushing. Based on First Solar's current recycling operations in Malaysia, electricity is sourced from captive natural gas plants.	Electricity, high voltage {MY}| electricity production, natural gas, at conventional power plant | Alloc Def, U

Recycling Method	Inventory item	Requirement per m^2 [source]	SimaPro dataset
	sulfuric acid for the leaching process	83 g [14]	Sulfuric acid {RER}| production | Alloc Def, U
	hydrogen peroxide for the leaching process	570 g [14]	Hydrogen peroxide, without water, in 50% solution state {RER}| hydrogen peroxide production, product in 50% solution state | Alloc Def, U
	sodium hydroxide for the precipitation process	100 g [14]	Sodium hydroxide, without water, in 50% solution state {RER}| chlor-alkali electrolysis, diaphragm cell | Alloc Def, U
Alternative 2: thermal+leach+ion exch+prcp	Electricity for furnace operation.	0.48 kWh. Refer section 6 in SI. Based on First Solar's current recycling operations in Malaysia, electricity is sourced from captive natural gas plants.	Electricity, high voltage {MY}| electricity production, natural gas, at conventional power plant | Alloc Def, U
	electricity for leaching process	2.2 kWh. We assume 50% of the energy reported in Table 1 in [14] is required for the leaching process. Based on First Solar's current recycling	Electricity, high voltage {MY}| electricity production, natural gas, at conventional power plant | Alloc Def, U

Recycling Method	Inventory item	Requirement per m^2 [source]	SimaPro dataset
		operations in Malaysia, electricity is sourced from captive natural gas plants.	
	sulfuric acid for the leaching process	83 g [14]	Sulfuric acid {RER} | production | Alloc Def, U
	hydrogen peroxide for the leaching process	570 g [14]	Hydrogen peroxide, without water, in 50% solution state {RER} | hydrogen peroxide production, product in 50% solution state | Alloc Def, U
	Amberlyst 15 (cation resin) for ion exchange process	234 g. Refer section **Error! Reference source not found.** in SI.	Cationic resin {CH} | production | Alloc Def, U
	Electricity for ion exchange process	$2.75x10^{-4}$ kWh. Refer section **Error! Reference source not found.** in SI.	Electricity, high voltage {MY} | electricity production, natural gas, at conventional power plant | Alloc Def, U
	Sulfuric acid to strip the cadmium	10052 g. Refer section **Error! Reference source not found.** in SI.	Sulfuric acid {RER} | production | Alloc Def, U

Recycling Method	Inventory item	Requirement per m^2 [source]	SimaPro dataset
	during the ion exchange process		
	Sodium hydroxide to precipitate the cadmium during the ion exchange process	33 g. Refer section **Error! Reference source not found.** in SI.	Sodium hydroxide, without water, in 50% solution state {RER}| chlor-alkali electrolysis, diaphragm cell | Alloc Def, U
	Sodium hydroxide to precipitate the tellurium that remains in the leachate.	67 g. Refer section **Error! Reference source not found.** in SI.	Sodium hydroxide, without water, in 50% solution state {RER}| chlor-alkali electrolysis, diaphragm cell | Alloc Def, U
Alternative 3: thermal+leach+prcp	Electricity for furnace operation.	0.48 kWh. Refer section 6 in SI. Based on First Solar's current recycling operations in Malaysia, electricity is sourced from captive natural gas plants.	Electricity, high voltage {MY}| electricity production, natural gas, at conventional power plant | Alloc Def, U
	electricity for leaching process	2.2 kWh. We assume 50% of the energy reported in Table 1 in [14] is required for the leaching process. Based on First Solar's current recycling operations in Malaysia,	Electricity, high voltage {MY}| electricity production, natural gas, at conventional power plant | Alloc Def, U

Recycling Method	Inventory item	Requirement per m^2 [source]	SimaPro dataset
		electricity is sourced from captive natural gas plants.	
	sulfuric acid for the leaching process	83 g [14]	Sulfuric acid {RER} | production | Alloc Def, U
	hydrogen peroxide for the leaching process	570 g [14]	Hydrogen peroxide, without water, in 50% solution state {RER} | hydrogen peroxide production, product in 50% solution state | Alloc Def, U
	sodium hydroxide for the precipitation process	100 g [14]	Sodium hydroxide, without water, in 50% solution state {RER} | chlor-alkali electrolysis, diaphragm cell | Alloc Def, U
Alternative 4: thermal+leach+solv ext+prcp	Electricity for furnace operation.	0.48 kWh. Refer section 6 in SI. Based on First Solar's current recycling operations in Malaysia, electricity is sourced from captive natural gas plants.	Electricity, high voltage {MY} | electricity production, natural gas, at conventional power plant | Alloc Def, U
	electricity for leaching process	2.2 kWh. We assume 50% of the energy reported in Table 1 in [14] is required for the	Electricity, high voltage {MY} | electricity production, natural gas,

Recycling Method	Inventory item	Requirement per m^2 [source]	SimaPro dataset
		leaching process. Based on First Solar's current recycling operations in Malaysia, electricity is sourced from captive natural gas plants.	at conventional power plant | Alloc Def, U
	sulfuric acid for the leaching process	83 g [14]	Sulfuric acid {RER}| production | Alloc Def, U
	hydrogen peroxide for the leaching process	570 g [14]	Hydrogen peroxide, without water, in 50% solution state {RER}| hydrogen peroxide production, product in 50% solution state | Alloc Def, U
	D2EHPA for solvent extraction of cadmium	1195 g. Refer section 3 in SI.	Organophosphorus-compound, unspecified {RER}| production | Alloc Def, U
	Kerosene for solvent extraction of cadmium	11800 g. Refer section 3 in SI.	Kerosene {Europe without Switzerland}| petroleum refinery operation | Alloc Def, U

Recycling Method	Inventory item	Requirement per m^2 [source]	SimaPro dataset
	Sulfuric acid for solvent extraction of cadmium	2880 g. Refer section 3 in SI.	Sulfuric acid {RER}| production | Alloc Def, U
	Sodium hydroxide for solvent extraction of cadmium	33 g. Refer section 3 in SI.	Sodium hydroxide, without water, in 50% solution state {RER}| chlor-alkali electrolysis, diaphragm cell | Alloc Def, U
	Electricity for solvent extraction of cadmium	2 kWh. Refer section 3 in SI. Based on First Solar's current recycling operations in Malaysia, electricity is sourced from captive natural gas plants.	Electricity, high voltage {MY}| electricity production, natural gas, at conventional power plant | Alloc Def, U
	Sodium hydroxide to precipitate the tellurium that remains in the leachate.	67 g. Refer section 3 in SI.	Sodium hydroxide, without water, in 50% solution state {RER}| chlor-alkali electrolysis, diaphragm cell | Alloc Def, U
Alternative 5: org solv+leach+ion exch+prcp	o-dichlorobenzene for dissolving the EVA	8840 g. Refer section 7 in SI.	O-dichlorobenzene {RER}| benzene chlorination | Alloc Def, U
	Electricity for delaminating EVA	Uniform distribution ranging between 6.5 to 37.4 kWh.	Electricity, high voltage {MY}| electricity

Recycling Method	Inventory item	Requirement per m² [source]	SimaPro dataset
	by heating in o-DCB	Refer section 7 in SI. Based on First Solar's current recycling operations in Malaysia, electricity is sourced from captive natural gas plants.	production, natural gas, at conventional power plant | Alloc Def, U
	electricity for leaching process	2.2 kWh. We assume 50% of the energy reported in Table 1 in [14] is required for the leaching process. Based on First Solar's current recycling operations in Malaysia, electricity is sourced from captive natural gas plants.	Electricity, high voltage {MY}| electricity production, natural gas, at conventional power plant | Alloc Def, U
	sulfuric acid for the leaching process	83 g [14]	Sulfuric acid {RER}| production | Alloc Def, U
	hydrogen peroxide for the leaching process	570 g [14]	Hydrogen peroxide, without water, in 50% solution state {RER}| hydrogen peroxide production, product in 50% solution state | Alloc Def, U
	Amberlyst 15 (cation resin) for	234 g. Refer section **Error! Reference source not found.** in SI.	Cationic resin {CH}| production | Alloc Def, U

Recycling Method	Inventory item	Requirement per m^2 [source]	SimaPro dataset
	ion exchange process		
	Electricity for ion exchange process	$2.75x10^{-4}$ kWh. Refer section **Error! Reference source not found.** in SI.	Electricity, high voltage {MY}| electricity production, natural gas, at conventional power plant | Alloc Def, U
	Sulfuric acid to strip the cadmium during the ion exchange process	10052 g. Refer section **Error! Reference source not found.** in SI.	Sulfuric acid {RER}| production | Alloc Def, U
	Sodium hydroxide to precipitate the cadmium during the ion exchange process	33 g. Refer section **Error! Reference source not found.** in SI.	Sodium hydroxide, without water, in 50% solution state {RER}| chlor-alkali electrolysis, diaphragm cell | Alloc Def, U
	Sodium hydroxide to precipitate the tellurium that remains in the leachate.	67 g. Refer section **Error! Reference source not found.** in SI.	Sodium hydroxide, without water, in 50% solution state {RER}| chlor-alkali electrolysis, diaphragm cell | Alloc Def, U

Recycling Method	Inventory item	Requirement per m^2 [source]	SimaPro dataset
Alternative 6: org solv+leach+prcp	o-dichlorobenzene for dissolving the EVA	8840 g. Refer section 7 in SI.	O-dichlorobenzene {RER}| benzene chlorination | Alloc Def, U
	Electricity for delaminating EVA by heating in o-DCB	Uniform distribution ranging between 6.5 to 37.4 kWh. Refer section 7 in SI. Based on First Solar's current recycling operations in Malaysia, electricity is sourced from captive natural gas plants.	Electricity, high voltage {MY}| electricity production, natural gas, at conventional power plant | Alloc Def, U
	electricity for leaching process	2.2 kWh. We assume 50% of the energy reported in Table 1 in [14] is required for the leaching process. Based on First Solar's current recycling operations in Malaysia, electricity is sourced from captive natural gas plants.	Electricity, high voltage {MY}| electricity production, natural gas, at conventional power plant | Alloc Def, U
	sulfuric acid for the leaching process	83 g [14]	Sulfuric acid {RER}| production | Alloc Def, U
	hydrogen peroxide for the leaching process	570 g [14]	Hydrogen peroxide, without water, in 50% solution state {RER}| hydrogen peroxide

Recycling Method	Inventory item	Requirement per m² [source]	SimaPro dataset
			production, product in 50% solution state | Alloc Def, U
	sodium hydroxide for the precipitation process	100 g [14]	Sodium hydroxide, without water, in 50% solution state {RER}| chlor-alkali electrolysis, diaphragm cell | Alloc Def, U
Alternative 7: org solv+leach+solv ext+prcp	o-dichlorobenzene for dissolving the EVA	8840 g. Refer section 7 in SI.	O-dichlorobenzene {RER}| benzene chlorination | Alloc Def, U
	Electricity for delaminating EVA by heating in o-DCB	Uniform distribution ranging between 6.5 to 37.4 kWh. Refer section 7 in SI. Based on First Solar's current recycling operations in Malaysia, electricity is sourced from captive natural gas plants.	Electricity, high voltage {MY}| electricity production, natural gas, at conventional power plant | Alloc Def, U
	electricity for leaching process	2.2 kWh. We assume 50% of the energy reported in Table 1 in [14] is required for the leaching process. Based on First Solar's current recycling operations in Malaysia,	Electricity, high voltage {MY}| electricity production, natural gas, at conventional power plant | Alloc Def, U

Recycling Method	Inventory item	Requirement per m^2 [source]	SimaPro dataset
		electricity is sourced from captive natural gas plants.	
	sulfuric acid for the leaching process	83 g [14]	Sulfuric acid {RER} | production | Alloc Def, U
	hydrogen peroxide for the leaching process	570 g [14]	Hydrogen peroxide, without water, in 50% solution state {RER} | hydrogen peroxide production, product in 50% solution state | Alloc Def, U
	D2EHPA for solvent extraction of cadmium	1195 g. Refer section 3 in SI.	Organophosphorus-compound, unspecified {RER} | production | Alloc Def, U
	Kerosene for solvent extraction of cadmium	11800 g. Refer section 3 in SI.	Kerosene {Europe without Switzerland} | petroleum refinery operation | Alloc Def, U
	Sulfuric acid for solvent extraction of cadmium	2880 g. Refer section 3 in SI.	Sulfuric acid {RER} | production | Alloc Def, U
	Sodium hydroxide for solvent	33 g. Refer section 3 in SI.	Sodium hydroxide, without water, in 50%

Recycling Method	Inventory item	Requirement per m^2 [source]	SimaPro dataset
	extraction of cadmium		solution state {RER}| chlor-alkali electrolysis, diaphragm cell | Alloc Def, U
	Electricity for solvent extraction of cadmium	2 kWh. Refer section 3 in SI. Based on First Solar's current recycling operations in Malaysia, electricity is sourced from captive natural gas plants.	Electricity, high voltage {MY}| electricity production, natural gas, at conventional power plant | Alloc Def, U
	Sodium hydroxide to precipitate the tellurium that remains in the leachate.	67 g. Refer section 3 in SI.	Sodium hydroxide, without water, in 50% solution state {RER}| chlor-alkali electrolysis, diaphragm cell | Alloc Def, U
Transportation	Road	Refer Section 9 in SI for the values.	Transport, freight, lorry 16-32 metric ton, EURO5 {RoW}| transport, freight, lorry 16-32 metric ton, EURO5 | Alloc Def, U
	Ship	Refer Section 9 in SI for the values.	Transport, freight, sea, transoceanic ship {GLO}| processing | Alloc Def, U

5. Calculating aggregated environmental stochastic score

For illustrative purposes and simplicity, this section demonstrates the aggregation of outranking scores into an aggregated probabilistic environmental score for 3 recycling methods across 3 impact categories. The same principles can be extended to the 7 recycling alternatives and the 18 ReCiPe impact categories discussed in the main paper. This method was proposed by Prado et al [15] and is based on PROMETHEE II complete ranking [16].

Table 39 Log normal distributions with standard deviations and means for environmental impacts of 3 recycling methods for 3 ReCiPe impact categories. For example, method X has a lognormal distribution Xcc for climate change impacts and the mean and standard distribution are μCC-X and σCC-X, respectively.

	Recycling method X	Recycling method Y	Recycling method Z
Climate Change (CC)	X_{cc} [μ_{CC-X}, σ_{CC-X}]	Y_{CC} [μ_{CC-Y}, σ_{CC-Y}]	Z_{CC} [μ_{CC-Z}, σ_{CC-Z}]
Ozone Depletion (OD)	X_{OD} [μ_{OD-X}, σ_{OD-X}]	Y_{OD} [μ_{OD-Y}, σ_{OD-Y}]	Z_{CC} [μ_{OD-Z}, σ_{OD-Z}]
Human Toxicity (HT)	X_{HT} [μ_{HT-X}, σ_{HT-X}]	Y_{HT} [μ_{HT-Y}, σ_{HT-Y}]	Z_{CC} [μ_{HT-Z}, σ_{HT-Z}]

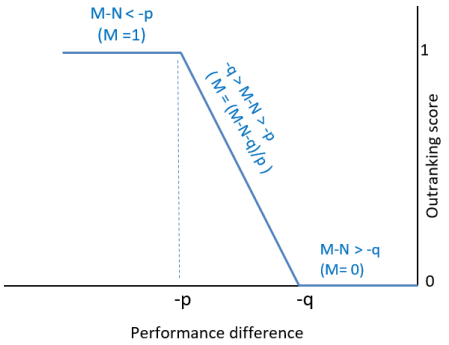

Figure 60 Linear preference function to calculate positive flows. M and N are data points from the stochastically generated values (from mean and standard deviations in Table 39) for a particular environmental impact category for two recycling alternatives, respectively. To calculate negative flows, M is subtracted from N and the difference is similarly converted into an outranking score.

In Figure 60, the preference threshold (p) is the smallest difference in the stochastically generated values in a particular environmental impact category for one recycling alternative to be preferred over another [17]. Similarly, indifference threshold (q) is the largest difference yielding no preference between two recycling alternatives in a particular environmental impact category.

The preference and indifference thresholds can be elicited from experts [18] or quantified from the uncertainty in the underlying characterization data [15]. This research uses the latter approach based on a previous study [15] that calculates the p and q as

$$p=(\sigma_{cdc\_1}+\sigma_{cdc\_2})\div 2$$

$$q=p\div 2$$

where, σ_{cdc_x} is the standard deviation for recycling alternative 'x' in a particular environmental impact category (σ values are reported in section 8 of Appendix E).

In Figure 60, M and N are the stochastically generated data points for a particular impact category (from Table 39) for the two recycling alternatives being compared. If the difference between M and N is less than –p then the alternative with value M is preferred over alternative with value N and M is assigned a value 1. Similarly, if the difference is greater than –q then alternative with value M is outperformed by alternative with value N and M is set to 0. When the difference lies between –p and –q there is a partial preference of M over N and M is assigned a value between 0 and 1.

The positive outranking flow of X with respect to Y in the CC impact category, $\alpha_{XY\text{-}CC}$, will range between 0 and 1 and is calculated from

$$\alpha_{XY\text{-}CC} = PF\{X_{cc} - Y_{cc}\}$$

PF is the preference function (Figure 60) which is applied to the difference between the stochastically generated values for the CC impact category of X and Y. The positive outranking flow is a measure of X being preferred over Y.

Correspondingly, the negative outranking flow, $\alpha_{YX\text{-}CC}$, is a measure of other alternatives (e.g. Y) being preferred over X and is calculated from

$$\alpha_{YX\text{-}CC} = PF\{Y_{cc} - X_{cc}\}$$

Similarly, the remaining positive and negative outranking flows are calculated for all the impact categories for the 6 combinations – XY, XZ, YX, YZ, ZX and ZY.

The total positive outranking flow of X with respect to Y, weighted by stochastically generated weights (W) for each impact category, is given by

$$\pi_{XY} = (\alpha_{XY\text{-}CC} \times W_{CC}) + (\alpha_{XY\text{-}OD} \times W_{OD}) + (\alpha_{XY\text{-}HT} \times W_{HT})$$

where W_{cc}, W_{OD} and W_{HT} are beta-randomly distributed random variables (1000 samples each) such that

$$W_{CC} + W_{OD} + W_{HT} = 1$$

Similarly, the remaining positive and negative outranking flows - π_{XZ}, π_{XZ}, π_{YX}, π_{YZ}, π_{ZX} and π_{ZY} - are calculated.

The aggregated net probabilistic environmental score (Φ) for each of the 3 recycling methods is calculated from the sum of the net flows (positive minus negative flows) and is given by

$$\Phi_X = (\pi_{XY} - \pi_{YX}) + (\pi_{XZ} - \pi_{ZX})$$

$$\Phi_Y = (\pi_{YX} - \pi_{XY}) + (\pi_{YZ} - \pi_{ZY})$$

$$\Phi_Z = (\pi_{ZY} - \pi_{YZ}) + (\pi_{ZX} - \pi_{XZ})$$

Φ_x, Φ_x and Φ_z are distributed between -1 (environmentally least favorable) and +1 (environmentally most favorable).

6. Thermal delamination EVA in furnace

Table 40 Experimental observations for thermal delamination of EVA in a furnace

Trial Number	Temperature of furnace (Celsius)	Time heated in furnace ($\mathbf{T_{run}}$,min)	Time in closed furnace after furnace is switched off ($\mathbf{T_{close}}$, min)	Time in open furnace after furnace is switched off ($\mathbf{T_{open}}$, min)	EVA Remaining after $T_{run}+T_{close}+T_{open}$ minutes (%)	Delaminated after $T_{run}+T_{close}+T_{open}$ minutes?	Flames observed after $T_{run}+T_{close}+T_{open}$ minutes?	Glass cracked after $T_{run}+T_{close}+T_{open}$ minutes?
1	500	2	0	0	-	No	-	-
2	500	3	0	0	-	No	-	-
3	500	4	0	0	-	No	-	-
4	500	5	0	0	-	No	-	-
5	500	6	0	0	-	No	-	-
6	500	7	0	0	0	Yes	Yes	Yes
7	500	7	7	0	0	Yes	Yes	Yes
8	500	7	9	0	0	Yes	Yes	Yes
9	500	7	10	0	0	Yes	Yes	Yes
10	500	7	11	0	0	Yes	No	Yes
11	500	7	11	6	0	Yes	No	Yes
12	500	7	11	8	0	Yes	No	Yes
13	500	7	11	9	0	Yes	No	No

Two 8x8 inch glass samples were laminated with EVA and heated in a Vulcan 3-1750 box furnace [19] at 500 C for T_{run} minutes. The furnace is then switched off and the sample

is allowed to cool inside the closed furnace for T_{close} minutes. The furnace is then opened and the sample is allowed to cool for T_{open} minutes as the sample cracks if it is removed immediately after opening furnace. The EVA remaining in the sample is determined by a mass balance by weighing the sample before and after the thermal delamination.

- Trials 1 to 6 show that 7 minutes is the minimum value for T_{run} to completely delaminate the sample (refer "Time heated in furnace (**T_{run}**,min)" and "Delaminated after $T_{run}+T_{close}+T_{open}$ minutes?" columns)
- Trials 5 to 10 show that 11 minutes is the minimum value for T_{close} to prevent flames (refer "Time in closed furnace after furnace is switched off (**T_{close}**, min)" and "Flames observed after $T_{run}+T_{close}+T_{open}$ minutes?" columns)
- Trials 11 to 13 show that 9 minutes is the minimum value for T_{open} to prevent cracking of glass (refer "Time in open furnace after furnace is switched off (**T_{open}**, min)" and "Glass cracked after $T_{run}+T_{close}+T_{open}$ minutes?" columns)

Therefore, the total process time is 27 minutes with the furnace requiring electricity for the first 7 minutes.

Trials 6, 10 and 13 were repeated twice to confirm the values for T_{run}, T_{close}, and T_{open}. Furthermore, trial 13 was repeated with 4 samples of 8x8 inch glass samples (total area of 0.16 m^2) and 100% delamination was observed without flames or cracking.

Based on an energy meter reading, the electricity required for operating the furnace for 12 hours is 8.46 kWh. Therefore, for the 7-minutes the furnace requires 0.08 kWh electricity to delaminate 0.16 m^2 of the module and this corresponds to 0.48 kWh/m^2 of the module.

7. **Material and energy required to delaminate EVA by heating in an organic solvent**

Table 41 Experimental observations for delamination of EVA by heating in an organic solvent

Sl No	Solvent	Temperature (Celsius)	Delamination time (hours)	Energy required (kWh/m^2)
1	TCE	70	32	-
2	TCE	70	48	-
3	TCE	70	27	-
4	Toluene	85	36	-
5	Toluene	85	53	
6	Toluene	85	49	
7	o-DCB	165	23	37.4
8	o-DCB	165	17	27.6
9	o-DCB	165	10.5	17.07
10	o-DCB	165	7.5	12.2
11	o-DCB	165	4	6.5

The 2x2 inch glass samples (laminated with EVA) are immersed in an organic solvent in a closed beaker (to prevent evaporation) and heated on a hotplate. The results in **Table 41** show that heating in o-DCB requires the shortest time for delamination (Sl No 9). This is

due to the higher heating temperature as ortho-dichlorobenzene has a higher boiling point (180.5 C) than trichloroethylene (87.2 C) and Toluene (110.6 C).

The volume of a 1 m^2 First Solar module with a 0.0068 m thickness is 0.0068 m^3. Therefore, a minimum volume of 0.0068m^3 of o-DCB is required to immerse the module completely in solvent. This volume corresponds to 8.84 kg of o-DCB (density of o-DCB is 1300 kg/m^3). No evaporation of o-DCB is observed during the experimental trials with a closed beaker and this research assumes 10% more (0.0068 x 1.1 = 0.0075m^3 or 7.5L or 9.7kg) than the minimum value to account for possible process inefficiencies at a commercial scale (e.g. when the 1 m^2 is removed from the solvent tank after delamination).

Based on an energy meter reading, 2.87 kWh is required to heat and maintain 0.5L of o-DCB at 165^{o}C for 24 hours. The energy values for o-DCB in the table are calculated by normalizing 2.87 kWh/0.5 L (over 24 hours) to 6.8 L of o-DCB required for 1 m^2 of the module over the delamination time.

8. Summary of the mean and standard deviation of the 18 impact categories in ReCiPe for the seven recycling alternatives

Table 42 Mean and standard distribution for the 18 impact categories in ReCiPe for the seven recycling alternatives as generated by SimaPro [20]

		mech+leach+prcp (incumbent)		thermal+leach+ion exch+prcp		thermal+leach+prcp		thermal+leach+solv ext+prcp		org solv+leach+ion exch+prcp		org solv+leach+prcp		org solv+leach+solv ext+prcp	
Impact category	Unit	Mean	SD	Mean	SD	Mean	SD	Mean	SD	Mean	SD	Mean	SD	Mean	SD
Agricultural land occupation	m2a	2.72E-02	1.76E-02	1.13E-01	1.10E-01	2.72E-02	1.72E-02	3.57E-01	2.20E-01	7.11E-01	4.42E-01	6.02E-01	3.73E-01	9.68E-01	5.30E-01
Climate change	kg CO2 eq	3.62E+00	1.45E+00	3.35E+00	1.03E+00	2.49E+00	8.89E-01	1.99E+01	6.20E+00	4.39E+01	1.40E+01	4.21E+01	1.36E+01	5.99E+01	1.63E+01
Fossil depletion	kg oil eq	1.36E+00	5.71E-01	1.21E+00	3.76E-01	9.22E-01	3.56E-01	1.91E+01	8.59E+00	1.95E+01	6.65E+00	1.88E+01	6.42E+00	3.75E+01	1.06E+01
Freshwater ecotoxicity	kg 1,4-DB eq	3.05E-02	2.15E-01	5.07E-02	4.19E-01	2.13E-02	2.08E-01	9.42E-02	6.48E+00	1.18E+00	4.43E+00	7.95E-01	4.19E+00	1.31E+00	9.49E+00
Freshwater eutrophication	kg P eq	3.72E-04	2.47E-04	1.26E-03	3.80E-03	3.66E-04	2.44E-04	1.95E-02	1.05E-02	1.37E-02	9.63E-03	1.22E-02	9.03E-03	3.17E-02	1.47E-02
Human toxicity	kg 1,4-DB eq	1.81E+00	5.79E+01	-1.61E+00	1.13E+02	8.89E-02	5.62E+01	-1.62E+01	1.75E+03	3.20E+01	1.25E+03	-5.88E+01	1.13E+03	3.66E+01	2.56E+03
Ionising radiation	kBq U235 eq	2.09E-01	2.13E-01	3.76E-01	4.55E-01	2.06E-01	2.41E-01	4.54E+00	3.33E+00	3.68E+00	4.46E+00	3.35E+00	4.14E+00	8.25E+00	8.48E+00
Marine ecotoxicity	kg 1,4-DB eq	2.46E-02	1.74E-01	4.90E-02	3.40E-01	1.81E-02	1.69E-01	1.22E-01	5.25E+00	4.88E-01	3.57E+00	1.90E-01	3.39E+00	6.40E-01	7.68E+00
Marine eutrophication	kg N eq	3.65E-04	1.49E-04	8.01E-04	3.48E-04	3.28E-04	1.35E-04	1.58E-02	8.15E-03	7.11E-03	2.86E-03	6.41E-03	2.69E-03	2.18E-02	8.61E-03
Metal depletion	kg Fe eq	8.81E-02	5.60E-02	4.62E-01	4.46E-01	7.95E-02	4.59E-02	9.93E-01	5.75E-01	1.96E+00	1.21E+00	1.56E+00	9.88E-01	2.54E+00	1.42E+00
Natural land transformation	m2	9.34E-04	6.42E-04	7.73E-04	5.24E-04	6.40E-04	4.08E-04	1.48E-02	8.62E-03	7.02E-03	3.91E-03	6.75E-03	3.75E-03	2.19E-02	1.06E-02
Ozone depletion	kg CFC-11 eq	1.67E-07	6.50E-08	2.12E-07	8.78E-08	1.57E-07	6.71E-08	4.50E-06	2.78E-06	8.02E-06	3.99E-06	7.68E-06	3.67E-06	1.22E-05	4.86E-06
Particulate matter formation	kg PM10 eq	2.79E-03	1.08E-03	1.70E-02	8.26E-03	2.15E-03	7.66E-04	5.09E-02	1.83E-02	8.74E-02	3.18E-02	7.01E-02	2.99E-02	1.20E-01	3.86E-02
Photochemical oxidant formation	kg NMVOC	5.98E-03	2.27E-03	1.74E-02	6.79E-03	4.55E-03	1.68E-03	9.84E-02	3.70E-02	2.21E-01	9.63E-02	1.98E-01	8.92E-02	2.98E-01	1.08E-01
Terrestrial acidification	kg SO2 eq	1.01E-02	4.38E-03	7.46E-02	3.78E-02	7.55E-03	2.91E-03	1.79E-01	6.50E-02	2.46E-01	8.07E-02	1.73E-01	6.83E-02	3.47E-01	1.00E-01
Terrestrial ecotoxicity	kg 1,4-DB eq	2.10E-04	1.49E-03	1.90E-04	2.91E-03	1.29E-04	1.44E-03	2.86E-03	5.25E-02	5.04E-03	3.04E-02	2.86E-03	2.90E-02	8.10E-03	6.98E-02
Urban land occupation	m2a	7.30E-03	3.23E-03	2.38E-02	1.64E-02	6.25E-03	2.74E-03	1.80E-01	7.90E-02	2.99E-01	1.48E-01	2.72E-01	1.42E-01	4.51E-01	1.80E-01
Water depletion	m3	2.72E+00	1.00E+00	6.17E+00	3.16E+00	2.65E+00	1.02E+00	3.92E+01	1.61E+01	7.27E+01	3.18E+01	6.64E+01	2.97E+01	1.05E+02	3.79E+01

9. Shipping and road transportation distances for centralized recycling

Table 43 Road transportation distances from the deployment site in California to the centralized recycling facility in Ohio. Transportation by road accounts for 100% of the transportation (in ton-km).

Source	Destination	Transportation Mode	Distance (km)	Ton-km (t-km)
Topaz Solar Plant, California	Perrysburg, Ohio	Road - Lorry (16-32 metric ton)	3750	62

Table 44 Road and shipping transportation distances from the deployment site in China to the centralized recycling facility in Malaysia. Transportation by ship and road accounts for 97% and 3% of the transportation (in ton-km), respectively.

Source	Destination	Transportation Mode	Distance (km)	Ton-km (t-km)
Beijing, China	Tianjin Port, China	Road - Lorry (16-32 metric ton)	182	3
Tianjin Port, China	Penang Port, Malaysia	Ship - Transoceanic freight ship	5815	97
Penang Port, Malaysia	First Solar, 8, Jalan Hi Tech 3 / 3 & Phase 3, Kulim Hi-tech Park, 09000 Kulim, Kedah, Malaysia	Road - Lorry (16-32 metric ton)	24	0.4

The ton-km value is calculated by multiplying the distance (km) by 16.66×10^{-3} ton which is the weight of $1m^2$ of a CdTe module [21]. The distances were calculated using Google maps.

10. **Contributions of the energy and material inventory items towards the 18 impact categories in ReCiPe (calculated in SimaPro)**

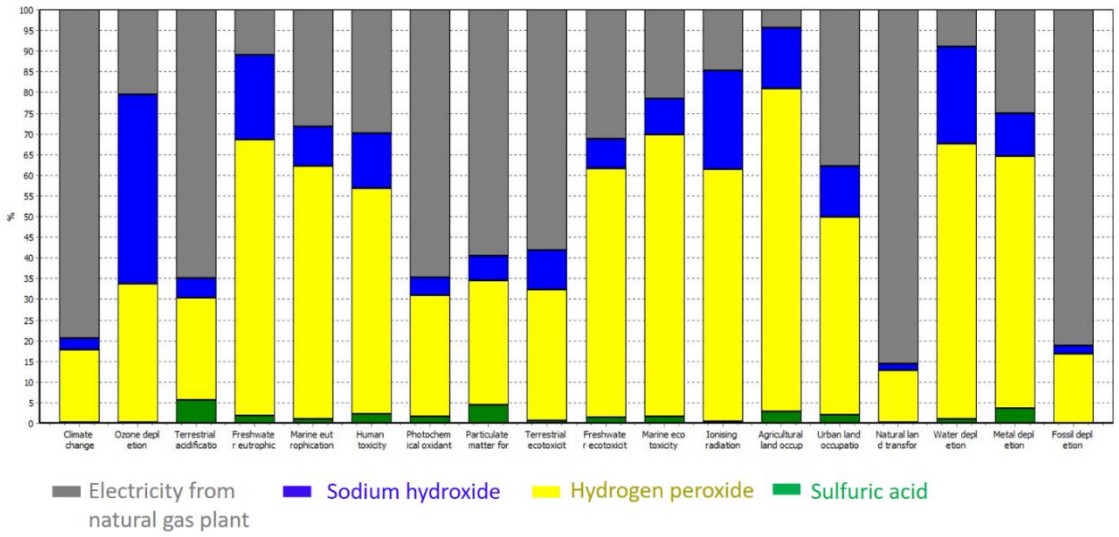

Figure 61 Contributions of the energy and material inventory requirements of the incumbent "mech+leach+prcp" method towards the 18 environmental impact categories in ReCiPe.

Electricity use in the "mech+leach+prcp" recycling method contributes the most to climate change (80%), natural land transformation (85%), and fossil depletion (82%) impact categories (Figure 61).

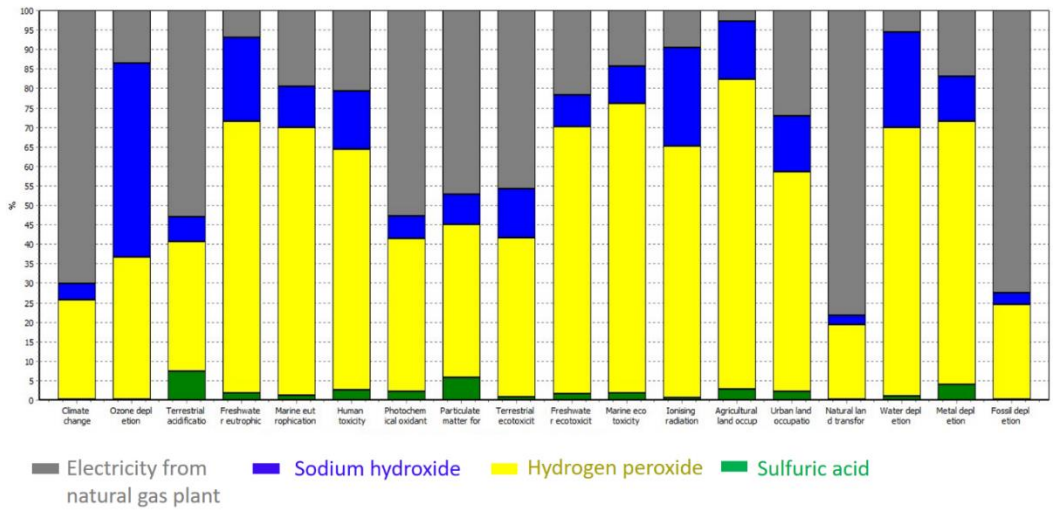

Figure 62 Contributions of the energy and material inventory requirements of the "thermal+leach+prcp" alternative towards the 18 environmental impact categories in ReCiPe.

Electricity use in the "thermal+leach+prcp" recycling alternative contributes the most to natural land transformation (78%), and fossil depletion (75%) impact categories. Similarly, sodium hydroxide use contributes the most to ozone depletion (50%) impact category (Figure 62).

11. Global sensitivity analysis identifying the ten most significant input parameters

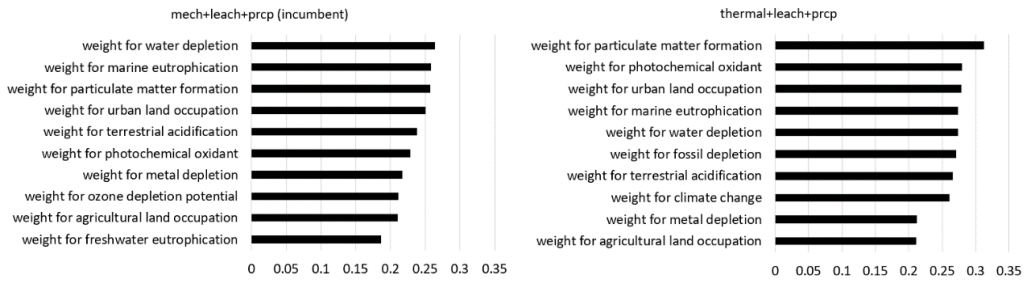

Figure 63 Global sensitivity analysis results showing the values of the sensitivity indices for the ten most significant input parameters (out of a total of 144 input parameters). The environmental ranking of the incumbent "mech+leach+prcp" (left) and the novel "thermal+leach+prcp" (right) recycling alternatives are most sensitive to the weights assigned to the environmental impact categories in ReCiPe impact assessment method.

12. Environmental ranking of the seven recycling alternatives with minimum uncertainty in the pedigree matrix for the material and energy inventory

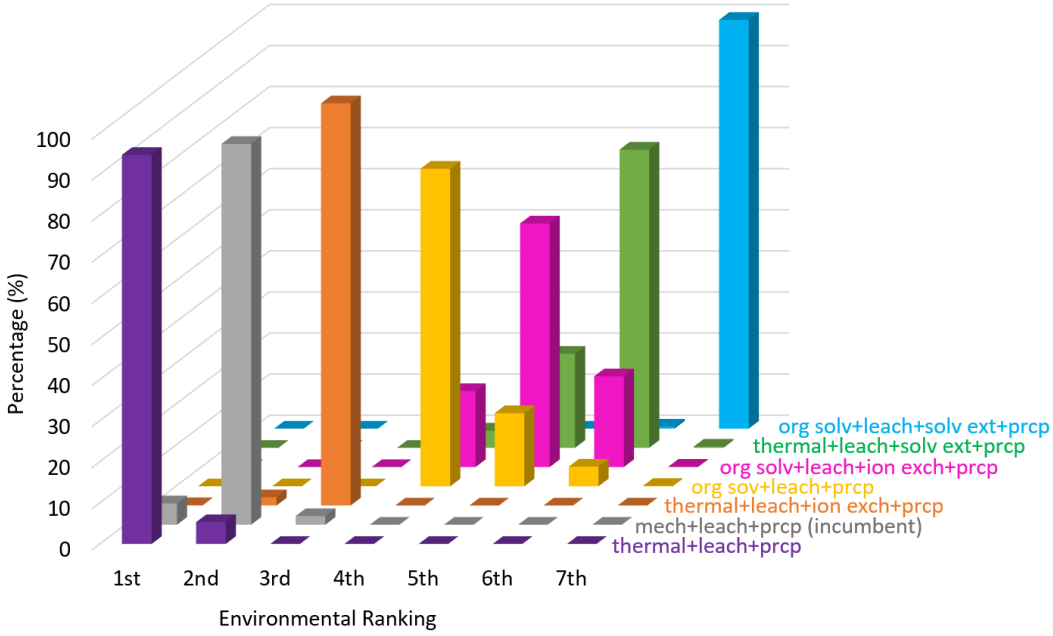

Figure 64 Environmental rankings for the 7 recycling alternatives with rank 1 being most environmentally preferable. The rankings are calculated based on minimum uncertainty in the energy and material inventory values in the pedigree matrix. The x-axis shows the ranks and the y-axis depicts the percentage value out of a 1000 runs that a particular recycling alternative obtains a rank.

13. **Environmental impact of transportation by road and ship**

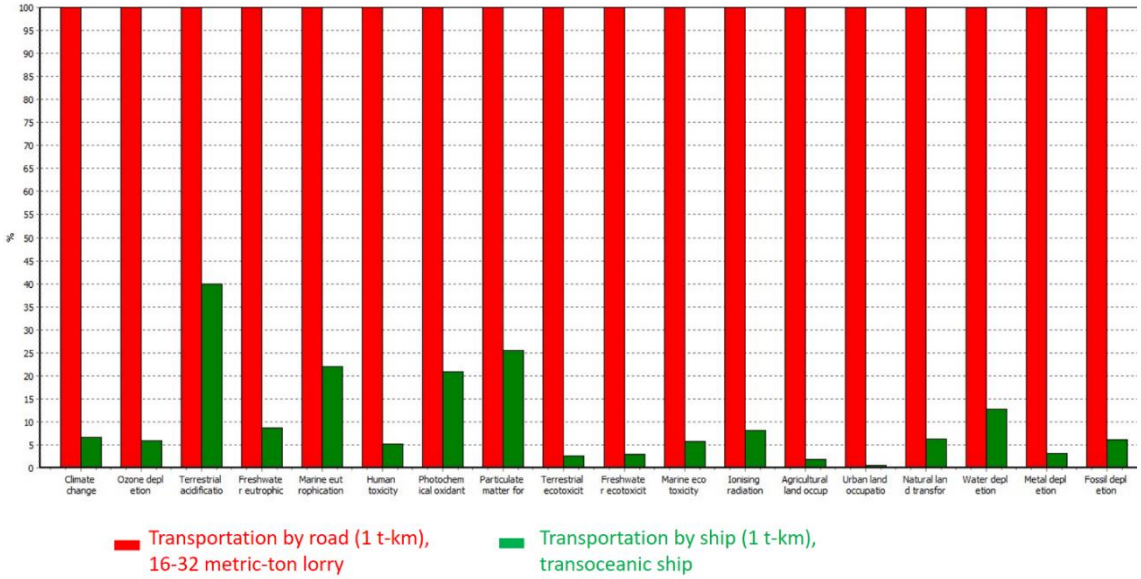

Figure 65 Environmental comparison of transportation by ship and road. The results are generated in SimaPro [20] **and are calculated for 1 ton-km. The impacts of transportation by road are greater than ship in all the 18 impact categories in ReCiPe.**

14. **Environmental ranking for decentral recycling in China and centralized in Malaysia when recycling operations in China utilize electricity generated from PV systems.**

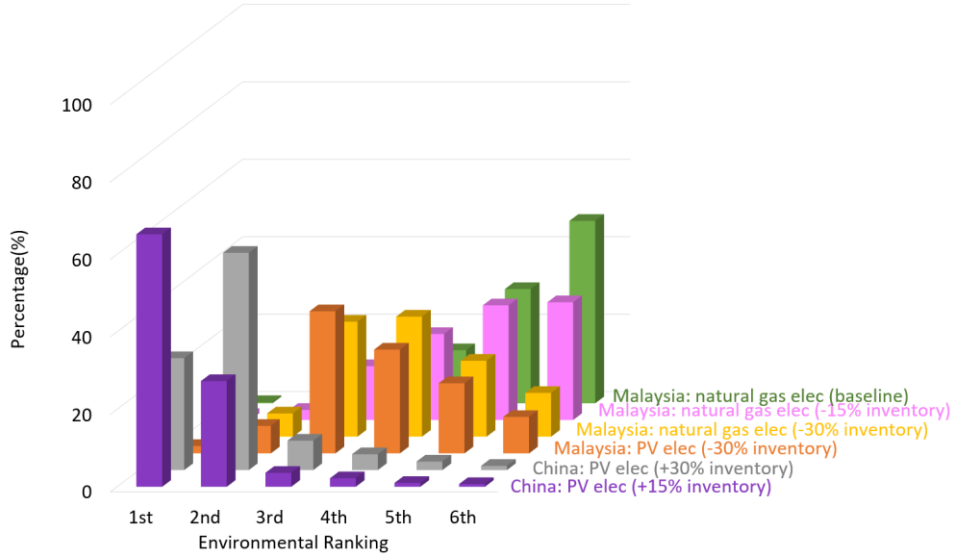

Figure 66 Environmental ranking for decentral recycling in China with electricity generated from PV systems and centralized recycling in Malaysia.

Environmental rankings when the "thermal+leach+prcp" recycling alternative is adopted in both the centralized and decentralized plants in Malaysia and China, respectively (rank 1 being the most environmentally favorable). The + and - percentage values represent the increased and decreased inventory requirements (compared to the baseline scenario) due to lower and higher process efficiencies in decentralized and centralized plants, respectively. The results depict that decentralized recycling in China with PV electricity is environmentally preferable to centralized recycling in Malaysia.

References

[1] Sigma-Aldrich, "Amberlyst 15 Specifications." [Online]. Available: http://www.sigmaaldrich.com/catalog/product/sial/06423?lang=en&region=US. [Accessed: 01-Jan-2015].

[2] V. Fthenakis and W. Wang, "System and method for separating tellurium from cadmium waste," US7731920 B2, 2010.

[3] W. Wang and V. Fthenakis, "Kinetics study on separation of cadmium from tellurium in acidic solution media using ion-exchange resins," *J. Hazard. Mater.*, vol. 125, no. 1–3, pp. 80–88, 2005.

[4] V. M. Fthenakis and W. Wang, "Extraction and separation of Cd and Te from cadmium telluride photovoltaic manufacturing scrap," *Prog. Photovoltaics Res. Appl.*, vol. 14, no. 4, pp. 363–371, 2006.

[5] J. K. Choe, M. H. Mehnert, J. S. Guest, T. J. Strathmann, and C. J. Werth, "Comparative assessment of the environmental sustainability of existing and emerging perchlorate treatment technologies for drinking water," *Environ. Sci. Technol.*, vol. 47, no. 9, pp. 4644–4652, 2013.

[6] A. Amini, Y. Kim, J. Zhang, T. Boyer, and Q. Zhang, "Environmental and economic sustainability of ion exchange drinking water treatment for organics removal," *J. Clean. Prod.*, vol. 104, pp. 413–421, 2015.

[7] NREL, "Polycrystalline Thin-Film Materials and Devices R&D." [Online]. Available: http://www.nrel.gov/pv/thinfilm.html. [Accessed: 01-Jan-2015].

[8] A. Mezei, M. Ashbury, M. Canizares, R. Molnar, H. Given, A. Meader, K. Squires, F. Ojebuoboh, T. Jones, and W. Wang, "Hydrometallurgical recycling of the semiconductor material from photovoltaic materials—part II: metal recovery," in *Hydrometallurgy*, 2008, pp. 224–237.

[9] Sigma Aldrich, "Bis(2-ethylhexyl) phosphate specification," 2015. [Online]. Available: http://www.sigmaaldrich.com/catalog/product/aldrich/237825?lang=en&region=US.

[10] Ehsan Vahidi et Al., "Modeling of synergistic effect of Cyanex 302 and D2EHPA on separation of nickel and cadmium from sulfate leach liquors of spent Ni–Cd batteries," *Eng. Technol.*, vol. 6, no. 12, p. 53, 2012.

[11] V. Kumar, M. Kumar, M. K. Jha, J. Jeong, and J. C. Lee, "Solvent extraction of cadmium from sulfate solution with di-(2-ethylhexyl) phosphoric acid diluted in kerosene," *Hydrometallurgy*, vol. 96, no. 3, pp. 230–234, 2009.

[12] A. Babakhani, F. Rashchi, A. Zakeri, and E. Vahidi, "Selective separation of nickel and cadmium from sulfate solutions of spent nickel-cadmium batteries using mixtures of

D2EHPA and Cyanex 302," *J. Power Sources*, vol. 247, pp. 127–133, 2014.

[13] E. Vahidi and F. Zhao, "Life Cycle Analysis for Solvent Extraction of Rare Earth Elements from Aqueous Solutions," *Rewas 2016 Towar. Mater. Resour. Sustain.*, pp. 113–120, 2016.

[14] P. Sinha, M. Cossette, and J.-F. Ménard, "End-of-Life CdTe PV Recycling with Semiconductor Refining," in *PVSEC 2012*, pp. 8–11.

[15] V. Prado-Lopez, T. P. Seager, M. Chester, L. Laurin, M. Bernardo, and S. Tylock, "Stochastic multi-attribute analysis (SMAA) as an interpretation method for comparative life-cycle assessment (LCA)," *Int. J. Life Cycle Assess.*, vol. 19, no. 2, pp. 405–416, 2014.

[16] J.-P. Brans and B. Mareschal, "Promethee Methods," *Mult. Criteria Decis. Anal. State Art Surv.*, pp. 163–196, 2005.

[17] V. Prado, K. Rogers, and T. P. Seager, "Integration of MCDA Tools in Valuation of Comparative Life Cycle Assessment," *Life Cycle Assess. Handb. A Guid. Environ. Sustain. Prod.*, pp. 413–431, 2012.

[18] I. Linkov, F. K. Satterstrom, B. Yatsalo, A. Tkachuk, G. A. Kiker, J. Kim, and K. Gardner, "Comparative assessment of several multi-criteria decision analysis tools for management of contaminated sediments," *Environ. Secur. Harb. Coast. areas*, pp. 195–215, 2007.

[19] Vulcan, "Vulcan Box Furnace - Owner & Operator's Manual." [Online]. Available: http://www.coleparmer.com/Assets/manual_pdfs/33855-10.pdf.

[20] PRe Consultants, "Simapro version 8.0.3.14," 2015. [Online]. Available: http://www.pre-sustainability.com/simapro.

[21] First Solar, "First Solar Series 4™ PV Module," 2015. [Online]. Available: http://www.firstsolar.com/en/Technologies-and-Capabilities/PV-Modules/First-Solar-Series-4-Modules/Documents/Series-4-V2-Datasheet?dl=1.